

2018

# Exploration Of Zirconium-Catalyzed Intermolecular Hydrophosphination With Primary Phosphines: Photocatalytic Single And Double Hydrophosphination

Christine Anne Bange  
*University of Vermont*

Follow this and additional works at: <https://scholarworks.uvm.edu/graddis>

 Part of the [Inorganic Chemistry Commons](#)

---

## Recommended Citation

Bange, Christine Anne, "Exploration Of Zirconium-Catalyzed Intermolecular Hydrophosphination With Primary Phosphines: Photocatalytic Single And Double Hydrophosphination" (2018). *Graduate College Dissertations and Theses*. 872.  
<https://scholarworks.uvm.edu/graddis/872>

This Dissertation is brought to you for free and open access by the Dissertations and Theses at ScholarWorks @ UVM. It has been accepted for inclusion in Graduate College Dissertations and Theses by an authorized administrator of ScholarWorks @ UVM. For more information, please contact [donna.omalley@uvm.edu](mailto:donna.omalley@uvm.edu).

EXPLORATION OF ZIRCONIUM-CATALYZED INTERMOLECULAR  
HYDROPHOSPHINATION WITH PRIMARY PHOSPHINES: PHOTOCATALYTIC  
SINGLE AND DOUBLE HYDROPHOSPHINATION

A Dissertation Presented

by

Christine Anne Bange

to

The Faculty of the Graduate College

of

The University of Vermont

In Partial Fulfillment of the Requirements  
For the Degree of Doctor of Philosophy  
Specializing in Chemistry

May, 2018

Defense Date: March 23, 2018  
Dissertation Examination Committee:

Rory Waterman, Ph.D., Advisor  
Madalina I. Furis, Ph.D., Chairperson  
Matthew D. Liptak, Ph.D.  
Adam C. Whalley, Ph.D.  
Cynthia J. Forehand, Ph.D., Dean of the Graduate College

## ABSTRACT

Catalytic hydrophosphination has enormous potential in the selective preparation of value-added organophosphines, despite the challenge of the reaction. This dissertation aims to address the hurdles in catalytic hydrophosphination with respect to substrate scope, selectivity, and reaction conditions using  $[\kappa^5\text{-}N,N,N,N,C\text{-(Me}_3\text{SiNCH}_2\text{CH}_2)_2\text{NCH}_2\text{CH}_2\text{NSiMe}_2\text{CH}_2]\text{Zr}$  (**1**).

Compound **1** readily engages with a suite of primary phosphines. These are challenging substrates for this reaction, but **1** readily provides high conversions with these substrates. Increasingly large primary phosphines, including chiral phosphines, undergo catalysis with **1**. Furthermore, a variety of underreported unsaturated substrates can be functionalized in catalytic hydrophosphination with **1**. Alkynes are underreported substrates, but **1** showed not only catalytic reactivity with internal alkynes, but also the first example of a double hydrophosphination with these substrates. Almost entirely absent from catalytic hydrophosphination are unactivated alkenes, yet **1** catalyzes them with TON and TOF that now rival those of styrenes. Additionally, a new tandem inter- and intramolecular diene hydrophosphination was reported to give cyclic phosphine products.

The selectivity in catalytic hydrophosphination **1** in all processes is novel in many regards. In alkyne hydrophosphination, vinyl phosphines or double hydrophosphination products could be isolated as secondary phosphines, depending on reaction conditions. For alkenes, secondary or tertiary phosphines can be formed by modification of the reaction stoichiometry. Isolated secondary phosphines were further elaborated into chiral tertiary phosphines. Catalytic hydrophosphination with a chiral, air-stable primary phosphine gave chiral secondary phosphine products. Efforts to synthesize a chiral ligand to close the gap on catalysts (and therefore substrates) for asymmetric hydrophosphination are discussed.

Catalysis with **1** proceeds under photolysis. Direct irradiation of **1** by ultraviolet or visible light during alkene hydrophosphination substantially enhanced catalytic activity. For example, previous reports of styrene hydrophosphination with **1** showed TON = 18 and TOF = 1.5 h<sup>-1</sup>. Under irradiation, the process is substantially more efficient (TON = 20 and TOF = 60 h<sup>-1</sup>) and the substrate scope is expanded. Computational and spectroscopic data indicate that photoexcitation results in a charge transfer in the active catalyst, which appears to accelerate catalysis by promoting substrate insertion based on a linear free-energy relationship.

The impressive substrate scope, mild conditions, and increased catalytic activity from photoexcitation, rather than heat, are among the best reported for the reaction. Identification of a photoexcitation event that promotes substrate insertion may enable enhanced reactivity from other metal catalysts for this transformation.

## CITATIONS

Material from this dissertation has been published in the following form:

Bange, C. A.. (2016). Zirconium-catalyzed intermolecular hydrophosphination using a chiral, air-stable primary phosphine. *Dalton Transactions*, 45, 1863-1867.

Bange, C. A.. (2016). Challenges in Catalytic Hydrophosphination. *Chemistry - A European Journal*, 22, 12598-12605.

Bange, C. A.. (2016). Zirconium-Catalyzed Intermolecular Double Hydrophosphination of Alkynes with a Primary Phosphine. *ACS Catalysis*, 6, 6413-6416.

Bange, C. A.. (2016). Zirconium-Catalyzed Alkene Hydrophosphination and Dehydrocoupling with an Air-stable Primary Phosphine. *Inorganics*, 4, 26.



## **DEDICATION**

For Ryan

## ACKNOWLEDGEMENTS

The research work presented here was supported by the National Science Foundation (NSF Grants CHE-1265608 and CHE-1565658). I would also like to thank the University of Vermont Chemistry Department and University of Vermont Graduate Student Senate for awards and travel funding. This allowed me to present my work at two American Chemical Society conferences over the years.

It has been a sincere honor to work for Rory Waterman. Rory has shown me incredible kindness, patience, support, and guidance since day one. Rory has a talent for bringing out the best in people. Many graduate students leave Vermont wishing they could emulate him, and I am no exception.

I would like to thank many members of the Waterman group for their support over the years, and my fellow graduate students for many years of friendship and fond memories. My committee members, Prof. Madalina Furis, Prof. Matthew Liptak, Prof. Adam Whalley, deserve deep gratitude for helpful discussions and feedback. Each of them has made substantial contributions to this work.

I would like to sincerely thank Kathy and Rob, who have always treated me like one of their own. I have looked up to them for support and guidance many times during the years and I found love and answers each time.

I would like to thank my family for their steadfast love and encouragement. I entered into graduate school at a very difficult time in our lives, yet they overwhelmingly supported me. I was deeply touched that my sister was there for me even during her darkest days and I hope that she knows she is a huge inspiration in my life. My parents have shown me every love and kindness in the world. They worked so hard and sacrificed so much for me to have the life I do. Their unwavering faith in my pursuits and education has made a tremendous difference.

This dissertation is dedicated to Ryan, who means more to me than I can express. His love, support, and encouragement has driven me each step of this process. He has been the best friend I have ever known, and he makes me feel truly loved.

## TABLE OF CONTENTS

	Page
ACKNOWLEDGEMENTS.....	ii
LIST OF TABLES.....	x
LIST OF FIGURES.....	xii
LIST OF ABBREVIATIONS.....	xxi
CHAPTER 1: GENERAL INTRODUCTION.....	1
1.1. Phosphines.....	1
1.2. P–C bond formation via metal-catalyzed hydrophosphination.....	2
1.3 Mechanistic understandings of metal-catalyzed hydrophosphination.....	17
1.4. Hydroarsination.....	19
1.5. Conclusions.....	21
1.6. References.....	23
CHAPTER 2: ZIRCONIUM-CATALYZED INTERMOLECULAR HYDROPHOSPHINATION WITH PRIMARY PHOSPHINES.....	34
2.1. Introduction.....	34
2.1.1. Primary phosphine chemistry.....	34
2.1.2. Catalytic hydrophosphination of primary phosphines.....	39
2.2. Results and discussion.....	44
2.2.1. Catalytic hydrophosphination of alkenes with PhPH <sub>2</sub> and CyPH <sub>2</sub> .....	44
2.2.2. Hydrophosphination of alkenes with air-stable primary phosphines.....	51
2.2.3. Formation of tertiary phosphine products.....	58
2.2.4. Formation of secondary phosphines.....	59
2.3. Conclusions.....	61
2.4. Experimental methods.....	61

2.4.1. General procedure for hydrophosphination reactions with PhPH <sub>2</sub> and CyPH <sub>2</sub> .....	64
2.4.2. General procedure for hydrophosphination reactions with <b>2</b> .....	63
2.4.3. Procedure for hydrophosphination reaction targeting <b>3a</b> .....	63
2.4.4. Procedure for formation of <b>4</b> and <b>5</b> .....	63
2.5. References.....	64

## CHAPTER 3: ZIRCONIUM-CATALYZED DOUBLE HYDROPHOSPHINATION OF ALKYNES WITH PRIMARY PHOSPHINES ..... 71

3.1. Introduction.....	71
3.2. Results and discussion .....	78
3.2.1. Single hydrophosphination to make vinyl phosphines .....	78
3.2.2. Double hydrophosphination to make diphosphines.....	82
3.2.3. Hydrophosphination with MesPH <sub>2</sub> .....	96
3.2.4. Functionalization with double hydrophosphination products.....	98
3.2.5. Hydrophosphination and isomerization of bis(diethylamido)acetylene .....	101
3.3. Conclusions .....	103
3.4. Experimental methods .....	105
3.4.1. General methods .....	105
3.4.2. General procedure for hydrophosphination reactions.....	106
3.4.3. Procedure for hydrophosphination reactions with bis(diethylamido)acetylene to produce <b>2j</b> .....	107
3.4.4. General procedure for isomerization reactions with <b>2j</b> .....	108
3.4.5. Procedure for hydrophosphination of acetylene .....	109
3.4.6. Procedure for formation of <b>5</b> .....	109
3.4.7. Procedure for catalytic hydrophosphination with MesPH <sub>2</sub> .....	109
3.5. References.....	110

## CHAPTER 4: EFFORTS TOWARDS SYNTHESIS OF A CHIRAL LIGAND FOR ZIRCONIUM-CATALYZED HYDROPHOSPHINATION TO FORM *P*-CHIRAL PHOSPHINES ..... 114

4.1. Introduction.....	114
4.1.1. Synthetic and stoichiometric routes to <i>P</i> -stereogenic phosphines .....	114
4.1.2. Catalytic routes to <i>P</i> -stereogenic phosphines .....	116
4.1.3. Hydrophosphination to generate <i>P</i> - and/or <i>C</i> -chiral phosphines.....	119

4.2. Results and discussion .....	123
4.3. Conclusions .....	133
4.4. Experimental methods .....	136
4.4.1. General methods .....	136
4.4.2. Formation of compound <b>15</b> .....	136
4.4.3. Formation of compound <b>16</b> .....	138
4.4.4. Deprotection of <b>8</b> with sulfuric acid to form <b>5</b> .....	138
4.5. References.....	138
CHAPTER 5: LIGHT-DEPENDENT ALKENE HYDROPHOSPHINATION: THE ROLE OF IRRADIATION .....	143
5.1. Introduction.....	143
5.2. Results and discussion .....	144
5.2.1. Ultraviolet-visible spectroscopy .....	144
5.2.2. Alkene hydrophosphination promoted by light .....	147
5.2.3. Alkene hydrophosphination with <b>1</b> .....	154
5.2.4. Light-driven alkyne hydrophosphination with <b>1</b> .....	166
5.2.5. TDDFT calculations .....	168
5.2.6. Fluorescence spectroscopy on <b>2</b> .....	173
5.2.7. Mechanistic insights .....	176
5.2.8. Optimization of photocatalytic hydrophosphination with <b>1</b> .....	179
5.2.9. Excitation of <b>2</b> for catalytic dehydrocoupling of PhPH <sub>2</sub> .....	183
5.3. Conclusions .....	185
5.4. Experimental methods .....	186
5.4.1. General methods .....	186
5.4.2. Spectral energy distributions of the lamps.....	187
5.4.3. General procedure for hydrophosphination reactions.....	188
5.4.4. Procedure for Hammett plot generation.....	189
5.4.5. Procedure for dehydrocoupling of PhPH <sub>2</sub> .....	190
5.4.6. Determination of extinction coefficient for <b>2</b> .....	190
5.5. References.....	191
CHAPTER 6: SEQUENTIAL CATALYTIC INTERMOLECULAR AND INTRAMOLECULAR HYDROPHOSPHINATION OF DIENES TARGETING PHOSPHORUS-CONTAINING RINGS .....	195

6.1. Introduction.....	195
6.2. Results and discussion .....	198
6.3. Conclusions .....	210
6.4. Experimental methods .....	210
6.4.1. General methods .....	210
6.4.2. Synthesis of <b>2a</b> .....	211
6.4.3. General procedure for hydrophosphination reactions with PhPH <sub>2</sub> targeting phosphacycles .....	211
6.4.4. Representative NMR spectra .....	212
6.5. References.....	236
 CHAPTER 7: ZIRCONIUM-CATALYZED HYDROARSINATION WITH PRIMARY ARSINES.....	 239
7.1. Introduction.....	239
7.2. Results and discussion .....	247
7.3. Conclusion .....	252
7.4. Experimental methods .....	254
7.4.1. General methods .....	254
7.4.2. General procedure for catalytic hydroarsination with <b>1</b> .....	254
7.4.3. Procedure for Hammett plot generation.....	254
7.4.4. Synthesis of arsenic precursors.....	256
7.4.5. NMR spectra of hydroarsination reactions .....	269
7.5. References.....	287
 CHAPTER 8: GENERAL CONCLUSION.....	 290
 CHAPTER 9: COMPREHENSIVE BIBLIOGRAPHY .....	 292

## LIST OF TABLES

Table	Page
Table 2.1: Zirconium-catalyzed intermolecular hydrophosphination of styrenes with PhPH <sub>2</sub> .....	46
Table 2.2: Zirconium-catalyzed intermolecular hydrophosphination of alkenes and dienes with PhPH <sub>2</sub> .....	48
Table 2.3: Catalytic Hydrophosphination with <b>2</b> to form secondary phosphine products.....	52
Table 3.1: Zirconium-catalyzed single hydrophosphination of alkynes targeting vinyl phosphines .....	79
Table 3.2: Double hydrophosphination to make diphosphines.....	83
Table 3.3: Hydrophosphination of bis(diethylamido)acetylene.....	101
Table 3.4: Hydrophosphination of bis(diethylamido)acetylene with PhPH <sub>2</sub> to produce <b>2j</b> .....	107
Table 3.5: Isomerization of bis(diethylamido)acetylene with PhPH <sub>2</sub> to produce <b>2j</b> ....	108
Table 5.1: Lamp specifications .....	153
Table 5.2: Catalytic hydrophosphination of styrene derivatives with <b>1</b> under blacklight.....	155
Table 5.3: Catalytic hydrophosphination of styrenes under 253.7 nm.. .....	157
Table 5.4: Catalytic hydrophosphination of unactivated alkenes. ....	159
Table 5.5: Catalytic hydrophosphination of dienes substrates, unactivated substrates, and Michael acceptors.....	162
Table 5.6: Catalytic hydrophosphination using CyPH <sub>2</sub> and MesPH <sub>2</sub> .....	164



Table 5.7: Structure optimization around Zr as implemented in ORCA 4.0 .....	170
Table 5.8: Band intensity ratios and differences for GGA functionals.....	171
Table 5.9: Lifetimes of fluorescence decay in <b>2</b> .....	176
Table 5.10: Initial concentrations of reactants in hydrophosphination competition experiments.....	199
Table 5.11: <sup>1</sup> H integration ratios of styrene and styrene derivatives in hydrophosphination competition experiments.....	189
Table 6.1: Catalytic hydrophosphination of 1,4-pentadiene with PhPH <sub>2</sub> to form vinyl phosphine <b>2a</b> and phosphacycle <b>2b</b> .....	199
Table 6.2: Catalytic hydrophosphination of <b>2a</b> to form <b>2b</b> .....	201
Table 6.3: Catalytic hydrophosphination of 1,5-hexadiene with PhPH <sub>2</sub> to form alkenyl phosphine <b>3a</b> , phosphacycles <b>3b</b> and <b>3c</b> , and diphosphine <b>3d</b> .....	203
Table 6.4: Catalytic hydrophosphination of 2-methyl-1,5-hexadiene with PhPH <sub>2</sub> to form vinyl phosphines <b>4a</b> and <b>4b</b> and phosphacycles <b>4c-4e</b> .....	204
Table 6.5: Catalytic hydrophosphination of 1,7-octadiene with PhPH <sub>2</sub> to form vinyl phosphine <b>5a</b> and phosphacycles <b>5b</b> and <b>5c</b> .....	205
Table 7.1: Catalytic hydroarsination with <b>1</b> .....	249
Table 7.2: Initial concentrations of reactants in hydroarsination competition experiments.....	255
Table 7.3: <sup>1</sup> H integration ratios of styrene and styrene derivatives in hydroarsination competition experiments.....	255

## LIST OF FIGURES

Figure	Page
Figure 2.1: Air-stable primary phosphines protected by steric bulk.....	36
Figure 2.2: Air-stable primary phosphines <b>2</b> and <b>3</b> .....	38
Figure 2.3: Metal catalysts capable of primary phosphine hydrophosphination .....	41
Figure 2.4: X-ray crystal structure of <b>4</b> with thermal ellipsoids drawn at the 50% probability level. ....	55
Figure 3.1: <i>E</i> and <i>Z</i> isomers from the single hydrophosphination of diphenylacetylene with two equivalents of PhPH <sub>2</sub> and 5 mol % <b>1</b> .....	80
Figure 3.2: One-pot double hydrophosphination of methyl phenyl acetylene to form the diphosphines from the vinyl phosphines.....	84
Figure 3.3: <sup>31</sup> P- <sup>1</sup> H HMBC spectrum of the one-pot hydrophosphination of methyl phenylacetylene.....	85
Figure 3.4: Hydrophosphination of methyl phenyl acetylene targeting vinyl phosphines run in the absence of light (top) or irradiation from an LED lamp (bottom).....	88
Figure 3.5: Attempted hydrophosphination of phenylacetylene.....	91
Figure 3.6: Crude <sup>31</sup> P{ <sup>1</sup> H} NMR spectrum of the hydrophosphination of acetylene gas .....	93

Figure 3.7: $^1\text{H}$ NMR spectrum of <b>5</b> .....	95
Figure 3.8: Hydrophosphination of methyl phenyl acetylene with $\text{MesPH}_2$ .....	97
Figure 3.9: $^{31}\text{P}\{^1\text{H}\}$ NMR spectrum of the diphosphine with a chiral reporter .....	100
Figure 3.10: Isomerization of the vinyl phosphines in the presence of excess $\text{PhPH}_2$ .....	102
Figure 4.1: $^1\text{H}$ NMR spectrum of <b>7</b> showing formation of a single isomer.....	124
Figure 4.2: $^1\text{H}$ NMR spectrum of <b>8</b> .....	125
Figure 4.3: $^1\text{H}$ NMR spectrum of ( <i>S</i> )- <i>N</i> 1, <i>N</i> 1-bis(( <i>S</i> )-2-aminopropyl)propane-1,2-diamine ( <b>5</b> ) .....	127
Figure 4.4: $^1\text{H}$ NMR spectrum of <b>16</b> .....	131
Figure 4.5: A crude reaction forming compounds <b>6</b> (eqn 4.4).....	133
Figure 4.6: $^1\text{H}$ NMR spectrum of <b>15</b> .....	137
Figure 5.1: UV-vis spectra of <b>2</b> in various solvents .....	146
Figure 5.2: UV-vis spectra of <b>2</b> and <b>3</b> in hexanes .....	147
Figure 5.3: Stacked $^1\text{H}$ NMR spectra of the hydrophosphination of styrene under blacklight.....	149
Figure 5.4: Overlap of the spectral energy distribution of the OSRAM Sylvania Ultra LED A19 Lamp – generation 5, operating power of 6 W and output of 450 lumens (red dash), VEI UV Blacklight Party Lamp, operating power of 13 W (black dash), and UV-vis absorbance of <b>2</b> . ....	151

Figure 5.5: TDDFT predicted absorbance spectra for <b>2</b> .....	169
Figure 5.6: Donor and acceptor orbitals for the low energy band predicted in each spectrum.....	172
Figure 5.7: Overlay of fluorescence and UV-vis spectrum of <b>2</b> in hexanes. ....	174
Figure 5.8: Time-resolved photoluminescence spectrum of <b>2</b> with triexponential fit....	175
Figure 5.9: Relative rate constants of competition experiments after 15 min .....	177
Figure 5.10: Jablonski diagram for photoexcitation of <b>2</b> .....	178
Figure 5.11: Light intensity as a function of distance from the lamp .....	179
Figure 5.12: Percent consumption of styrene with 2 equiv. of PhPH <sub>2</sub> and 5 mol % <b>1</b> in an NMR tube taped to the surface of a Vei party lamp blacklight.....	180
Figure 5.13: Hydrophosphination of styrene with 2 equiv. of PhPH <sub>2</sub> and 5 mol % <b>1</b> in an NMR tube taped to the surface of a Vei party lamp blacklight.....	181
Figure 5.14: Effect of solvent on % consumption of styrene... ..	183
Figure 5.15: Dehydrocoupling of PhPH <sub>2</sub> at ambient temperature with <b>1</b> .....	184
Figure 5.16: Spectral energy distribution of an OSRAM Sylvania Ultra LED A19 Lamp – Generation 5, operating power of 6 W and output of 450 lumens .....	187
Figure 5.17: Spectral energy distribution of VEI UV Blacklight Party Lamp, operating power of 13 W. ....	188

Figure 5.18: Spectral energy distribution of a Rexim G23 UV-A 360 nm Lamp, operating power of 9 W. ....	188
Figure 5.19: Stacked $^{31}\text{P}\{^1\text{H}\}$ NMR spectra of the dehydrocoupling of $\text{PhPH}_2$ with <b>1</b> at ambient temperature.....	190
Figure 5.20: Determination of the extinction coefficient for <b>2</b> in hexanes measured at 364.5 nm in a 1.0 mm cuvette.....	191
Figure 5.21: Determination of the extinction coefficient of <b>2</b> in benzene measured at 360.0 nm in a 1.0 cm cuvette.....	191
Figure 6.1: Cyclic phosphines as ligands for asymmetric catalysis.....	196
Figure 6.2: Assignment of the isomers <b>3b</b> and <b>3c</b> by $^{31}\text{P}$ - $^1\text{H}$ HMBC .....	206
Figure 6.3: Assignment of the isomers <b>4a-4e</b> by $^{31}\text{P}$ - $^1\text{H}$ HMBC .....	207
Figure 6.4: DEPT-135 NMR spectrum of a reaction mixture of <b>5a-5c</b> . ....	208
Figure 6.5: Representative initial $^1\text{H}$ NMR spectrum of the hydrophosphination of 1,4-pentadiene.....	212
Figure 6.6: Representative final $^1\text{H}$ NMR spectrum of the hydrophosphination of 1,4-pentadiene.....	213
Figure 6.7: Representative $^{31}\text{P}\{^1\text{H}\}$ NMR spectrum of the hydrophosphination of 1,4-pentadiene.....	214

Figure 6.8: Representative $^{31}\text{P}$ - $^1\text{H}$ HMBC NMR spectrum of the hydrophosphination of 1,4-pentadiene.....	215
Figure 6.9: Representative initial $^1\text{H}$ NMR spectrum of the ring closure of <b>2a</b> to make <b>2b</b> .....	216
Figure 6.10: Representative initial $^{31}\text{P}\{^1\text{H}\}$ NMR spectrum of the ring closure of <b>2a</b> to make <b>2b</b> .....	217
Figure 6.11: Representative final $^1\text{H}$ NMR spectrum of the ring closure of <b>2a</b> to make <b>2b</b> .....	218
Figure 6.12: Representative final $^{31}\text{P}\{^1\text{H}\}$ NMR spectrum of the ring closure of <b>2a</b> to make <b>2b</b> .....	219
Figure 6.13: Representative $^{31}\text{P}\{^1\text{H}\}$ NMR spectrum of the ring closure of <b>2a</b> to make <b>2b</b> .....	220
Figure 6.14: Representative initial $^1\text{H}$ NMR spectrum of the hydrophosphination of 1,5-hexadiene.....	221
Figure 6.15: Representative final $^1\text{H}$ NMR spectrum of the hydrophosphination of 1,5-hexadiene.....	222
Figure 6.16: $^{31}\text{P}\{^1\text{H}\}$ NMR spectrum of the hydrophosphination of 1,5-hexadiene. ..	223
Figure 6.17: $^{31}\text{P}$ NMR spectrum of the hydrophosphination of 1,5-hexadiene .....	224
Figure 6.18: $^{31}\text{P}$ - $^1\text{H}$ HMBC NMR spectrum of the hydrophosphination of 1,5-hexadiene .....	225

Figure 6.19: $^{31}\text{P}\{^1\text{H}\}$ NMR spectrum of the hydrophosphination of 1,5-hexadiene...	226
Figure 6.20: Representative initial $^1\text{H}$ NMR spectrum of the hydrophosphination of 2-methyl-hex-1-ene .....	227
Figure 6.21: Representative final $^1\text{H}$ NMR spectrum of the hydrophosphination of 2-methyl-hex-1-ene .....	228
Figure 6.22: Representative $^{31}\text{P}\{^1\text{H}\}$ NMR spectrum of the hydrophosphination of 2-methyl-hex-1-ene .....	229
Figure 6.23: Representative $^{31}\text{P}$ NMR spectrum of the hydrophosphination of 2-methyl-hex-1-ene.....	230
Figure 6.24: Representative $^{31}\text{P}$ - $^1\text{H}$ HMBC NMR spectrum of the hydrophosphination of 2-methyl-hex-1-ene .....	231
Figure 6.25: Representative initial $^1\text{H}$ NMR spectrum of the hydrophosphination of 1,7-octadiene.....	232
Figure 6.26: Representative final $^1\text{H}$ NMR spectrum of the hydrophosphination of 1,7-octadiene.....	233
Figure 6.27: Representative $^{31}\text{P}\{^1\text{H}\}$ NMR spectrum of the hydrophosphination of 1,7-octadiene.....	234
Figure 6.28: Representative $^{31}\text{P}$ NMR spectrum of the hydrophosphination of 1,7-octadiene.....	235
Figure 6.29: Representative $^{31}\text{P}$ - $^1\text{H}$ HMBC NMR spectrum of the hydrophosphination of 1,7-octadiene.....	236

Figure 7.1: Attempted hydroarsination with <b>1</b> and MesAsH <sub>2</sub> .....	242
Figure 7.2: UV-vis absorbance spectrum of <b>2</b> in hexanes .....	247
Figure 7.3: Hammett competition experiment for hydroarsination .....	248
Figure 7.4: Calculation of the extinction coefficient for <b>2</b> .....	256
Figure 7.5: <sup>1</sup> H NMR spectrum of bis(diethylamino)chloroarsine .....	257
Figure 7.6: <sup>13</sup> C{ <sup>1</sup> H} NMR spectrum of bis(diethylamino)chloroarsine .....	258
Figure 7.7: IR spectrum of bis(diethylamino)chloroarsine.....	258
Figure 7.8: <sup>1</sup> H NMR spectrum of <i>N,N,N',N'</i> -tetraethyl-1-( <i>p</i> -tolyl)arsinediamine.....	260
Figure 7.9: <sup>13</sup> C{ <sup>1</sup> H} NMR spectrum of <i>N,N,N',N'</i> -tetraethyl-1-( <i>p</i> -tolyl)arsinediamine .....	261
Figure 7.10: IR spectrum of <i>N,N,N',N'</i> -tetraethyl-1-( <i>p</i> -tolyl)arsinediamine.....	261
Figure 7.11: <sup>1</sup> H NMR spectrum of dichloro- <i>p</i> -tolylarsine.....	263
Figure 7.12: <sup>13</sup> C{ <sup>1</sup> H} NMR spectrum of dichloro- <i>p</i> -tolylarsine.....	264
Figure 7.13: IR spectrum of dichloro- <i>p</i> -tolylarsine .....	264
Figure 7.14: <sup>1</sup> H NMR spectrum of <i>p</i> -tolylarsine .....	266
Figure 7.15: <sup>13</sup> C{ <sup>1</sup> H} NMR spectrum of <i>p</i> -tolylarsine .....	267
Figure 7.16: <sup>1</sup> H NMR spectrum of <b>2</b> .....	268



Figure 7.17: $^{13}\text{C}\{^1\text{H}\}$ NMR spectrum of <b>2</b> .....	269
Figure 7.18: Initial $^1\text{H}$ NMR spectrum of the hydroarsination of styrene with <i>p</i> -tolylarsine.....	270
Figure 7.19: Final $^1\text{H}$ NMR spectrum of the hydroarsination of styrene with <i>p</i> -tolylarsine.....	271
Figure 7.20: Initial $^1\text{H}$ NMR spectrum of the hydroarsination of <i>p</i> -methoxystyrene with <i>p</i> -tolylarsine .....	272
Figure 7.21: Final $^1\text{H}$ NMR spectrum of the hydroarsination of <i>p</i> -methoxystyrene with <i>p</i> -tolylarsine .....	273
Figure 7.22: Initial $^1\text{H}$ NMR spectrum of the hydroarsination of <i>p</i> -trifluoromethylstyrene with <i>p</i> -tolylarsine .....	274
Figure 7.23: Final $^1\text{H}$ NMR spectrum of the hydroarsination of <i>p</i> -trifluoromethylstyrene with <i>p</i> -tolylarsine .....	275
Figure 7.24: Initial $^1\text{H}$ NMR spectrum of the hydroarsination of <i>p</i> -bromostyrene with <i>p</i> -tolylarsine .....	276
Figure 7.25: Final $^1\text{H}$ NMR spectrum of the hydroarsination of <i>p</i> -bromostyrene with <i>p</i> -tolylarsine .....	277
Figure 7.26: Crude $^1\text{H}$ NMR spectrum of $(p\text{-tolyl})\text{As}(\text{H})\text{CH}_2\text{CH}_2\text{CN}$ .....	278
Figure 7.27: Crude $^{13}\text{C}\{^1\text{H}\}$ NMR spectrum of $(p\text{-tolyl})\text{As}(\text{H})\text{CH}_2\text{CH}_2\text{CN}$ .....	279
Figure 7.28: Crude IR spectrum of $(p\text{-tolyl})\text{As}(\text{H})\text{CH}_2\text{CH}_2\text{CN}$ .....	279

Figure 7.29: $^1\text{H}$ NMR spectrum of ( <i>p</i> -tolyl)As(H)CH <sub>2</sub> CH <sub>2</sub> C(O)OMe .....	280
Figure 7.30: $^{13}\text{C}\{^1\text{H}\}$ NMR spectrum of ( <i>p</i> -tolyl)As(H)CH <sub>2</sub> CH <sub>2</sub> C(O)OMe .....	281
Figure 7.31: IR spectrum of ( <i>p</i> -tolyl)As(H)CH <sub>2</sub> CH <sub>2</sub> C(O)OMe .....	281
Figure 7.32: $^1\text{H}$ NMR spectrum of ( <i>p</i> -tolyl)As(H)CH <sub>2</sub> CH <sub>2</sub> C(O)OEt.....	282
Figure 7.33: $^{13}\text{C}\{^1\text{H}\}$ NMR spectrum of ( <i>p</i> -tolyl)As(H)CH <sub>2</sub> CH <sub>2</sub> C(O)OEt.....	283
Figure 7.34: IR spectrum of ( <i>p</i> -tolyl)As(H)CH <sub>2</sub> CH <sub>2</sub> C(O)OEt .....	283
Figure 7.35: Initial $^1\text{H}$ NMR spectrum of the hydroarsination of 2,3-dimethyl-1,3-butadiene with <i>p</i> -tolylarsine.....	284
Figure 7.36: Final $^1\text{H}$ NMR spectrum of the hydroarsination of 2,3-dimethyl-1,3-butadiene with <i>p</i> -tolylarsine.....	285
Figure 7.37: $^{13}\text{C}-^1\text{H}$ HMBC NMR spectrum of the hydroarsination of 2,3-dimethyl-1,3-butadiene with <i>p</i> -tolylarsine .....	286
Figure 7.38: $^{13}\text{C}$ DEPT-135 NMR spectrum of the hydroarsination of 2,3-dimethyl-1,3-butadiene with <i>p</i> -tolylarsine .....	287

## LIST OF ABBREVIATIONS

(N <sub>3</sub> N)	(Me <sub>3</sub> SiNCH <sub>2</sub> CH <sub>2</sub> ) <sub>3</sub> N
Ac	Acetyl
Acac	Acetylacetonate
Ar	Aryl
BOC	<i>tert</i> -Butyloxycarbonyl
BOC <sub>2</sub> O	Di- <i>tert</i> -butyl dicarbonate
Bu	Butyl
Cat.	Catalyst
Cy	Cyclohexyl
d	Distance or days
DABCO	1,4-Diazabicyclo[2.2.2]octane
DCM	Dichloromethane
de	Diastereomeric excess
DEPT	Distortionless enhancement by polarization transfer
DFT	Density functional theory
DIBAL-H	Di <i>isobutyl</i> aluminum hydride
DIMET	2,6-Dimesityl-4-methylphenyl
DMF	Dimethylformamide
DuPhos	(-)-1,2-Bis[(2 <i>R</i> , 5 <i>R</i> )-2,5-dimethylphospholano]benzene
e <sup>-</sup>	Electron

ee	Enantiomeric excess
Eqn	Equation
Et	Ethyl
FLP	Frustrated Lewis pair
FT-IR	Fourier Transform Infrared Spectrometer
GGA	Generalized Gradient Approximation
h	Hours
HMBC	Heteronuclear multiple bond coupling
hmpa	Hexamethylphosphoramide
HOMO	Highest occupied molecular orbital
Hz	Hertz
I	Intensity
IR	Infrared
kcal	Kilocalories
KO <sup>t</sup> Bu	Potassium <i>tert</i> -butoxide
L	Ligand
LED	Light-emitting diode
LUMO	Lowest occupied molecular orbital
Me	Methyl
Mes	Mesityl = 2,4,6-trimethylphenyl
MO	Molecular orbital
MOF	Metal-organic framework

MOP	2'-methoxy-[1,1'-binaphthalen]-2-yl
NHC	<i>N</i> -Heterocyclic carbene
NMR	Nuclear magnetic resonance (spectroscopy)
Norbornyl	2-bicyclo-[2.2.1]heptyl
Nosyl	2-nitrobenzene-1-sulfonyl chloride
Ph	Phenyl
PTFE	Polytetrafluoroethylene
R	Generic substituent
SOMO	Singly Occupied Molecular Orbital
t	Time
<sup>t</sup> Bu	<i>tert</i> -Butyl
TDDFT	Time-dependent density functional theory
temp.	Temperature
THF	Tetrahydrofuran
TLC	Thin-layer chromatography
TMS	Trimethylsilyl
TOF	Turnover frequency
Tolyl	Methylphenyl
TON	Turnover number
Tosyl	Toluenesulfonyl
Tren	Tris(2-aminoethyl)amine
UV	Ultraviolet

UV-vis	Ultraviolet-visible (spectroscopy)
W	Watts
X	Anionic ligand
ZORA	Zeroth order regular approximation

## CHAPTER 1: GENERAL INTRODUCTION

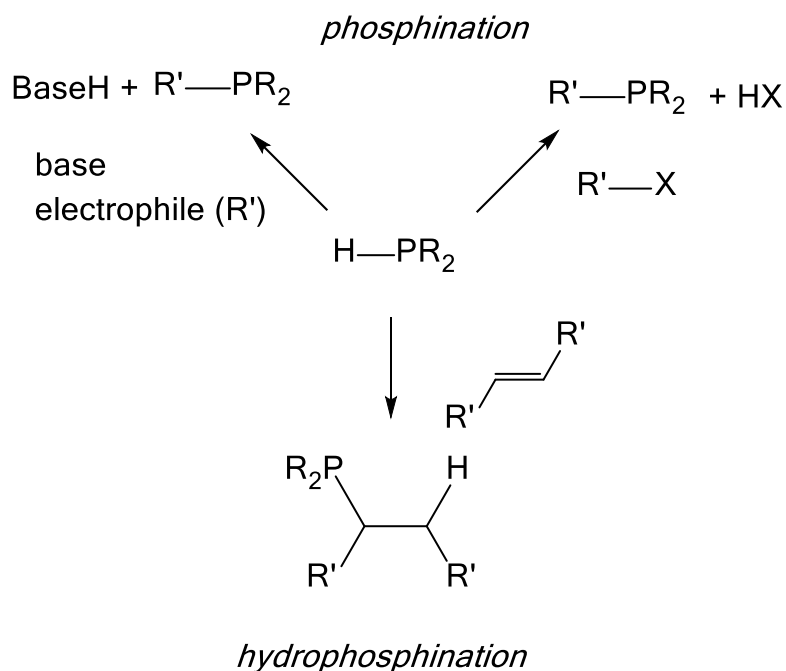
### 1.1 Phosphines

The ubiquity of phosphorus compounds in biological systems, biochemistry, medicine, industry, agriculture, and chemistry is difficult to understate.<sup>1-2</sup> Phosphines bearing a P–H bond attract a good deal of interest for not only being synthetic precursors to these valuable compounds but also for being a unique functional group. The P–H group exhibits a wide breath of reactivity, from oxidation and reduction, cross- and oxidative-coupling, alkylation, heterofunctionalization, C–H activation, to name a few.<sup>1-3</sup> Recent developments in phosphorus chemistry have expanded into advanced materials, such as high thermostable and organic-inorganic polymers, and multifunctional materials, including ones used in the biomedical industry.<sup>1-2</sup>

However, the stark requirement of phosphorus-based compounds is concerning because the world is running out of phosphorus. Some estimates calculate that we will reach peak phosphorus production in the upcoming years, and some estimates state that we have already passed it.<sup>4</sup> Because the agricultural industry consumes the lion's share of phosphorus compounds for both fertilizers and pesticides sustainable ways to make organophosphines is of critical long-term importance. A particular threat to this issue is that so many of the (already limited!) routes to the necessary organophosphines are not atom-economical. Despite the plethora of necessary molecules and attractive materials based on phosphorus, the methodologies that make them still have vast room for improvement.

Historically employed synthetic routes to phosphorus (III) compounds can be loosely divided into two categories (Scheme 1.1). Phosphination produces

organophosphines via classic nucleophilic/electrophilic chemistry. Despite the simplicity and reliability of this transformation, the major caveat is the inherently poor atom-economy. This transformation requires additional reagents and produces waste products that must be separated from the desired organophosphine products.<sup>5</sup>



**Scheme 1.1:** Routes to phosphorus (III) compounds

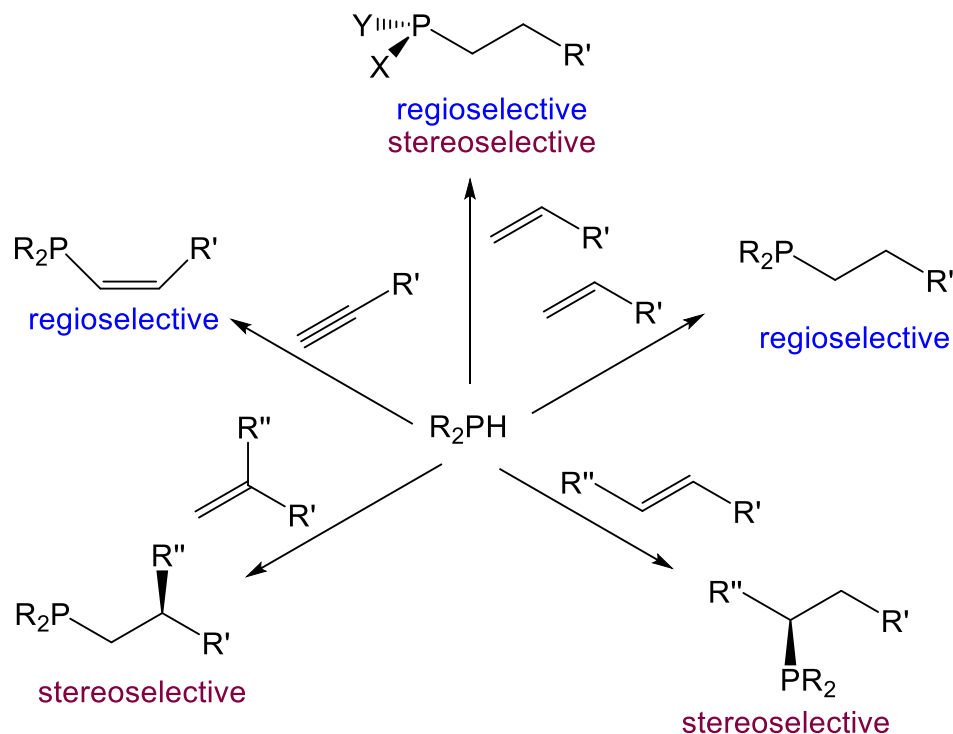
An alternative route is hydrophosphination, which is the addition of P–H across and unsaturated fragment, commonly a carbon–carbon double bond. This reaction has enormous potential to selectively provide a vast array of phosphine products, despite the challenge of the reaction.<sup>6</sup>

### 1.2 P–C bond formation via metal-catalyzed hydrophosphination

Unlike the related hydroamination, hydrophosphination does not necessarily require a catalyst. With impetus from heat, light, or a radical initiator,<sup>7</sup> hydrophosphination can proceed, but often these non-catalytic routes afford mixtures of phosphine products.

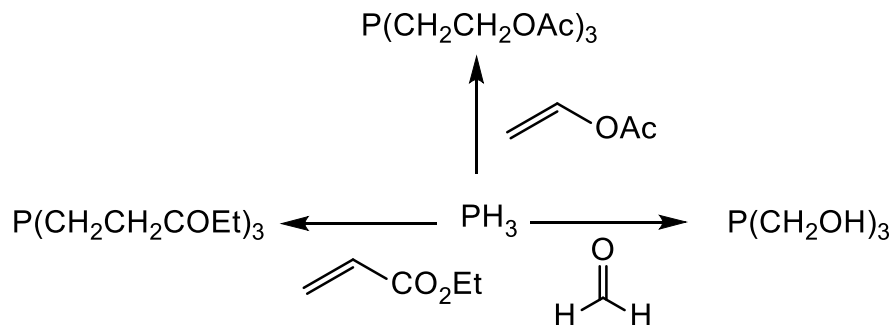


The main advantage of catalytic hydrophosphination over non-catalytic P–C bond formation via P–H addition is product selectivity (Scheme 1.2).<sup>5</sup> The potential for regio- and stereoselectivity in catalytic hydrophosphination has prompted investigation of metal catalysts to provide the desired product selectivity.



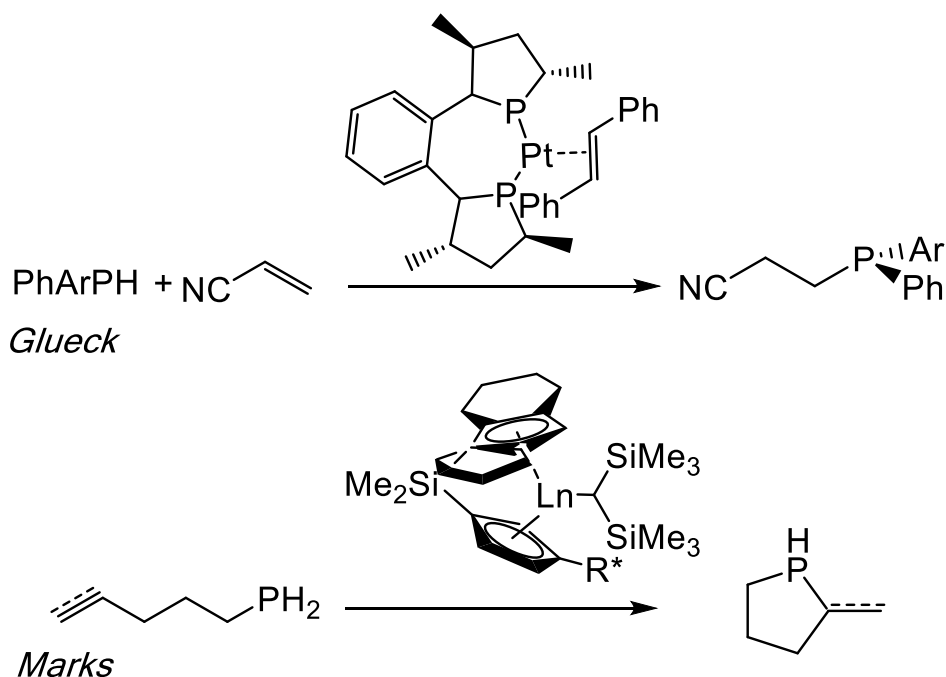
**Scheme 1.2:** Hydrophosphination to selectively generate phosphines

This reaction may be considered a mature transformation as metal-catalyzed hydrophosphination was reported almost 25 years ago,<sup>8</sup> and spontaneous and radical additions of P–H bond to unsaturated substrates are decades older than that.<sup>7</sup> Catalytic hydrophosphination was first explored by Pringle's group using phosphine for the hydrophosphination of a handful of electron-rich substrates to make tertiary phosphines using simple platinum salts (Scheme 1.3).<sup>8</sup>



**Scheme 1.3:** Hydrophosphination of  $\text{PH}_3$  catalyzed by various Pt salts

After Pringle's seminal report early reports of catalytic hydrophosphination came from both Mark's<sup>9</sup> and Glueck's<sup>10</sup> research groups (Scheme 1.4).



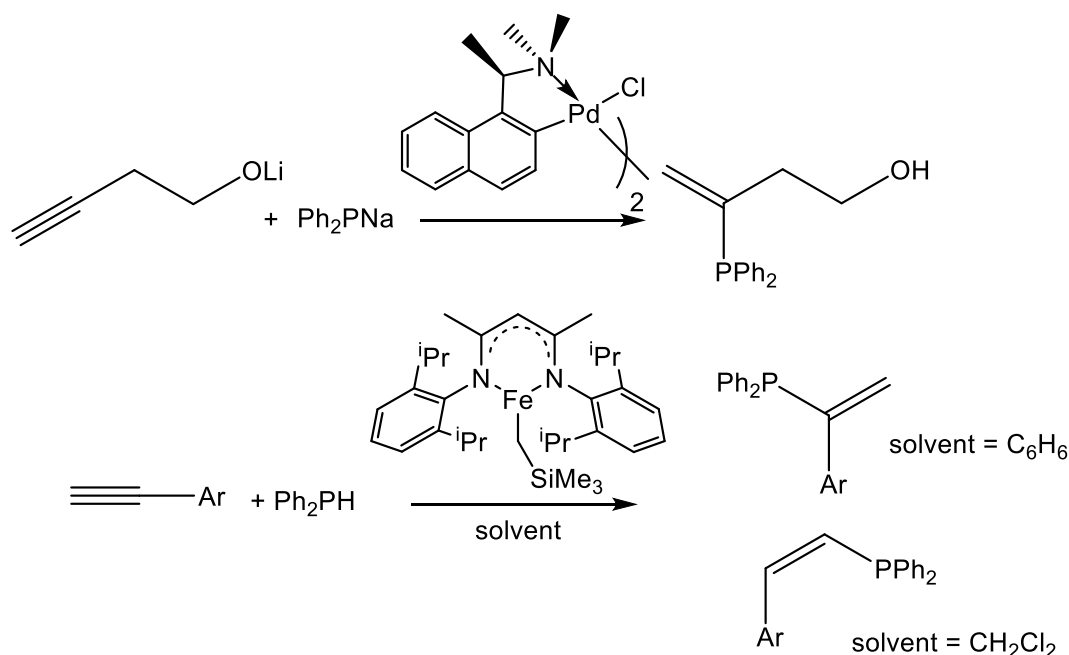
**Scheme 1.4:** Early examples of hydrophosphination catalysts

Glueck's platinum catalyst used secondary phosphines to provide either *P*- or *C*-chiral hydrophosphination products. Marks's lanthanide catalyst performed an intramolecular hydrophosphination reaction on alkenyl or alkynyl phosphines to make cyclic phosphines.

After these initial reports metal catalyzed hydrophosphination has grown substantially. The family of catalysts capable of this transformation has expanded to include more earth-abundant metals, products are formed with increasingly impressive enantioselectivities,<sup>11</sup> and the mechanistic understandings of these catalytic systems is being unearthed.<sup>5</sup>

However, there is much work to be done in metal-catalyzed hydrophosphination. The current set of challenges that drive the field come in three distinct areas: catalyst, substrate, and selectivity. Selectivity is at the core of metal-catalyzed hydrophosphination. Chemists are keenly aware of the limitations of resources, including phosphorus,<sup>12</sup> and the use of more earth-abundant and sustainable catalysts to efficiently utilize the limited phosphorus feedstock is of critical long-term importance.

Catalytic hydrophosphination to *selectively* generate phosphine products is an ongoing challenge. The selectivity issue generally spans three regions: regioselectivity, chemoselectivity of P–H bonds, and stereoselectivity (Scheme 1.2). Modern hydrophosphination catalysts almost always select for the anti-Markovnikov hydrophosphination product, often with perfect selectivity. Thermally induced hydrophosphination with secondary<sup>13-14</sup> and primary phosphines<sup>14</sup> also provides nearly perfect anti-Markovnikov selectivity. Metal catalysts that prefer Markovnikov products are rare, and restricted to only a handful of examples (Scheme 1.5).<sup>15-17</sup>

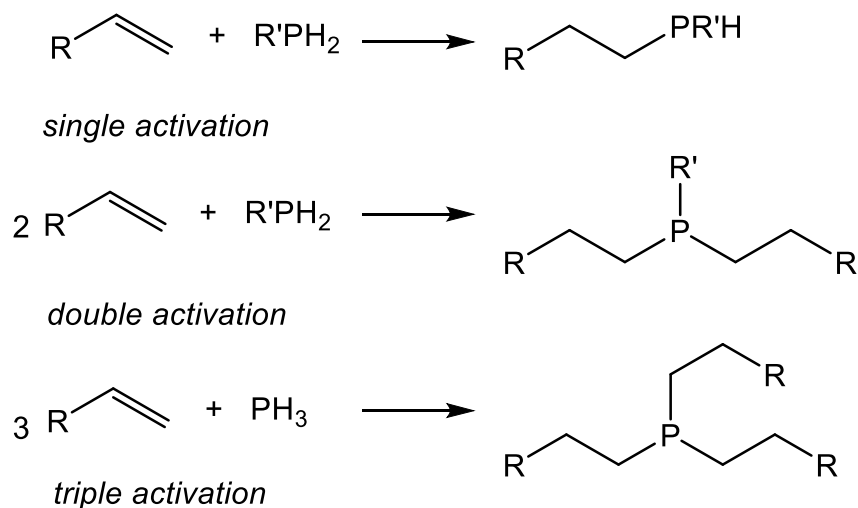


**Scheme 1.5:** Metal catalysts capable of Markovnikov selectivity in hydrophosphination

While researchers appear to have perfected anti-Markovnikov addition, this was not necessarily achieved through design. A handful of iron-based systems have been identified for their ability to switch preferences. For example, hydrophosphination of styrene substrates with  $\text{FeCl}_2$  and  $\text{FeCl}_3$  provide anti-Markovnikov and Markovnikov products, respectively. A  $\beta$ -diketiminato iron compound was found to prefer anti-Markovnikov products when catalysis was performed in DCM and Markovnikov products when catalysis was performed in benzene.<sup>18</sup> The authors postulate that Markovnikov selectivity is a radical-mediated process, whereas the anti-Markovnikov selectivity is due to a change in oxidation state.

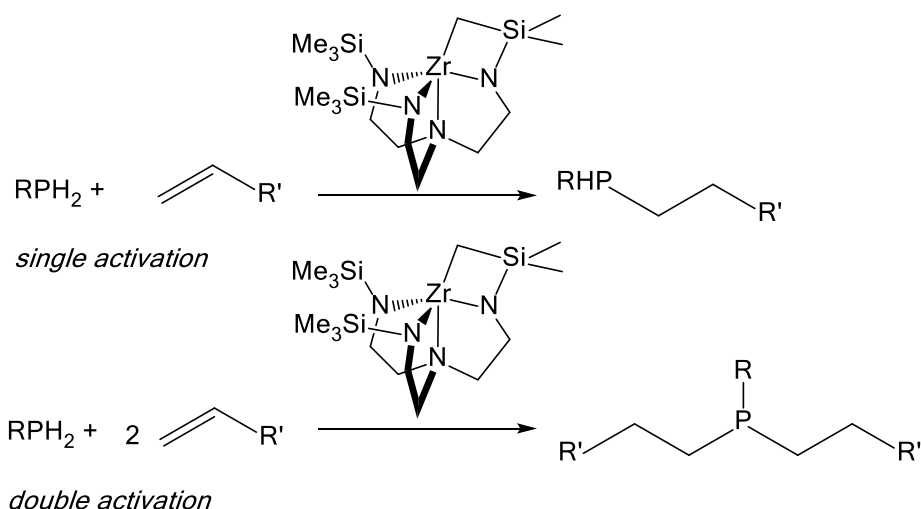
The addition of a secondary phosphine (i.e.,  $\text{R}_2\text{PH}$ ) across a double-bonded substrate (e.g., an alkene) presents no challenge in chemoselectivity. However, other substrates that may be activated more than once in the catalysis, such as primary

phosphines and  $\text{PH}_3$  are not as straightforward. Despite some early successes, primary phosphines have been largely absent as substrates in this catalysis until recently.<sup>19-33</sup> These substrates can add a single P–H equivalent to form a secondary phosphine product or both P–H bonds can be activated to give a tertiary product. (Scheme 1.6).



**Scheme 1.6:** Single, double, and triple activation of primary phosphines and  $\text{PH}_3$

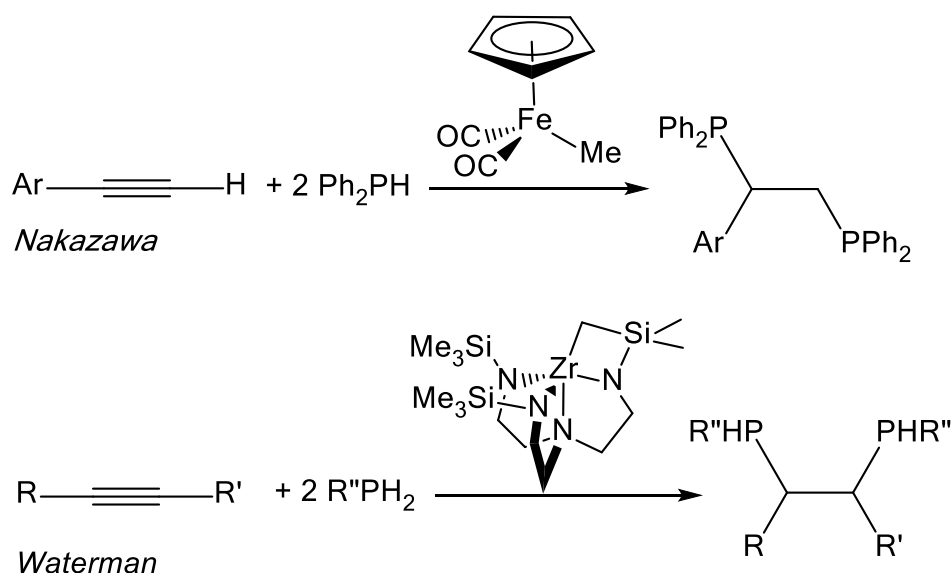
The terms single and double activation will be used for the former and latter transformation, respectively, to distinguish from the addition of two P–H equivalents on a single unsaturated substrate (q.v. double hydrophosphination). Selectivity for the secondary phosphine product is particularly attractive due to the potential for further functionalization at the P–H bond. The resurgence of interest in primary phosphine substrates came with our report of zirconium-catalyzed hydrophosphination of alkenes.<sup>32</sup> In that work it was demonstrated that the double activation of primary phosphines provides tertiary products. What was important in this example is that the single activation event was more facile, which resulted in secondary phosphine products that are isolable in good to excellent yields (Scheme 1.7).



**Scheme 1.7:** Zirconium-catalyzed single or double activation of alkenes with primary phosphines<sup>32</sup>

Because the single activation product is more encumbered than the primary phosphine substrate, it is reasonable to anticipate that steric factors would govern the chemoselectivity in these reactions. However, P–C bond formation following the single activation event may provide a more reactive P–H bond in the secondary phosphine. Catalysts that are highly reactive toward P–H bonds, regardless of steric factors, may significantly erode a selectivity for the single activation event.<sup>5</sup>

The addition of two P–H equivalents across a single substrate such as an alkyne (i.e., double hydrophosphination) is a simple, direct route to 1,2-bis(phosphino)ethanes, which is well-utilized class of ligands. In 2012 Nakazawa reported the first example of this transformation, which was catalyzed by simple iron derivatives with terminal alkynes and  $\text{Ph}_2\text{PH}$  (Scheme 1.8).<sup>34</sup>

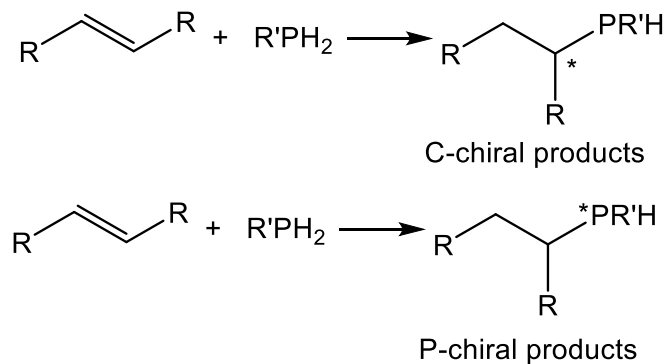


**Scheme 1.8:** Seminal reports of catalytic double hydrophosphination of alkynes with secondary<sup>35-36</sup> and primary phosphines<sup>37</sup>

This is clearly a rare and challenging reaction. No subsequent reports had surfaced until 2016. Nakazawa followed on that iron chemistry to demonstrate selective single hydrophosphination of alkynes followed by a second hydrophosphination event to afford unsymmetrical derivatives.<sup>38</sup> Examples of rhodium,<sup>36</sup> copper,<sup>39</sup> and samarium systems<sup>40-41</sup> for double hydrophosphination utilizing  $\text{Ph}_2\text{PH}$  have emerged. Waterman found that a simple, commercially available, bench-stable iron catalyst is also capable of providing double hydrophosphination reactivity with secondary phosphines and terminal alkynes. In all cases, only 1,2-addition products have been observed.

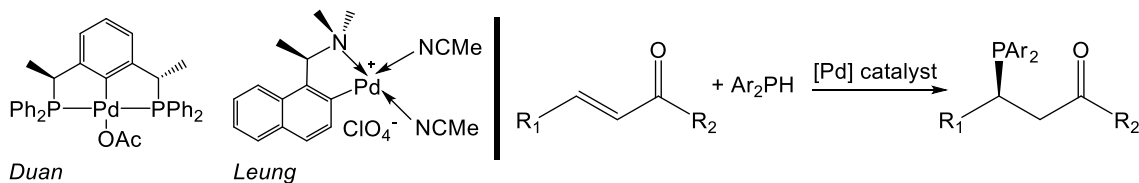
All current examples of double hydrophosphination are specific for terminal, aryl-substituted alkynes. We reported that zirconium catalysts perform the double hydrophosphination of *internal* alkynes.<sup>37</sup> This chemistry was the first to feature primary phosphine substrates that selectively generate secondary phosphine products, which were absent in previous reports.

Metal-catalyzed *asymmetric* hydrophosphination is an immensely desirable transformation with enormous potential to generate *P*-chiral and *C*-chiral phosphine products (Scheme 1.9). The ability of catalytic hydrophosphination to provide stereoselective product formation is of intense value to the chemical community, but this transformation remains quite challenging.



**Scheme 1.9:** Asymmetric hydrophosphination to produce *P*- or *C*-chiral phosphines

Leung, Pullarkat, and Duan have extensively studied the development of palladium-catalyzed hydrophosphination to generate *C*-chiral phosphine products.<sup>11</sup> A report from Leung<sup>42</sup> appeared almost simultaneously with one from Duan and coworkers<sup>43</sup> for the hydrophosphination of enones with secondary phosphines using palladium catalysts to achieve ee values of up to 99% (Scheme 1.10).



**Scheme 1.10:** Examples of palladium-catalyzed asymmetric hydrophosphination to generate *C*-chiral phosphines

Installation of a chiral center at carbon has been highly successful for these systems.

Examples in this area have repeatedly demonstrated ee values of 99% for late transition-



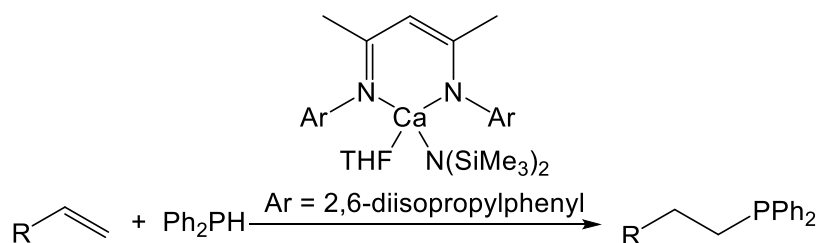
metal catalysts with secondary phosphines.<sup>11</sup> This chemistry has not yet been developed for unactivated substrates, primary phosphines, or metals other than palladium. Some of these limitations may be due in part to the consistently low temperatures (i.e.,  $< -25\text{ }^{\circ}\text{C}$ ) required to achieve high ee values.<sup>11</sup> High ee values have only been reported for unactivated substrates where enones,<sup>42, 44-51</sup> bis(enones),<sup>46, 52</sup> ketimines,<sup>53</sup> and sulfonic esters,<sup>54</sup> achieve ee values of greater than 95%. Values of this magnitude have yet to be seen for other substrates. Asymmetric hydrophosphination of electron-poor alkenes and alkynes has a high watermark of 42% ee at phosphorus,<sup>55</sup> demonstrating the reliance on electron-donating substituents for these transformations.<sup>56</sup> Expansion of this type of hydrophosphination reactivity to more substrates is, as yet, unrealized.

Early investigation of hydrophosphination catalysis centered on coinage metals and lanthanides.<sup>11, 56-57</sup> Despite the dominance of these metals in the reaction, there has been a dramatic increase in the diversity of catalysts used in this transformation over the last decade.

Limitations on the supply of coinage metals will, eventually, impact the ability to use these metals in catalysis. Iron is an attractive catalyst for hydrophosphination because it is both electron-rich and earth abundant, and work with iron has already demonstrated a wide breadth of reactivity.<sup>14, 17, 28, 35, 38, 58-63</sup> For example, oxo-bridged dimers have shown good reactivity and selectivity in the hydrophosphination of styrene derivatives. These catalysts can readily perform single or double activation reactions with primary phosphine substrates to give secondary or tertiary products in modest to excellent yields.<sup>14</sup> Iron has been at the fore of new reactivities including selective single and double

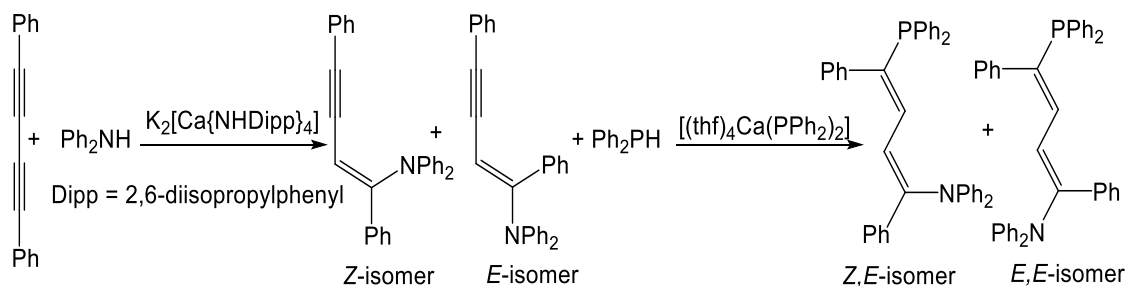
hydrophosphination of alkynes (*vide supra*)<sup>35, 38</sup> and selective, tunable Markovnikov- or anti-Markovnikov catalysis (Scheme 1.5).<sup>17</sup> An recently reported iron compound was found to be the first and only catalyst capable of isocyanate hydrophosphination.<sup>64</sup> Waterman also found that a simple commercially-available iron compound catalyzes the hydrophosphination of styrene derivatives with secondary phosphines at ambient temperature (*vide supra*).<sup>65</sup> This example allows for hydrophosphination products to be obtained from a readily-available, bench-stable iron catalyst. Naturally, these catalysts have not yet matured to the levels of other late metal hydrophosphination catalysts, but their resurgence suggests that more is to come.

Alkaline earth elements are good candidates for sustainable hydrophosphination catalysts. Indeed, a family of calcium catalysts has demonstrated proclivity for the reaction.<sup>66-74</sup> Hill has reported the hydrophosphination of alkenes, alkynes and carbodiimides with  $\beta$ -diketiminato calcium complexes.<sup>69-70</sup> Mechanistic investigation reveals a reliance on  $\sigma$ -bond metathesis for P–H bond activation, similar to  $d^0$  transition-metal and lanthanide catalysts (Scheme 1.11).<sup>69</sup>



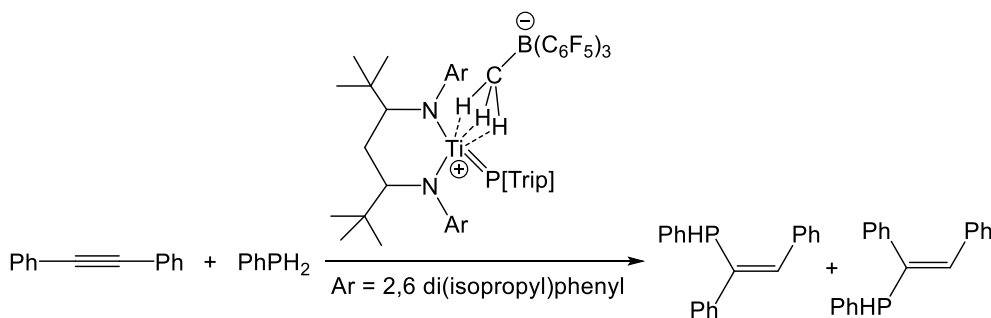
**Scheme 1.11:** Calcium-catalyzed hydrophosphination with  $\text{Ph}_2\text{PH}$

More recently, Westerhausen has demonstrated that calcium catalysts can stereoselectively catalyze the hydrophosphination of hydroaminated diynes, which are under-explored substrates in hydrophosphination (Scheme 1.12).<sup>73</sup>



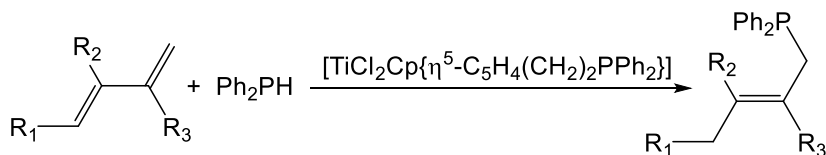
**Scheme 1.12:** Calcium-catalyzed hydrophosphination of diynes

Early-transition metals, which are often abundant and underutilized in homogenous catalysis, have grown in their own right as hydrophosphination catalysts.<sup>26, 32-33, 75-78</sup> In 2006, Mindiola reported the single hydrophosphination of diphenylacetylene with  $\text{PhPH}_2$ ,<sup>77</sup> which is unique because of the participation of a terminal phosphinidene ligand in the catalysis and the uncommon [2+2] cycloaddition (Scheme 1.13).



**Scheme 1.13:** Mindiola's titanium-catalyzed hydrophosphination with  $\text{PhPH}_2$

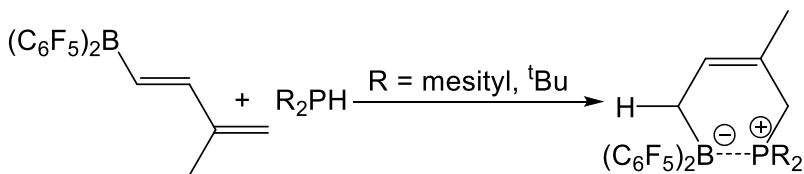
Since then, examples of early-metal catalysts capable of hydrophosphination have grown. Le Gendre demonstrated that simple titanium derivatives are capable diene hydrophosphination to give exclusively the 1,4-addition product (Scheme 1.14).<sup>76</sup>



**Scheme 1.14:** Titanium-catalyzed hydrophosphination of a conjugated diene

It is worth noting that our triamidoamide-ligated zirconium complex has shown to readily engage in hydrophosphination under mild conditions with both primary and secondary phosphines to selectively generate either secondary or tertiary product phosphines, depending on modification of the selective reaction conditions (Scheme 1.7).<sup>32-33, 78</sup>

P-block and non-metals have been emergent in the field of catalysis, and these only have room for growth in hydrophosphination catalysis. Frustrated Lewis Pair (FLP) hydrophosphination has only been reported as a stoichiometric process (Scheme 1.15),<sup>23, 79-81</sup> but recent DFT calculations suggests that FLPs may be able to act as hydrophosphination catalysts.<sup>82</sup>



**Scheme 1.15:** Stoichiometric hydrophosphination with an FLP

Catalytic FLP hydrophosphination is currently an uncharted area with much promise for development, but catalytic main-group hydrophosphination is already gaining ground.<sup>19, 30</sup> Preliminary studies of tin-catalyzed hydrophosphination with  $PhPH_2$  has demonstrated modest conversion to hydrophosphination products for classic substrates like phenylacetylene and styrene.<sup>19</sup> Catalytic hydrophosphination with these species appears not to be driven not by the Lewis acidity of the tin, highlighting an important distinction between those systems and stoichiometric FLP chemistry.

Investigation of lanthanide catalysts for hydrophosphination originates with seminal intramolecular examples from Marks and coworkers.<sup>9, 83</sup> Intermolecular

hydrophosphination using  $\text{Ph}_2\text{PH}$  with lanthanide catalysts has an impressive substrate scope. This category of catalysts has functionalized heterocumulenes,<sup>39, 84</sup> imines,<sup>40, 85-87</sup> enynes,<sup>88</sup> dienes,<sup>41, 71, 87, 89</sup> and allenes.<sup>87</sup> Examples of rare-earth catalysis with primary phosphines is growing.<sup>9, 21, 26-27, 90-91</sup> Samarium compounds have their own unique claims in hydrophosphination, with some of the first examples of hydrophosphination/cyclizations,<sup>9, 88, 92</sup> and an uncommon carbene and diyne hydrophosphination (Scheme 1.12).<sup>86</sup> Ytterbium compounds have a rich history as hydrophosphination catalysts, and among this family are rare examples of heterocumulene<sup>39</sup> and alkyne hydrophosphination catalysts.<sup>41, 71, 85-87, 89</sup> A thorium compound was found to be able to perform a single intermolecular hydrophosphination reaction on two alkynes,<sup>93</sup> and a samarium compound was found to be a double hydrophosphination catalyst for imines.<sup>40</sup> A recent report of a cerium-hydride metal-organic framework (MOF) was found to be able to catalyze the hydrophosphination of unactivated alkenes.<sup>94</sup> The breadth of substrates that have been addressed with lanthanide catalysts demonstrates their success as hydrophosphination catalysts, and the more recent reports of these transformations suggests that they have yet more to offer.

Secondary phosphines are ubiquitous in metal-catalyzed hydrophosphination, and divergence from the canonical  $\text{Ph}_2\text{PH}$  substrate is relatively rare, which provides little information on electronic factors at phosphorus. Development of metal-catalyzed hydrophosphination of primary phosphines to generate secondary phosphines has lagged behind,<sup>32-33</sup> partially due to the challenge of selective formation of secondary or tertiary phosphine products (Scheme 1.1). Other factors, such as the greater acidity of P–H protons

of primary phosphines or the scarcer commercial availability of these substrates may be culpable. Following early successes from Glueck and Mindiola, metal-catalyzed primary phosphine hydrophosphination has seen a reemergence over the past two years.<sup>19-33</sup>

Despite being the phosphorus substrate used in Pringle's initial hydrophosphination work,<sup>8</sup> catalytic hydrophosphination with phosphine ( $\text{PH}_3$ ) has been developed only for three, electron-rich substrates (Scheme 1.3).<sup>8, 95-97</sup> So far hydrophosphination of common alkenes and alkynes with  $\text{PH}_3$  is not yet realized, but offers considerable potential in the synthesis of primary and secondary phosphine products. To date, there has not yet been a hydrophosphination reaction involving  $\text{PH}_3$  that offers selective formation of primary or secondary hydrophosphination products. Such a transformation would prove useful for a variety of designer organophosphines, but is doubtlessly stymied by the reluctance to work with  $\text{PH}_3$ .

Hydrophosphination has been well-developed for activated substrates, particularly electron-deficient alkenes, which leaves unactivated substrates are underrepresented in hydrophosphination.<sup>25, 32-33, 69, 85, 92, 94, 98</sup> Indeed, the most successful asymmetric hydrophosphination catalysis occurs with activated alkene substrates.<sup>11</sup> The factors that allow for functionalization of unactivated alkenes are not well-understood.

Metal compounds that can catalyze the hydrophosphination of alkynes are relatively rare, but growing.<sup>34-35, 71, 89, 92-93, 99-102</sup> Alkynes reported in this catalysis are generally limited to terminal alkynes, and in all cases the phosphine substrate is a secondary phosphine. Reports of hydrophosphination catalysts that selectively generate vinyl phosphine products are of considerable interest, such as ours,<sup>37</sup> and two related ones.<sup>38, 93</sup>

Only five catalysts are known that can perform a double hydrophosphination reaction of an alkyne substrates.<sup>35-37, 40-41</sup> Other substrates featuring triple bonds, such as isocyanates<sup>64</sup> diynes<sup>73, 86</sup> and enynes<sup>83,84,86,98</sup> are even less common in hydrophosphination reactions, despite their greater reactivity than alkenes.

### 1.3 Mechanistic understandings of metal-catalyzed hydrophosphination

Mechanistic aspects of hydrophosphination have been explored in-depth recently.<sup>5</sup> Late transition-metal hydrophosphination catalysts tend to work only for activated substrates with electron-withdrawing groups. These systems often employ a base as a co-catalyst, and many proceed through some degree of nucleophilic attack from the metal phosphide, hence the need for activated substrates, particularly Michael acceptors. Rosenberg summarized two general outer-sphere mechanisms for these late-metal processes. One pathway involves metal bonding to the substrate, either directly or indirectly, preceding nucleophilic attack from the free phosphine. The second, more common route is formation of a nucleophilic metal-phosphide, followed by nucleophilic attack of the phosphide to the electropositive carbon center.<sup>5</sup> Leung and Pullarkat exploited the latter mechanism in the catalytic asymmetric hydrophosphination to generate *C*-chiral phosphines.

Early metal hydrophosphination typically proceeds via inner-sphere hydrophosphination from metal-phosphido intermediates, as is the case for our system. The metal-phosphides formed in these examples are sufficiently strong enough to functionalize phosphines,<sup>103-106</sup> either by nucleophilic attack or by insertion-based mechanisms. Early-metal and other  $d^0$  metal hydrophosphination catalysts do not require basic-cocatalysts to

proceed and are the only ones capable of hydrophosphination of unactivated alkenes and alkynes.<sup>5</sup> However, there are no examples of  $d^0$  metal catalysts capable of asymmetric hydrophosphination to form *P*- or *C*-chiral phosphine products, despite the apparent plausibility of the transformation. That is, the metal-phosphides formed during catalysis should be activated enough such that substrate insertion proceeds in a specific orientation to provide asymmetric products.

Mechanistic understanding of all hydrophosphination systems is not yet fully understood, despite significant efforts from a handful of research groups.<sup>5</sup> For example, Leung and Pullarkat's palladium-catalyzed enantioselective hydrophosphination catalysts are well-explored. These authors have been able to fine-tune their system for increasingly high enantiomeric excesses. Glueck's catalyst families have been considered for their unique outer-sphere mechanisms, and Mark's lanthanide catalysts have been investigated computationally. Operations of early metal systems, like ours, are not well understood. Furthermore, most mechanistic understandings come from the perspective of bond-formation of the phosphines and the substrates, rather than from the perspective of the catalyst. Physical details of these systems, such as electronic structural details, are scarcely explored. Besides the radical-mediated processes, light-dependent hydrophosphination remains scarcely explored.

Understanding the role of light in our system would offer an advantageous platform for further developments. Our catalyst is impressive and unique in several regards. It is one of the (still) rare primary phosphine hydrophosphination catalysts and one of the few that can successfully form bonds with unactivated substrates, and it does so under mild



conditions. It is one of only a handful of double hydrophosphination catalysts and the only catalyst capable of a double hydrophosphination reaction involving primary phosphines and/or internal alkynes. Its special features are only activated under light, making it exceptional in the hydrophosphination catalyst family. A deeper understanding of just that interaction would be of stand-alone interest, but it also would open the doors for further development. For example, light activation allows for increasingly larger primary phosphines to participate in P–C bond formation, which expands the limited field of primary phosphine hydrophosphination.

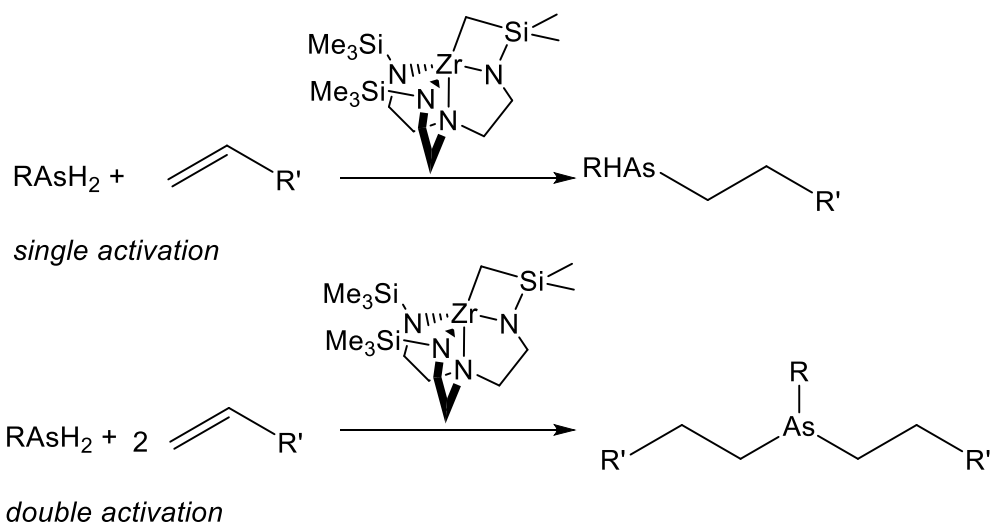
Entirely lacking in  $d^0$  metal catalysts are enantioselective ones. Marriage of both primary phosphine and potentially enantioselective features would offer an unprecedented platform to secondary P-chiral phosphines that could be functionalized to P-chiral tertiary phosphines by either conventional methods or by our catalyst. Very little is understood about the mechanisms of double hydrophosphination catalysts, and understanding of this process would allow expansion of this nascent field. Regardless, further exploration of the operational aspects of our catalyst, either on its own or under catalytic hydrophosphination, is intriguing.

## 1.4 Hydroarsination

While hydrophosphination is a developing field, hydroarsination is scarcely explored. Organoarsenic chemistry has found applications in a vast number of transformations, including chemistry,<sup>107-111</sup> materials science,<sup>112</sup> and anti-cancer agents.<sup>113</sup> Arsenic chemistry is still developing,<sup>107</sup> but a notable achievement is arsenic-based ligands. Some triarylarsine ligands have outperformed phosphorus analogues.<sup>113-116</sup>

Arsenic has a well-deserved historical reputation for its toxicity, particularly arsine oxides and compounds with As–Cl bonds.<sup>107</sup> Development of arsenic chemistry that circumvents usage of As–Cl compounds would advance arsenic bond-forming chemistry. One route is through hydroarsination. Like hydrophosphination, hydroarsination proceeds through the atom-economical addition of As–H across an unsaturated fragment to generate a new arsine. Examples of catalytic hydroarsination are quite limited in number.<sup>108-109, 111, 117-123</sup> All transformations functionalize either secondary arsines, or in one case an arsenylborane.<sup>119</sup>

Previous work in the Waterman group on hydroarsination has targeted bond-forming reactions of terminal alkynes and secondary arsines to provide tertiary arsines in limited yields. Given the nascent understanding of the light-dependence of this catalyst during hydrophosphination, further consideration of hydroarsination is warranted. For example, hydroarsination of primary arsines to selectively generate either secondary or tertiary arsines would be of interest (Scheme 1.16).



**Scheme 1.16:** Potential catalytic hydroarsination reactions with primary arsines

Efforts to investigate and develop hydroarsination would prove useful for the synthesis of organoarsenic compounds. Preliminary results have shown that catalysis behaves differently for hydroarsination than hydrophosphination<sup>119, 122, 124</sup> so exciting chemistry could be in store!

## 1.5 Conclusions

Greater development of earth-abundant catalysts featuring metals like zirconium is needed, particularly those that afford products with stereoselectivity. The substrate scope for stereoselective hydrophosphination must be expanded, and mechanistic understanding of how metal catalysts operate could be improved upon.

While many unsaturated substrates have been investigated, substantial gaps remain. Most prominent is the lack of unactivated substrates (e.g., alkenes); however, hydrophosphination of some functionalities is simply unknown. The nature of the phosphine substrate can be expanded as well. Only recently have air-stable primary phosphine derivatives been employed.<sup>33, 125</sup> Likewise, hydrophosphination of using sterically encumbered phosphines has been underreported.<sup>33, 126</sup> Examples of catalytic hydrophosphination to generate secondary *P*- and *C*-chiral phosphine products would be of great interest, and it appears that a  $d^0$  metal catalyst could be well-suited for this transformation. Investigation of hydroarsination may prove exciting, given preliminary results.

The growth of metal-catalyzed hydrophosphination has identified many successes, but also many gaps. Maturation and development of this field offers undeniable ease to

many attractive organophosphorus compounds. A key success to metal-catalyzed hydrophosphination lies in uncovering mechanistic aspects of this transformation.

The work presented in this dissertation aims to address these challenges with **1** (Scheme 1.7). Primary phosphine hydrophosphination is realized for a large variety of both alkenes and primary phosphines. This work was the first to feature unactivated alkenes, primary phosphines, and selective formation of either secondary or tertiary phosphine products, depending on reaction conditions. Given the success of unactivated alkenes in catalytic hydrophosphination with **1**, catalytic sequential intermolecular and intramolecular hydrophosphination of dienes to make phosphacycles is explored. Furthermore, attempts at making a chiral ligand variant for **1** for catalytic asymmetric hydrophosphination are discussed. Elaboration of hydroelementation with **1** to primary arsines is presented. Preliminary results on catalytic hydroarsination with primary arsines reveals similarities, but also some divergence from catalytic hydrophosphination.

Catalytic *double* hydrophosphination of internal alkynes with primary phosphines was realized with **1**. At the time of publication this was one of the first examples of this type of reactivity, and the first to feature both primary phosphines and internal alkynes. That work closed the gap on substrates and phosphines for this reaction.

The most surprising secret of catalytic hydrophosphination with **1** revealed itself during the double hydrophosphination with alkynes. Catalytic hydrophosphination with **1** requires visible light for catalysis. This led to an investigation into the light-dependent behavior of **1** for a variety of phosphines and alkenes. Transformations that were previously inaccessible became possible and the substrate scope expanded to include a family of

primary phosphines and underreported substrates. The improvement of irradiation was substantial. For example, catalytic hydrophosphination with styrene proceeds with a TON = 18 and TOF = 1.5 h<sup>-1</sup> in the absence of direct irradiation. Direct irradiation of the same reaction with ultraviolet light substantially enhanced catalysis (TON = 20 and TOF = 60 h<sup>-1</sup>). Catalytic hydrophosphination with **1** seemed indifferent to heat, which made it both rare and intriguing. Identification of an earth-abundant metal catalyst that can achieve these conversions without impetus from heat or other reagents was impressive, and suggests that hydrophosphination could advance to address the challenges in sustainable phosphorus chemistry.

## 1.6 References

- (1) Corbridge, D. E. C., *Phosphorus: Chemistry, Biochemistry, and Technology*. 6 ed.; CRC Press: Boca Raton, Florida, 2013; p 1473.
- (2) Troev, K. D., *Reactivity of P-H Group of Phosphorus Based Compounds*. Academic Press: London, 2017.
- (3) Fleming, J. T.; Higham, L. J., *Coord. Chem. Rev.* **2015**, 297–298, 127-145.
- (4) Cordell, D.; White, S., *Sustainability* **2011**, 3, 2027.
- (5) Rosenberg, L., *ACS Catal.* **2013**, 3, 2845-2855.
- (6) Bange, C. A.; Waterman, R., *Chem. Eur. J.* **2016**, 22, 12598-12605.
- (7) Reuter, M.; Orthner, L. Trihydroxymethylphosphine. DE1035135, 1958.
- (8) Pringle, P. G.; Smith, M. B., *J. Chem. Soc., Chem. Commun.* **1990**, 1701-1702.
- (9) Douglass, M. R.; Marks, T. J., *J. Am. Chem. Soc.* **2000**, 122, 1824-1825.

- (10) Wicht, D. K.; Kourkine, I. V.; Kovacik, I.; Glueck, D. S.; Concolino, T. E.; Yap, G. P. A.; Incarvito, C. D.; Rheingold, A. L., *Organometallics* **1999**, *18*, 5381-5394.
- (11) Pullarkat, S. A., *Synthesis* **2016**, *48*, 493-503.
- (12) Nakamura, E.; Sato, K., *Nat. Mater.* **2011**, *10*, 158-161.
- (13) Moglie, Y.; Gonzalez-Soria, M. J.; Martin-Garcia, I.; Radivoy, G.; Alonso, F., *Green Chem.* **2016**, *18*, 4896-4907.
- (14) Gallagher, K. J.; Espinal-Viguri, M.; Mahon, M. F.; Webster, R. L., *Adv. Synth. Catal.* **2016**, *358*, 2460-2468.
- (15) Pullarkat, S. A.; Yi, D.; Li, Y.; Tan, G.-K.; Leung, P.-H., *Inorg. Chem.* **2006**, *45*, 7455-7463.
- (16) Mimeau, D.; Gaumont, A.-C., *J. O. C.* **2003**, *68*, 7016-7022.
- (17) Routaboul, L.; Toulgoat, F.; Gatignol, J.; Lohier, J.-F.; Norah, B.; Delacroix, O.; Alayrac, C.; Taillefer, M.; Gaumont, A.-C., *Chem. Eur. J.* **2013**, *19*, 8760-8764.
- (18) King, A. K.; Gallagher, K. J.; Mahon, M. F.; Webster, R. L., *Chem. Eur. J.* **2017**, *23*, 9039-9043.
- (19) Erickson, K. A.; Dixon, L. S. H.; Wright, D. S.; Waterman, R., *Inorg. Chim. Acta* **2014**, *422*, 141-145.
- (20) Isley, N. A.; Linstadt, R. T. H.; Slack, E. D.; Lipshutz, B. H., *Dalton Trans.* **2014**, *43*, 13196-13200.
- (21) Basalov, I. V.; Dorcet, V.; Fukin, G. K.; Carpentier, J.-F.; Sarazin, Y.; Trifonov, A. A., *Chem. Eur. J.* **2015**, *21*, 6033-6036.

- (22) Belli, R. G.; Burton, K. M. E.; Rufh, S. A.; McDonald, R.; Rosenberg, L., *Organometallics* **2015**, *34*, 5637-5646.
- (23) Chen, G.-Q.; Kehr, G.; Daniliuc, C. G.; Wibbeling, B.; Erker, G., *Chem. Eur. J.* **2015**, *21*, 12449-12455.
- (24) Erickson, K. A.; Stelmach, J. P. W.; Mucha, N. T.; Waterman, R., *Organometallics* **2015**, *34*, 4693-4699.
- (25) Geer, A. M.; Serrano, A. L.; de Bruin, B.; Ciriano, M. A.; Tejel, C., *Angew. Chem. Int. Ed.* **2015**, *54*, 472-475.
- (26) Kissel, A. A.; Mahrova, T. V.; Lyubov, D. M.; Cherkasov, A. V.; Fukin, G. K.; Trifonov, A. A.; Del Rosal, I.; Maron, L., *Dalton Trans.* **2015**, *44*, 12137-12148.
- (27) Basalov, I. V.; Yurova, O. S.; Cherkasov, A. V.; Fukin, G. K.; Trifonov, A. A., *Inorg. Chem.* **2016**, *55*, 1236-1244.
- (28) Pritzwald-Stegmann, J. R. F.; Loennecke, P.; Hey-Hawkins, E., *Dalton Trans.* **2016**, *45*, 2208-2217.
- (29) Serrano, A. L.; Casado, M. A.; Ciriano, M. A.; de Bruin, B.; Lopez, J. A.; Tejel, C., *Inorg. Chem.* **2016**, *55*, 828-839.
- (30) Stelmach, J. P.; Bange, C. A.; Waterman, R., *Dalton Trans.* **2016**, *45*, 6204-6209.
- (31) Yao, W.; Ma, M.; Zhang, N.; Li, Y.; Pullarkat, S. A.; Leung, P.-H., *J. Organomet. Chem.* **2016**, *801*, 1-5.
- (32) Ghebreab, M. B.; Bange, C. A.; Waterman, R., *J. Am. Chem. Soc.* **2014**, *136*, 9240-9243.

- (33) Bange, C. A.; Ghebreab, M. B.; Ficks, A.; Mucha, N. T.; Higham, L.; Waterman, R., *Dalton Trans.* **2016**, 45, 1863-1867.
- (34) Itazaki, M.; Katsube, S.; Kamitani, M.; Nakazawa, H., *Chem Commun.* **2016**, 52, 3163-3166.
- (35) Kamitani, M.; Itazaki, M.; Tamiya, C.; Nakazawa, H., *J. Am. Chem. Soc.* **2012**, 134, 11932-11935.
- (36) Di Giuseppe, A.; De Luca, R.; Castarlenas, R.; Perez-Torrente, J. J. J.; Crucianelli, M.; Oro, L. A., *Chemical Commun.* **2016**, 52, 5554-5557.
- (37) Bange, C. A.; Waterman, R., *ACS Catal.* **2016**, 6, 6413-6416.
- (38) Itazaki, M.; Katsube, S.; Kamitani, M.; Nakazawa, H., *Chem. Commun.* **2016**, 52, 3163-3166.
- (39) Gu, X.; Zhang, L.; Zhu, X.; Wang, S.; Zhou, S.; Wei, Y.; Zhang, G.; Mu, X.; Huang, Z.; Hong, D.; Zhang, F., *Organometallics* **2015**, 34, 4553-4559.
- (40) Li, J.; Lamsfus, C. A.; Song, C.; Liu, J.; Fan, G.; Maron, L.; Cui, C., *ChemCatChem* **2017**, 9, 1368-1372.
- (41) Yuan, J.; Hu, H.; Cui, C., *Chem. Eur. J.* **2016**, 22, 5778-5785.
- (42) Huang, Y.; Pullarkat, S. A.; Li, Y.; Leung, P.-H., *Chem. Commun.* **2010**, 46, 6950-6952.
- (43) Feng, J.-J.; Chen, X.-F.; Shi, M.; Duan, W.-L., *J. Am. Chem. Soc.* **2010**, 132, 5562-5563.
- (44) Yang, M.-J.; Liu, Y.-J.; Gong, J.-F.; Song, M.-P., *Organometallics* **2011**, 30, 3793-3803.



- (45) Huang, Y.; Pullarkat, S. A.; Li, Y.; Leung, P.-H., *Inorg. Chem.* **2012**, *51*, 2533-2540.
- (46) Huang, Y.; Pullarkat, S. A.; Teong, S.; Chew, R. J.; Li, Y.; Leung, P.-H., *Organometallics* **2012**, *31*, 4871-4875.
- (47) Chew, R. J.; Teo, K. Y.; Huang, Y.; Li, B.-B.; Li, Y.; Pullarkat, S. A.; Leung, P.-H., *Chem. Commun.* **2014**, *50*, 8768-8770.
- (48) Gan, K.; Sadeer, A.; Xu, C.; Li, Y.; Pullarkat, S. A., *Organometallics* **2014**, *33*, 5074-5076.
- (49) Hao, X.-Q.; Huang, J.-J.; Wang, T.; Lv, J.; Gong, J.-F.; Song, M.-P., *J. Org. Chem.* **2014**, *79*, 9512-9530.
- (50) Hao, X.-Q.; Zhao, Y.-W.; Yang, J.-J.; Niu, J.-L.; Gong, J.-F.; Song, M.-P., *Organometallics* **2014**, *33*, 1801-1811.
- (51) Yang, X.-Y.; Tay, W. S.; Li, Y.; Pullarkat, S. A.; Leung, P.-H., *Organometallics* **2015**, *34*, 5196-5201.
- (52) Huang, Y.; Chew, R. J.; Li, Y.; Pullarkat, S. A.; Leung, P.-H., *Org. Lett.* **2011**, *13*, 5862-5865.
- (53) Huang, Y.; Chew, R. J.; Pullarkat, S. A.; Li, Y.; Leung, P.-H., *J. Org. Chem.* **2012**, *77*, 6849-6854.
- (54) Lu, J.; Ye, J.; Duan, W.-L., *Chem. Commun.* **2014**, *50*, 698-700.
- (55) Join, B.; Mimeau, D.; Delacroix, O.; Gaumont, A.-C., *Chem. Commun.* **2006**, 3249-3251.
- (56) Koshti, V.; Gaikwad, S.; Chikkali, S. H., *Coord. Chem. Rev.* **2014**, *265*, 52-73.

- (57) Rosenberg, L., *ACS Catal.* **2013**, 3, 2845-2855.
- (58) Sugiura, J.; Kakizawa, T.; Hashimoto, H.; Tobita, H.; Ogino, H., *Organometallics* **2005**, 24, 1099-1104.
- (59) Price, A. J.; Edwards, P. G., *Chem. Commun.* **2000**, 899-900.
- (60) King, A. K.; Buchard, A.; Mahon, M. F.; Webster, R. L., *Chem. Eur. J.* **2015**, 21, 15960-15963.
- (61) Huang, J.-S.; Yu, G.-A.; Xie, J.; Wong, K.-M.; Zhu, N.; Che, C.-M., *Inorg. Chem.* **2008**, 47, 9166-9181.
- (62) Gallagher, K. J.; Webster, R. L., *Chem. Commun.* **2014**, 50, 12109-12111.
- (63) Brown, C. A.; Nile, T. A.; Mahon, M. F.; Webster, R. L., *Dalton Trans.* **2015**, 44, 12189-12195.
- (64) Sharpe, H. R.; Geer, A. M.; Lewis, W.; Blake, A. J.; Kays, D. L., *Angew. Chem. Int. Ed.* **2017**, 56, 4845-4848.
- (65) Pagano, J. K.; Bange, C. A.; Farmiloe, S. E.; Waterman, R., *Organometallics* **2017**, 36, 3891-3895.
- (66) Al-Shboul, T. M. A.; Goerls, H.; Westerhausen, M., *Inorg. Chem. Commun.* **2008**, 11, 1419-1421.
- (67) Al-Shboul, T. M. A.; Palfi, V. K.; Yu, L.; Kretschmer, R.; Wimmer, K.; Fischer, R.; Goerls, H.; Reiher, M.; Westerhausen, M., *J. Organomet. Chem.* **2010**, 696, 216-227.
- (68) Carpentier, J.-F.; Liu, B.; Sarazin, Y. In *Charge-neutral and cationic complexes of large alkaline earths for ring-opening polymerization and fine chemicals catalysis*, John Wiley & Sons, Inc.: 2014; pp 359-378, 351 plate.

- (69) Crimmin, M. R.; Barrett, A. G. M.; Hill, M. S.; Hitchcock, P. B.; Procopiou, P. A., *Organometallics* **2007**, *26*, 2953-2956.
- (70) Crimmin, M. R.; Barrett, A. G. M.; Hill, M. S.; Hitchcock, P. B.; Procopiou, P. A., *Organometallics* **2008**, *27*, 497-499.
- (71) Hu, H.; Cui, C., *Organometallics* **2012**, *31*, 1208-1211.
- (72) Rosca, S.-C.; Roisnel, T.; Dorcet, V.; Carpentier, J.-F.; Sarazin, Y., *Organometallics* **2014**, *33*, 5630-5642.
- (73) Younis, F. M.; Krieck, S.; Al-Shboul, T. M. A.; Goerls, H.; Westerhausen, M., *Inorg. Chem.* **2016**, *55*, 4676-4682.
- (74) Ward, B. J.; Hunt, P. A., *ACS Catal.* **2017**, *7*, 459-468.
- (75) Sakae, R.; Yamamoto, Y.; Komeyama, K.; Takaki, K., *Chem. Lett.* **2010**, *39*, 276-277.
- (76) Perrier, A.; Comte, V.; Moise, C.; Le Gendre, P., *Chem. Eur. J.* **2010**, *16*, 64-67.
- (77) Zhao, G.; Basuli, F.; Kilgore, U. J.; Fan, H.; Aneetha, H.; Huffman, J. C.; Wu, G.; Mindiola, D. J., *J. Am. Chem. Soc.* **2006**, *128*, 13575-13585.
- (78) Roering, A. J.; Leshinski, S. E.; Chan, S. M.; Shalumova, T.; MacMillan, S. N.; Tanski, J. M.; Waterman, R., *Organometallics* **2010**, *29*, 2557-2565.
- (79) Moquist, P.; Chen, G.-Q.; Mueck-Lichtenfeld, C.; Bussmann, K.; Daniliuc, C. G.; Kehr, G.; Erker, G., *Chem. Sci.* **2015**, *6*, 816-825.
- (80) Jian, Z.; Kehr, G.; Daniliuc, C. G.; Wibbeling, B.; Erker, G., *Dalton Trans.* **2017**, *46*, 11715-11721.
- (81) Dupre, J.; Gaumont, A.-C.; Lakhdar, S., *Org. Lett.* **2017**, *19*, 694-697.

- (82) Liu, L.; Chan, C.; Zhu, J.; Cheng, C.-H.; Zhao, Y., *J. Org. Chem.* **2015**, *80*, 8790-8795.
- (83) Douglass, M. R.; Ogasawara, M.; Hong, S.; Metz, M. V.; Marks, T. J., *Organometallics* **2002**, *21*, 283-292.
- (84) Behrle, A. C.; Schmidt, J. A. R., *Organometallics* **2013**, *32*, 1141-1149.
- (85) Takaki, K.; Komeyama, K.; Kobayashi, D.; Kawabata, T.; Takehira, K., *J. Alloys Compd.* **2006**, *408-412*, 432-436.
- (86) Takaki, K.; Komeyama, K.; Takehira, K., *Tetrahedron* **2003**, *59*, 10381-10395.
- (87) Takaki, K.; Koshoji, G.; Komeyama, K.; Takeda, M.; Shishido, T.; Kitani, A.; Takehira, K., *J. Org. Chem.* **2003**, *68*, 6554-6565.
- (88) Komeyama, K.; Kawabata, T.; Takehira, K.; Takaki, K., *J. Org. Chem.* **2005**, *70*, 7260-7266.
- (89) Takaki, K.; Takeda, M.; Koshoji, G.; Shishido, T.; Takehira, K., *Tetrahedron Lett.* **2001**, *42*, 6357-6360.
- (90) Basalov, I. V.; Rosca, S. C.; Lyubov, D. M.; Selikhov, A. N.; Fukin, G. K.; Sarazin, Y.; Carpentier, J.-F.; Trifonov, A. A., *Inorg. Chem.* **2014**, *53*, 1654-1661.
- (91) Kawaoka, A. M.; Douglass, M. R.; Marks, T. J., *Organometallics* **2003**, *22*, 4630-4632.
- (92) Douglass, M. R.; Stern, C. L.; Marks, T. J., *J. Am. Chem. Soc.* **2001**, *123*, 10221-10238.
- (93) Garner, M. E.; Parker, B. F.; Hohloch, S.; Bergman, R. G.; Arnold, J., *J. Am. Chem. Soc.* **2017**, *139*, 12935-12938.

- (94) Ji, P.; Sawano, T.; Lin, Z.; Urban, A.; Boures, D.; Lin, W., *J. Am. Chem. Soc.* **2016**, *138*, 14860-14863.
- (95) Costa, E.; Pringle, P. G.; Worboys, K., *Chem. Commun.* **1998**, 49-50.
- (96) Hoye, P. A. T.; Pringle, P. G.; Smith, M. B.; Worboys, K., *J. Chem. Soc., Dalton Trans.* **1993**, 269-274.
- (97) Monkowius, U. V.; Nogai, S. D.; Schmidbaur, H., *J. Am. Chem. Soc.* **2004**, *126*, 1632-1633.
- (98) Ganushevich, Y. S.; Miluykov, V. A.; Polyancev, F. M.; Latypov, S. K.; Lönnecke, P.; Hey-Hawkins, E.; Yakhvarov, D. G.; Sinyashin, O. G., *Organometallics* **2013**, *32*, 3914-3919.
- (99) Kazankova, M. A.; Efimova, I. V.; Kochetkov, A. N.; Afanas'ev, V. V.; Beletskaya, I. P.; Dixneuf, P. H., *Synlett* **2001**, 497-500.
- (100) Kazankova, M. A.; Shulyupin, M. O.; Borisenko, A. A.; Beletskaya, I. P., *Russ. J. Org. Chem.* **2002**, *38*, 1479-1484.
- (101) Kondoh, A.; Yorimitsu, H.; Oshima, K., *J. Am. Chem. Soc.* **2007**, *129*, 4099-4104.
- (102) Ohmiya, H.; Yorimitsu, H.; Oshima, K., *Angew. Chem. Int. Ed.* **2005**, *44*, 2368-2370.
- (103) Rosenberg, L., *Coord. Chem. Rev.* **2012**, *256*, 606-626.
- (104) Barre, C.; Boudot, P.; Kubicki, M. M.; Moiese, C., *Inorg. Chem.* **1995**, *34*, 284-291.

- (105) Holland, P. L.; Andersen, R. A.; Bergman, R. G., *Comments on Inorganic Chemistry* **1999**, *21*, 115-129.
- (106) Glueck, D. S., *Dalton Trans.* **2008**, 5276-5286.
- (107) Gregson, A. M.; Wales, S. M.; Bailey, S. J.; Keller, P. A., *J. Organomet. Chem.* **2015**, *785*, 77-83.
- (108) Berger, H. O.; Noeth, H., *J. Organomet. Chem.* **1983**, *250*, 33-48.
- (109) Bungabong, M. L.; Tan, K. W.; Li, Y.; Selvaratnam, S. V.; Dongol, K. G.; Leung, P.-H., *Inorg. Chem.* **2007**, *46*, 4733-4736.
- (110) Burt, J.; Levason, W.; Reid, G., *Coord. Chem. Rev.* **2014**, *260*, 65-115.
- (111) Cheow, Y. L.; Pullarkat, S. A.; Li, Y.; Leung, P.-H., *J. Organomet. Chem.* **2012**, *696*, 4215-4220.
- (112) Williams, J. O., *Angew. Chem. Int. Ed.* **1989**, *28*, 1110-1120.
- (113) Lu, D.; Coote, M. L.; Ho, J.; Kilah, N. L.; Lin, C.-Y.; Salem, G.; Weir, M. L.; Willis, A. C.; Wild, S. B.; Dilda, P. J., *Organometallics* **2012**, *31*, 1808-1816.
- (114) Denmark, S. E.; Ober, M. H., *Adv. Synth. Catal.* **2004**, *346*, 1703-1714.
- (115) Kojima, A.; Boden, C. D. J.; Shibasaki, M., *Tetrahedron Lett.* **1997**, *38*, 3459-3460.
- (116) Kojima, A.; Honzawa, S.; Boden, C. D. J.; Shibasaki, M., *Tetrahedron Lett.* **1997**, *38*, 3455-3458.
- (117) Liu, F.; Pullarkat, S. A.; Li, Y.; Chen, S.; Leung, P.-H., *Eur. J. Inorg. Chem.* **2009**, 4134-4140.

- (118) Maitra, K.; Catalano, V. J.; Clark, J., III; Nelson, J. H., *Inorg. Chem.* **1998**, *37*, 1105-1111.
- (119) Marquardt, C.; Balazs, G.; Baumann, J.; Virovets, A. V.; Scheer, M., *Chem. Eur. J.* **2017**, *23*, 11423-11429.
- (120) Roering, A. J.; Davidson, J. J.; MacMillan, S. N.; Tanski, J. M.; Waterman, R., *Dalton Trans.* **2008**, 4488-4498.
- (121) Stubenhofer, M.; Lassandro, G.; Balazs, G.; Timoshkin, A. Y.; Scheer, M., *Chem. Commun.* **2012**, *48*, 7262-7264.
- (122) Tay, W. S.; Yang, X.-Y.; Li, Y.; Pullarkat, S. A.; Leung, P.-H., *Chem. Commun.* **2017**, *53*, 6307-6310.
- (123) Turbervill, R. S. P.; Goicoechea, J. M., *Eur. J. Inorg. Chem.* **2014**, *2014*, 1660-1668.
- (124) Roering, A. J.; Davidson, J. J.; MacMillan, S. N.; Tanski, J. M.; Waterman, R., *Dalton Trans.* **2008**, 4488-4498.
- (125) Bange, C.; Mucha, N.; Cousins, M.; Gehsmann, A.; Singer, A.; Truax, T.; Higham, L.; Waterman, R., *Inorganics* **2016**, *4*, 26.
- (126) Ganushevich, Y. S.; Miluykov, V. A.; Polyancev, F. M.; Latypov, S. K.; Lonnecke, P.; Hey-Hawkins, E.; Yakhvarov, D. G.; Sinyashin, O. G., *Organometallics* **2013**, *32*, 3914-3919.

## **CHAPTER 2: ZIRCONIUM-CATALYZED INTERMOLECULAR HYDROPHOSPHINATION WITH PRIMARY PHOSPHINES**

### **2.1 Introduction**

#### **2.1.1 Primary phosphine chemistry**

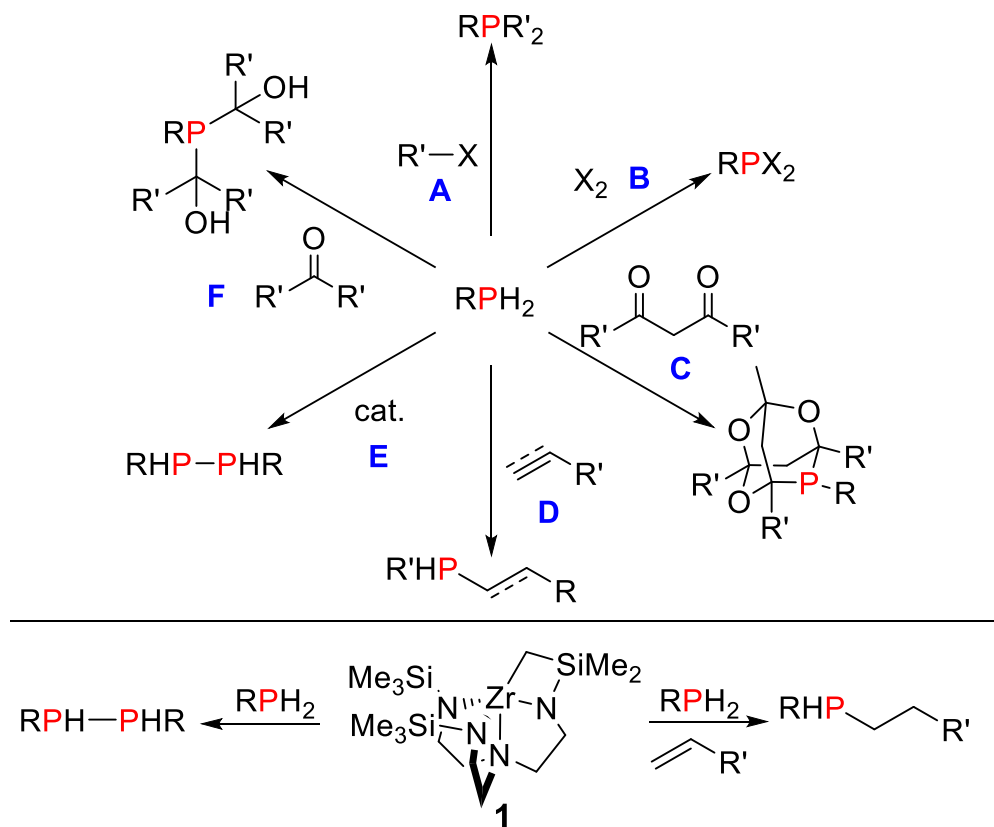
Despite the use of primary phosphines in asymmetric catalysis, macrocyclic synthesis, medicinal chemistry, and polymer science, synthetic routes that capitalize on primary phosphines are underreported.<sup>1-7</sup> Advancement of primary phosphine chemistry would be advantageous, not only for better understanding and utilization of this class of molecules but for a more direct approach to many attractive higher-order secondary and tertiary phosphine products. Primary phosphines are primed for further synthetic modification. The phosphorus center can be harnessed as either a nucleophile or an electrophile, and the relatively weak P–H bond is readily functionalized. The steric and electronic properties of higher-order phosphines can be controlled relatively easily, which makes primary and secondary phosphines attractive platform for further synthetic modification.

The most apparent setback to the development of primary phosphine chemistry is the nature of the primary phosphine itself. Many of these compounds are toxic, volatile, and/or pyrophoric in an aerobic atmosphere.<sup>4, 8</sup> Low molecular weight phosphines are the most susceptible to this type of exothermic, aerobic oxidation, which is disappointing considering that most metal-catalyzed methods that can functionalize primary phosphines come with the condition that they be small enough to cooperate with a metal catalyst.<sup>6, 9</sup>

Primary phosphines are generally more acidic than  $\text{PH}_3$  but less acidic than their secondary counterparts.<sup>6</sup> Activation of  $\text{PH}_3$  requires a base for addition to even the most



electrophilic alkenes, but primary phosphines can add spontaneously to electron-deficient alkenes, albeit with long reaction times and essentially nonexistent selectivity. Classic synthetic methods to functionalize primary phosphines are outlined in Scheme 2.1.<sup>9</sup>

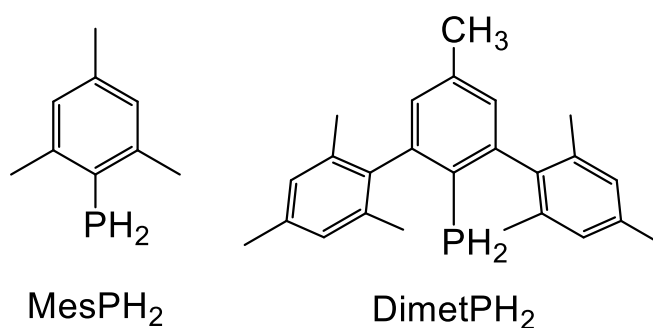


**Scheme 2.1:** Overview of methods to functionalize a primary phosphine (top) and catalytic functionalizations of primary phosphines studied in the Waterman group (bottom)

The generality of the methods outlined in Scheme 2.1 is more limited than it suggests. For example, a condensation-type reaction with a ketone and a primary phosphine will also produce the competitive phosphine oxide in addition to the phosphine diol (Scheme 2.1, **C** and **F**).<sup>6</sup> Catalytic dehydrocoupling of primary phosphines tends to produce cyclic phosphines in addition to the diphenylphosphine (Scheme 2.1 **E**).<sup>10</sup> Most of the methods only work for a limited number of phosphines and reagents, and the conversions may not

be substantial. The Waterman group has historically studied two particular reactions involving primary phosphines and compound  $[K^5 - N, N, N, N, C-(Me_3SiNCH_2CH_2)_2NCH_2CH_2NSiMe_2CH_2]Zr$  (**1**) (Scheme 2.1, bottom). Both catalytic dehydrocoupling<sup>11</sup> and hydrophosphination<sup>12-16</sup> of primary phosphines by **1** tackled some of the issues with primary phosphine chemistry, but limitations remain. Improvement and expansion of the arsenal of techniques for primary phosphine reactivity is an enticing challenge.

Given the understandable reservations about working with primary phosphines, several research groups have targeted ways to make air-stable primary phosphines. The most common ways to increase resistance to aerobic oxidation are either through added steric bulk, usually significant and carefully placed, or through a high degree of electron conjugation. The former method has been explored historically. The first moderately air-stable phosphine, mesitylphosphine (mesityl = Mes = 2,4,6-trimethylphenyl), was reported forty years ago.<sup>17</sup> Twenty years later the first completely air-stable primary phosphine, DimetPH<sub>2</sub> (Dimet = 2,6-dimesityl-4-methylphenyl) was reported<sup>18</sup> (Figure 2.1).



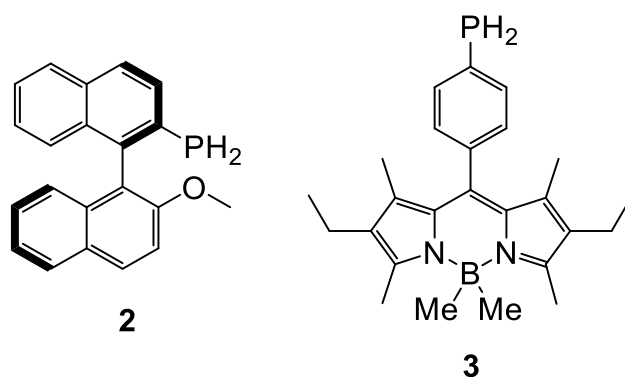
**Figure 2.1:** Air-stable primary phosphines protected by steric bulk

Sterically encumbered primary phosphines are afforded kinetic protection by their substituents, which impart significant resistance to oxidation.<sup>4</sup> This effect is so strong that primary phosphines with sufficient bulk can be isolated and handled freely in air.<sup>19</sup> In recent years, there has been substantial growth in the report of this class of phosphines,<sup>7, 9</sup> but the tradeoffs remain. The steric congestion responsible for the kinetic stability also impedes further functionalization.

Oxidation of a primary phosphine to a phosphine oxide is thermodynamically favorable due to the strength of the phosphorus–oxygen bond.<sup>9</sup> The putative steps of aerobic oxidation of phosphines to phosphine oxides involve photolytic phosphine radical cation formation and subsequent reaction with molecular oxygen, though the details remain unknown.<sup>9, 20</sup> Examples of isolated phosphine radical cations in which the phosphine has a high degree of steric encumbrance have surfaced.<sup>21-22</sup> The protection offered by sterically bulky or rigid substituents would result in a greater stability in the radical cations and subsequent resistance to interaction with molecular oxygen, explaining their observed kinetic stability towards oxidation.<sup>9, 20</sup>

A second approach to ensuring air-stability on a primary phosphine relies on a relatively high degree of  $\pi$ -conjugation. This hypothesis was designed and studied by the Higham group through synthetic and computational methods.<sup>20, 23-26</sup> The fundamental idea of this work is that the greater the degree of  $\pi$ -conjugation, the greater the air stability. A key component to this working model is the energies of the Highest Occupied Molecular Orbital (HOMO) of the phosphine and that of the Singly Occupied Molecular Orbital (SOMO) of the radical cations. Phosphines with a high degree of  $\pi$ -conjugation have

relatively little phosphorus contribution to the HOMO and experimentally observed air stability. Phosphines lacking substantial  $\pi$ -conjugation have HOMOs with a significantly higher degree of phosphorus contribution and are experimentally more prone to oxidation. Exploration of the relative energies of the SOMO revealed that primary phosphines with a SOMO  $> -10$  eV are experimentally air-stable and those with SOMO energies  $< -10$  eV are air-sensitive.<sup>20</sup> The Higham group has proposed that radical cations generated from a more stable SOMO have greater reactivity towards oxidation than those originating from SOMOs of lower stability.



**Figure 2.2:** Air-stable primary phosphines **2** and **3**

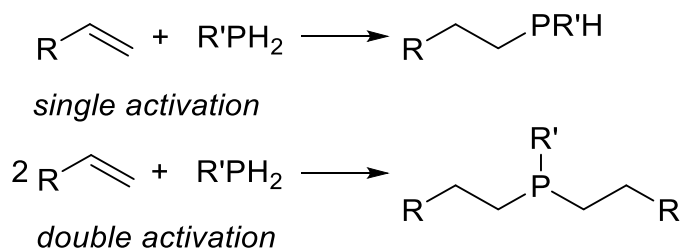
With this knowledge, the Higham group has made several air-stable primary phosphines possessing a high degree of  $\pi$ -conjugation. Two of these are shown in Figure 2.2. Primary phosphine (2'-methoxy-[1,1'-binaphthalen]-2-yl)phosphine (**2**) can be synthesized on gram scale and is precursor to valuable tunable structural and electronic phosphine products.<sup>24-25, 27-29</sup> Phosphine **2** is known to perform well as a ligand in asymmetric catalysis.<sup>24, 27</sup> Another air-stable primary phosphine, 8-[(4-phosphino)phenyl]-4,4-dimethyl-1,3,5,7-tetramethyl-2,6-diethyl-4-bora-3a,4a-diaza-s-indacene (**3**) is of interest as an imaging probe.<sup>30-32</sup>

### 2.1.2 Catalytic hydrophosphination of primary phosphines

The high value of primary phosphine derivatives argues for further exploration of their chemistry. The relative scarcity of examples and the limitations of the current art offer a platform for further development. Much of the recent work involving reactivity with primary phosphines is based on metal-mediated transformations, either stoichiometric or catalytic.<sup>1-7</sup>

Primary phosphines are hybridized in such a way that the lone-pair orbital has more *s*-character and is a relatively poor donor.<sup>33</sup> However, secondary and tertiary phosphines have lone pairs that are better donors, which presents metal-based functionalization with a problem. Metal-catalyzed routes to forming secondary and tertiary phosphines from lower-order phosphines generate products that are better suited to metal coordination. This often results in preferential coordination of the product to the metal center over the intended ligand, or preferential coordination of the product over insertion of the phosphine and/or substrate. This phenomenon is known as product inhibition and can shut down catalysis entirely.<sup>2</sup> One response to this problem in metal-catalyzed hydrophosphination lies in exploitation of the P–H activation while sidestepping coordination either by deliberate steric congestion or electronic manipulation.

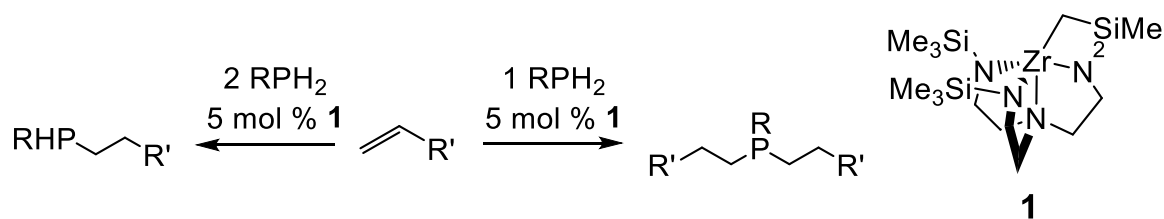
Primary phosphine hydrophosphination has an additional challenge. The primary phosphine offers *two* opportunities for functionalization, such that either a single or a double activation can occur (Scheme 2.2). Therefore, selective functionalization to furnish either the single or the double activation of the primary phosphine must be developed.



**Scheme 2.2:** Single and double activation of primary phosphines via hydrophosphination

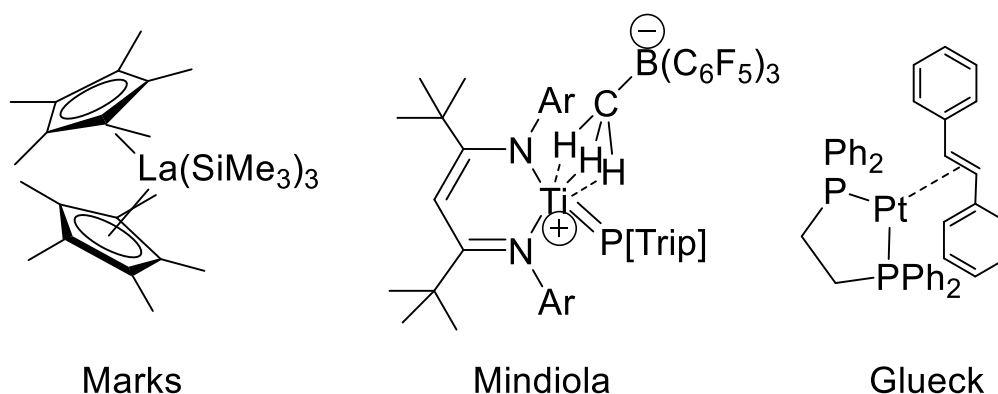
Hydrophosphination of primary phosphines to generate tertiary phosphines is well-established,<sup>2-4</sup> but metal-catalyzed hydrophosphination of primary phosphines to form exclusively secondary phosphines is a relatively recent phenomenon. Despite the greater steric demands of the newly-generated secondary phosphines, the lack of selectivity for formation of tertiary phosphines via metal-catalyzed hydrophosphination often stems from the metal catalyst itself. Catalysts that display the prerequisite high reactivity for P–H bonds also inherently suffer from poor control. That is, active metal catalysts cannot readily discriminate between either primary or secondary P–H bonds, resulting in a mixture of products. One solution to this problem may be to slow down the catalyst reactivity for P–H bonds, but this introduces a new difficulty. Retardation of the reaction progress also tends to allow for a buildup of the secondary phosphine product and thus increase the chance that it may be activated. Longer reaction times have also led to catalyst degradation and loss of chemoselectivity in one report.<sup>34</sup>

Seminal work from Glueck's,<sup>35</sup> Marks's,<sup>36-39</sup> and Mindiola's<sup>40</sup> groups reported the first examples of catalytic hydrophosphination using primary phosphines, but the field remained stagnant for about ten years until a report by Waterman in 2014.<sup>15</sup> That work demonstrated the double activation of primary phosphines to generate tertiary phosphines under mild conditions using **1** (Scheme 2.3).



**Scheme 2.3:** Hydrophosphination with primary phosphines to form either secondary or tertiary phosphine products

A noteworthy feature of this work was that exclusively secondary phosphine products could be obtained by use of two equivalents of the primary phosphine.<sup>15</sup> This selectivity, along with the exceptional substrate scope, set a high bar for further exploration.



**Figure 2.3:** Metal catalysts capable of primary phosphine hydrophosphination

Hydrophosphination catalysts that cooperate with primary phosphines are still limited,<sup>34-35, 40-42</sup> despite the resurfacing of this chemistry as of late.<sup>15</sup> Catalysts that employ lanthanide<sup>34, 38, 43-44</sup> and late transition metals<sup>35</sup> have been among the first to tackle primary phosphines (Figure 2.3). Some of the only calculated thermodynamic parameters are reported for the lanthanide catalysts. Mark's lanthanide hydrophosphination process encompassing phosphine protonolysis, substrate insertion, and subsequent product protonolysis, is mildly exothermic.<sup>38</sup> Trifonov's primary phosphine work alludes to these

thermodynamic considerations, but the parameters are not as well-defined.<sup>34, 43-44</sup> Some of the earliest known primary phosphine hydrophosphination comes from Glueck, whose platinum catalysts were able to hydrophosphinate acrylonitrile with  $\text{PhPH}_2$  via an insertion-based pathway to provide the tertiary phosphine product.<sup>45</sup> Regardless, there is still room for advancement in both catalyst design and mechanistic understandings.

Recent investigations by Trifonov and colleagues on the calcium- and lanthanum-catalyzed hydrophosphination of styrene (the benchmark substrate in hydrophosphination) with  $\text{PhPH}_2$  resulted in formation of secondary phosphine products with high chemoselectivity.<sup>43</sup> Preliminary investigations suggest that this selectivity results from a large difference in the rates of addition of the  $\text{PhPH}_2$  and the secondary phosphine product. However, hydrophosphination with  $\text{Ph}_2\text{PH}$  and styrene occurred much faster for the same catalyst system, suggesting that hydrophosphination is not merely the result of steric factors, but rather a nuance from the primary phosphine. The greater acidity of  $\text{Ph}_2\text{PH}$  than  $\text{PhPH}_2$  was not investigated in these lanthanide-catalyzed reactions but cannot be ruled out as a source of the reactivity difference.

However, the supply of many metal catalysts is limited.<sup>46</sup> One response to this problem is the exploration of more sustainable metal catalysts for hydrophosphination. Earth-abundant metals and main-group elements have emerged as primary phosphine hydrophosphination catalysts in more recent years,<sup>47-49</sup> with principal contributions from the Waterman group.<sup>12-13, 15, 40, 50</sup> Additionally, a series of iron catalysts have been reported for primary phosphine hydrophosphination under relatively mild conditions,<sup>51-55</sup> though it



should be noted that simple iron salts such as  $\text{FeCl}_2$  and  $\text{FeCl}_3$  can catalyze the hydrophosphination of styrene derivatives with  $\text{Ph}_2\text{PH}$ .<sup>56</sup>

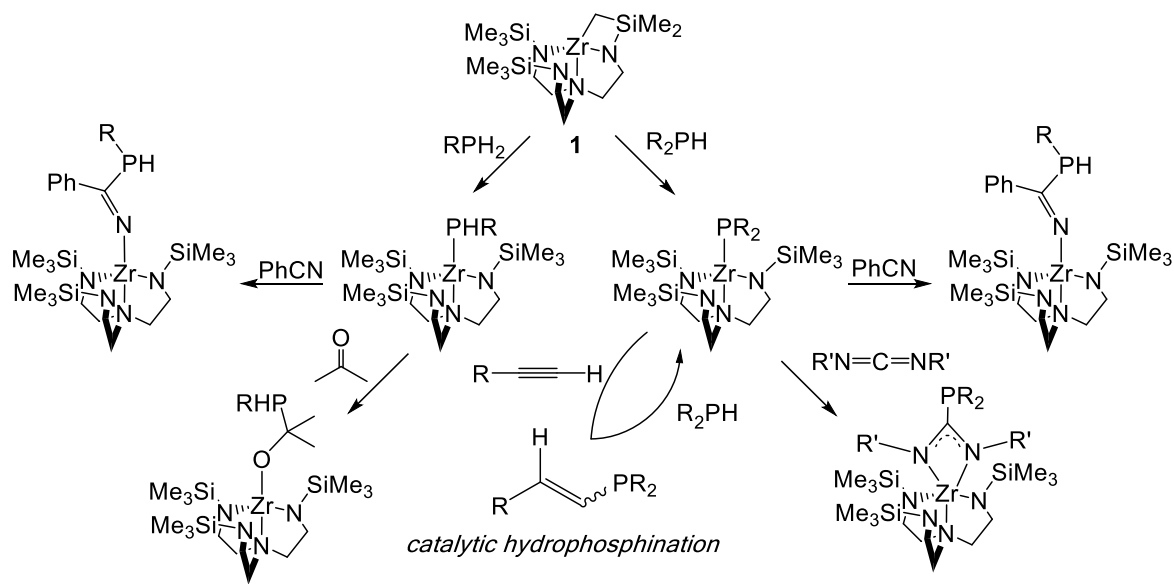
Limitations in metal-catalyzed primary phosphine hydrophosphination still remain. Late transition metals have a stronghold on hydrophosphination in general, though that grip is slipping. The dwindling supply of precious metal catalysts cannot continue support this transformation, and more sustainable metals must be investigated. While substantial progress has been made among earth-abundant metals,<sup>5, 40, 51, 53</sup> boundaries remain. We reported an example of a main group compound as a hydrophosphination catalyst,<sup>57</sup> however, P-block elements that catalyze this transformation are suggested but unrealized.<sup>49</sup> So far mostly small primary phosphines have been reported for hydrophosphination, whereas larger, sterically encumbered phosphines remain uncommon.

Work presented in this chapter aims to address challenges in metal-catalyzed hydrophosphination with regard to the substrate scope of both the phosphine and the unsaturated substrate, the selectivity, and the reaction conditions. Increasingly large phosphines are shown to be viable candidates for primary phosphine hydrophosphination. Hydrophosphination of chiral phosphines produces hydrophosphination products with intact chirality on the backbone. Furthermore, historically absent substrates (e.g. unactivated alkenes) are viable candidates for the transformation. These reactions proceed under mild conditions (i.e. ambient temperature) to offer either secondary or tertiary phosphines, depending on selection of the reaction stoichiometry. Development of a method that can selectively make secondary or tertiary phosphine products for a suite of substrates under mild conditions responds to some of the challenges of the reaction.

## 2.2: Results and Discussion

### 2.2.1: Catalytic hydrophosphination of alkenes with $\text{PhPH}_2$ and $\text{CyPH}_2$

The relative ease with which small, polar, unsaturated substrates insert into the Zr–P bond of phosphide derivatives of **1**<sup>10, 58</sup> suggested an attractive opportunity to capitalize on bond-forming reactivity between phosphines and unsaturated substrates (Scheme 2.4). This seminal investigation in the Waterman group on catalytic hydrophosphination with **1** targeted substrates possessing a  $\text{C}=\text{O}$ ,  $\text{C}=\text{N}$ ,  $\text{C}\equiv\text{N}$ , or  $\text{C}=\text{S}$  moiety, or terminal alkynes.<sup>16</sup>



**Scheme 2.4:** Insertion chemistry and catalytic hydrophosphination of terminal alkynes with **1**

Hydrophosphination with polar substrates with  $\text{Ph}_2\text{PH}$  provided tertiary phosphine products.<sup>16</sup> Despite high selectivity of this process for formation of vinyl, anti-Markovnikov products and the tolerance of  $\text{C}=\text{E}$  bonds, catalytic hydrophosphination of  $\text{Ph}_2\text{PH}$  with **1** was less efficient than known systems.<sup>59-60</sup> This limitation was likely an expression of the steric congestion around the catalytic intermediates that limited catalytic

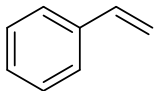
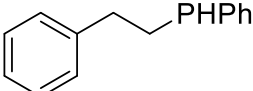
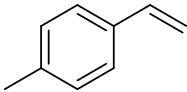
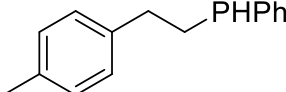
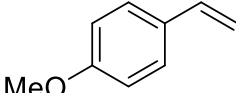
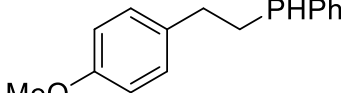
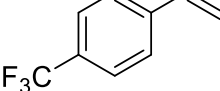
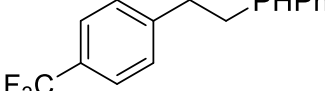
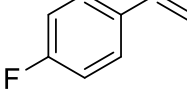
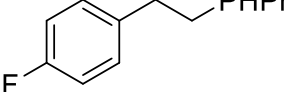
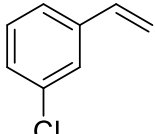
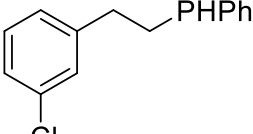
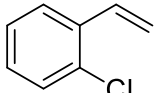
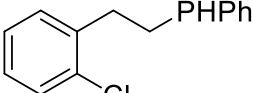
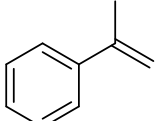
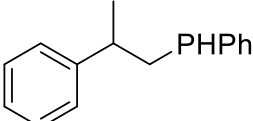
turnover. Functionalization of terminal alkynes also presented an unproductive catalytic pathway in which the terminal alkyne ring-opens on the Zr-CH<sub>2</sub> bond of **1** to form a stable, terminal zirconium alkynyl species. These uncooperative features limited catalytic hydrophosphination with **1**.

Reinvestigation of catalytic hydrophosphination with **1** with *primary* phosphines unleashed new possibilities.<sup>15</sup> Treatment of alkenes and diene substrates with PhPH<sub>2</sub> afforded exclusively secondary or tertiary phosphine products, depending on reaction conditions (Scheme 2.3).

When equal amounts of phosphine and substrate were used, the reaction provided a mixture of the secondary and tertiary phosphine products. Use of two equivalents of PhPH<sub>2</sub> afforded greater preference for the secondary phosphine product. This difference in reactivity is explained by the favored coordination of PhPH<sub>2</sub> to the zirconium metal center to form the primary zirconium phosphide over activation of the secondary phosphine product to form the secondary zirconium phosphide. The primary phosphide delivers secondary phosphine products, whereas the secondary phosphide returns tertiary products. Use of an excess of the PhPH<sub>2</sub> ensures that the catalytically active primary zirconium phosphide outnumbers the secondary zirconium phosphide.

Thus, treatment of styrene with *two* equivalents of PhPH<sub>2</sub> at ambient temperature in the presence of 5 mol % of **1** afforded complete consumption of styrene to provide the secondary phosphine product. This relative ease of functionalization was extended to a family of styrene derivatives (Table 2.1).

**Table 2.1:** Zirconium-catalyzed intermolecular hydrophosphination of styrenes with PhPH<sub>2</sub>. Reactions were run at ambient temperature. \*Reaction heated to 60 °C. Conversions were determined using <sup>1</sup>H NMR spectroscopy after complete consumption of the substrate.

$2 \text{ PhPH}_2 + \text{R-Substrate} \xrightarrow[\text{C}_6\text{D}_6, 22^\circ\text{C}]{5 \text{ mol } \% \text{ 1}} \text{R-Product}$				
Entry	Substrate	Time (h)	Product	Conversion (%)
a		12		89 (72)
b		12		87 (69)
c		12		85
d		12		94
e		12		82
f		12		90
g		12		93
h		24		93 (80)*

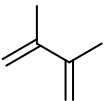
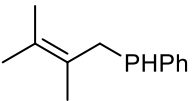

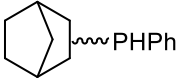

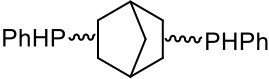
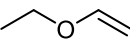
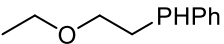
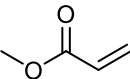
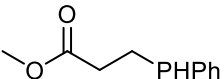
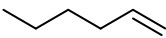
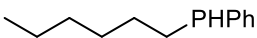


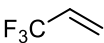
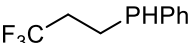
In all cases, the conversion was high to excellent. Separation of the secondary phosphine away from small amounts of tertiary phosphine side products and unreacted PhPH<sub>2</sub> provided high isolated yields of phosphine products (Table 2.1). In some cases PhPH<sub>2</sub> could be separated in sufficiently high yields such that it could be recycled for further reactivity.

Functionalization of the styrene substrates at either the *para*- or *meta*-positions did not affect hydrophosphination, even when halogenated substrates were used (Table 2.1). While styrenes with electron-withdrawing groups outperformed styrenes with electron-donating groups at the *para* position, the difference in reactivity was not substantial. Functionalization of  $\alpha$ -methylstyrene requires a longer reaction time and mild heating but affords the secondary hydrophosphination product in high yields. These steric and electronic tolerances speak to the high generality of hydrophosphination with **1**, but also hint at a mechanism in which the zirconium–phosphide dominates (*vide infra*).

Styrenes have been the benchmark substrates in hydrophosphination chemistry in recent years.<sup>5</sup> Reports of hydrophosphination with Michael acceptors appear to a lesser extent but are popular among late-transition metals. However, electron-deficient substrates have been almost entirely absent. Reports of unactivated substrates in hydrophosphination chemistry are limited, but growing. This neglect is surprising, the electronics of the  $\alpha$ -olefin are concentrated almost entirely at the double bond, and the sterics are minimal. Like styrenes and Michael acceptors,  $\alpha$ -olefins are widely commercially available. The observation that so few metal catalysts have been able to produce phosphines with these starting materials prompted an investigation into olefins, both cyclic and linear, and diene

substrates. Initial work targeting these substrates for catalytic hydrophosphination with **1** has shown good conversion with primary phosphines (Table 2.2.)

**Table 2.2:** Zirconium-catalyzed intermolecular hydrophosphination of alkenes and dienes with PhPH<sub>2</sub>. Conversions were determined using <sup>1</sup>H NMR spectroscopy after complete consumption of the substrate.

$2 \text{ PhPH}_2 + \text{R} \text{---} \text{CH=CH}_2 \xrightarrow[\text{C}_6\text{D}_6, 22^\circ\text{C}]{5 \text{ mol } \% \text{ 1}} \text{R} \text{---} \text{CH}_2\text{CH}_2\text{P(Ph)}_2$					
Entry	Substrate	Time (h)	T (°C)	Product	Conversion (%)
a		24	22		91 (72)
b		24	22		88 (82)
c		24	22		40
d		24	60		42
e		6	22		96 (90)
f		96	60		47
g		120	90		5
h		120	90		22

Despite the requirement for longer reaction times and elevated temperatures, unactivated substrates proved to be amenable for hydrophosphination with **1** (Table 2.2). Cyclic alkenes and dienes, such as norbornene and norbornadiene provide hydrophosphination products after 24 hours at ambient temperature. Norbornadiene provides some degree of polymerized phosphine products, resulting in a lower reported

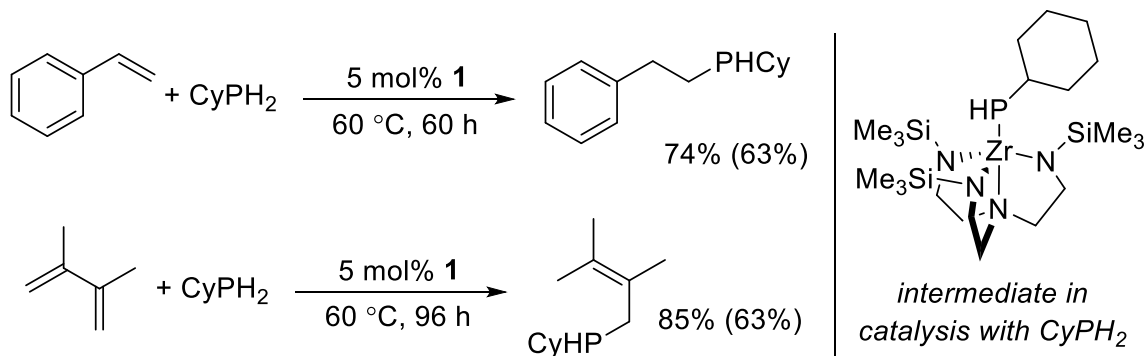
yield. Unactivated linear alkenes such as ethyl vinyl ether (Table 2.2, entry e) and 1-hexene (Table 2.2, entry f) require elevated temperatures and longer reaction times, but were still successful candidates for hydrophosphination. Even with lower efficiency than styrene substrates, hydrophosphination of unactivated alkenes was impressive at the time of publication for its novelty. Previous reports of hydrophosphination catalysts reported no success with these substrates, despite the cooperation of styrene and diene substrates.<sup>61</sup>

The selective formation of secondary phosphine products in hydrophosphination with **1** is intriguing and offered an advancement over several known systems at the time.<sup>35, 40, 62-63</sup> The secondary phosphines formed from hydrophosphination of styrene substrates all show characteristic <sup>31</sup>P NMR signals between -51.1 and -58.7 ppm.<sup>64</sup> The P-H <sup>1</sup>H NMR resonances appear between 4.01 and 4.12 ppm with a  $J_{PH} = 205 - 210$  Hz.

Interestingly, hydrophosphination with 2,3-dimethyl-1,3-butadiene provided the 1,4-addition product in high isolated yield (Table 2.2, entry a).<sup>15</sup> Installation of the P-C bond at the terminal end of the diene with P-H bond formation at the other site of unsaturation with concomitant shift of the second pair of electrons is different.<sup>15-16</sup> The (1,3)-electron shift is not accounted for in a simple insertion-based mechanism. The observation of polymerized products from hydrophosphination of norbornene and norbornadiene also is inconsistent with an insertion-based mechanism (Table 2.2, entries b and c).

Hydrophosphination with cyclohexylphosphine, CyPH<sub>2</sub>, of styrene and 2,3-dimethyl-1,3-butadiene provided hydrophosphination products in good conversions (Scheme 2.5). Compounds from CyPH<sub>2</sub> hydrophosphination display P-H <sup>1</sup>H NMR

resonances that are significantly downfield than those of PhPH<sub>2</sub> hydrophosphination. This difference is an anticipated reflection of the relative electronic shielding differences of the P–H bond. Cyclohexylphosphine has considerably more electron density on the P atom than derivatives of PhPH<sub>2</sub>. As limited as primary phosphines are in the literature as substrates, non-aromatic primary phosphines are even rarer.



**Scheme 2.5:** Hydrophosphination with CyPH<sub>2</sub> via a phosphide derivative of **1**. Conversions were determined using <sup>1</sup>H NMR spectroscopy after complete consumption of the substrate. Isolated yields are shown in parenthesis.

Despite the lower efficiency of this catalytic process, CyPH<sub>2</sub> is the largest phosphine for which productive hydrophosphination has occurred with **1**. This limitation is probably an expression of the relative size demands of the zirconium cyclohexylphosphide derivative of **1** that is responsible for catalysis (Scheme 2.5).<sup>11, 65</sup> This agrees with the previously observed size restraints on catalytic hydrophosphination with **1** with Ph<sub>2</sub>PH,<sup>16</sup> and underscores that steric factors, rather than electronic factors, guide hydrophosphination chemistry with **1**.



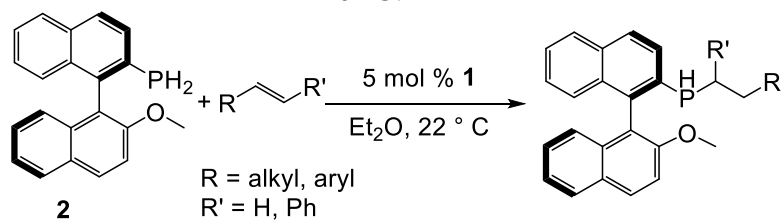
### 2.2.2: Hydrophosphination of alkenes with air-stable primary phosphines

While hydrophosphination of small primary phosphines is still somewhat underdeveloped, hydrophosphination of larger primary phosphines is sorely underreported in hydrophosphination chemistry.<sup>5</sup> This absence is not surprising. The steric congestion responsible for the kinetic stability also impedes further functionalization. The nascent generation of primary phosphine hydrophosphination catalysts is still undergoing some proof-of-concept studies, and challenging substrates like outsized primary phosphines are only beginning to come into reach.

Expansion of hydrophosphination chemistry with **1** to this class of air-stable, primary phosphines was intriguing for two main reasons. First, it offered a testament to the remarkable tolerance of **1** for primary phosphine identity, as demonstrated by reactions with CyPH<sub>2</sub>.<sup>15</sup> Second, it offered a way to further expand primary phosphine bond-forming chemistry. Use of an air-stable, chiral primary phosphine in hydrophosphination offers access to an expanded family of similar target phosphines that also were air-stable and potentially chiral.<sup>13</sup> These products would be of arguable value. Derivatives of **2** are known to perform well in asymmetric catalysis,<sup>24, 27</sup> and compound **3** is of interest as an imaging probe (Figure 2.2).

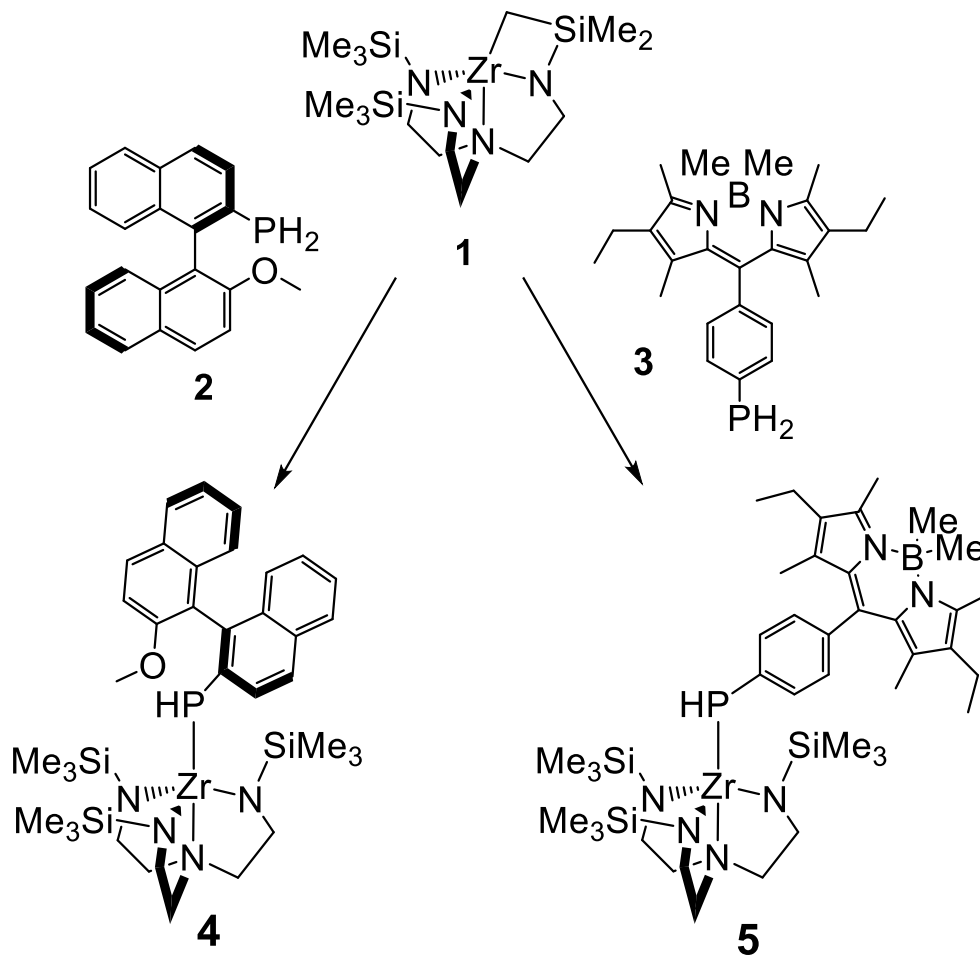
Treatment of a variety of styrenes, Michael acceptor, and imine substrates with **2** provided air-stable, chiral hydrophosphination products as exclusively secondary phosphines, as expected from previous investigations with **1**<sup>15</sup> (Table 2.3).

**Table 2.3:** Catalytic Hydrophosphination with **2** to form secondary phosphine products.  
<sup>a</sup>Yield was measured by integration of the <sup>31</sup>P{<sup>1</sup>H} NMR spectrum. <sup>b</sup>Required heating to 40 °C.



Entry	Time/h	Product	Conversion (%) <sup>a</sup>	Diastereomeric Ratio
a	48	(R)-MeO-MOP-	55 (40)	1 : 1.16
b	48	(R)-MeO-MOP-	42	1 : 2.37
c	48	(R)-MeO-MOP-	63	1 : 1.33
e	24	(R)-MeO-MOP-	74 (66)	1 : 1.20
e	48	(R)-MeO-MOP-	72 (69)	1 : 1.78
f	24	(R)-MeO-MOP-	87 (82)	1 : 1.32
g <sup>b</sup>	48	(R)-MeO-MOP-	8	1 : 1.06
h	24	(R)-MeO-MOP-	80 (72)	1 : 1.12

The influence of the substitution of the styrene substrate is noticeable. Substrates bearing electron-donating groups outperform those with electron-withdrawing groups (Table 2.3). This is markedly different than hydrophosphination with  $\text{PhPH}_2$ . That investigation identified styrene substrates bearing electron-withdrawing groups were favored.<sup>15</sup>



**Scheme 2.6:** Catalytically active intermediates in hydrophosphination with **1**

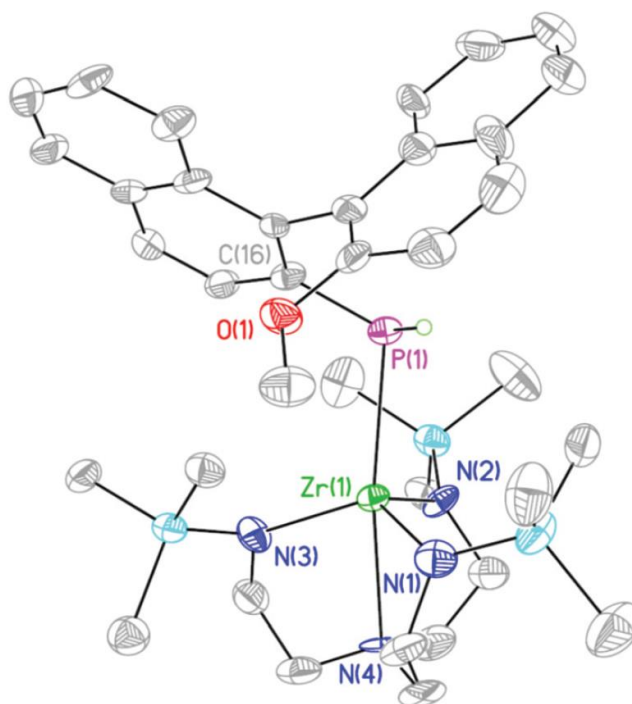
In both hydrophosphination studies Michael acceptors outperform styrene substituents in conversions, as anticipated.<sup>13, 15</sup> Michael acceptors do not necessarily require a catalyst for hydrophosphination, though noncatalytic reactions often suffer from

poor selectivity and limited conversions. Hydrophosphination of methyl methacrylate with **2** in the absence of **1** failed to give detectable levels of hydrophosphination products after four days; whereas, hydrophosphination of methyl methacrylate with **1** provides high yields of the product after 24 hours with **2**, and excellent yields after six hours with  $\text{PhPH}_2$ .<sup>13, 15</sup>

The chemical shifts of hydrophosphination products in Table 2.3 fall between -52.2 to -57.7 ppm, which is characteristic of secondary phosphines bearing both an alkyl and aryl substituent<sup>12-13, 15</sup> and similar to hydrophosphination products with  $\text{PhPH}_2$  (Tables 2.1 and 2.2).<sup>15</sup> The similarity of the  $^{31}\text{P}$  NMR resonances argues that either little differences exist between the P–H bond nature in all products, as anticipated from previous investigations. The hydrophosphination product of *N*-benzylideneaniline has a pair of resonances at -25.7 and -28.3 ppm from the P–C–N bond (Table 2.3, entry e). All compounds show the characteristic scalar P–H coupling constants of 200–220 Hz. As expected, the other hydrophosphination products display one distinct  $^{31}\text{P}$  NMR resonance for each diastereomer.

The selectivity of the hydrophosphination process is high in some regards. All products are formed as only anti-Markovnikov products and only as secondary phosphines. The chirality on the backbone remains intact, and the air-stability is preserved. However, the products are formed as mixtures of diastereomers; the diastereomeric excess (d.e.) of these transformation is small, with values less than 15%. This observation suggests that the impact of the binaphthyl substituent on **2** is not sufficiently large enough to control diastereoselectivity. Selectivity in the product phosphines is largely a function of kinetics

and not the secondary phosphine itself. Inversion barriers in solution for secondary phosphines are high (29–36 kcal mol<sup>-1</sup>),<sup>1</sup> suggesting that epimerization of the hydrophosphination products is not responsible for the low diastereoselectivity. Instead, the culprit is likely **4**. This phosphide is likely too big to invert rapidly enough during catalysis to give high product selectivity at the newly-formed P–C bond.<sup>66–67</sup> This species possesses only a single resonance in the <sup>31</sup>P{<sup>1</sup>H} NMR spectrum and a single P–H resonance in the <sup>1</sup>H NMR spectrum. X-ray crystallography was employed to coax out more structural information relevant for catalysis. Isolation of **4** gave analytically pure red crystals of the complex (Figure 2.4).



**Figure 2.4:** X-ray crystal structure of **4** with thermal ellipsoids drawn at the 50% probability level. One of two molecules in the unit cell are shown. Hydrogen atoms except H(1), which was located on phosphorus, are omitted for clarity.

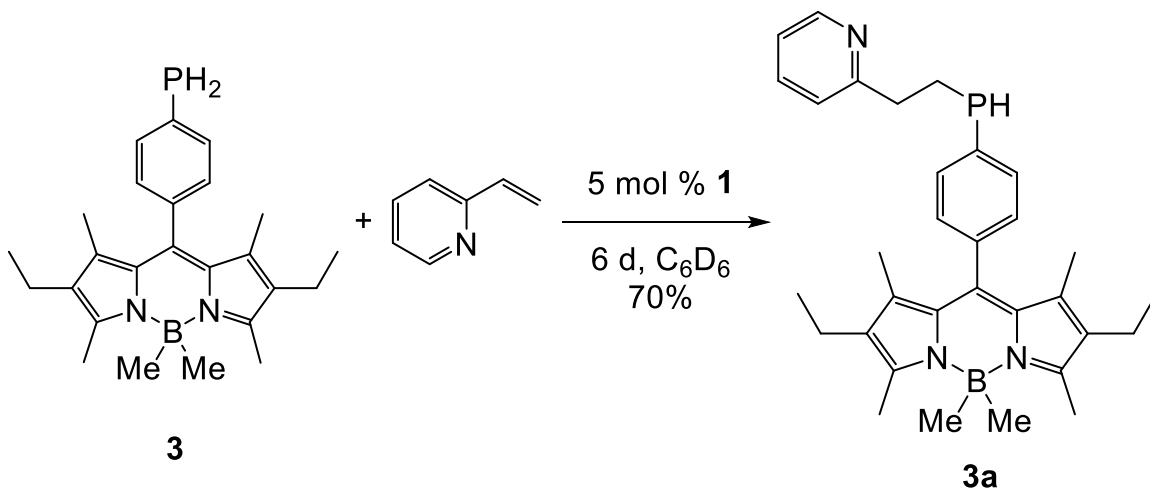
The isolated crystals of **4** contained two independent molecules within the unit cell that differ by the chirality at phosphorus. The isolation of both isomers of the zirconium phosphide and the observed phosphide inversion on the NMR time scale suggest that substrate insertion does not compete with phosphide inversion, which would result in the poor diastereoselectivity. Instead, the poor diastereoselectivity likely results from thermodynamic epimerization. To test this idea, compound **2b** was isolated by selective sublimation of **2**, which resulted in the diastereomeric ratio of 1:1.03 for the secondary phosphine product.

The Zr–P bond length is 2.736(4) Å; making it the tied for the longest for this library of Zr–PRR' compounds, and comparable to of Zr–PHCy (2.734(1)Å). These bond-length similarities suggest that steric factors predominate over electronic factors for these distances. The phosphide ligands of the structurally characterized primary zirconium phosphidos of this class, (N<sub>3</sub>N)Zr–PPh and (N<sub>3</sub>N)Zr–PHCy, display no significant  $\pi$ -bonding. The resemblance of the bond lengths of not only the Zr–P bond but also the Zr–amide bonds of both **4** and (N<sub>3</sub>N)Zr–PHCy demonstrate that catalytic hydrophosphination with **1** to form **4** is viable. The Zr–P bond length of **4** is sufficiently long enough that a substrate can insert into the Zr–P bond to make the new phosphine. This is clearly supported by the formation of hydrophosphination products (Table 2.3) and lends credence to the argument that steric factors, rather than electronic factors, dictate hydrophosphination reactivity.

Formation of both diastereomers from **4** is understandable given the way the MOP phosphide backbone rests on the catalyst in the crystal structure (Figure 2.4). It folds down

over the Zr–P bond and hinders it from reactivity. This may be responsible for both the diminished catalytic turnovers in Table 2.3 and for the modest diastereoselectivity. An incoming substrate is equally blocked from insertion at either side of the Zr–P bond. It is also worth noting that the chirality of **2** is sufficiently far enough from the active Zr–P bond such that it cannot influence the reactivity.

The versatility of the primary phosphine in catalytic hydrophosphination with **1** was encouraging. Few examples of sterically encumbered primary phosphines appear as substrates for metal-catalyzed hydrophosphination. This led us to investigate catalytic hydrophosphination of **3**, which is a potential biologically active fluorophore. Hydrophosphination of **3** with 2-vinylpyridine gives the anticipated secondary phosphine **3a** as the anti-Markovnikov adduct (Scheme 2.7).<sup>12</sup>



**Scheme 2.7:** Catalytic hydrophosphination of 2-vinylpyridine to form **3a**

As expected, compound **3a** retains its fluorescence. Excitation at 485 nm resulted in a maximum emission at 529 nm in THF, which aligns closely with that of the parent molecule ( $\lambda_{em} = 526$  nm in THF).<sup>23, 68</sup> The retention of fluorescence during catalytic

hydrophosphination suggests that product phosphines could also be candidates for highly desirable, niche uses as is the case for their parent molecule.<sup>23, 31-32, 68-70</sup>

The air stability of these hydrophosphination products was assessed in the standard manner.<sup>20, 26</sup> The secondary phosphine was dissolved in benzene-*d*<sub>6</sub> and left in an open NMR tube. The reaction was monitored by <sup>31</sup>P{<sup>1</sup>H} NMR spectroscopy periodically for seven days, at which no change was observed. The resistance of these phosphines to oxidation is an anticipated result, but it is worth noting that there are few air-stable secondary phosphines without a protecting group.<sup>1</sup> The resemblance of the hydrophosphination products in Table 2.3 and **3a** to their parent molecules and experimental resistance to oxidation also suggests that the desirable air-stability is passed on to the product phosphines. Instead, resistance to aerobic oxidation comes from the high degree of  $\pi$ -conjugation and a resulting raised HOMO energy. As expected, these attributes are also present in the hydrophosphination products, resulting in their measured increased aerobic stability. The resistance to oxidation, retention of chirality for hydrophosphination products of **2** and fluorescence for **3a** in the product secondary and tertiary phosphines demonstrates that these phosphines are of value.

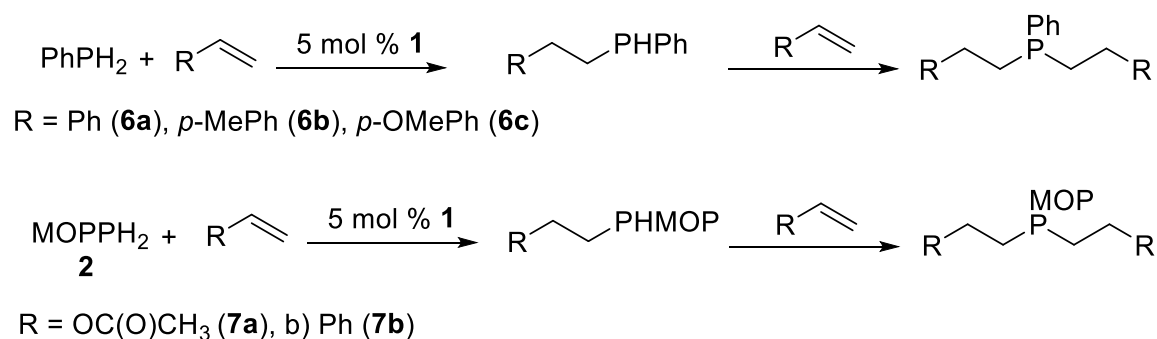
### 2.2.3 Formation of tertiary phosphine products

Hydrophosphination reactions involving primary phosphines often gives competitive and unselective amounts of both the secondary and tertiary phosphine products (*vide supra*). One challenge is to select for formation of either product.

Addition of two equivalents of an unsaturated substrate to a primary phosphine forms a tertiary phosphine via the secondary phosphine, as is intuitive. Modification of the



reaction conditions with **1** by using equal amounts of the phosphine and styrene returned the anticipated secondary phosphine product first (Table 2.1). A second, separate, hydrophosphination event in the same pot provides the tertiary phosphine products after slightly increased reaction times (Scheme 2.8).



**Scheme 2.8:** Catalytic hydrophosphination with **1** to form tertiary phosphines **6** and **7** via secondary phosphines

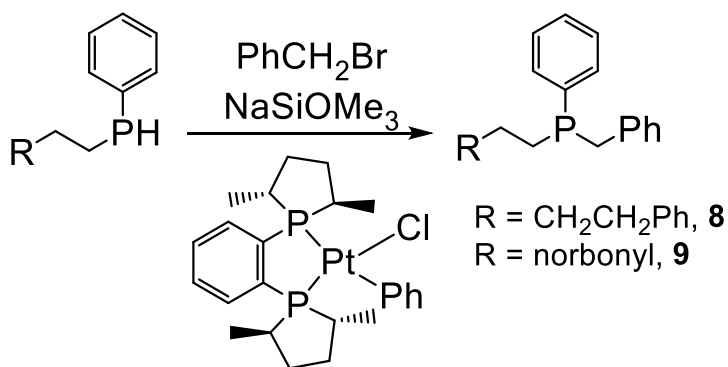
After extended reaction times tertiary phosphine products appear at the conventional <sup>31</sup>P chemical shifts of tertiary phosphines at -34.2 and -34.3 ppm. Compounds **6a-6c** were isolated in high yields under otherwise identical conditions. The reactions to form tertiary phosphines are more sluggish than those to form secondary phosphines, which is probably attributable to the increased steric demand of the tertiary phosphine products. However, the relative support of phosphine identity in catalytic hydrophosphination with **1** supports an ongoing theme in which **1** can tolerate significant steric encumbrance on the phosphide and still provide hydrophosphination products.

#### 2.2.4 Functionalization of secondary phosphines

The attractiveness of controllable formation of secondary phosphines is demonstrated by consideration of their potential. Secondary phosphine chemistry is more developed than primary phosphine chemistry, particularly for desirable transformations,

such as formation of chiral phosphines. Secondary phosphines have a more rich history in cross-coupling and other catalytic processes than their primary counterparts.<sup>6</sup> However, secondary phosphines are nearly impossible to reduce to their primary counterparts, whereas primary phosphines can be readily modified to secondary phosphines.

One known method to formation of asymmetric tertiary phosphines from achiral secondary phosphines was developed by Glueck.<sup>67</sup> This reactivity was elaborated upon using hydrophosphination products from catalytic hydrophosphination with  $\text{PhPH}_2$  and **1** (Scheme 2.9).



**Scheme 2.9:** Asymmetric alkylation of hydrophosphination products

The enantiomeric excess (ee) of the product was scarcely measureable for **8**, but a high degree of steric encumbrance is required to for significant ee values. Reaction of product **1j** to produce **9** gave an ee of 61% as measured with a chiral reporter.<sup>71</sup> However, secondary phosphine chemistry is more mature than primary phosphine chemistry. Addition to the substrate pool by easy functionalization of primary phosphines to secondary phosphines represents an attractive, underreported tapline into a rich field of study.

## 2.3 Conclusions

In summary, triamidoamine-ligated zirconium compound **1** catalyzes both the single and the double activation of primary phosphines with alkenes to selectively generate secondary or tertiary phosphine products. The extension of this catalysis to challenging substrates, such as 1-hexene or large primary phosphines has expanded the substrate pool for which intramolecular hydrophosphination is possible. These developments challenge the relatively limited reports of primary phosphine chemistry and offer practical, mild, and general synthetic routes to organophosphine derivatives from primary phosphines.

## 2.4 Experimental methods

### 2.4.1 General methods

All air-sensitive manipulations were performed under a positive pressure of nitrogen using standard Schlenk line or in a M. Braun glove box. Dry, oxygen-free solvents were employed throughout. Benzene-*d*<sub>6</sub> was purchased then degassed and dried over NaK alloy and distilled under reduced pressure. NMR spectra were recorded with either a Bruker AXR 500 MHz spectrometer in benzene-*d*<sub>6</sub> and are reported with reference to residual solvent signals (C<sub>6</sub>D<sub>6</sub>,  $\delta$  7.16 and 128.0) and to an external 85% H<sub>3</sub>PO<sub>4</sub> ( $\delta$  0.0) standard for <sup>31</sup>P NMR spectra. Infrared spectra were collected on a Bruker Alpha FT-IR spectrometer with an ATR head. Mass spectra were collected on an Applied Biosystems 4000QTrap Pro. Absorption spectra were recorded with a QuantaMaster 4 fluorescence spectrophotometer using tetrahydrofuran as a solvent. Compounds were excited at 485 nm and excitation and emission slits were both set to 1 nm. PhPH<sub>2</sub> and CyPH<sub>2</sub> were purchased from Strem Chemicals and used without further purification. Phosphines (*R*)-[2'-methoxy(1,1'-

binaphthalen)-2-yl]phosphine<sup>72</sup> (**2**) and 8-[(4-phosphino)phenyl]-4,4-dimethyl-1,3,5,7-tetramethyl-2,6-diethyl-4-bora-3a,4a-diaza-*s*-indacene<sup>23</sup> (**3**) were prepared according to literature procedures. Compound [ $\kappa^5$ -*N,N,N,N,C*-(Me<sub>3</sub>SiNCH<sub>2</sub>CH<sub>2</sub>)<sub>2</sub>NCH<sub>2</sub>CH<sub>2</sub>NSiMe<sub>2</sub>CH<sub>2</sub>]Zr (**1**) was prepared according to the literature procedure.<sup>11</sup> All other chemicals were obtained from commercial suppliers and dried by appropriate means.

#### 2.4.2 General procedure for hydrophosphination reactions with PhPH<sub>2</sub> or CyPH<sub>2</sub><sup>15</sup>

A scintillation vial was charged with 0.2 mmol primary phosphine and 0.1 mmol alkene or diene in the presence of 5 mol % of **1** in 2 mL benzene-*d*<sub>6</sub> solvent. The mixture solutions were stirred at ambient temperature for noted time period. The consumption of substrate to product was monitored by <sup>31</sup>P and <sup>1</sup>H NMR spectroscopy. Yields were determined from integration of the substrate converted by <sup>1</sup>H NMR and <sup>31</sup>P NMR spectra<sup>73</sup> or using internal standard dcamethylferrocene in the <sup>1</sup>H NMR spectrum. The catalyst was removed when passed through a silica column (1 cm) eluting with diethyl ether (ca. 2 mL). The solvent of elute was then removed under reduced pressure to give colorless oil. For large scale reactions, 0.3–0.5 mmol of alkenes or dienes substrate was used. Distillation using a short path apparatus removed excess primary phosphines to give the secondary phosphine derivatives as clear, colorless oils. Primary phosphine can be recovered during fractional distillation (~70%, high purity) or by collecting all residual fractions, deprotonation with *n*BuLi, filtration of the solid, and careful reprotonation with degassed water (~90%, low purity).

Heating was necessary when using CyPH<sub>2</sub> or unactivated alkenes substrates. Hydrophosphination reactions with ethylene and 3,3,3-trifluoropropene substrate were performed in a PTFE-valved NMR tube under similar reaction conditions. Tertiary phosphines **6a-c** were prepared by reaction of two equiv. of alkene substrate with one equiv. of phosphine under same catalytic conditions.

Spectroscopic data is consistent to that reported in the literature for known products.

#### **2.4.3 General procedure for hydrophosphination reactions with **2**<sup>13</sup>**

A Teflon-sealed reaction vial was charged with 0.18 mmol of unsaturated substrate, dissolved in Et<sub>2</sub>O, and equipped with a magnetic stir bar. The reaction vessel was charged with 0.90 mmol of **2** and 0.0045 mmol (5 mol %) of **1**. The reactions were stirred at ambient temperature for 48 h. The crude reaction mixture was filtered through Celite to remove **1**.

#### **2.4.4 Procedure for hydrophosphination reaction targeting **3a**<sup>12</sup>**

A J-Young NMR tube was given 16.1 mg (0.040 mmol) of **3**, 4.2 mg (0.040 mmol) of 2-vinyl pyridine, 0.9 mg of **1** (0.002 mmol) and dissolved in benzene-*d*<sub>6</sub>. The J-Young NMR tube was capped and heated to 80 °C for 6 days to achieve 70 % NMR conversion to **3a**.

#### **Procedure for formation of **4** and **5**<sup>12-13</sup>**

A scintillation vial was charged with **1** (1 equiv) and 3 mL of benzene (for the formation of **4**) or toluene (for the formation of **5**). To the solution of **1**, either **2** or **3** (1.05 equiv) was added and the resultant solution was stirred at ambient temperature for 30 minutes. Volatiles were removed under reduced pressure until incipient crystallization. Gentle warming redissolved the solids, and the solution was cooled to −30 °C for ~16 h to afford

red crystals of **4** (276 mg, 0.361 mmol, 82%) or dissolved in hexanes and cooled to -30 °C for 4 days to form **5**.

## 2.5 References

- (1) Corbridge, D. E. C., *Phosphorus: Chemistry, Biochemistry, and Technology*. 6 ed.; CRC Press: Boca Raton, Florida, 2013; p 1473.
- (2) Rosenberg, L., *ACS Catal.* **2013**, 3, 2845-2855.
- (3) Koshti, V.; Gaikwad, S.; Chikkali, S. H., *Coord. Chem. Rev.* **2014**, 265, 52-73.
- (4) Fleming, J. T.; Higham, L. J., *Coord. Chem. Rev.* **2015**, 297-298, 127-145.
- (5) Bange, C. A.; Waterman, R., *Chem. Eur. J.* **2016**, 22, 12598-12605.
- (6) Troev, K. D., *Reactivity of P-H Group of Phosphorus Based Compounds*. Academic Press: London, 2017.
- (7) Brynda, M., *Coord. Chem. Rev.* **2005**, 249, 2013-2034.
- (8) Hiney, R. M.; Higham, L. J.; Mueller-Bunz, H.; Gilheany, D. G., *Angew. Chem. Int. Ed.* **2006**, 45, 7248-7251.
- (9) Fleming, J. T.; Higham, L. J., *Coord. Chem. Rev.* **2015**, 297-298, 127-145.
- (10) Waterman, R., *Curr. Org. Chem.* **2008**, 12, 1322-1339.
- (11) Waterman, R., *Organometallics* **2007**, 26, 2492-2494.
- (12) Bange, C.; Mucha, N.; Cousins, M.; Gehsmann, A.; Singer, A.; Truax, T.; Higham, L.; Waterman, R., *Inorganics* **2016**, 4, 26.
- (13) Bange, C. A.; Ghebreab, M. B.; Ficks, A.; Mucha, N. T.; Higham, L.; Waterman, R., *Dalton Trans.* **2016**, 45, 1863-1867.
- (14) Bange, C. A.; Waterman, R., *ACS Catal.* **2016**, 6, 6413-6416.

- (15) Ghebreab, M. B.; Bange, C. A.; Waterman, R., *J. Am. Chem. Soc.* **2014**, *136*, 9240-9243.
- (16) Roering, A. J.; Leshinski, S. E.; Chan, S. M.; Shalumova, T.; MacMillan, S. N.; Tanski, J. M.; Waterman, R., *Organometallics* **2010**, *29*, 2557-2565.
- (17) Becker, G.; Mundt, O.; Roessler, M.; Schneider, E., *Z. Anorg. Allg. Chem.* **1978**, *443*, 42-52.
- (18) Rigon, L.; Ranaivonjatovo, H.; Escudie, J., *Phosphorus, Sulfur Silicon Relat. Elem.* **1999**, *152*, 153-167.
- (19) Yoshifuji, M.; Shibayama, K.; Inamoto, N.; Matsushita, T.; Nishimoto, K., *J. Am. Chem. Soc.* **1983**, *105*, 2495-2497.
- (20) Stewart, B.; Harriman, A.; Higham, L. J., *Organometallics* **2011**, *30*, 5338-5343.
- (21) Pan, X.; Chen, X.; Li, T.; Li, Y.; Wang, X., *J. Am. Chem. Soc.* **2013**, *135*, 3414-3417.
- (22) Sasaki, S.; Sutoh, K.; Shimizu, Y.; Kato, K.; Yoshifuji, M., *Tetrahedron Lett.* **2014**, *55*, 322-325.
- (23) Davies, L. H.; Stewart, B.; Harrington, R. W.; Clegg, W.; Higham, L. J., *Angew. Chem. Int. Ed.* **2012**, *51*, 4921-4924, S4921/4921-S4921/4966.
- (24) Ficks, A.; Martinez-Botella, I.; Stewart, B.; Harrington, R. W.; Clegg, W.; Higham, L. J., *Chem. Commun.* **2011**, *47*, 8274-8276.
- (25) Hiney, R. M.; Ficks, A.; Muller-Bunz, H.; Gilheany, D. G.; Higham, L. J., Air-stable chiral primary phosphines part (i) synthesis, stability and applications. In

*Organometallic Chemistry: Volume 37*, The Royal Society of Chemistry: 2011; Vol. 37, pp 27-45.

(26) Stewart, B.; Harriman, A.; Higham, L. J., Air-stable chiral primary phosphines part (ii) predicting the air-stability of phosphines. In *Organometallic Chemistry: Volume 38*, The Royal Society of Chemistry: 2012; Vol. 38, pp 36-47.

(27) Ficks, A.; Hiney, R. M.; Harrington, R. W.; Gilheany, D. G.; Higham, L. J., *Dalton Trans.* **2012**, *41*, 3515-3522.

(28) Ficks, A.; Harrington, R. W.; Higham, L. J., *Dalton Trans.* **2013**, *42*, 6302-6305.

(29) Ficks, A.; Clegg, W.; Harrington, R. W.; Higham, L. J., *Organometallics* **2014**, *33*, 6319-6329.

(30) Nigam, S.; Burke, B. P.; Davies, L. H.; Domarkas, J.; Wallis, J. F.; Waddell, P. G.; Waby, J. S.; Benoit, D. M.; Seymour, A.-M.; Cawthorne, C.; Higham, L. J.; Archibald, S. J., *Chem. Commun.* **2016**, *52*, 7114-7117.

(31) Davies, L. H.; Harrington, R. W.; Clegg, W.; Higham, L. J., *Dalton Trans.* **2014**, *43*, 13485-13499.

(32) Davies, L. H.; Kasten, B. B.; Benny, P. D.; Arrowsmith, R. L.; Ge, H.; Pascu, S. I.; Botchway, S. W.; Clegg, W.; Harrington, R. W.; Higham, L. J., *Chem. Commun.* **2014**, *50*, 15503-15505.

(33) Drago, R. S., *Organometallics* **1995**, *14*, 3408-3417.

(34) Basalov, I. V.; Dorcet, V.; Fukin, G. K.; Carpentier, J.-F.; Sarazin, Y.; Trifonov, A. A., *Chem. Eur. J.* **2015**, *21*, 6033-6036.



- (35) Wicht, D. K.; Kourkine, I. V.; Kovacik, I.; Glueck, D. S.; Concolino, T. E.; Yap, G. P. A.; Incarvito, C. D.; Rheingold, A. L., *Organometallics* **1999**, *18*, 5381-5394.
- (36) Douglass, M. R.; Marks, T. J., *J. Am. Chem. Soc.* **2000**, *122*, 1824-1825.
- (37) Douglass, M. R.; Ogasawara, M.; Hong, S.; Metz, M. V.; Marks, T. J., *Organometallics* **2002**, *21*, 283-292.
- (38) Douglass, M. R.; Stern, C. L.; Marks, T. J., *J. Am. Chem. Soc.* **2001**, *123*, 10221-10238.
- (39) Kawaoka, A. M.; Douglass, M. R.; Marks, T. J., *Organometallics* **2003**, *22*, 4630-4632.
- (40) Zhao, G.; Basuli, F.; Kilgore, U. J.; Fan, H.; Aneetha, H.; Huffman, J. C.; Wu, G.; Mindiola, D. J., *J. Am. Chem. Soc.* **2006**, *128*, 13575-13585.
- (41) Douglass, M. R.; Stern, C. L.; Marks, T. J., *J. Am. Chem. Soc.* **2001**, *123*, 10221-10238.
- (42) Erickson, K. A.; Dixon, L. S. H.; Wright, D. S.; Waterman, R., *Inorg. Chim. Acta* **2014**, *422*, 141-145.
- (43) Basalov, I. V.; Yurova, O. S.; Cherkasov, A. V.; Fukin, G. K.; Trifonov, A. A., *Inorg. Chem.* **2016**, *55*, 1236-1244.
- (44) Kissel, A. A.; Mahrova, T. V.; Lyubov, D. M.; Cherkasov, A. V.; Fukin, G. K.; Trifonov, A. A.; Del Rosal, I.; Maron, L., *Dalton Trans.* **2015**, *44*, 12137-12148.
- (45) Wicht, D. K.; Kourkine, I. V.; Kovacik, I.; Glueck, D. S.; Concolino, T. E.; Yap, G. P. A.; Incarvito, C. D.; Rheingold, A. L., *Organometallics* **1999**, *18*, 5381-5394.

- (46) Cox, P. A., *The Elements: Their Origin, Abundance, and Distribution*. Oxford University Press: Oxford 1989.
- (47) Ganushevich, Y. S.; Miluykov, V. A.; Polyancev, F. M.; Latypov, S. K.; Lonnecke, P.; Hey-Hawkins, E.; Yakhvarov, D. G.; Sinyashin, O. G., *Organometallics* **2013**, *32*, 3914-3919.
- (48) Edwards, P. G.; Malik, K. M. A.; Ooi, L.-l.; Price, A. J., *Dalton Trans.* **2006**, 433-441.
- (49) Chen, G.-Q.; Kehr, G.; Daniliuc, C. G.; Wibbeling, B.; Erker, G., *Chem. Eur. J.* **2015**, *21*, 12449-12455.
- (50) Erickson, K. A.; Dixon, L. S. H.; Wright, D. S.; Waterman, R., *Inorg. Chim. Acta* **2014**, *422*, 141-145.
- (51) Espinal-Viguri, M.; King, A. K.; Lowe, J. P.; Mahon, M. F.; Webster, R. L., *ACS Catal.* **2016**, *6*, 7892-7897.
- (52) Espinal-Viguri, M.; Mahon, M. F.; Tyler, S. N. G.; Webster, R. L., *Tetrahedron* **2017**, *73*, 64-69.
- (53) Gallagher, K. J.; Espinal-Viguri, M.; Mahon, M. F.; Webster, R. L., *Adv. Synth. Catal.* **2016**, *358*, 2460-2468.
- (54) King, A. K.; Buchard, A.; Mahon, M. F.; Webster, R. L., *Chem. Eur. J.* **2015**, *21*, 15960-15963.
- (55) King, A. K.; Gallagher, K. J.; Mahon, M. F.; Webster, R. L., *Chem. Eur. J.* **2017**, *23*, 9039-9043.

- (56) Routaboul, L.; Toulgoat, F.; Gatignol, J.; Lohier, J.-F.; Norah, B.; Delacroix, O.; Alayrac, C.; Taillefer, M.; Gaumont, A.-C., *Chem. Eur. J.* **2013**, *19*, 8760-8764.
- (57) Stelmach, J. P. W.; Bange, C. A.; Waterman, R., *Dalton Trans.* **2016**, *45*, 6204-6209.
- (58) Ghebreab, M. B.; Shalumova, T.; Tanski, J. M.; Waterman, R., *Polyhedron* **2010**, *29*, 42-45.
- (59) Crimmin, M. R.; Barrett, A. G. M.; Hill, M. S.; Hitchcock, P. B.; Procopiou, P. A., *Organometallics* **2008**, *27*, 497-499.
- (60) Crimmin, M. R.; Barrett, A. G. M.; Hill, M. S.; Hitchcock, P. B.; Procopiou, P. A., *Organometallics* **2007**, *26*, 2953-2956.
- (61) Hu, H.; Cui, C., *Organometallics* **2012**, *31*, 1208-1211.
- (62) Gusarova, N. K.; Shaikhutdinova, S. I.; Kazantseva, T. I.; Malysheva, S. F.; Sukhov, B. G.; Belogorlova, N. A.; Dmitriev, V. I.; Trofimov, B. A., *Russ. J. Gen. Chem.* **2002**, *72*, 371-375.
- (63) Basalov, I. V.; Rosca, S. C.; Lyubov, D. M.; Selikhov, A. N.; Fukin, G. K.; Sarazin, Y.; Carpentier, J.-F.; Trifonov, A. A., *Inorg. Chem.* **2014**, *53*, 1654-1661.
- (64) Busacca, C. A.; Farber, E.; De Young, J.; Campbell, S.; Gonnella, N. C.; Grinberg, N.; Haddad, N.; Lee, H.; Ma, S.; Reeves, D.; Shen, S.; Senanayake, C. H., *Org. Lett.* **2009**, *11*, 5594-5597.
- (65) Roering, A. J.; Maddox, A. F.; Elrod, L. T.; Chan, S. M.; Ghebreab, M. B.; Donovan, K. L.; Davidson, J. J.; Hughes, R. P.; Shalumova, T.; MacMillan, S. N.; Tanski, J. M.; Waterman, R., *Organometallics* **2009**, *28*, 573-581.

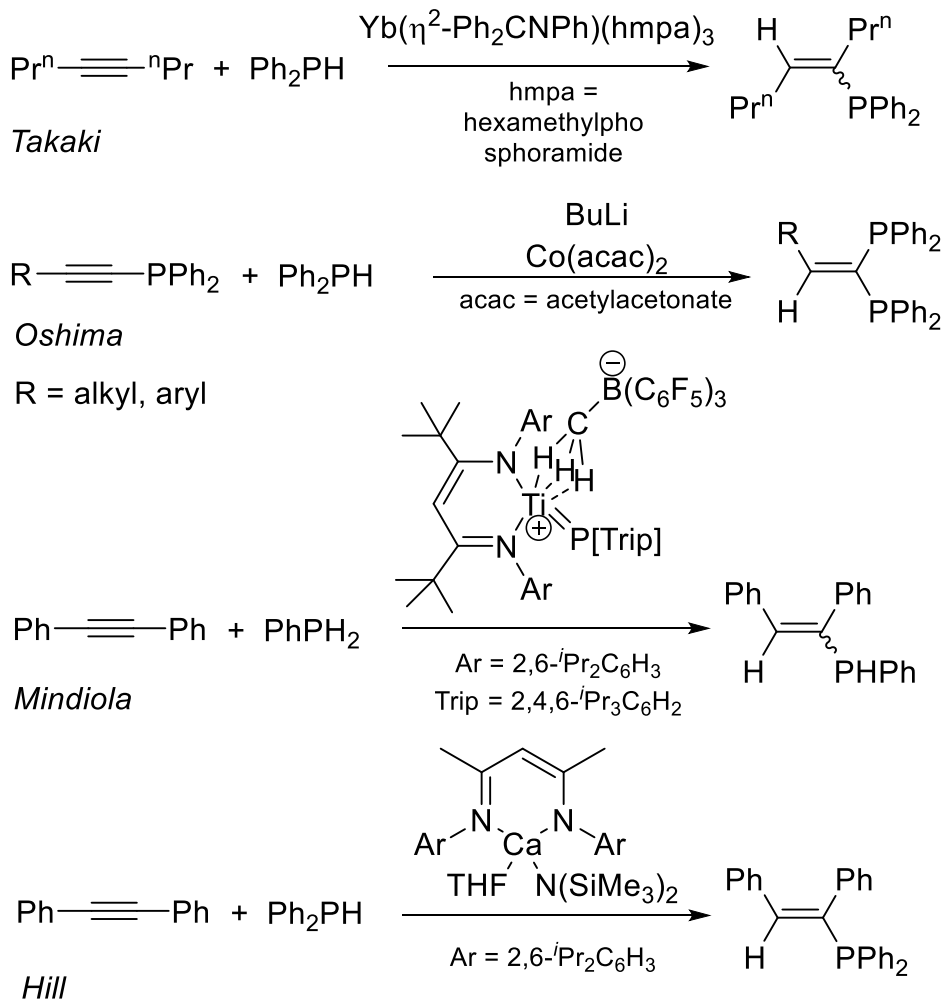
- (66) Glueck, D. S., *Chem. Eur. J.* **2008**, *14*, 7108-7117.
- (67) Scriban, C.; Glueck, D. S., *J. Am. Chem. Soc.* **2006**, *128*, 2788-2789.
- (68) Davies, L. H.; Wallis, J. F.; Probert, M. R.; Higham, L. J., *Synthesis* **2014**, *46*, 2622-2628.
- (69) Davies, L. H.; Stewart, B.; Higham, L. J., *Organomet. Chem.* **2014**, *39*, 51-71.
- (70) Nigam, S.; Burke, B. P.; Davies, L. H.; Domarkas, J.; Wallis, J. F.; Waddell, P. G.; Waby, J. S.; Benoit, D. M.; Seymour, A.-M.; Cawthorne, C.; Higham, L. J.; Archibald, S. J., *Chem. Commun.* **2016**, *52*, 7114-7117.
- (71) Scriban, C.; Glueck, D. S.; Zakharov, L. N.; Kassel, W. S.; DiPasquale, A. G.; Golen, J. A.; Rheingold, A. L., *Organometallics* **2006**, *25*, 5757-5767.
- (72) Ficks, A.; Sibbald, C.; Ojo, S.; Harrington, R. W.; Clegg, W.; Higham, L. J., *Synthesis* **2013**, *45*, 265-271.
- (73) Fluck, E.; Issleib, K., *Chem. Ber.* **1965**, *98*, 2674-2680.

## CHAPTER 3: ZIRCONIUM-CATALYZED DOUBLE HYDROPHOSPHINATION OF ALKYNES WITH PRIMARY PHOSPHINES

### 3.1 Introduction

The limited number of examples of metal catalysts that functionalize alkynes compared to alkenes suggests that alkyne hydrophosphination may be more nuanced.<sup>1</sup> Because the carbon–carbon triple bond of an alkyne displays greater reactivity than an alkene, it is perhaps understandable that the relative scarcity of alkyne hydrophosphination catalysts may be due to greater factors than just the alkyne itself. For example, the C–H proton of a terminal alkyne is relatively acidic.<sup>2</sup> The formation of terminal metal alkynyl species or metal hydride species upon introduction of the alkyne may be in part to blame for the underdevelopment of catalytic alkyne hydrophosphination relative to alkene hydrophosphination.<sup>3</sup>

Only few hydrophosphination catalysts are reported with internal alkynes, and the mechanistic details of these catalysts are only somewhat understood. In general, late-transition metal catalysts operate via nucleophilic attack of the phosphide on an electron-rich unsaturated substrate and frequently require a base as a co-catalyst.<sup>4</sup> Early transition-metal, alkaline earth, and lanthanide  $d^0$  systems do not require a base as a co-catalyst, and generally proceed through insertion-type chemistry.<sup>4</sup> A notable exception here is a triphosphinidene catalyst that proceeds via [2+2] cycloaddition.<sup>5</sup> These  $d^0$  metal catalysts were the first to operate with unactivated alkenes and alkynes, a feat that late-metal catalysts have yet to achieve.<sup>4</sup>



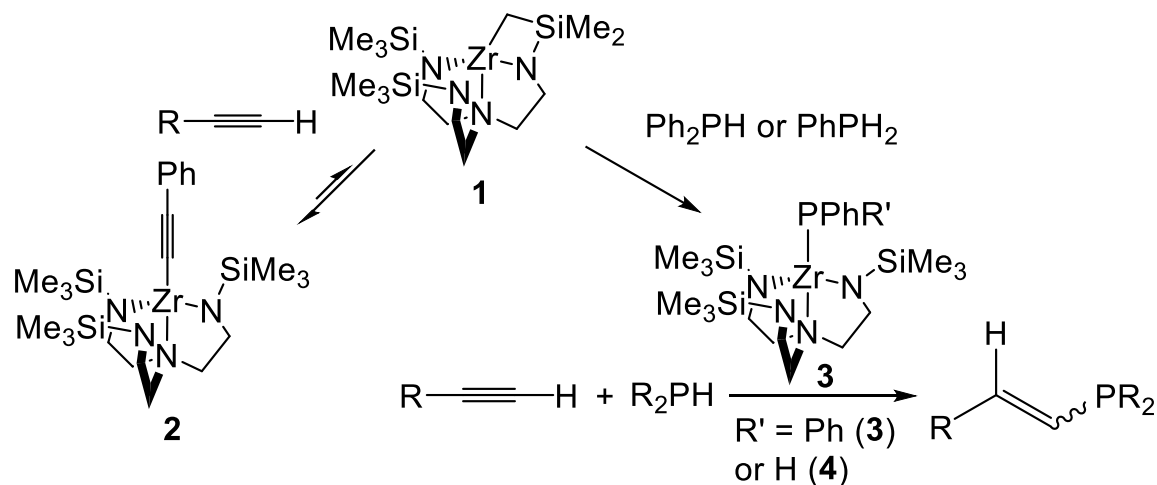
**Scheme 3.1:** Metal catalysts for alkyne hydrophosphination

A handful of alkyne hydrophosphination catalysts are shown in Scheme 3.1. All of these catalysts produce vinyl phosphines from a single hydrophosphination of the alkyne. Takaki's  $d^0$  ytterbium catalyst was one of the first to tackle unactivated alkynes (Scheme 3.1, entry 1).<sup>6</sup> Oshima's catalyst proceeded with excellent selectivity for the single hydrophosphination of a variety of alkynes, including unactivated species<sup>7</sup> (Scheme 3.1, entry 2). While both Mindiola's<sup>5</sup> and Hill's<sup>8</sup> catalyst functionalize diphenylacetylene, Hill's proceeds *via* alkyne insertion, whereas Mindiola's proceeds *via* [2+2] cycloaddition

to the alkyne (Scheme 3.1, entries 3 and 4). Hill's system selects for the *E* isomer, whereas Mindiola's produces mixtures of both *E* and *Z*.<sup>5, 8</sup>

Late metal hydrophosphination catalysts often require nucleophilic attack of the phosphide on the alkyne as the crucial P–C bond forming step in catalysis.<sup>4</sup> Because the majority of metal catalysts for hydrophosphination are late-metal systems, development of alkyne hydrophosphination catalysts may be thwarted by the electronic nature of these catalysts. The alkyne might be too electron-rich to cooperate with nucleophilic attack.

Investigation of [ $\kappa^5$ –*N,N,N,N*, *C*–(Me<sub>3</sub>SiNCH<sub>2</sub>CH<sub>2</sub>)<sub>2</sub>NCH<sub>2</sub>CH<sub>2</sub>NSiMe<sub>2</sub>CH<sub>2</sub>]*Zr* **1** for alkyne hydrophosphination unveiled new reactivity. While **1** has been studied as an alkyne hydrophosphination catalyst in its hydrophosphination debut, this reactivity was limited (Scheme 3.2).<sup>3</sup>



**Scheme 3.2:** Hydrophosphination of terminal alkynes and secondary phosphines with **1**

Terminal alkyne hydrophosphination with  $Ph_2PH$  and **1** is susceptible to ring-opening to form the stable terminal zirconium-alkynyl compound **2**.<sup>3</sup> Compound **2** is so stable that hydrophosphination with  $Ph_2PH$  was restricted by the reversion of **2** to **1**. This

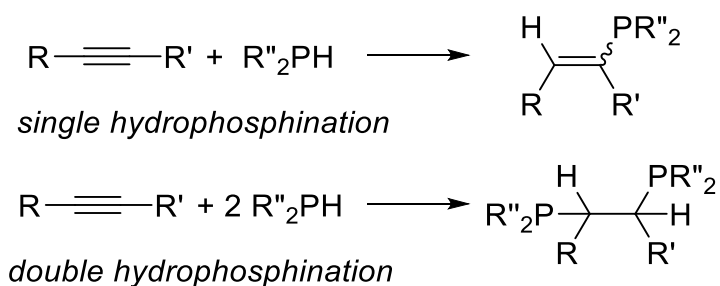
counterproductive pathway resulted in sluggish catalysis based on substrate inhibition. It is worth noting that  $\text{Ph}_2\text{PH}$  is also culpable in the limited reactivity. Secondary phosphines are simply too big for productive hydrophosphination with **1**. Formation and regeneration of **3**, the active species in hydrophosphination, was thought to contribute to the overall limited catalytic turnover. Regardless, alkynes had been deliberately shunned in the Waterman group for catalytic hydrophosphination with **1** for some time.

Reinvestigation of alkynes substrates as hydrophosphination candidates came after observation of the enhanced reactivity of **1** with primary phosphines.<sup>1, 9-11</sup> Previous investigations revealed that the reaction of terminal alkynes with  $\text{PhPH}_2$  gave consistent, analogous results to hydrophosphination with  $\text{Ph}_2\text{PH}$ .<sup>3</sup> This comes as no surprise. The formation of the analogous metal alkynyl species to **2** still appeared in the reaction of phenylacetylene with  $\text{PhPH}_2$  (Scheme 3.2).

After the success of alkenes and primary phosphines for hydrophosphination with this catalyst, primary phosphines became a mainstay in our hydrophosphination chemistry with **1**.<sup>1, 9-11</sup> This new chemistry availed alkynes because primary phosphine hydrophosphination proved to be more efficient. While terminal alkynes still posed the threat of unproductive ring-opening to make analogues of **2**, internal alkynes did not.

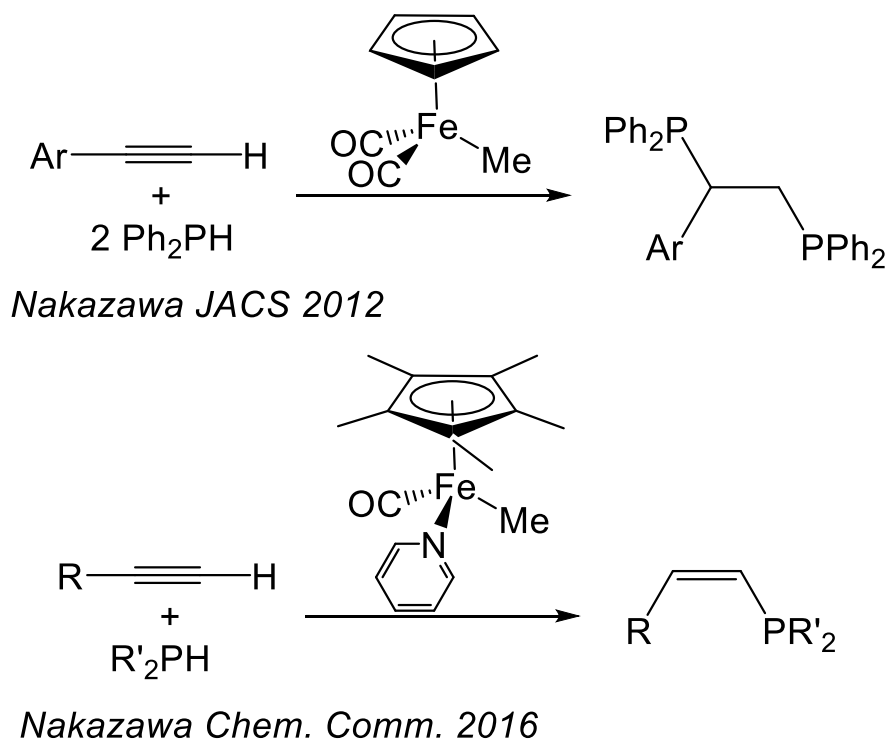
Alkynes present two opportunities for functionalization. That is, a single hydrophosphination event can occur to make a vinyl phosphine, or two sequential hydrophosphination events can occur as a double hydrophosphination<sup>1</sup> (Scheme 3.3).





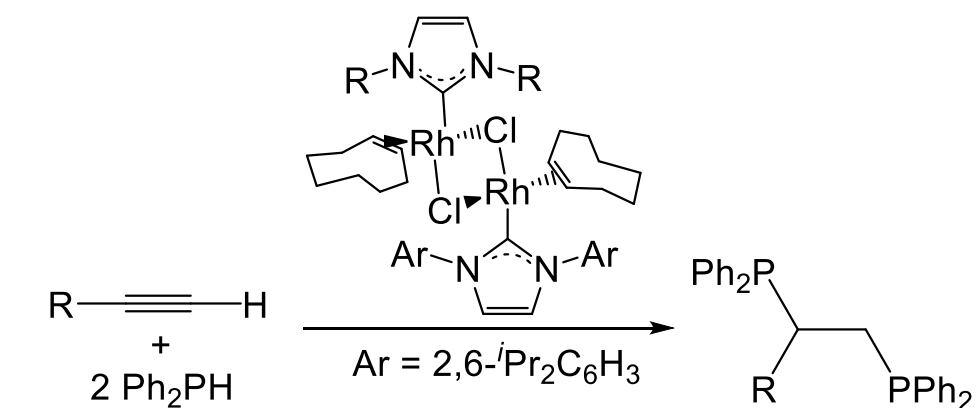
**Scheme 3.3:** Single and double hydrophosphination of alkynes

The first example of the latter reaction was reported by Nakazawa in 2012.<sup>12</sup> That work featured terminal aryl alkyne hydrophosphination with  $\text{Ph}_2\text{PH}$  to make double hydrophosphination products selective for the 1,2-addition. The authors later expanded on that idea with a related iron catalyst to generate vinyl phosphines selectively from alkynes using only one equivalent of  $\text{Ph}_2\text{PH}$ <sup>13</sup> (Scheme 3.4).

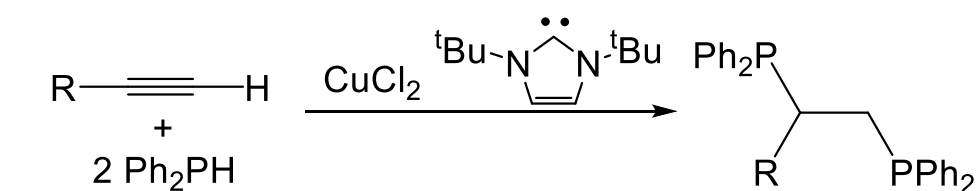


**Scheme 3.4:** Nakazawa's system for the single or double hydrophosphination of alkynes

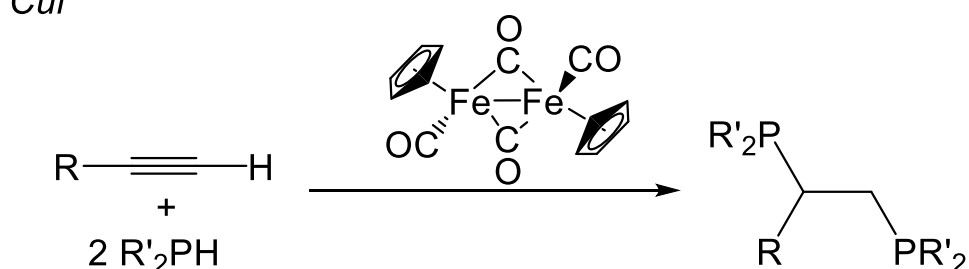
More recently systems emerged. Oro presented a suite of rhodium catalysts<sup>14</sup> and Cui found a simple  $\text{CuCl}_2/\text{NHC}$  system<sup>15</sup> for the double hydrophosphination of terminal alkynes with  $\text{Ph}_2\text{PH}$  (Scheme 3.5, entries 1 and 2). While both systems required terminal alkynes and sterically minimized secondary phosphines, Oro's system suffered from poor conversions and minimal selectivity. Cui's copper catalyst was highly efficient by the limited standards of this difficult transformation.<sup>15</sup> Our group recently reported the double hydrophosphination of terminal alkynes with a family of secondary phosphines using a commercially available iron catalyst (Scheme 3.5, entry 3).



*Oro*



*Cui*



*Waterman*

**Scheme 3.5:** Late-metals for the double hydrophosphination of alkynes

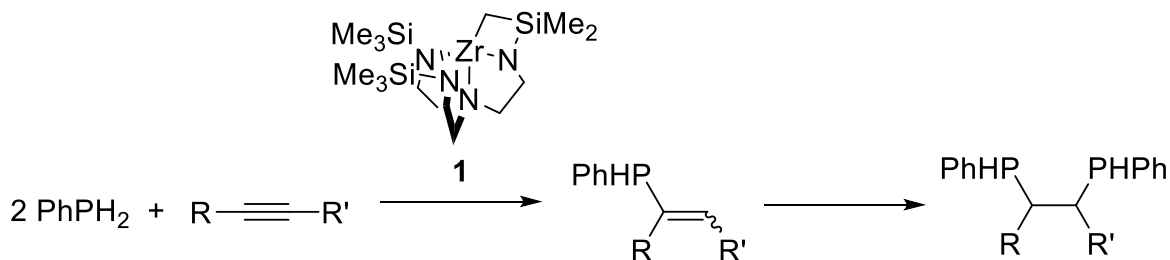
While the nascent double hydrophosphination of terminal alkynes has grown substantially in recent years, significant hurdles remain.<sup>1</sup> For example, primary phosphines were absent in this reactivity entirely until our report. Double hydrophosphination of alkynes with primary phosphines to selectively provide secondary phosphines would be of interest; these 1,2-bis(phosphines) enjoy a wide audience as ligands. The ability to further functionalize these products to make tertiary phosphines, potentially P-chirogenic, was

enticing. Furthermore, the currently known double hydrophosphination systems only cooperate with terminal, electron-rich alkynes.<sup>12-15</sup> Systems that can catalyze a double hydrophosphination of alkynes on unactivated substrates remained unseen. The work in this chapter addresses the substrate gaps in catalytic alkyne double hydrophosphination with respect to both the alkynes (e.g. internal, unactivated) and the phosphine scope.

### 3.2 Results and Discussion

#### 3.2.1 Single hydrophosphination to make vinyl phosphines

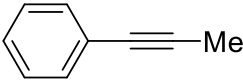
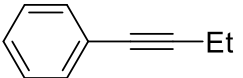
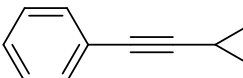
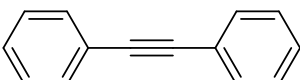
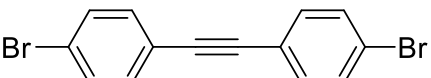
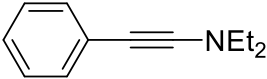
Consideration of our system for the *double* hydrophosphination of alkynes with PhPH<sub>2</sub> came as an unintended result of attempting alkyne hydrophosphination. Treatment of two equivalents of PhPH<sub>2</sub> to alkyne substrate provided mixtures of the single hydrophosphination and double hydrophosphination products<sup>16</sup> (Scheme 3.6).



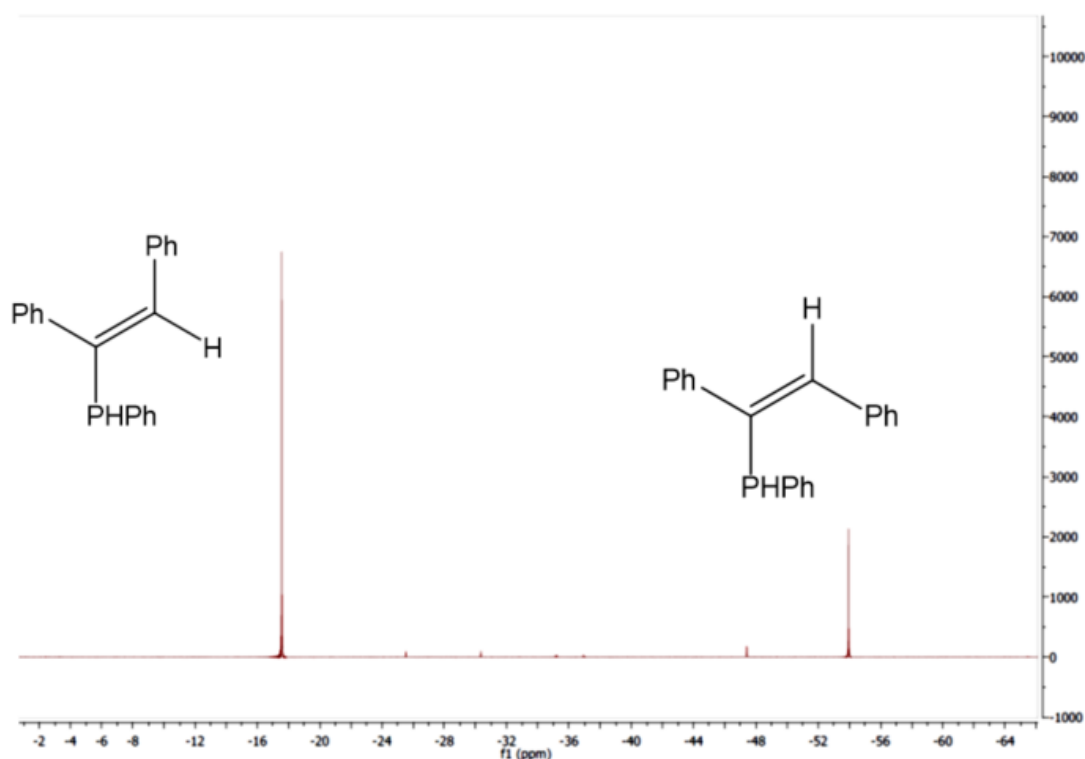
**Scheme 3.6:** Single and double hydrophosphination of alkynes with **1**

Catalysis proceeds via formation of the catalytically active zirconium phosphide **4**. Reinvestigation of challenging substrates also considered a far more prolific substrate: internal alkynes. These species are uncommon substrates for hydrophosphination, even ones with relatively little steric encumbrance. However, treatment of two equivalents of PhPH<sub>2</sub> to internal alkyne substrate with 5 mol % of **1** in the presence of a 9-W LED visible light results in production of the vinyl phosphine (Table 3.1).

**Table 3.1:** Zirconium-catalyzed single hydrophosphination of alkynes targeting vinyl phosphines. <sup>a</sup>Reactions run in a PTFE-valved NMR tube, heated, to 80 °C under visible irradiation. Conversion to product phosphines determined by <sup>31</sup>P NMR integration. Values in parentheses represent isolated yields. <sup>b</sup>Reaction run at ambient temperature.

$2 \text{ PhPH}_2 + \text{R} \text{---} \text{C} \equiv \text{C} \text{---} \text{R}' \xrightarrow[\text{C}_6\text{D}_6, \text{ LED light}]{5 \text{ mol } \% \text{ 1}, 80^\circ\text{C}, 15 \text{ h}} \text{PhHP} \begin{matrix} \diagup \\ \text{R} \end{matrix} \text{C} = \text{C} \begin{matrix} \diagdown \\ \text{R}' \end{matrix}$			
Entry	Substrate	Conversion (%)	<i>E</i> : <i>Z</i> Ratio
1a		99 (78)	5.1 : 1
1b		99	1.9 : 1
1c		96	1.8 : 1
1d		89 (64)	3.1 : 1
1e		75	3.7 : 1
1f	Me—C≡C—Me	96 (76)	3.5 : 1
1g	Et—C≡C—Et	88 (70)	1 : 1.5
1g	Bu—C≡C—Bu	59 (41)	1 : 1.8
1h		46	1 : 1.2
1h	Et <sub>2</sub> N—C≡C—NEt <sub>2</sub>	85	15.5 : 1

The product phosphines are formed as a mixture of *E* and *Z* isomers and can be isolated in yields up to 78%. Isomer assignments were made following a report from Mindiola.<sup>5</sup>



**Figure 3.1:** *E* and *Z* isomers from the single hydrophosphination of diphenylacetylene with two equivalents of  $\text{PhPH}_2$  and 5 mol % **1**

The *E* and *Z* isomers have substantially different  $^{31}\text{P}$  chemical shifts. While the *Z* isomer resonates in the typical region for secondary phosphines, the *E* isomer has a considerably downfield chemical shift due to a lower electron density at phosphorus. The P–H protons resonate at 5.07 ppm ( $J_{\text{PH}} = 218$  Hz) and 5.38 ppm ( $J_{\text{PH}} = 224$  Hz) for the *E* and *Z* isomers, respectively. The upfield chemical shift of the P–H proton of the *E* isomer is consistent with a greater shielding at the proton, and greater deshielding at the phosphorus atom.

The preference for a stereoisomer is modest in all cases. While alkyne insertion at the Zr–PPh bond prefers the *anti*-Markovnikov product, orientation to selectively give an *E* or a *Z* isomer is not expressed. Alkyne insertion is quantitatively slower than that of

alkene insertion, which is probably an expression of the steric demands of the system. It cannot contort in such a way to relieve steric strain in the way that alkene substrates can. The alkyne has two possibilities upon insertion into the Zr–PPh bond. It can either orient the substrate up or down, providing the *Z* or the *E* isomer, respectively. The preference for putting the aryl substrate down is low, resulting in the slightly favorable formation of the *E* isomer. Alkyl substrates favor the *Z* isomer because they impose less steric hindrance than their aryl counterparts.

A recent report from Arnold's group on the catalytic hydrophosphination of either 3-hexyne or diphenylacetylene with primary phosphines showed the same preference for the *E* isomer.<sup>17</sup> However, these transformations were catalyzed by a thorium metallacycle, whose electronic properties are rather different than those of **1**, and only two substrates were reported, so comparison between these systems is limited. The reported alkyne double hydrophosphination catalysts with *secondary* phosphines show either a preference for the *Z* isomer<sup>12-13, 15</sup> or no preference at all.<sup>14</sup>

Hydrophosphination of unsymmetrical aryl/alkyl-substituted alkynes provides the secondary phosphine products with complete selectivity for formation of the new P–C bond at the alkyl-substituted position. This preference is novel for hydrophosphination reactions of this type, but may be a mere expression of sterics. Insertion of the substrate into the Zr–P bond may require specific orientation for proper alignment to occur, which may prerequisite hydrophosphination reactivity. The relatively high degree of electron-density at the alkyl side and lack of steric encumbrance, may allow for these substrates to better functionalized at the alkyl site.

This selectivity may be governed by more factors. Hydrophosphination of diarylacetylenes proceeded to give vinyl phosphines, indicating that the reaction is not in some way limited by the aromatics of the system. This is consistent with the working hypothesis that P–C bond-forming catalysis proceeds via insertion. Alkyl-alkynes are less restricted by sterics than aryl-alkynes, and this gives rise to the selectivity observed. However, the observed reaction of diaryl-alkynes suggests that catalysis is still productive even in the face of some degree of steric encumbrance.

Unactivated alkynes react readily to provide the corresponding vinyl phosphines (Table 3.1, entries 1f-1h). Hydrophosphination of 2-butyne provides the greatest conversion under these conditions as compared to the related dialkyl-substituted alkynes, which further demonstrates a steric dependence.

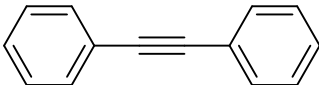
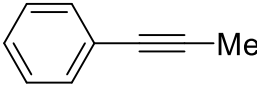
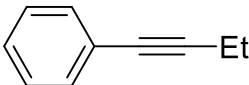
### **3.2.2 Double hydrophosphination to make diphosphines**

Treatment of a vinyl phosphine product with a second equivalent of  $\text{PhPH}_2$  provides the corresponding 1,2-bis(phosphino)ethane derivative as a mixture of *rac* and *meso* isomers. These secondary diphosphines can be produced either from an independent hydrophosphination event of the vinyl phosphine, or from a one-pot reaction of the starting alkyne and two equivalents of  $\text{PhPH}_2$  (Table 3.2).

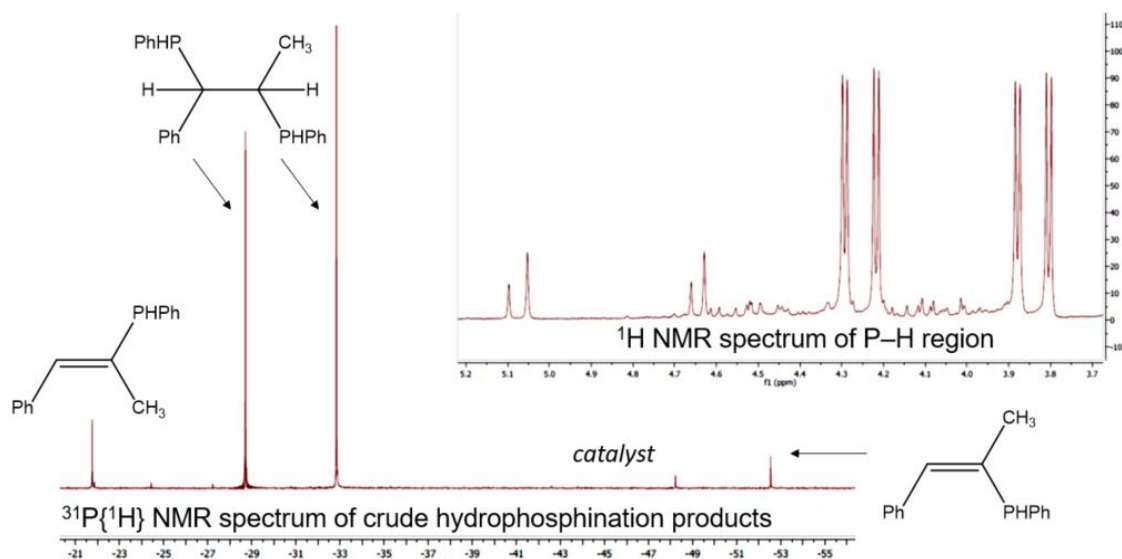


**Table 3.2:** Double hydrophosphination to make diphosphines. Reactions run in PTFE-valved NMR tubes, heated to 80 °C under visible irradiation. Conversion to product phosphines determined by  $^{31}\text{P}$  NMR integration.

$$2 \text{ PhPH}_2 + \text{R} \equiv \text{R}' \xrightarrow[\text{C}_6\text{D}_6, \text{ LED light}]{5 \text{ mol } \% \text{ 1}, 80^\circ\text{C}} \text{PhHP} \begin{array}{c} \diagup \\ \text{C} \\ \diagdown \end{array} \begin{array}{c} \text{R} \\ \text{R}' \end{array}$$

Entry <sup>a</sup>	Substrate	Time (d)	Conversion (%)
2a		9	78 (62)
2b		3	92 (71)
2c		6	88
2d	Me—≡—Me	4	96
2e	Et—≡—Et	4	78 (55)
2f	Bu—≡—Bu	7	73

Double hydrophosphination reactions from an alkyne first give the vinyl phosphine before the double hydrophosphination product. For example, hydrophosphination of methyl phenyl acetylene gives vinyl phosphine products detected at -21.8 ppm (*E* isomer) and -52.5 ppm (*Z* isomer), which then undergo the second hydrophosphination event to form *rac* and *meso* isomers at -28.7 and -32.9 ppm (Figure 3.2). The second, double hydrophosphination event can be noticed from the disappearance of P–H vinyl protons at 4.88 and 4.84 ppm ( $J_{\text{PH}} = 218$  and 212 Hz, respectively) and corresponding appearance of the diphosphine P–H protons at 4.09 and 4.02 ppm ( $J_{\text{PH}} = 207$  Hz, for each isomer).

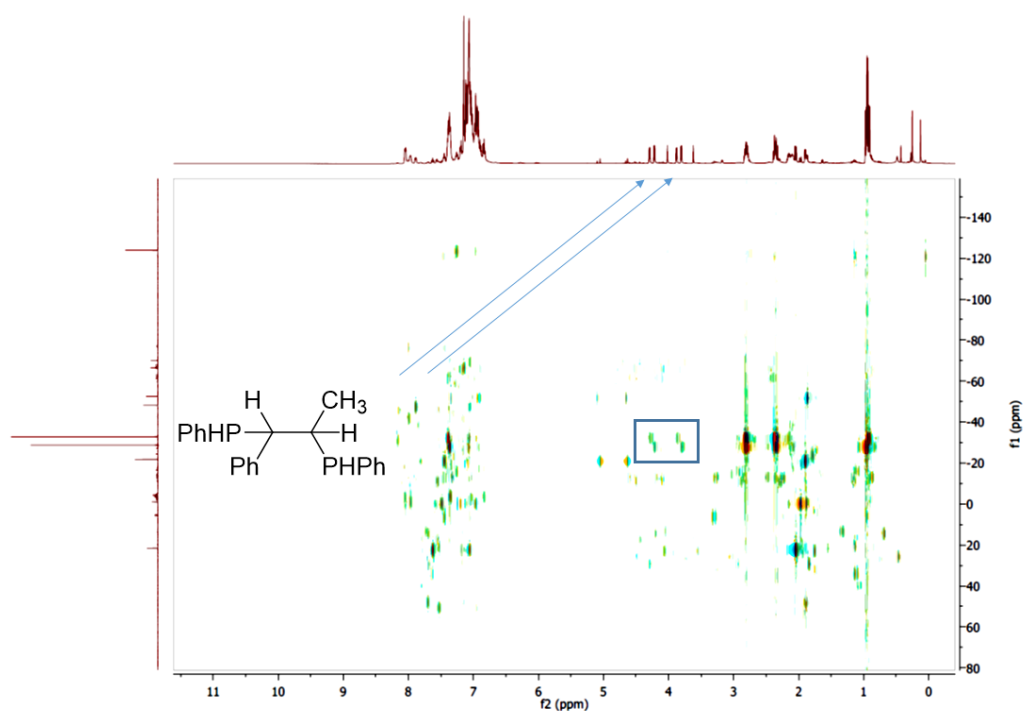


**Figure 3.2:** One-pot double hydrophosphination of methyl phenyl acetylene to form the diphosphines from the vinyl phosphines

All diphosphines are formed as mixtures of *rac* and *meso* isomers in high yields with  $^{31}\text{P}\{^1\text{H}\}$  NMR chemical shifts in the range of -28 to -41 ppm. The  $^1\text{H}$  NMR spectra also show P–H resonances as doublets of doublets for the double hydrophosphination products. These P–H resonances appear more upfield than their vinyl phosphine precursors, consistent with an increase in electron density around the nucleus, as anticipated. The P–H protons for these species appear as doublets of doublets with secondary phosphine P–H couplings. In all cases the 1,1-addition product was not detected.

Characterization of this novel class of phosphines presented some difficulties. To start, none of the diphosphines were known. These secondary phosphines were identifiable by NMR spectroscopy due to diagnostic P–H coupling as monitored by  $^1\text{H}$  and  $^{31}\text{P}$  NMR spectroscopy. Heteronuclear multiple bond coupling (HMBC) was employed to correlate  $^{31}\text{P}$  and  $^1\text{H}$  NMR spectra. This experiment gives information about P–H coupling that are two or three bonds away from each other.<sup>18</sup> For example, an HMBC spectrum of the crude

double hydrophosphination of methyl phenyl acetylene to form a mixture of the single and double hydrophosphination products shows the P–H bond correlations between the  $^1\text{H}$  phosphine protons and the  $^{31}\text{P}$  chemical shift (Figure 3.3). Protons from the vinyl phosphines and diphosphines are correlated, as expected, where P–H bonds from the vinyl phosphines appear at 4.88 and 4.84 ppm and are correlated to their  $^{31}\text{P}$  resonances at -28.7 and -32.9 ppm. Products of the double hydrophosphination product are identified by the box in Figure 3.3. These secondary phosphines can be assigned to the double hydrophosphination products. The methyl groups and tertiary C–H resonances from the diphosphine are also identified. The resonances between 2 and 3 ppm in the  $^1\text{H}$  NMR spectrum correlate to the major diphosphine isomers, and the methyl group resonance appears here as well.



**Figure 3.3:**  $^{31}\text{P}$ - $^1\text{H}$  HMBC spectrum of the one-pot hydrophosphination of methyl phenylacetylene

Other characterization methods such as  $^{31}\text{P}$  NMR spectroscopy coupled to proton also identified only secondary phosphine products. Products belonging to tertiary phosphine products, such as those from the dehydrocoupling from vinyl phosphines, were not detected. Vibrations from P–H bonds were detected during infrared spectroscopic investigation between  $2200\text{--}2300\text{ cm}^{-1}$  as is characteristic for secondary phosphines.<sup>19</sup>

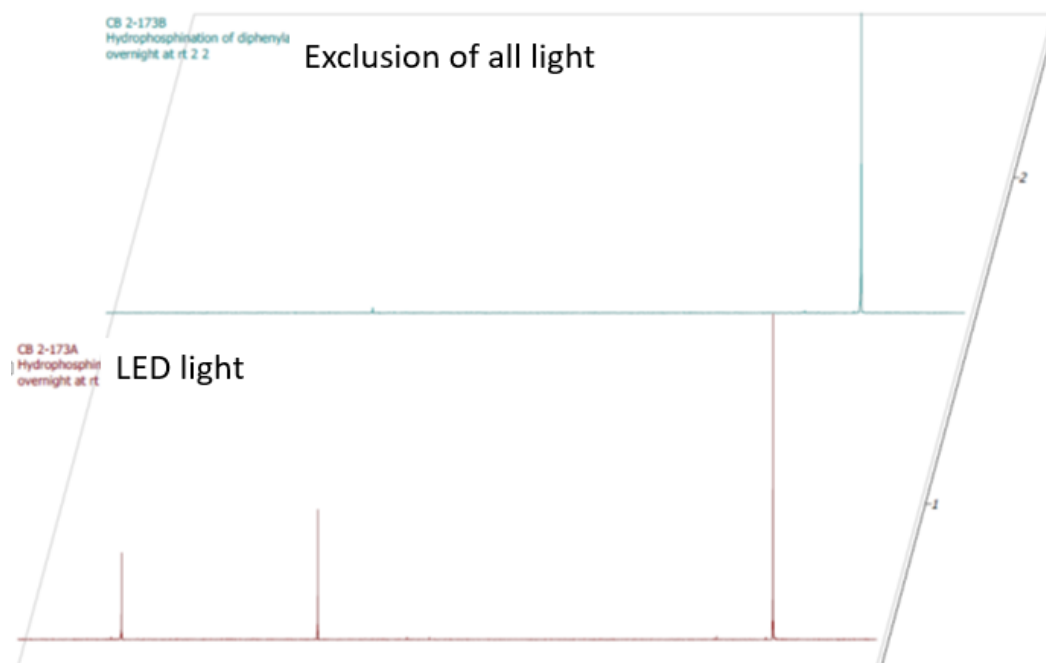
Unactivated alkynes are a challenging class of substrates for hydrophosphination.<sup>1</sup> However, these substrates are readily converted by **1** to double hydrophosphination products (Table 3.2, entries 2d–2f). The TONs for these unactivated substrates (TON = 14–19) are nearly identical to the TONs of aryl alkynes (TON = 15–18), suggesting that unactivated substrates are no less efficient than their more activated counterparts. This similarity may represent inhibition only by steric factors as hydrophosphination of diphenylacetylene had both a lower TON and TOF (TOF =  $8.7\text{ days}^{-1}$ ) than all other internal alkynes tested (TOF =  $10.4\text{ -- }30.7\text{ days}^{-1}$ ). The observation that catalytic hydrophosphination with **1** has comparable activity for both activated and unactivated alkynes represents a rare exception in this field.

The double hydrophosphination of alkynes required long reaction times (3–9 days) and elevated temperatures for conversion. Despite high NMR conversions, isolated yields of these products were relatively low due to challenges in purification. Diphosphines **2a**, **2b** and **2e** were isolated by ultra short-path distillation in several fractions. Unreacted alkyne and  $\text{PhPH}_2$  were first removed by reduced pressure and then the unreacted vinyl phosphine was removed by the first distillation. A second ultra-short path distillation returned the diphosphine in limited yields. Attempts to purify the diphosphine by

crystallization were successful in only a handful of cases. Secondary phosphines are known to be tricky to purify. Many research groups rely on intentional oxidation or borane protection before employing column chromatography. These methods were deliberately shunned to avoid further purification problems or lower isolated yields.

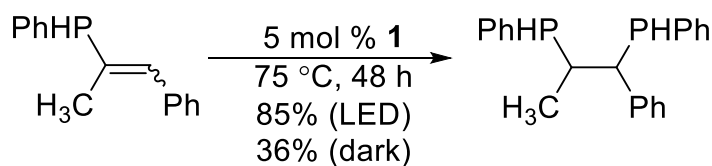
The long reaction times and elevated temperatures allowed for the unintentional, competitive dehydrocoupling to occur. This is an anticipated result since **1** is a known primary phosphine dehydrocoupling catalyst under similar conditions.<sup>20</sup> Double hydrophosphination run at lower temperatures returned both single and double hydrophosphination products without dehydrocoupling for some substrates (Figure 3.3), indicating that the dehydrocoupling does not precede hydrophosphination. That is, alkyne hydrophosphination from addition of PhHP–PPh to the substrate, either with or without **1**, is not explicitly required for bond-formation. Hydrophosphination of the vinyl phosphine with PhPH<sub>2</sub> targeting the double hydrophosphination product also concomitantly produced the competitive PhHP–PPh during catalysis during the long reaction times required for the second hydrophosphination event. Attempts to thwart competitive dehydrocoupling by lower temperatures or shorter reaction times also diminished the conversions to both single and double hydrophosphination products for most substrates, as expected.

In all hydrophosphination reactivity with **1** light irradiation from an LED bulb was required for catalysis. Reactions run in the absence of light failed to give detectable levels of hydrophosphination products under otherwise identical conditions (Figure 3.4).



**Figure 3.4:** Hydrophosphination of methyl phenyl acetylene targeting vinyl phosphines run in the absence of light (top) or irradiation from an LED lamp (bottom)

While the first catalytic hydrophosphination event to make the vinyl phosphines showed a complete requirement for light, it was suspected that light was not as important in the second event. For example, hydrophosphination of the vinyl phosphine products obtained from the hydrophosphination of methyl phenyl acetylene provided diminished, but significant, conversions to the double hydrophosphination products under the exclusion of light (Scheme 3.7).



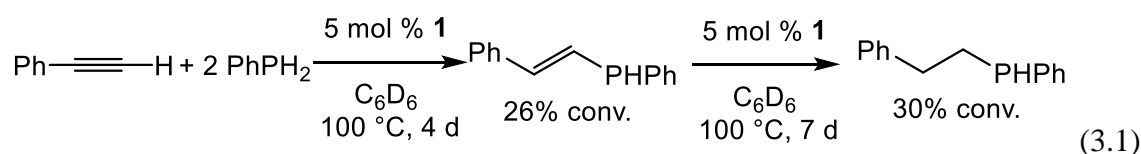
**Scheme 3.7:** Light dependence on the second hydrophosphination event

While thermal, catalytic hydrophosphination in the absence of light showed significant product conversions, it is not as light-dependent as the initial hydrophosphination step.

The light requirement for catalytic hydrophosphination remained intriguing. It is unlikely that a radical is involved in catalytic hydrophosphination with **1**, although radicals can hydrophosphinate a handful of substrates.<sup>21</sup> To test this idea, cyclopropyl phenyl acetylene was synthesized to test for the presence of a radical. The cyclopropyl group remained intact during catalysis, which discredits the idea that catalytic hydrophosphination proceeds via a radical intermediate, despite the strong light dependence.

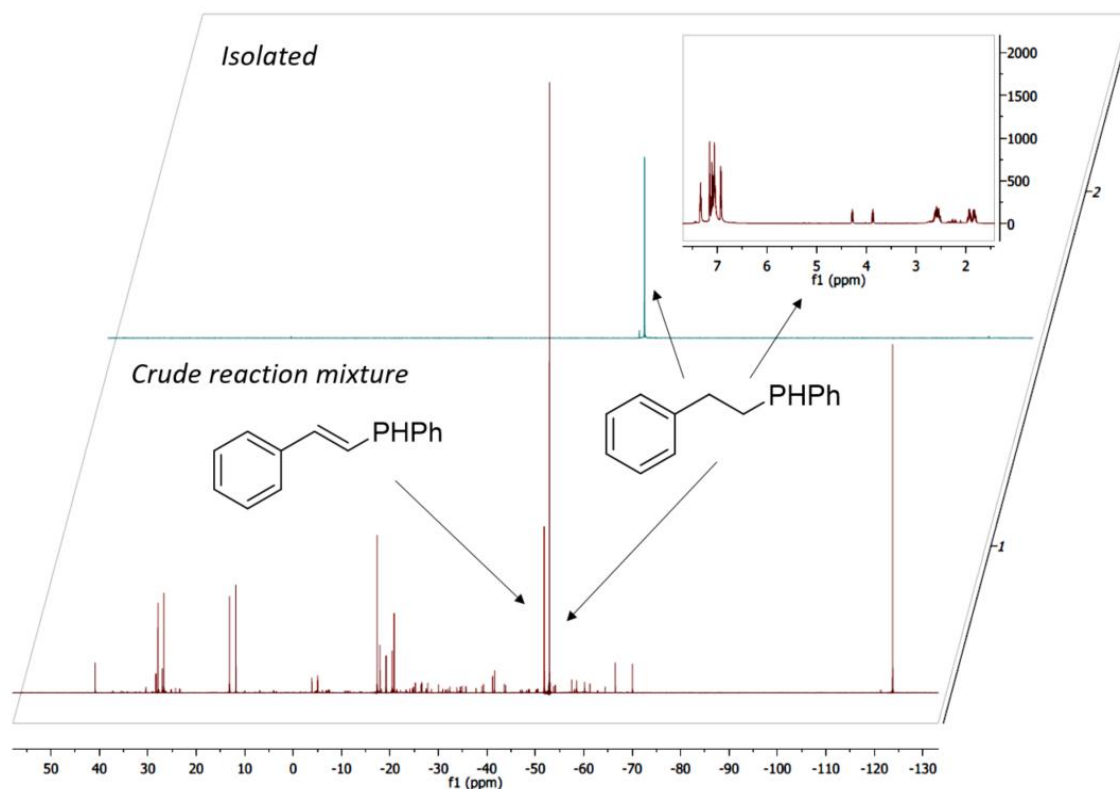
Terminal alkynes are known candidates for double hydrophosphination.<sup>12-14</sup> However, these substrates were not compatible for hydrophosphination with **1** and PhPH<sub>2</sub>. Attempted hydrophosphination of 1-hexyne only returned 5% conversion to the vinyl phosphine after eight days at 80 °C with a loss of *anti*-Markovnikov selectivity. Control reactions without **1** provided virtually identical results, indicating that this reaction is a thermal process rather than a catalytic one. The failure of **1** to hydrophosphinate terminal alkynes is anticipated. It is understood that terminal alkynes ring-open with **1** to form a stable terminal alkynyl compound that does not readily revert back to **1**.<sup>3</sup> However, terminal alkyne heterofunctionalization with either diphenyl phosphine or diphenylarsine with **1** provided products after extended reaction times and elevated temperatures.<sup>3, 22</sup> The catalyst inhibition was observed in spite of overall successful functionalization.

Treatment of phenylacetylene with two equivalents of PhPH<sub>2</sub> in the presence of **1** resulted in limited conversions to the single hydrophosphination product (eqn 3.1).



Extended reaction times failed to deliver the second hydrophosphination product and instead delivered the *hydrogenation* product, PhCH<sub>2</sub>CH<sub>2</sub>PPh<sub>2</sub> instead. This product is the known hydrophosphination product of styrene with PhPH<sub>2</sub>. This product has been prepared via catalytic hydrophosphination of styrene by **1**. The appearance of this product during the hydrophosphination of phenylacetylene is surprising. Compound **1** is a poor transfer hydrogenation catalyst,<sup>23</sup> though such forcing conditions were not tested in that report. Attempted hydrophosphination of phenylacetylene at these elevated temperatures and long reaction times provides, as anticipated, competitive dehydrocoupling of PhPH<sub>2</sub> to form PhHP–PPh<sub>2</sub> (*vide supra*) with concomitant buildup of H<sub>2</sub> in the sealed reaction vessel. Analysis of a crude <sup>31</sup>P NMR spectrum of this reaction after seven days revealed about 20% conversion of PhPH<sub>2</sub> to dehydrocoupled products (Figure 3.5).





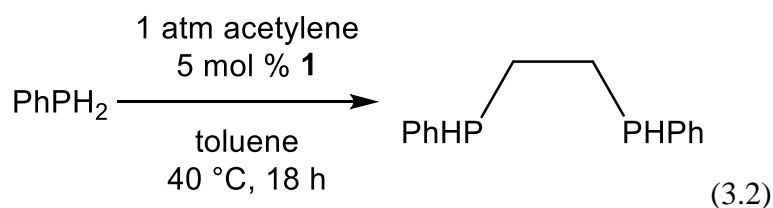
**Figure 3.5:** Attempted hydrophosphination of phenylacetylene

We hypothesize that the vinyl phosphine formed during the hydrophosphination of phenylacetylene with  $\text{PhPH}_2$  is converted to the hydrogenated product under these forcing conditions. It is worth noting that a related hydrophosphination system also suffered from competitive hydrogenation during the catalytic hydrophosphination of phenylacetylene.<sup>14</sup> Attempts to isolate the vinyl phosphine intermediate by vacuum distillation were hindered by the similar volatilities of both the vinyl and saturated phosphines. Isolation of the reaction product  $\text{PhCH}_2\text{CH}_2\text{PhPh}$  gave NMR spectra that were identical to those of the authentic compound.<sup>11, 24</sup> Hydrophosphination of *p*-tolylacetylene gave analogous results.

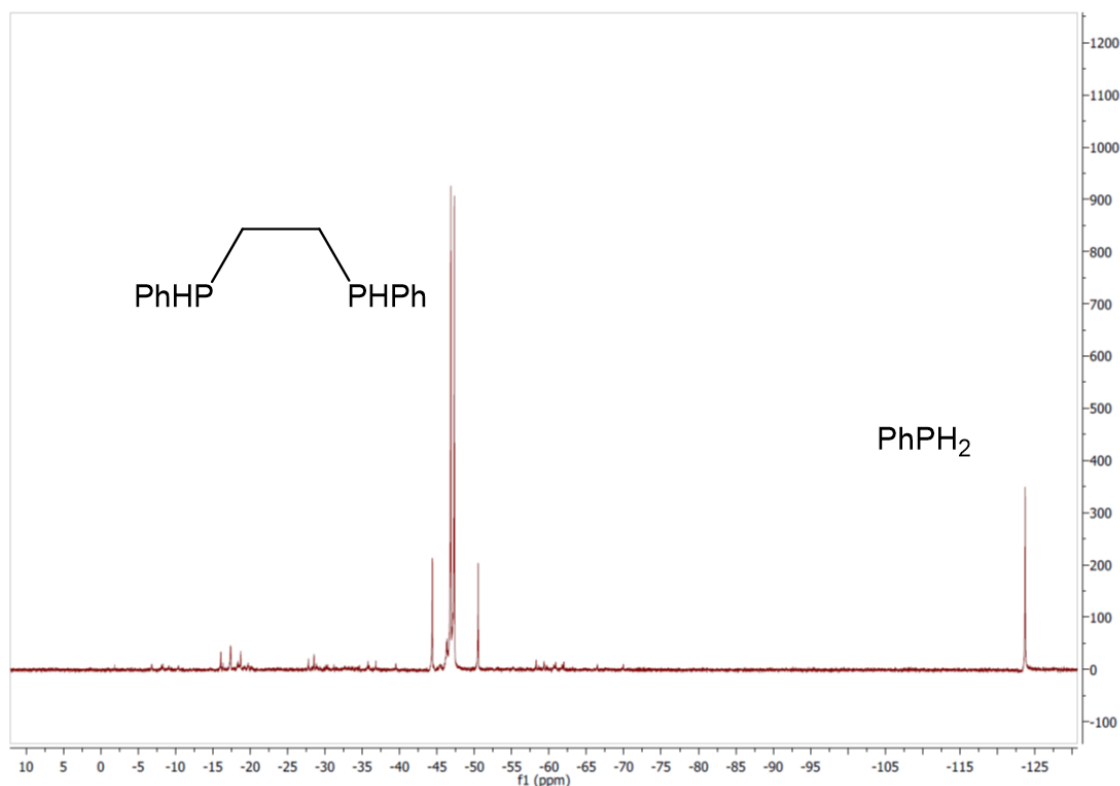
Secondary phosphines and primary phosphines have been known to undergo hydrophosphination with ethylene gas,<sup>25-28</sup> but hydrophosphination of acetylene was

unreported at the time of publication. However, functionalization of acetylene offers unparalleled opportunity for further synthesis of specialized diphosphines that are employed in an array of conventional transformations.

Heating a solution of  $\text{PhPH}_2$  in toluene with catalytic amounts of **1** under one atmosphere for acetylene resulted in 65% yield of 1,2-bis(phenylphosphino)ethane after 18 hours (eqn 3.2).



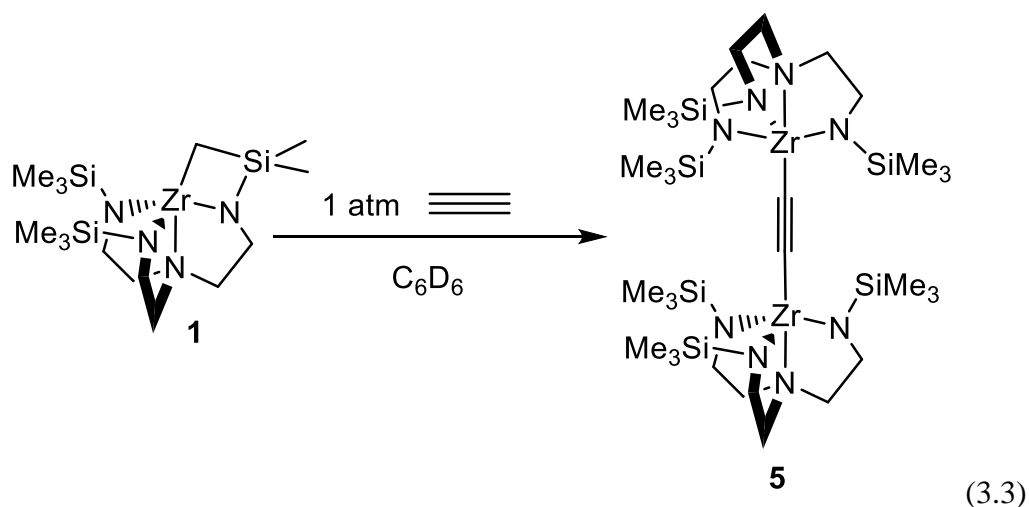
Removal of **1** by filtration through Celite followed by distillation affords the product as a 1:1 mixture of *rac* and *meso* isomers (Figure 3.6). Spectroscopic data for this product is identical to that previously reported.<sup>29</sup>



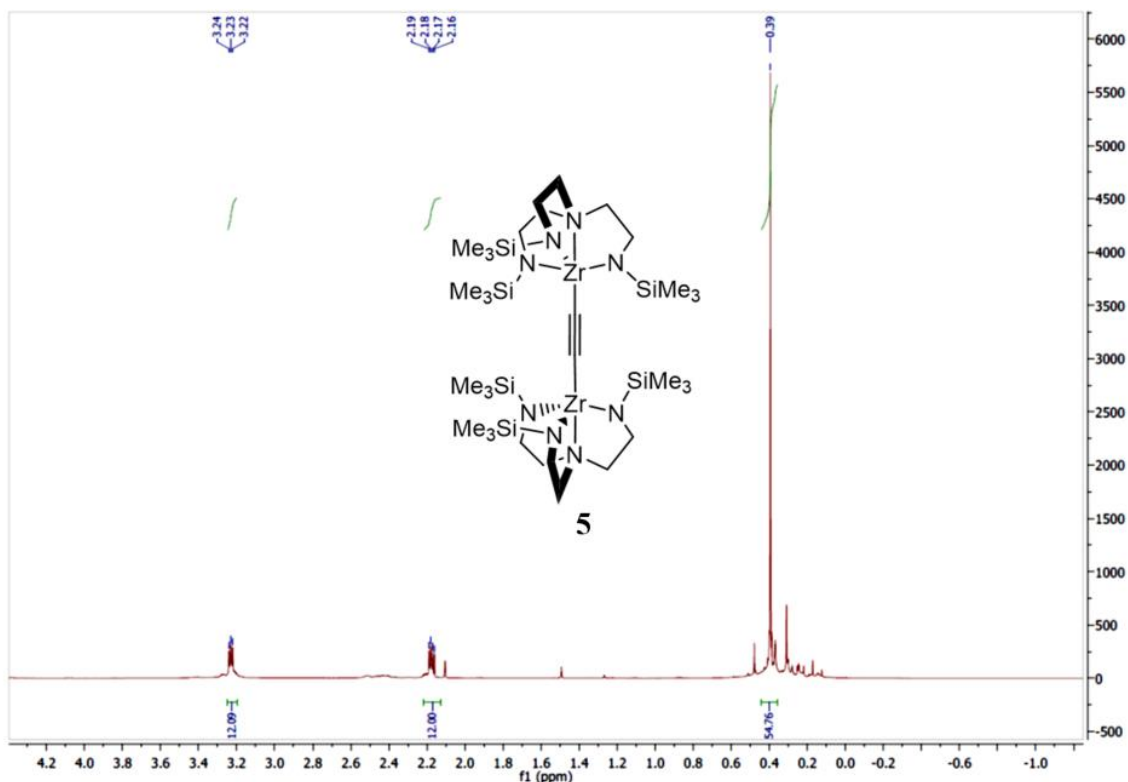
**Figure 3.6:** Crude  $^{31}\text{P}\{^1\text{H}\}$  NMR spectrum of the hydrophosphination of acetylene gas

Control experiments in which  $\text{PhPH}_2$  is heated in the absence of **1** fail to convert measurable amounts of 1,2-bis(phenylphosphino)ethane under otherwise identical conditions. It should be noted that the quality of acetylene gas is crucial for hydrophosphination to occur. Reactions run in samples of lesser purity failed to provide detectable amounts of hydrophosphination products.

Hydrophosphination of acetylene to 1,2-bis(phenylphosphino)ethane was surprising based on the reluctant catalytic activity of **1** with terminal alkynes. As expected, acetylene ring-opens **1** and forms the terminal acetylide compound **5** (eqn 3.3).



Compound **5** is a highly symmetric, bimetallic compound in which acetylene acts as a bridging ligand. This species displays four resonances in its  $^{13}\text{C}$  NMR spectrum, including a single alkyne peak at  $\delta$  94.2 ppm. The  $^1\text{H}$  NMR spectrum of **5** displays three single resonances. Two triplets at 3.2 and 2.2 ppm for the ligand backbone, and a singlet at 0.39 ppm for the trimethylsilyl substituents (Figure 3.7).



**Figure 3.7:**  $^1\text{H}$  NMR spectrum of **5**

Sublimation returned **5** as a nearly colorless solid, which is highly related to previously studied terminal alkynyl derivatives of **1**.<sup>3</sup> Treatment of **5** with one equivalent of  $\text{PhPH}_2$  gave no detectable ligand exchange after two days at 80 °C, which is similar to the sluggish reactivity of this class of zirconium alkynyl derivative  $(\text{N}_3\text{N})\text{ZrC}\equiv\text{CPh}$  towards  $\text{Ph}_2\text{PH}$ , despite the fact that both  $(\text{N}_3\text{N})\text{ZrC}\equiv\text{CPh}$  and **1** are active catalysts for the hydrophosphination of phenyl acetylene with  $\text{Ph}_2\text{PH}$ .

Two possibilities can be used to explain the catalytic reactivity in the face of apparent catalyst inhibition. First, it is hypothesized that **5** could revert back to **1** and acetylene or perhaps a single equivalent of  $(\text{N}_3\text{N})\text{ZrC}\equiv\text{CH}$  and **1** in the presence of  $\text{PhPH}_2$ . This was noted for the hydrophosphination of phenylacetylene and  $\text{Ph}_2\text{PH}$  in the presence

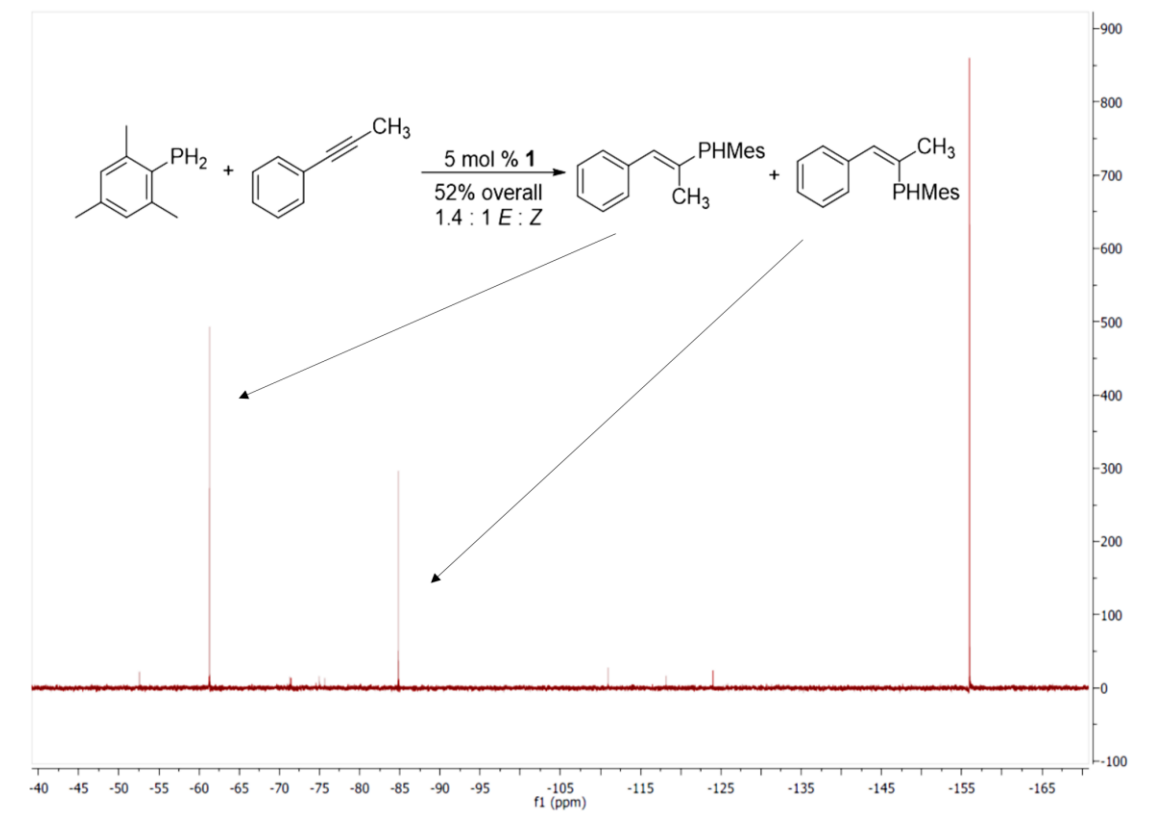
of **1**. A second hypothesis is that  $\text{PhPH}_2$  could participate in direct functionalization of **5**, resulting in liberation of the product vinyl phosphine (not detected). The former hypothesis seems more probable on the basis of literature precedent.<sup>3</sup>

Regardless, catalytic hydrophosphination of acetylene with  $\text{PhPH}_2$  is intriguing. Introduction of acetylene gas to the crude reaction mixture of  $\text{PhPH}_2$  and **1** results in an immediate color change from pale yellow to colorless, consistent with replacement of the phosphide ligand with that of acetylene. This is markedly different from hydrophosphination of internal alkynes with **1**, which keep their yellow color intact throughout. This indicates that internal alkyne hydrophosphination occurs using **3** as the active species in catalysis, as noted by the maintenance of the yellow color. Acetylene hydrophosphination may proceed by a different mechanism, as suggested by the color change, unless the formation of **3** occurs in such small amounts that the color is not visually detected.

### 3.2.3 Hydrophosphination with $\text{MesPH}_2$

An attractive idea was the possibility of doing a double hydrophosphination with two different phosphines to make a nonsymmetrical diphosphine. That is, a single hydrophosphination could be undertaken to provide the vinyl phosphine, which could then undergo a second hydrophosphination with a different primary phosphine to provide a heterosubstituted diphosphine. This reactivity would allow for virtually any diphosphine derivative to be achieved from a variety of simple starting materials. Derivatives of this type could give direct access to a variety of privileged ligand motifs and scaffolds that could be tailor-made.

Mesityl phosphine (mesityl = mes = 2,4,6-trimethylphenyl) was chosen for its ease of synthesis and moderate steric encumbrance. Treatment of  $\text{PCl}(\text{NEt}_2)_2$  with mesityl Grignard, followed by halogenation, provided  $\text{MesPCl}_2$ , which was then reduced to the desired  $\text{MesPH}_2$ .<sup>30</sup> Treatment of methyl phenyl acetylene with one equivalent of  $\text{MesPH}_2$  provided the targeted vinyl phosphines under catalytic conditions with **1** (Figure 3.8).

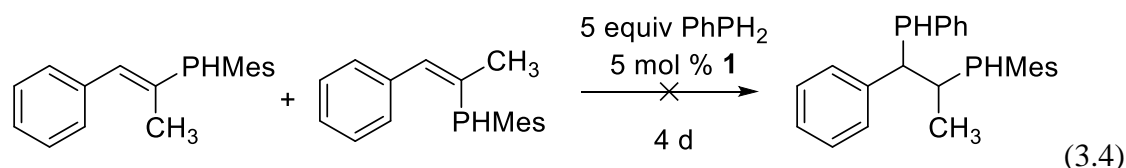


**Figure 3.8:** Hydrophosphination of methyl phenyl acetylene with  $\text{MesPH}_2$

As anticipated, the NMR conversions of the mesityl-substituted vinyl phosphines were substantially lower due to the increased steric bulk of the  $\text{MesPH}_2$  over  $\text{PhPH}_2$ . Vinyl phosphines made from the single hydrophosphination of methyl phenyl acetylene with  $\text{MesPH}_2$  display more upfield chemical shifts for the *E* and *Z* isomers. The selectivity for

catalytic hydrophosphination with **1** diminished. Alkyne hydrophosphination with MesPH<sub>2</sub> also requires irradiation for catalysis.

Treatment of the mesityl-substituted vinyl phosphines with excess PhPH<sub>2</sub> under catalytic conditions did not provide double hydrophosphination products, even after extended reaction times (eqn 3.4). The steric bulk of these vinyl phosphine products is simply too imposing to properly interact with the catalyst.



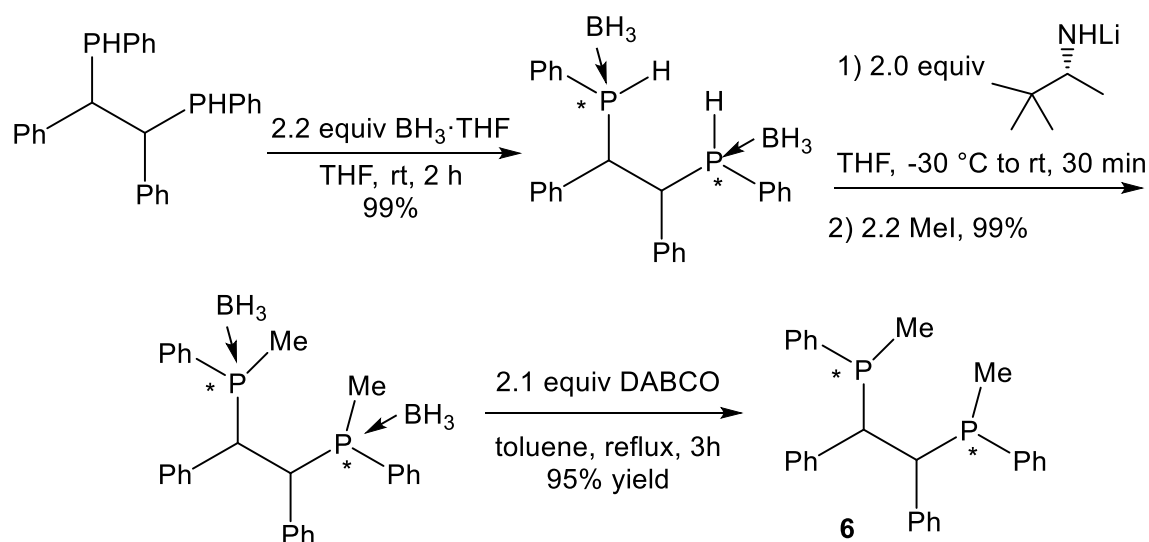
Attempts to diminish the steric hindrance of the system by using 3-hexyne instead of methyl phenyl acetylene still did not provide heterosubstituted diphosphines. Despite the promise of this reaction, the system suffered from inherently low tolerance for alkyne sterics during the second hydrophosphination event. The long reaction times required for even PhPH<sub>2</sub> double hydrophosphination (Table 3.2) are reflected in this limitation. Increased steric bulk of the products (and starting materials, in the case of the double hydrophosphination) impeded further catalytic reactivity.

### 3.2.4 Functionalization of double hydrophosphination products

Despite the limitations of the double hydrophosphination to provide asymmetric, heterosubstituted diphosphines, double hydrophosphination products from Table 3.2 can still become asymmetric. A large part of the appeal of generating secondary phosphines over tertiary phosphines is that secondary phosphine products can still be modified post-hydrophosphination. The high reactivity of the P–H bond allows for selective functionalization using known synthetic methodologies.<sup>21</sup>

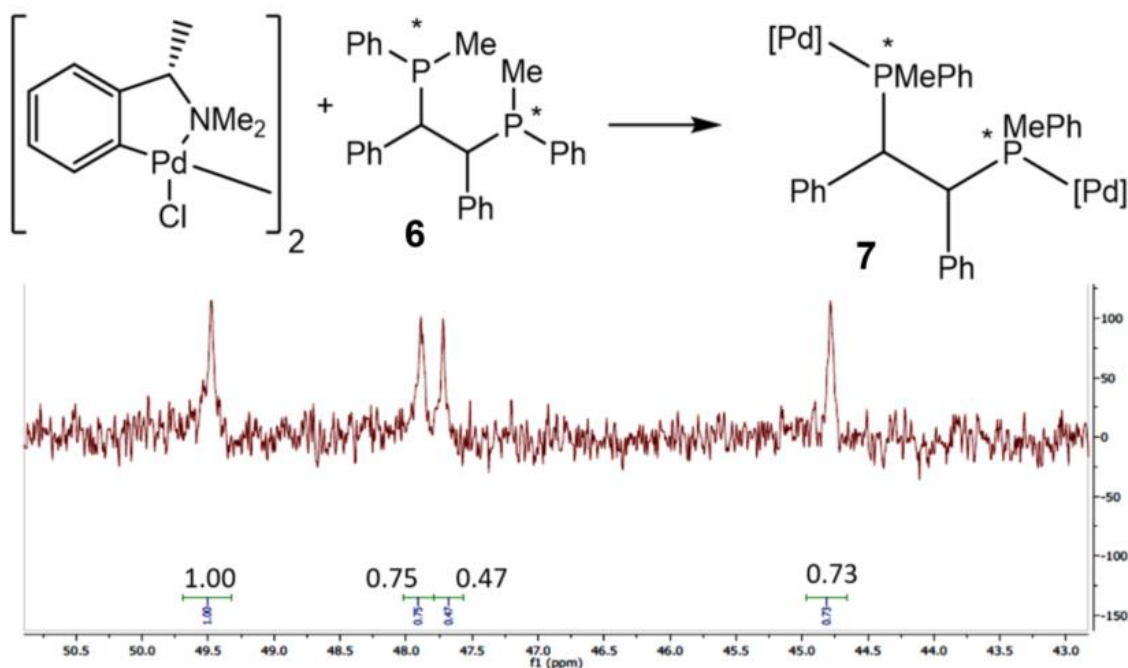


Protection of 1,2-diphenyl-1,2-bis(phenylphosphiny)ethane (Table 3.2, entry 2a) with borane,<sup>31</sup> followed by deprotonation with lithium (*R*)-(3,3-dimethylbutan-2-yl)amide and addition of the electrophile methyl iodide resulted in formation of the protected tertiary diphosphine (Scheme 3.8).



**Scheme 3.8:** Formation of asymmetric tertiary diphosphine from double hydrophosphination products

Deprotection of this species with DABCO (DABCO = 1,4-diazabicyclo[2.2.2]octane) removed the borane groups and provided the tertiary phosphine product **6**.<sup>32</sup> The final phosphine product had ambiguous chirality at the phosphorus center. Two singlets are observed in a ratio of 1:1.6. Because these resonances could be degenerate, a chiral reporter was employed to form **7**.<sup>33</sup> Upon binding to the metal center, the tertiary phosphines resonate at different frequencies, allowing for better detection of enantiomers (Figure 3.9).



**Figure 3.9:**  $^{31}\text{P}\{^1\text{H}\}$  NMR spectrum of the diphosphine with a chiral reporter

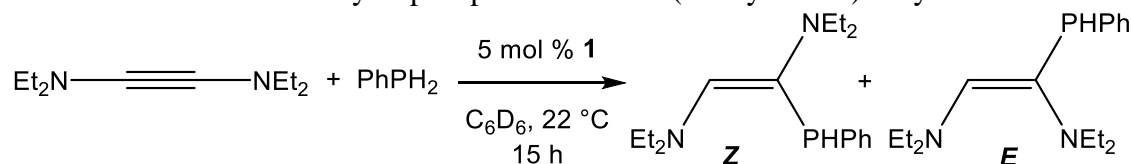
However, upon crystallization with **6**, four  $^{31}\text{P}$  resonances are seen. Compound **7** has two carbon and two phosphorus atoms that could be chiral. The presence of four  $^{31}\text{P}$  resonances does not clarify any structural details. However, because the inversion barrier for a tertiary phosphine is roughly 30 kcal per mol,<sup>34</sup> spontaneous inversion and corresponding loss of chirality at the phosphorus center is not a concern for this system. Because the ratio of isomers is not substantially high enough these efforts towards synthesizing chiral diphosphines were abandoned.

Compound **7** may not be big enough the methyl group introduced onto the phosphorus center may not be strong enough to influence the chirality at the phosphorus center. Future work targeting bulkier electrophiles may increase the ratio of isomers formed as newly tertiary phosphines.

### 3.4.5 Hydrophosphination and isomerization of bis(diethylamido)acetylene

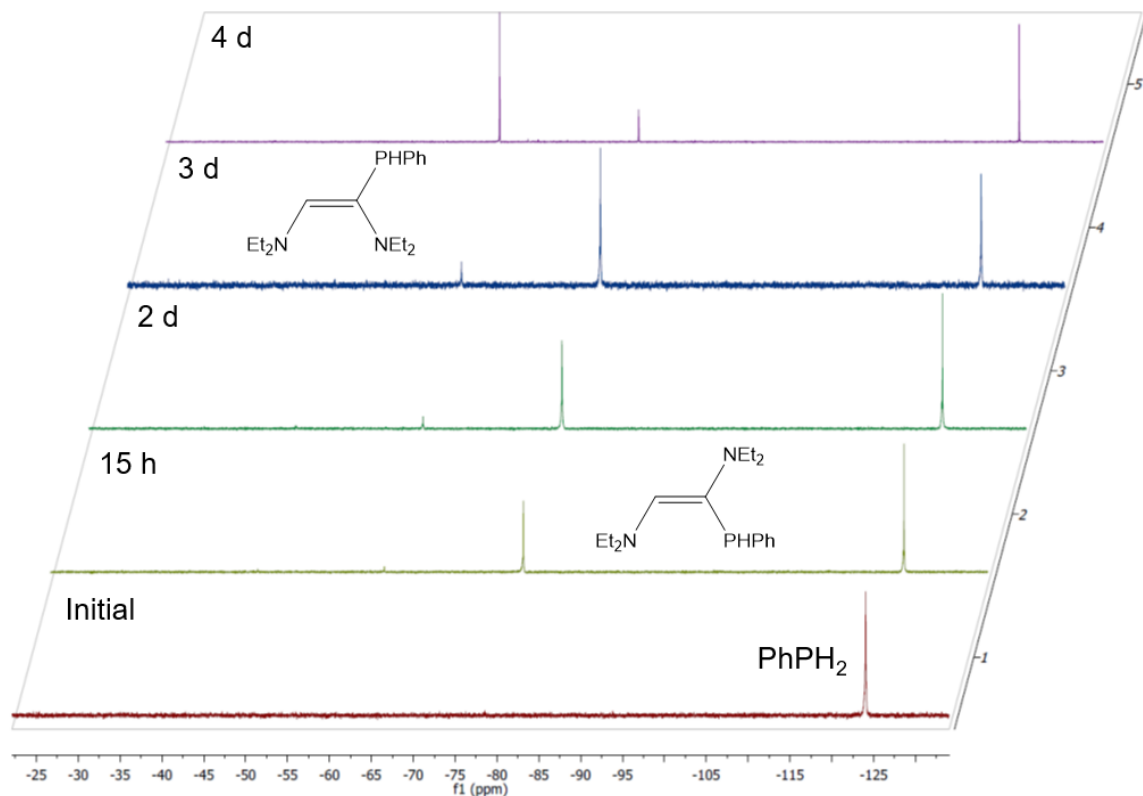
The highest selectivity was observed for bis(diethylamido)acetylene (Table 3.2, entry 1j), which readily provided hydrophosphination products after only 15 h at ambient temperature with a 15.5 : 1 selectivity for the *Z* isomer. Experiments in which only one equivalent of PhPH<sub>2</sub> was added to form the single hydrophosphination products resulted in a 78 : 1 ratio of the *E/Z* isomers (Table 3.3).

**Table 3.3:** Hydrophosphination of bis(diethylamido)acetylene



equivalents PhPH <sub>2</sub>	conversion (%)	ratio <i>Z</i> : <i>E</i>	final ratio <i>Z</i> : <i>E</i> (time)
1	25	78 : 1	7.6 : 1 (5 d)
2	80	15.5 : 1	1 : 3.7 (4 d)
10	99	4.7 : 1	1 : 3.1 (2 d)

Unlike the other vinyl phosphines, these products readily isomerized in the presence of excess primary phosphine (Figure 3.10). No formation of double hydrophosphination products were detected, even after extended reaction times and elevated temperatures.



**Figure 3.10:** Isomerization of the vinyl phosphines in the presence of excess  $\text{PhPH}_2$  (Table 3.3, entry 1)

Vinyl phosphine products formed from the hydrophosphination of bis(diethylamido)acetylene do not isomerize as either an isolated species or in the presence of **1** at ambient temperature. Isomerization is observed upon heating, either with or without **1** (see experimental considerations for details).

The electronics of this vinyl phosphine differ significantly than the other species. The relative ease of formation of the single hydrophosphination products at ambient temperature for this electron-donating alkyne suggests an insertion-based hydrophosphination mechanism. However, the inability of this substrate to undergo double hydrophosphination is surprising. Steric constraints are not substantial and the electronic nature has not significantly changed after the single hydrophosphination.

The ratio of vinyl isomers formed upon the single hydrophosphination is the highest to date for any alkyne hydrophosphination making vinyl phosphines.

### 3.3 Conclusions

In summary, this work represents the first example of a double hydrophosphination of an alkyne with a primary phosphine. The system is selective for either the single or the double hydrophosphination of alkynes, depending on the reaction time. Isolated vinyl phosphines can be reintroduced to catalytic conditions to make the double hydrophosphination products. Acetylene gas was also used as a substrate for the hydrophosphination with  $\text{PhPH}_2$ , despite somewhat unproductive formation of the acetylide-bridged zirconium dimer. This work closes some of the gaps on the substrates for double hydrophosphination with regard to both the alkyne and primary phosphine. To date, no report using either of these substrates has surfaced.

Despite attempts to functionalize the double hydrophosphination products, the chirality at phosphorus remained ambiguous. Attempts to make heterosubstituted diphosphines by a double hydrophosphination of an alkyne with both  $\text{PhPH}_2$  and  $\text{MesPH}_2$  was limited by the size of  $\text{MesPH}_2$ , as anticipated.

Double hydrophosphination continues to grow, but our contribution is still the only one to work with primary phosphines and unactivated substrates. This work represents a complement to the other two known hydrophosphination systems at the time, those of Nakazawa and Oro. The limitations on this subset of hydrophosphination reflect the broader limitations of hydrophosphination in general. That is, hydrophosphination of

primary phosphines to selectively furnish secondary phosphines is far from mature, and hydrophosphination of unactivated substrates continues to lag behind.

The identification of a lanthanide catalyst to make secondary vinyl phosphines<sup>17</sup> from primary phosphine hydrophosphination suggests that more  $d^0$  metal catalysts are capable of this transformation. Electron-rich metal catalysts have been the only emerging double hydrophosphination catalysts of late,<sup>12-15</sup> and all perform the expected double hydrophosphination with secondary phosphines.

Metal catalysts that are good candidates for the rarer primary phosphine double hydrophosphination may be identified in the years to come. One ongoing challenge is that the soft phosphines formed during catalysis can preferentially ligate to the metal center. Electron-deficient catalysts that work with primary phosphines are hard,  $d^0$  metal-based systems, such as Mindiola's titanium system,<sup>5</sup> and Mark's<sup>35-39</sup> and Arnold's<sup>17</sup> lanthanide systems. Softer metals, such as iron or rhodium, are better suited for secondary phosphines. This mismatch between the hard and soft properties of the hydrophosphination catalysts may help to explain why some catalysts cooperate better with phosphine identity than others. For example, Oro's soft/soft rhodium/phosphine pairing<sup>14</sup> was proposed to inhibit catalytic activity over Nakazawa's hard/soft mismatch.<sup>12-13</sup>

It is important to underscore that this argument is a loose generalization of the handful of known metal catalysts; the more important features lie in the mechanistic aspects of catalytic hydrophosphination. For example, Nakazawa's<sup>12-13</sup> and Cui's<sup>15</sup> systems proceed *via* coordination of the unsaturated substrate to the metal center, followed by insertion and elimination of the product phosphine. Oro proposes a classic oxidative

addition, migratory insertion, and reductive elimination system.<sup>14</sup> Our light-dependent single hydrophosphination process is based on insertion into the zirconium–phosphide to provide the vinyl phosphines, yet the mechanism to make double hydrophosphination products remains unclear. Vinyl phosphine insertion into the Zr–PPh bond of **3** is likely the case. Stoichiometric reactions of vinyl phosphines with **1** yielded no phosphide products. This observation also accounts for the high selectivity of secondary phosphine double hydrophosphination products over potential tertiary ones.

Mechanistic understanding of the double hydrophosphination event is needed to further identify good candidates for catalytic hydrophosphination, or to hack the system for interesting, novel transformations. For example, hydrophosphination to make P-chirogenic phosphines in a one-pot procedure or catalytic routes to make heterosubstituted diphosphines would be of interest. Hydrophosphination of  $\text{PH}_3$  to make primary diphosphines would provide direct access to a variety of ligand scaffolds. Double hydrophosphination of  $\text{C}\equiv\text{E}$  systems ( $\text{E} = \text{N}, \text{P}, \text{O}$ ) would provide molecules with tunable electronic properties. Consideration of these challenges comes with maturation of the field, and the emergence of metal catalysts capable of this transformation suggests that development is currently underway.

### **3.4 Experimental methods**

#### **3.4.1 General methods**

All air-sensitive manipulations were performed under a positive pressure of nitrogen using standard Schlenk line techniques or in an M. Braun glovebox. Diethyl ether and tetrahydrofuran were dried over sodium and transferred under vacuum. Benzene- $d_6$

was degassed and dried over NaK alloy. Celite-454® was purchased and heated to 180 °C under dynamic vacuum for overnight before use. Compound  $[K^5 - N, N, N, N, C - (Me_3SiNCH_2CH_2)_2NCH_2CH_2NSiMe_2CH_2]Zr$ <sup>20</sup>, but-1-yn-1-ylbenzene<sup>40</sup>, (cyclopropylethynyl)benzene<sup>41</sup>, 1,2-di-p-tolyne<sup>42</sup>, *N,N*-diethyl-2-phenylethyn-1-amine<sup>43</sup>, *N*<sup>1</sup>,*N*<sup>1</sup>,*N*<sup>2</sup>,*N*<sup>2</sup>-tetraethylethyne-1,2-diamine<sup>44</sup> and MesPH<sub>2</sub><sup>45</sup> were prepared according to literature procedures. Spectra for compounds **2d**,<sup>5</sup> PhCH<sub>2</sub>CH<sub>2</sub>Ph, <sup>24</sup> and bis(phenylphosphino)ethane,<sup>29</sup> have been reported previously. All other chemicals were obtained from commercial suppliers and dried by appropriate means. NMR spectra were collected on a Bruker AXR 500 MHz spectrometer in benzene-*d*<sub>6</sub> solution unless otherwise noted and are reported with reference to residual solvent signals (benzene-*d*<sub>6</sub>, δ 7.16 and 128.0) or to an external standard of 85% H<sub>3</sub>PO<sub>4</sub> (δ 0.0) for <sup>31</sup>P NMR spectra. ESI-mass spectra were collected on an Applied Biosystems 4000QTrap Pro. IR data were collected on a Shimadzu IRAffinity-1 FT-IR spectrometer. All hydrophosphination reactions were run with irradiation from a 9 W, 830 lumen LED lamp purchased from Greenlite™. Conversions are determined by integration of the <sup>31</sup>P{<sup>1</sup>H} NMR spectra. Pulse sequences for <sup>31</sup>P NMR spectra that are suitable for integration have been reported.<sup>11</sup>

### 3.4.2 General procedure for hydrophosphination reactions

A Teflon-sealed J-Young NMR tube was charged with 0.048 mmol of the unsaturated substrate and dissolved in benzene-*d*<sub>6</sub>. The reaction vessel was charged with 0.10 ml of a 0.9564 M solution of PhPH<sub>2</sub> in benzene-*d*<sub>6</sub> and 0.10 mL of a 0.0241 M solution of **1** in benzene-*d*<sub>6</sub> (5 mol %). The reactions were heated to 80 °C in an oil bath with irradiation from a 9 Watt, 830 lumen LED lamp. Products **2a**, **2d**, **2g**, and **2h** were isolated



by removal of the volatiles and sublimation under reduced pressure. Products **3a** and **3b** were obtained by filtration of the crude reaction mixture through Celite® and recrystallization in hexanes.

### 3.4.3 General procedure for hydrophosphination reactions with bis(diethylamido)acetylene to produce **2j**

A Teflon-sealed J-Young NMR tube was charged with bis(diethylamido)acetylene, and given corresponding amounts of the stock solutions in benzene-*d*<sub>6</sub> (Table4). The reactions were left at ambient temperature with irradiation from a 9 W, 830 lumen LED lamp and were periodically monitored by NMR spectroscopy. Product **2j** was isolated by filtration of the catalyst through Celite® and removal of the volatile materials.

**Table 3.4:** Hydrophosphination of bis(diethylamido)acetylene with PhPH<sub>2</sub> to produce **2j**

Entry	Mass bis(diethylamido) acetylene	mL 0.9564 M PhPH <sub>2</sub>	mL 0.0241 M <b>1</b>	NMR Conv.(%)	Initial Ratio Z : E	Final Ratio Z : E (t)
A	6.9 mg (0.041 mmol)	0.042 mL, 1 equiv	0.042 mL	25	78 : 1	7.6 : 1 (5 d)
B	7.5 mg (0.045 mmol)	0.093 mL, 2 equiv	0.093 mL	80	15.5 : 1	1 : 3.7 (4 d)
C	3.1 mg (0.018 mmol)	0.19 mL, 10 equiv	0.19 mL	99	4.7 : 1	1 : 3.1 (2 d)

### 3.4.4 General procedure for isomerization reactions of **2j**

A Teflon-sealed J-Young NMR tube was charged with 11.4 mg (0.068 mmol) a 15.5 : 1 ratio of the *Z* and *E* ratio of **2j**, and given corresponding amounts of the stock solutions in benzene-*d*<sub>6</sub> (Table 5). The reactions were left at ambient temperature with irradiation from a 9 W, 830 lumen LED lamp and were periodically monitored by NMR spectroscopy. Isomerization products were isolated by filtration of the catalyst through Celite® and removal of the volatile materials.

**Table 3.5:** Isomerization of bis(diethylamido)acetylene with PhPH<sub>2</sub> to produce **2j**. All reactions start with a 15.5 : 1 ratio of *Z* : *E*

Entry	mg PhPH <sub>2</sub>	mL 0.0241 M <b>1</b>	Temperature	Final ratio <i>Z</i> : <i>E</i> (time)
A	0	0	22 °C	No change
B	0	0.14	22 °C	No change
C	0	0.14	80 °C	1 : 1.2
D	0	0	80 °C	4.2 : 1
E	1.1 (0.010 mmol)	0.14	80 °C	1 : 7.6

The ratio of *Z* : *E* was monitored by <sup>31</sup>P NMR spectroscopy. In all cases the presence of phosphine and/or heat but not zirconium affects isomerization.

### 3.4.5 Procedure for hydrophosphination of acetylene

A 25-mL reflux Schlenk was charged with 125.6 mg (1.141 mmol) of PhPH<sub>2</sub> and 25.9 mg (0.057 mmol, 5 mol %) of **1**. The reaction vessel was given a magnetic stir bar and ca 10 mL of toluene. An acetylene atmosphere was introduced from a cylinder of acetylene that attached to a mineral oil bubbler. The reaction was heated to 40 °C for 18 h with irradiation from a 9 W, 830 lumen LED lamp. Spectral data for the product are consistent with known literature values.<sup>29</sup>

### 3.4.6 Procedure for formation of **5**

A Teflon-sealed J-Young NMR tube was given 14.4 mg (0.0316 mmol) of **1** and ca 0.3 mL of toluene. The NMR tube was freeze-pump-thawed for three consecutive cycles and then put under acetylene atmosphere for 10 minutes. Species **5** can be purified by sublimation under reduced pressure at 175 °C to give an off-white solid, though isolation of the species is proven difficult by apparent degradation of **5** to **1**.

### 3.4.7 Procedure for catalytic hydrophosphination with MesPH<sub>2</sub>

A Teflon-sealed J-Young NMR tube was charged with 0.048 mmol of the methylphenylacetylene and dissolved in benzene-*d*<sub>6</sub>. The reaction vessel was charged with 0.096 mmol of MesPH<sub>2</sub> and 0.10 mL of a 0.0241 M solution of **1** in benzene-*d*<sub>6</sub> (5 mol %). The reactions were heated to 80 °C in an oil bath for with irradiation from a 9 Watt, 830 lumen LED lamp. After 36 hours the vinyl phosphines were formed in 74% conversion as measured by <sup>1</sup>H NMR spectroscopy. Volatiles were removed under reduced pressure and the contents were dissolved in hexanes and filtered through Celite® and concentrated to provide the vinyl phosphines in 52% yield.

### 3.5 References

- (1) Bange, C. A.; Waterman, R. *Chem. Eur. J.* **2016**, 22, 12598-12605.
- (2) Eric V. Anslyn, D. A. D., *Modern Physical Organic Chemistry*. University Science Books: 2006.
- (3) Roering, A. J.; Leshinski, S. E.; Chan, S. M.; Shalumova, T.; MacMillan, S. N.; Tanski, J. M.; Waterman, R. *Organometallics* **2010**, 29, 2557-2565.
- (4) Rosenberg, L. *ACS Catal.* **2013**, 3, 2845-2855.
- (5) Zhao, G.; Basuli, F.; Kilgore, U. J.; Fan, H.; Aneetha, H.; Huffman, J. C.; Wu, G.; Mindiola, D. J. *J. Am. Chem. Soc.* **2006**, 128, 13575-13585.
- (6) Takaki, K.; Komeyama, K.; Kobayashi, D.; Kawabata, T.; Takehira, K. *J. Alloys Compd.* **2006**, 408-412, 432-436.
- (7) Kondoh, A.; Yorimitsu, H.; Oshima, K. *J. Am. Chem. Soc.* **2007**, 129, 4099-4104.
- (8) Crimmin, M. R.; Barrett, A. G. M.; Hill, M. S.; Hitchcock, P. B.; Procopiou, P. A. *Organometallics* **2007**, 26, 2953-2956.
- (9) Bange, C.; Mucha, N.; Cousins, M.; Gehsmann, A.; Singer, A.; Truax, T.; Higham, L.; Waterman, R. *Inorganics* **2016**, 4, 26.
- (10) Bange, C. A.; Ghebreab, M. B.; Ficks, A.; Mucha, N. T.; Higham, L.; Waterman, R. *Dalton Trans.* **2016**, 45, 1863-1867.
- (11) Ghebreab, M. B.; Bange, C. A.; Waterman, R. *J. Am. Chem. Soc.* **2014**, 136, 9240-9243.

- (12) Kamitani, M.; Itazaki, M.; Tamiya, C.; Nakazawa, H. *J. Am. Chem. Soc.* **2012**, *134*, 11932-11935.
- (13) Itazaki, M.; Katsube, S.; Kamitani, M.; Nakazawa, H. *Chem. Commun.* **2016**, *52*, 3163-3166.
- (14) Di Giuseppe, A.; De Luca, R.; Castarlenas, R.; Perez-Torrente, J. J. J.; Crucianelli, M.; Oro, L. A. *Chem. Commun.* **2016**, *52*, 5554-5557.
- (15) Yuan, J.; Hu, H.; Cui, C. *Chem. Eur. J.* **2016**, *22*, 5778-5785.
- (16) Bange, C. A.; Waterman, R. *ACS Catal.* **2016**, *6*, 6413-6416.
- (17) Garner, M. E.; Parker, B. F.; Hohloch, S.; Bergman, R. G.; Arnold, J. *J. Am. Chem. Soc.* **2017**, *139*, 12935-12938.
- (18) Claridge, T. D. w., *High-Resolution NMR Techniques in Organic Chemistry*. Elsevier: 2009; Vol. 27.
- (19) Corbridge, D. E. C., *Phosphorus: Chemistry, Biochemistry, and Technology*. 6 ed.; CRC Press: Boca Raton, Florida, 2013; p 1473.
- (20) Waterman, R. *Organometallics* **2007**, *26*, 2492-2494.
- (21) Troev, K. D., *Reactivity of P-H Group of Phosphorus Based Compounds*. Academic Press: London, 2017.
- (22) Roering, A. J.; Davidson, J. J.; MacMillan, S. N.; Tanski, J. M.; Waterman, R., *Dalton Trans.* **2008**, 4488-4498.
- (23) Erickson, K. A.; Stelmach, J. P. W.; Mucha, N. T.; Waterman, R., *Organometallics* **2015**, *34*, 4693-4699.

- (24) Obata, T.; Kobayashi, E.; Aoshima, S.; Furukawa, J., *Polym J* **1993**, 25, 1039-1048.
- (25) Geer, A. M.; Serrano, A. L.; de Bruin, B.; Ciriano, M. A.; Tejel, C. *Angew. Chem. Int. Ed.* **2015**, 54, 472-475.
- (26) Gusarova, N. K.; Chernysheva, N. A.; Klyba, L. V.; Shagun, V. A.; Yas'ko, S. V.; Smirnov, V. I.; Trofimov, B. A., *J. Organomet. Chem.* **2013**, 745-746, 126-132.
- (27) Kawaoka, A. M.; Marks, T. J. *J. Am. Chem. Soc.* **2004**, 126, 12764-12765.
- (28) Derrah, E. J.; Pantazis, D. A.; McDonald, R.; Rosenberg, L. *Angew. Chem. Int. Ed.* **2010**, 49, 3367-3370.
- (29) Brooks, P.; Gallagher, M. J.; Sarroff, A. *Aust. J. Chem.* **1987**, 40, 1341-1351.
- (30) Masuda, J. D.; Jantunen, K. C.; Ozerov, O. V.; Noonan, K. J. T.; Gates, D. P.; Scott, B. L.; Kiplinger, J. L. *J. Am. Chem. Soc.* **2008**, 130, 2408-2409.
- (31) Imamoto, T.; Oshiki, T.; Onozawa, T.; Kusumoto, T.; Sato, K. *J. Am. Chem. Soc.* **1990**, 112, 5244-5252.
- (32) Andrushko, N.; Boerner, A. In *Phosphine-boranes and related P-compounds as intermediates in the syntheses of chiral ligands and organocatalysts*, Wiley-VCH Verlag GmbH & Co. KGaA: 2008; pp 1275-1347.
- (33) Otsuka, S.; Nakamura, A.; Kano, T.; Tani, K. *J. Am. Chem. Soc.* **1971**, 93, 4301-4303.
- (34) Mislow, K.; Baechler, R. D. *J. Am. Chem. Soc.* **1971**, 93, 773-774.
- (35) Douglass, M. R.; Marks, T. J. *J. Am. Chem. Soc.* **2000**, 122, 1824-1825.

- (36) Douglass, M. R.; Ogasawara, M.; Hong, S.; Metz, M. V.; Marks, T. J. *Organometallics* **2002**, *21*, 283-292.
- (37) Douglass, M. R.; Stern, C. L.; Marks, T. J. *J. Am. Chem. Soc.* **2001**, *123*, 10221-10238.
- (38) Kawaoka, A. M.; Douglass, M. R.; Marks, T. J. *Organometallics* **2003**, *22*, 4630-4632.
- (39) Motta, A.; Fragala, I. L.; Marks, T. J. *Organometallics* **2005**, *24*, 4995-5003.
- (40) Deyris, P.-A.; Caneque, T.; Wang, Y.; Retailleau, P.; Bigi, F.; Maggi, R.; Maestri, G.; Malacria, M. *ChemCatChem* **2015**, *7*, 3266-3269.
- (41) Chen, G.-Q.; Zhang, X.-N.; Wei, Y.; Tang, X.-Y.; Shi, M. *Angew. Chem. Int. Ed.* **2014**, *53*, 8492-8497.
- (42) Wu, Y.; Wu, F.; Zhu, D.; Luo, B.; Wang, H.; Hu, Y.; Wen, S.; Huang, P. *Org. Biomol. Chem.* **2015**, *13*, 10386-10391.
- (43) Ciganek, E., *Org. React. (Hoboken, NJ, U. S.)* **2008**, *72*, 1-366.
- (44) Delavarenne, S. Y.; Viehe, H. G. *Chem. Ber.* **1970**, *103*, 1198-1208.
- (45) Takeda, Y.; Nishida, T.; Minakata, S. *Chem. Eur. J.* **2014**, *20*, 10266-10270.

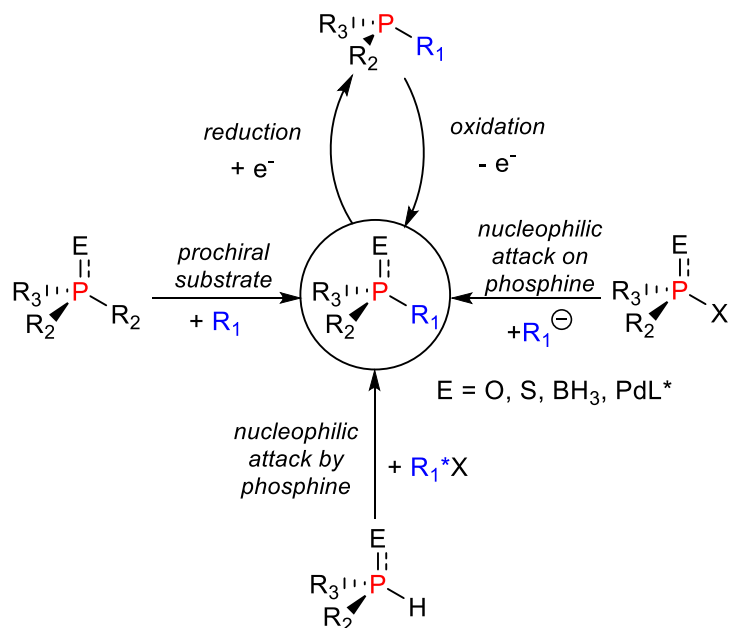
## CHAPTER 4: EFFORTS TOWARDS SYNTHESIS OF A CHIRAL LIGAND FOR ZIRCONIUM-CATALYZED HYDROPHOSPHINATION TO FORM *P*-CHIRAL PHOSPHINES

### 4.1 Introduction

Asymmetric phosphines garner wide attention and respect as ligands in asymmetric catalysis. However, asymmetric phosphines are not limited to ligand design. Chiral phosphorus compounds are used within the chemical community as synthons, such as Wittig reagents and chiral Brønsted acids. Further demand for chiral phosphines and phosphine oxides includes pesticides,<sup>1,2</sup> antibiotics,<sup>3,4</sup> antiviral agents,<sup>5</sup> and molecular materials.<sup>6-14</sup> Chiral phosphines can be made either by common synthetic methodologies or by catalytic routes.

#### 4.1.1: Synthetic and stoichiometric routes to *P*-stereogenic phosphines

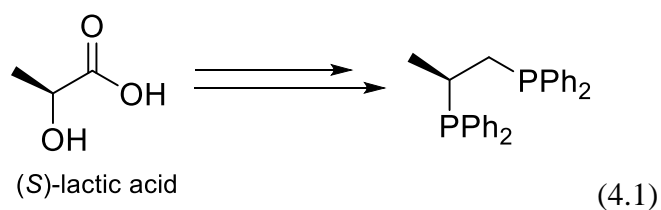
Phosphines can be prepared by traditional synthetic methodologies (Scheme 4.1).



**Scheme 4.1:** Survey of common synthetic methods to generate asymmetric phosphines and phosphine oxides



Nucleophilic attack by the phosphine on an asymmetric electrophilic organic molecule, often an organohalide, produces the new chiral phosphine (Scheme 4.1, bottom). An early and notable example is (*R*)-1,2-bis(diphenylphosphino)propane (equation 4.1), which was made from (*S*)-lactic acid by asymmetric hydrogenation, reduction, and phosphination (Scheme 4.1, right). This product phosphine was used as a ligand in catalytic asymmetric hydrogenation of prochiral ethyl 2-acetoxyacrylate to form ethyl (*S*)-2-acetoxypropanoate to effectively reproduce its precursor.<sup>15</sup>



It is also feasible to undergo a nucleophilic attack on the electrophilic phosphorus center by a nucleophile (Scheme 4.1, right), often an organolithium or organomagnesium reagent. Usually a chiral additive, or sterically bulky groups on the phosphine, are present to increase the enantioselectivity in these transformations. Despite the appeal of this method (any phosphorus electrophile, any nucleophile) the enantioselectivity is modest. Often further resolution techniques are required for appreciable product isolation.<sup>16</sup>

One straightforward approach to an asymmetric phosphine is the functionalization of a prochiral substrate with a chiral reagent (Scheme 4.1, left). A popular execution is enantioselective deprotonation of a phosphine either at the  $\alpha$ - or  $\beta$ - position with a chiral base, often (–)-sparteine or (–)-cystine, followed by carbonation, oxidative coupling, trapping with electrophilic reagents, or reduction. Despite the high diastereoselectivities of

the product phosphines, this method has only been shown to work with a specialized group of starting materials and reagents.<sup>16</sup>

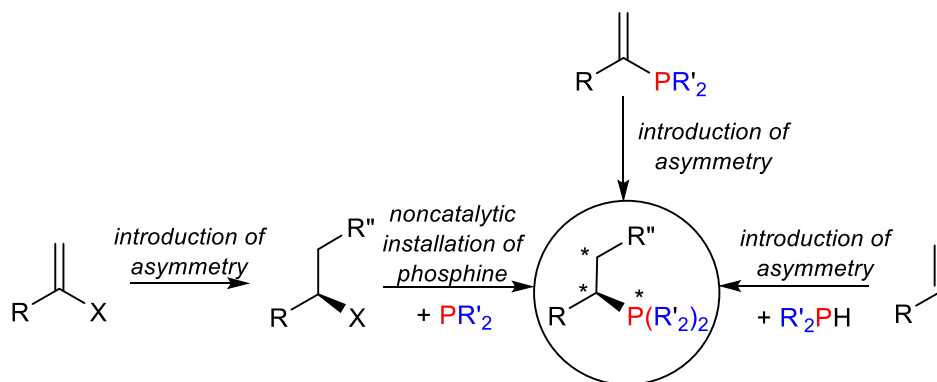
Methods that preserve the chirality on the phosphine oxide during the reduction process to a phosphine are limited to only a handful of examples.<sup>17-19</sup> Methods that preserve chirality on the phosphine during oxidation are somewhat more common but only have been employed for phosphine esters, phosphine amides, and oxazaphospholidines (Scheme 4.1, top).<sup>20</sup>

The modest stereoselectivities obtained during nucleophilic/electrophilic transformations and the requirement of chiral starting materials for further functionalization, many of which are expensive or not commercially available, significantly decreases the attractiveness and efficiency of these methods. Because the use of chiral auxiliaries also inherently requires multiple steps for both introduction, isolation, and purification, this method often is time- and reagent-consuming. Atom-economical methodologies to prepare this class of compounds or methodologies that are compatible with a more general class of phosphines and substrates are of immense interest and value.

#### **4.1.2: Catalytic routes to *P*-stereogenic phosphines**

Catalytic routes to *P*- and *C*-stereogenic phosphines are limited to three general approaches. First, chiral substrates are generated through other known asymmetric catalytic methodologies and then converted into chiral phosphines (Scheme 4.2, left). Second, chiral phosphines are achieved through catalytic asymmetric reduction of a prochiral organophosphine, such as a catalytic asymmetric hydrogenation (Scheme 4.2, top). Third,

chiral phosphines are produced by stereocontrol during a catalytic P–C bond forming reaction (Scheme 4.2, right).<sup>21</sup>



**Scheme 4.2:** Catalytic methods to asymmetric phosphines

A suite of examples employing the first two methodologies has been developed.<sup>21</sup> Synthetic strategies targeting prochiral substrates (Scheme 4.2, left) arose from the growth of asymmetric hydrogenation. That reaction has been responsible for the synthesis of a variety of chiral phosphines, often from simple ketone starting materials to give stereogenic alcohols, which are then converted to chiral phosphines by nucleophilic addition of a phosphide.<sup>15,22</sup> This method is commonly invoked for the synthesis of chiral bis(phosphines) from diketones. These substrates are hydrogenated to the corresponding chiral diol and cyclized to the cyclic sulfate before reaction with the phosphide.

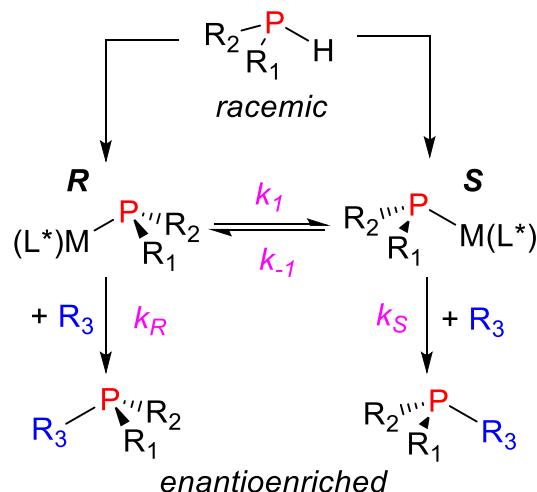
Installation of axial or planar chirality by catalytic coupling reactions can introduce chirality in the backbone of the molecule (Scheme 4.2, left). A specific site, often an aryl halide, can be converted to a phosphine.<sup>23,24</sup> Methods for asymmetric hydrogenation of alkenyl halides, then nucleophilic conversion to the phosphine, are less commonly employed.<sup>21</sup>

An achiral organophosphine can be made chiral by traditional enantioselective reactions, especially by installation of axial chirality on the substrate backbone (Scheme 4.2, top). Alternative techniques are kinetic resolution and desymmetrization reactions, which coax out chiral phosphines with varying degrees of effectiveness. For example, lipase has been shown to selectively acylate one enantiomer of a phosphine alcohol.<sup>25</sup> And, in a separate example, lipase resolved a P-stereogenic phosphine oxide.<sup>26</sup> Desymmetrization reactions of symmetric phosphines to give an enantioenriched products has been shown as a proof-of-concept for phosphine-boranes but provides products in limited yields. This method relies on the relative rate of deprotonation, followed by rapid reaction (e.g. coupling, ligand exchange) in the presence of a chiral additive (e.g. (-)-spartenine).<sup>27,28</sup> These strategies require that the rate of asymmetry introduction be faster than the rate of epimerization of the prochiral phosphine, which has limited the method to a handful of examples with specialty chiral additives.

#### 4.1.3: Hydrophosphination to generate *P*- and/or *C*-chiral phosphines

Selective addition of a P–H bond across an unsaturated bond, hydrophosphination, offers potential of stereocontrol of the newly formed P–C bond (Scheme 4.2, right). Two possible outcomes exist in this method, a stereocenter can be established at the carbon atom and/or the phosphorus atom. Because the inversion barrier for a tertiary phosphine is approximately 30 kcal mol<sup>-1</sup>,<sup>29</sup> spontaneous inversion and corresponding loss of chirality at the phosphorus center is not likely for most systems. While significant progress has been made at identifying substrates for which *C*-chiral products can be readily realized via hydrophosphination protocols,<sup>30</sup> formation of *P*-chiral products is an ongoing challenge.<sup>21,31</sup>

Catalytic hydrophosphination of racemic phosphines to yield enantioenriched products often stems from the formation of diastereomeric intermediates during catalysis (Scheme 4.3).<sup>21,32</sup> Metal-catalyzed hydrophosphination typically involves a metal-phosphide intermediate that interconverts rapidly on the NMR time scale.<sup>32</sup> The known inversion barriers to primary and secondary metal phosphides fall between 6 and 15 kcal mol<sup>-1</sup>.<sup>33-40</sup> If this equilibrium is faster than reaction with the substrate ( $R_3$ ), and if one enantiomer is favored, then enantioenriched products can be formed. The product ratio is directly proportional to the ratios of the equilibrium constants for cases where  $k_1, k_{-1} \gg k_R, k_S$ . This process is known as dynamic kinetic asymmetric transformation.<sup>41</sup>



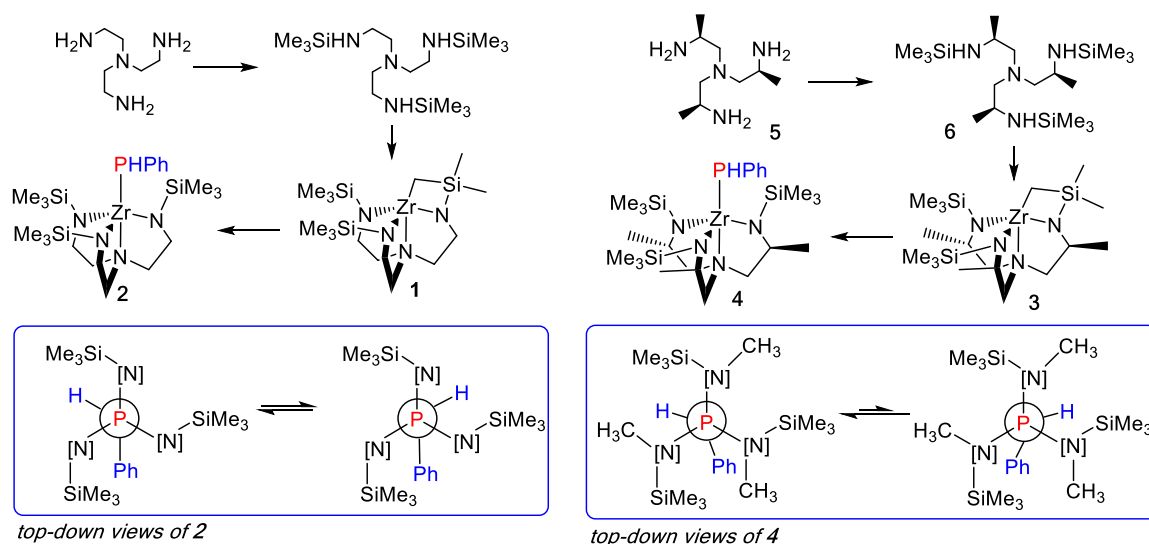
**Scheme 4.3:** Hydrophosphination of racemic phosphines to provide enantioenriched products<sup>21,32</sup>

Despite the simplicity and attractiveness of this idea, the transformation has only been demonstrated as a proof-of-concept for secondary phosphines to make tertiary products. In all reported cases the enantioselectivities of the product phosphines were modest, and development of this method into a synthetically viable route to enantioenriched products is not yet realized.<sup>21,43</sup> Growth of hydrophosphination is perhaps stymied by the dependence of small and electron-rich substrates in these reports. It is possible that the substrate reacts faster with the metal-phosphide intermediates than is desired, which would give rise to poor enantioselectivities (Scheme 4.3). Retardation of substrate insertion may address this stereocontrol issue. Use of unactivated alkenes and alkynes may sufficiently stall the rate of interaction of the substrate with the activated metal phosphide such that greater enantioselectivities can be reached in the final products.

While inversion barriers for compound **2** are unknown, the formation of *rac* and *meso* PhPH–PhPH upon dehydrocoupling of **2** with PhPH<sub>2</sub> suggests that inversion of the

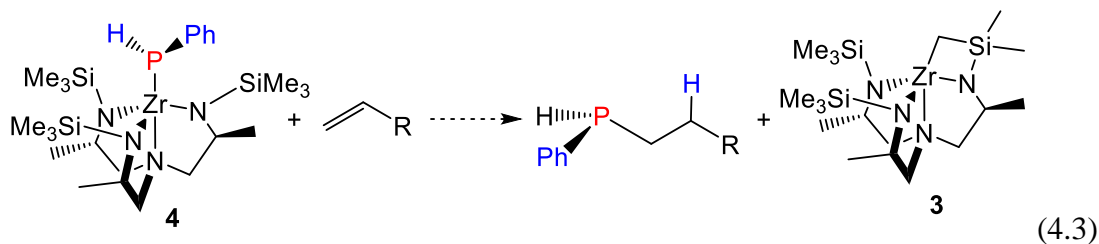
A related zirconium compound with a chiral ligand backbone (**3**) was sought to catalytically form asymmetric phosphines. A similar ligand to  $\text{N}(\text{CH}_2\text{CH}_2\text{NSiMe}_3)_3$ , (*S*)-*N*,*N*'-bis((*S*)-2-aminopropyl)propane-1,2-diamine (**5**) was chosen for its chirality in the backbone and known synthetic protocol.<sup>44,45</sup> Compound **5** would be protected to form **6** before making target zirconium derivative **3**. The hypothesis was that the zirconium

phosphide will be oriented in such a way during the P–C bond forming step to result in enantioenriched hydrophosphination products (Scheme 4.4).



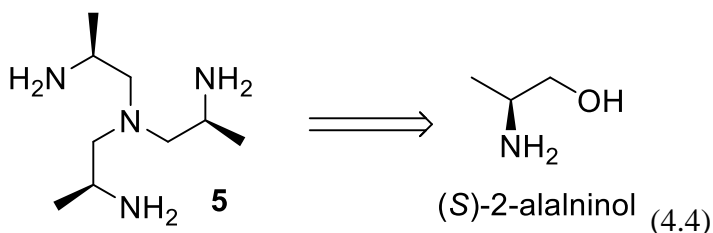
**Scheme 4.4:** Formation of chiral (tren)zirconium phosphides and top-down views showing preferential orientation of the phosphide

While the methyl group itself of **4** will only be a modest influence on the orientation of the phosphide, it may be enough to maintain the trimethylsilyl group's position on the amide that will in turn direct the phosphide orientation. An incoming substrate will also be oriented in such a way to interact with the phosphide to give an enantioenriched product (eq 4.3).



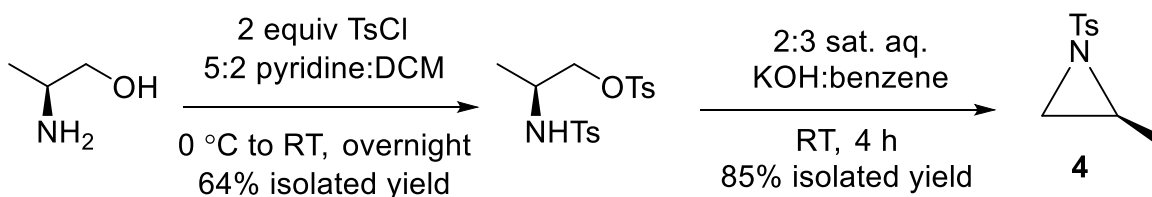
Synthesis of **5** follows a literature report from Moberg and coworkers.<sup>45</sup> This report uses alaninol, a commercially-available chiral amino alcohol, to form the product chiral tren **5** in three steps (eqn 4.4).





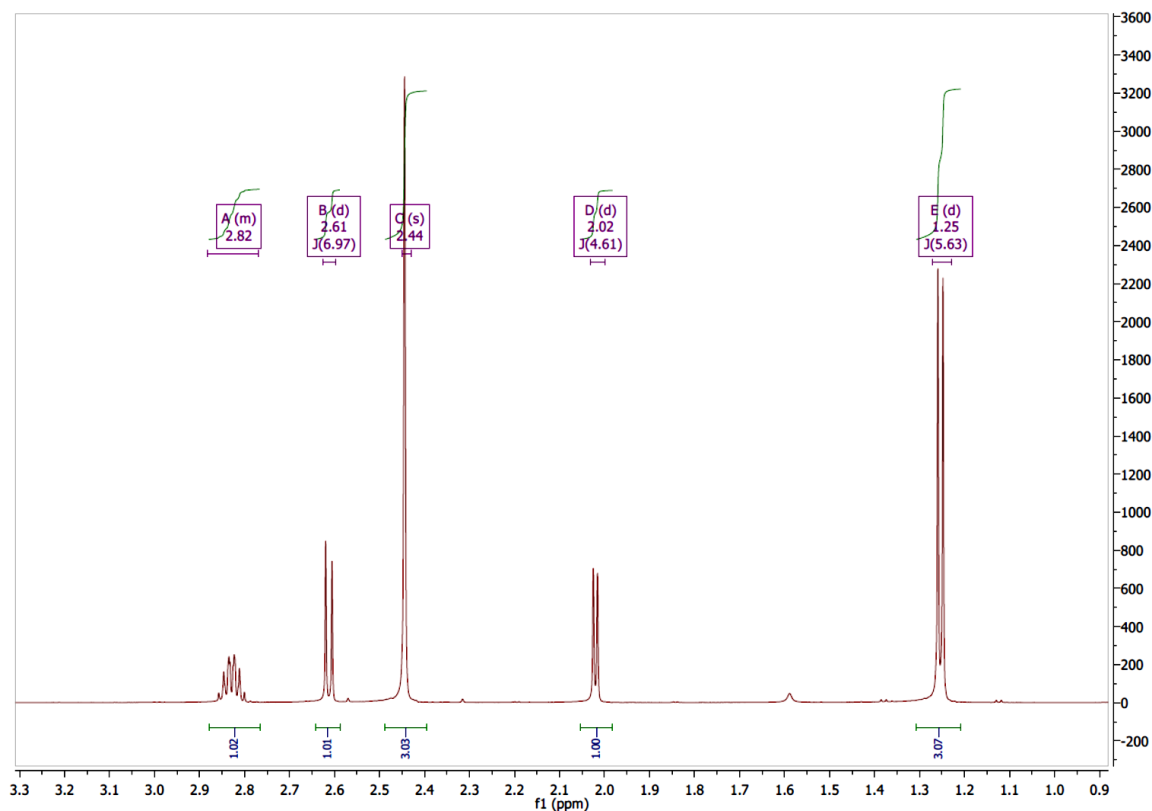
## 4.2 Results and discussion

The target molecule precursor (*S*)-2-methyl-1-tosylaziridine (**7**) was readily made from a two-step procedure. Protection of (*S*)-alaninol with two equivalents of tosyl chloride in a pyridine:DCM solvent cocktail furnished the protected alaninol (Scheme 4.5).



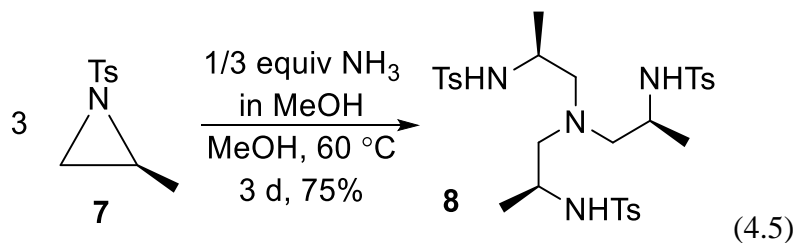
**Scheme 4.5:** Formation of aziridine **4** from chiral alaninol

Aziridine **7** can be formed by nucleophilic attack of the tosyl-protected alaninol under basic conditions (Scheme 4.5).<sup>46</sup> The product aziridine **7** displays a pair of doublets at 2.61 and 2.02 ppm ( $J = 7, 5$  Hz, respectively) for the methylene protons on the ring. The stereochemistry of the parent alaninol is conserved during the ring-closing step to form **4** as only a single methyl resonance is observed (Figure 4.1).



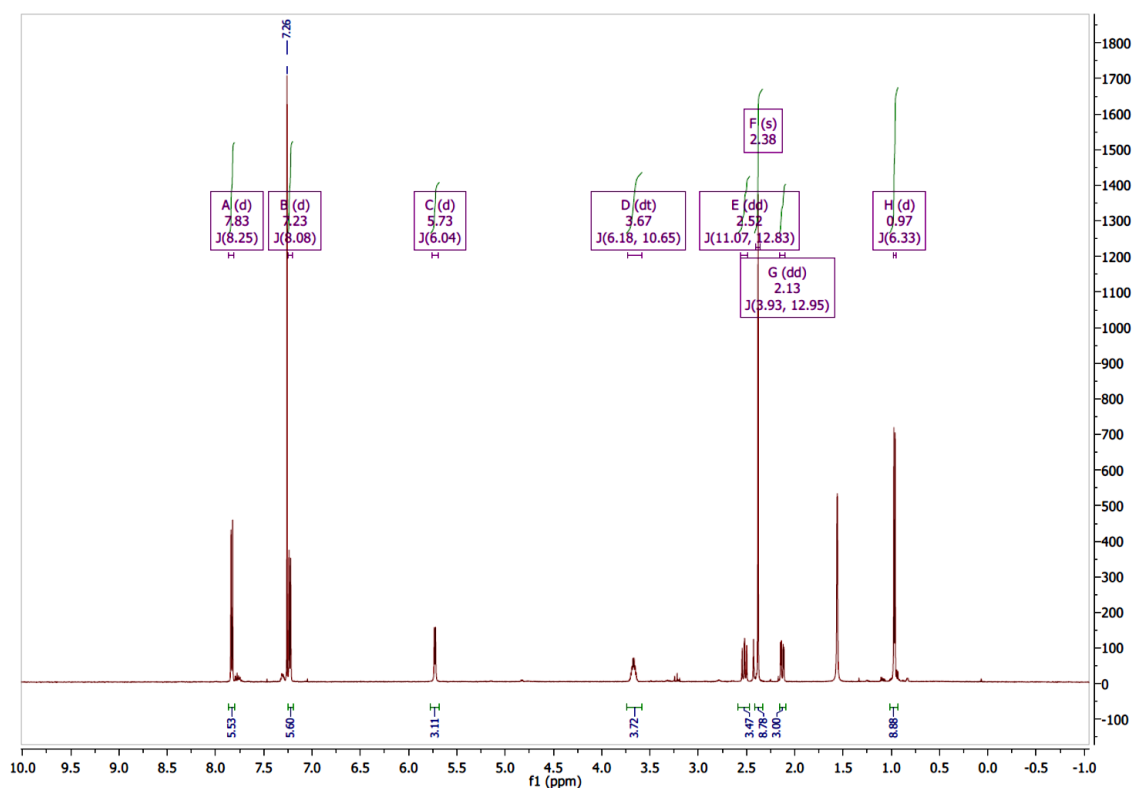
**Figure 4.1:**  $^1\text{H}$  NMR spectrum of **7** showing formation of a single isomer

Nucleophilic ring-opening of the aziridine **7** with ammonia in methanol provides the product *N,N',N''*-((2*S*,2'*S*,2''*S*)-nitrilotris(propane-1,2-diyl))tris(4-methylbenzenesulfonamide) (**8**) after several days under elevated temperatures<sup>44,45</sup> (eqn 4.5).



Products corresponding to a single or a double ring opening event (as opposed to the triple required for **8**) are not detected. Compound **8** is  $C_3$ -symmetric. This can be

detected by the formation of a triplet of quartets (3.70 ppm,  $J = 13$  Hz, 6 Hz) for the diastereomeric hydrogen atom, and the methylene protons appear as distinct doublets of doublets at 2.55 ppm and 2.16 ppm (Figure 4.2). This product can be isolated in approximately 75% yield after recrystallization from methanol.



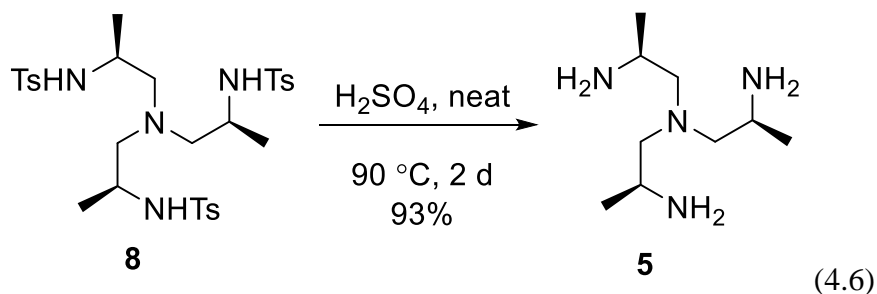
**Figure 4.2:**  $^1\text{H}$  NMR spectrum of **8**

Deprotonation of **8** to form **5** has proven challenging, indeed, deprotection of secondary *N*-tosylamines to form primary amines has only been demonstrated for a handful of substrates.<sup>47</sup> The sulfonamide is considered one of the most stable nitrogen protecting groups, which makes removal a considerable challenge.<sup>47</sup> Forcing conditions are often required for deprotection. A commonly employed method is refluxing HBr with either acetic acid or phenol followed by neutralization, but this method is limited to poor yields

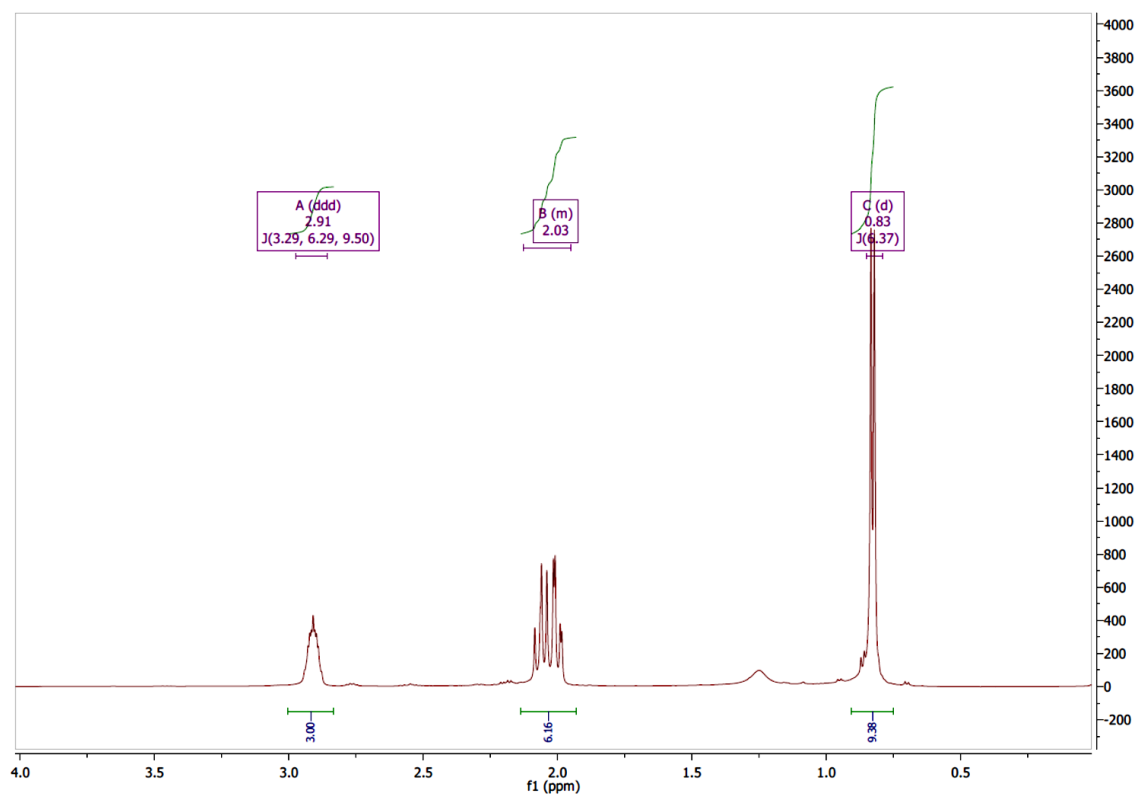
and requires significant amounts of reagents for product workup and isolation. Reduction of the tosyl moiety with an alkali metal and substoichiometric amounts of naphthalene at low temperatures can provide deprotection of the amine without epimerization. This method can also install an electrophile on the amine.<sup>48</sup> Deprotection of **8** with a ten-fold excess of sodium naphthalenide generated *in situ* was attempted several times. Comparison of the thin-layer chromatography plates containing a sample of tris(2-aminoethyl)amine next to a sample of **5** suggested that the tosyl groups had been removed to form the tren analogue **6**, but the product was never detected by <sup>1</sup>H NMR spectroscopy and not isolated, despite numerous attempts. The isolation was not attempted further as radical deprotection methodologies are known to sometimes epimerize chiral compounds.<sup>47</sup>

Deprotection mediated by a six-fold excess of SmI<sub>2</sub> in THF with a catalytic amount of DMPU has been shown to work for a variety of secondary *N*-tosylamines to form primary amines.<sup>49</sup> The six-fold excess required per mole of *N*-tosylamine allows for regeneration of the Sm(III) salts. This method only returned partially deprotected **5** and was not investigated further.

Despite the variety in the known deprotection methods for secondary *N*-tosylamines to primary amines,<sup>47</sup> none of these pathways provided deprotection of **8** to **5**. The original report from Moberg stated that deprotection using mercaptoacetic acid with KOH in DMF provided the product **5**.<sup>44</sup> A follow-up publication disclosed that this result was not often reproducible.<sup>45</sup> Their second report removed the tosyl groups by refluxing in HBr and phenol but provided the product in limited yield. As noted, this method was not reproducible.



Following a report by Mountford for a related compound,<sup>50</sup> compound **8** was partially dissolved in neat H<sub>2</sub>SO<sub>4</sub>, sealed, and heated to 90 °C for two days (eqn 4.6). Upon isolation the target compound **5** was obtained in 93% yield (Figure 4.3).

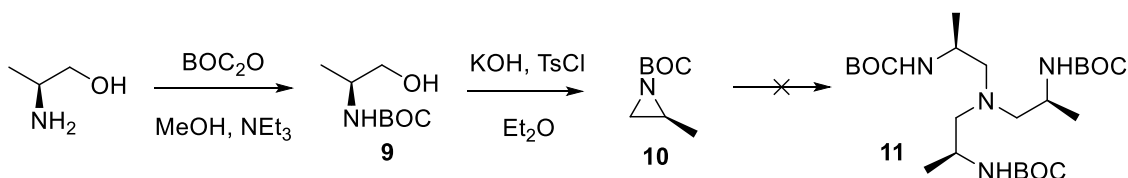


**Figure 4.3:** <sup>1</sup>H NMR spectrum of (*S*)-*N*1,*N*1-bis((*S*)-2-aminopropyl)propane-1,2-diamine (**5**)<sup>45</sup>

However, isolation of **5** was not always reproducible. Workup of the crude reaction mixture required a pH adjustment from 0 to 14 which diluted the product mixture

to such an extent that the product was soluble in both fractions. Attempts to remove the water under reduced pressure or to extract **6** out of the product were frequently unsuccessful.

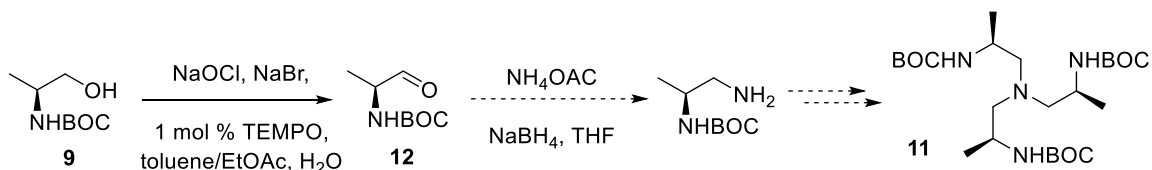
A more auspicious protecting group was sought to address the stubbornness of the tosyl deprotection step. The protecting group *tert*-butoxycarbonyl (BOC) is known to protect optically active amino acids with stereoconversion during either esterification or acidification.<sup>51</sup> This protecting group is well-regarded for its mild and numerous deprotection methods. The BOC substituent can be cleaved in the presence of acids or can be removed thermally with generation of CO<sub>2</sub> and 2-methylpropene.<sup>47</sup>



**Scheme 4.6:** Formation of *N*-BOC aziridine (**8**) and attempted synthesis of **11**

Reaction of (*s*)-alaninol with di-*tert*-butyl dicarbonate (BOC<sub>2</sub>O) provided the protected alaninol **9** under mild conditions<sup>52</sup> (Scheme 4.6). Aziridination of **9** to form **10** proceeded smoothly following *in situ* tosylation of the alcohol and with stereoconservation during nucleophilic attack. However, ring-opening of **10** to form **11** failed, presumably due to competitive nucleophilic attack from ammonia to the ester of the protecting group. It is also possible that methanol is sufficiently acidic enough to remove the BOC protecting group. An analysis of a crude reaction mixture during the nucleophilic ring-opening of **10** to **11** showed cleavage of the BOC protecting group and suggested epimerization of the reaction species. No products identified as **10** or **11** were recovered.

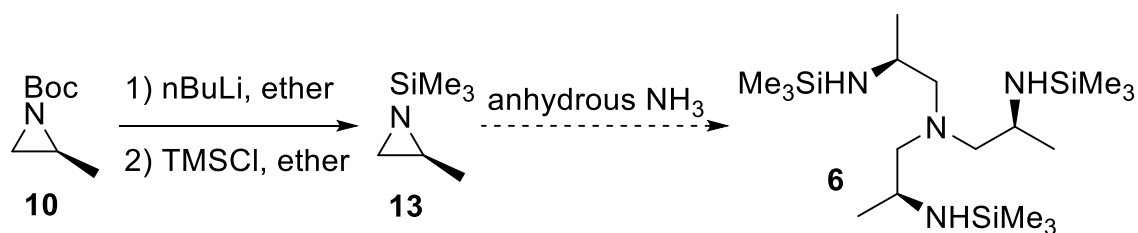
An alternative route around the issues of nonselective nucleophilic addition and accidental protecting group cleavage involves oxidation of the **9** to the *N*-BOC amino aldehyde **12** (Scheme 4.7).<sup>53</sup> This species was sought as it could go a condensation reaction with ammonium acetate to generate the imine, which would be reduced in the presence of sodium hydride. The newly-formed amine would then be able to undergo two more additions of this type to form the desired product **11**.



**Scheme 4.7:** Oxidation of **9** for sequential condensation and reduction to form **11**

Oxidation of **9** to **12** was carried out as quickly as possible to avoid loss of chirality at the C–N bond. However, after ten minutes of oxidation the product **12** had epimerized. This method was not pursued further.

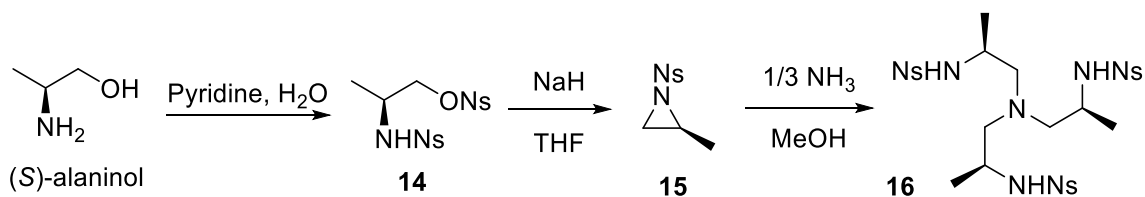
Uncontrolled nucleophilic addition, epimerization, and deprotection difficulties are inherent to the nature of the reaction methodologies shown in Schemes 4.5–4.8. One response to this problem is to take advantage of the ease of forming the protected aziridines **7** and **10**, but deprotect and reprotect with an alternative protecting group. Because trimethylsilyl groups will ultimately be installed on **5** to form **6**, trimethylsilyl was chosen for aziridine protection (Scheme 4.8). This newly-protected aziridine **13** could then undergo ring-opening to form target molecule **6**.



**Scheme 4.8:** Trimethylsilyl protection and ring-opening of the chiral aziridine

An ethereal sample of **10** was deprotected with butyllithium to form the amide, then quenched with trimethylsilylchloride to form **13**. However, the unprotected aziridine was not stable above  $-78\text{ }^{\circ}\text{C}$ . Indeed, after removal of the BOC protecting group the product had epimerized. Lithiation and quenching at  $-78\text{ }^{\circ}\text{C}$  without any warming failed to remove the protecting group.

Despite the difficulty of deprotection, the tosyl protecting group is attractive as it offers the most resistance to epimerization. A commercially available derivative, 2-nitrobenzenesulfonyl chloride (nosyl), was considered. Like tosylaziridines, nosylaziridines are known to be opened with nucleophiles preferentially over nucleophilic cleavage of the nosylate. A popular route to deprotection is refluxing the nosylamine with thiophenol under basic conditions in a polar solvent.<sup>47</sup>

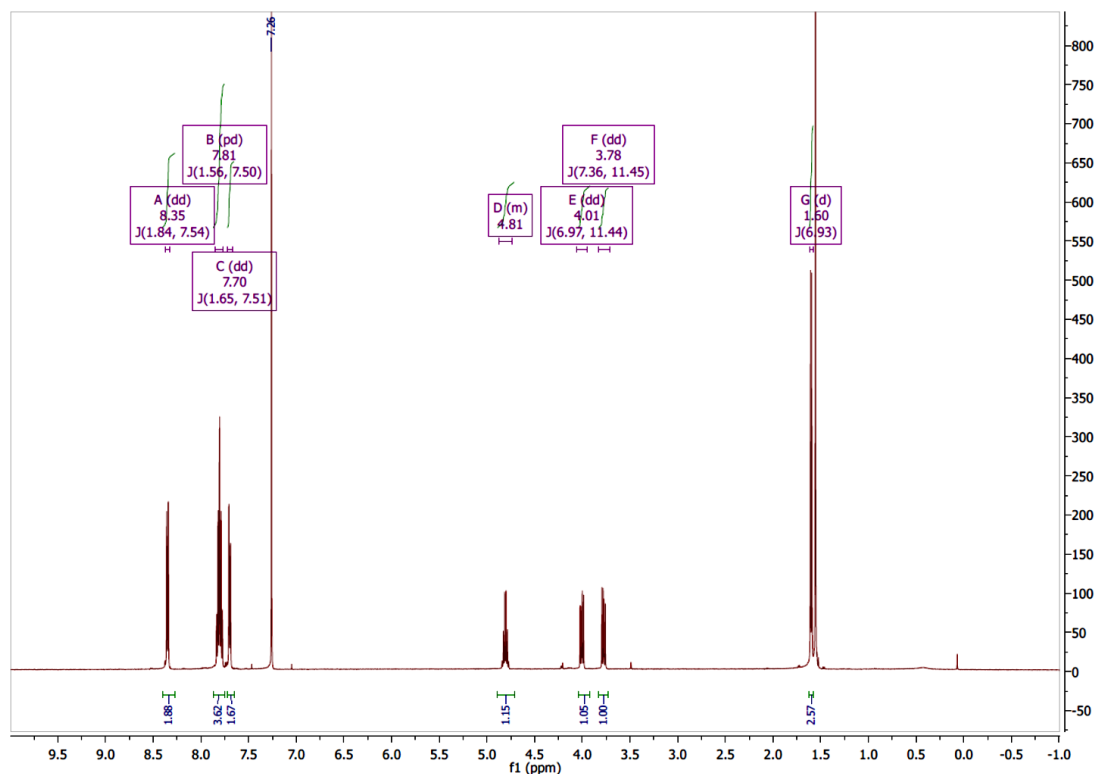


**Scheme 4.9:** Nosyl protection of (*S*)-alaninol en route to **16**

Compound **15** was prepared in an analogous way to **7** (Scheme 4.9). Compound **15** displays a similar pattern of doublets of doublets corresponding to the methylene

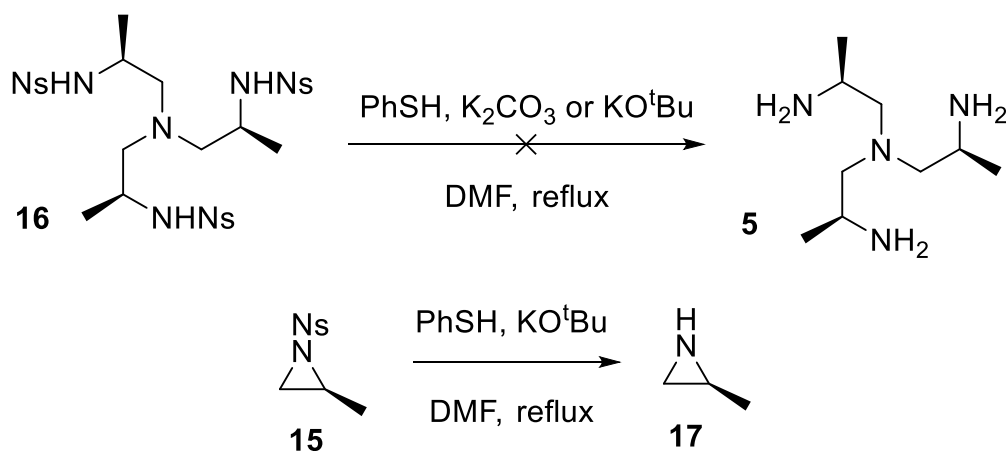


protons on the aziridine ring (Figure 4.4). The chemical shifts of **15** are noticeably more downfield to those of **7** due to the electron-withdrawing nature of the nosyl group.



**Figure 4.4:**  $^1\text{H}$  NMR spectrum of **16**

An attempted deprotection of **16** to **5** *via* refluxing **16** with an excess of thiophenol and base in dimethylformamide (DMF) was employed (Scheme 4.10). Isolation of the product **5** proved difficult. This product was detected by thin-layer chromatography but was never isolated despite numerous attempts. It is likely that deprotection of this moiety only occurred partially, as was suggested by TLC. That makes the product challenging to separate based on extractions. An attempted distillation of **5** out of the crude reaction mixture only returned thiophenol and other unidentified side products.

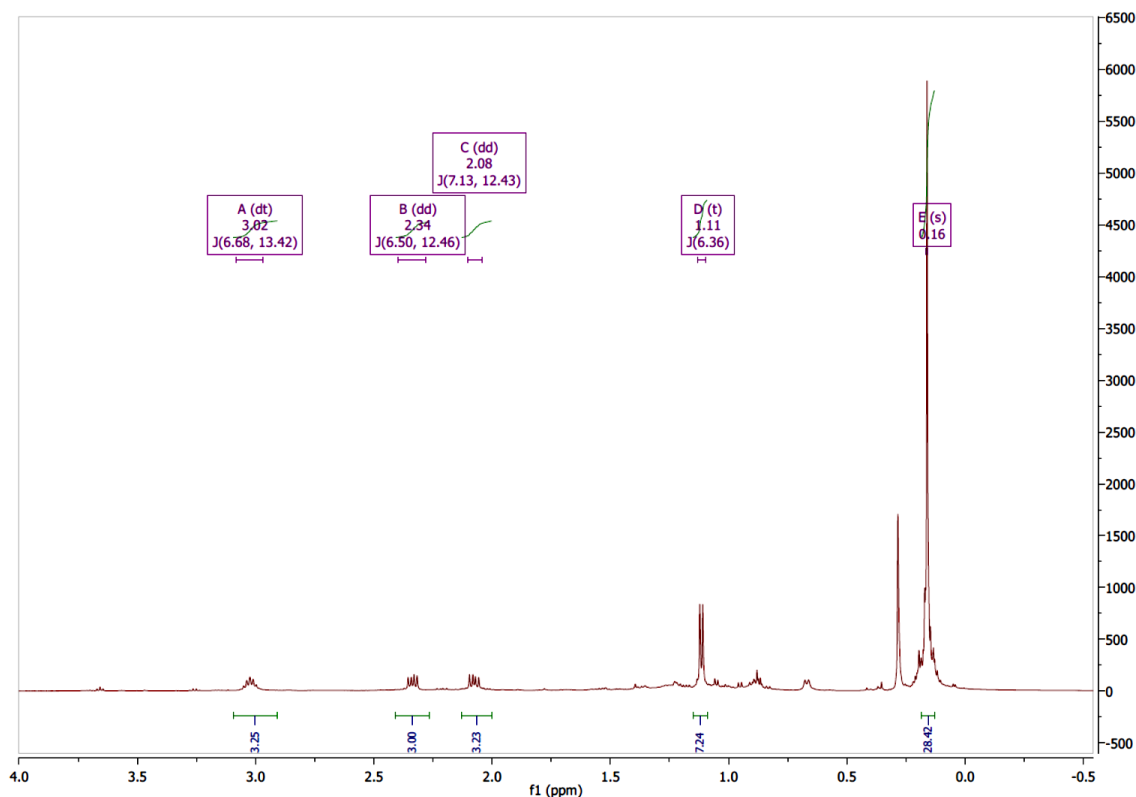


**Scheme 4.10:** Deprotection of the nosyl group

Because protected secondary amines are known to be easier to deprotect than their tertiary counterparts, **15** was deprotected by the same method. Indeed, a  $^1H$  NMR spectrum of the crude reaction mixture showed formation of **17**.<sup>54</sup> Despite the successful removal of the nosyl group, this product was not isolated due to separation difficulties from the reaction mixture.

A common method to reduce arylsulfonamides is by generation of magnesium in methanol, followed by either refluxing or sonication.<sup>55-57</sup> Generation of magnesium in methanol resulted in a detonation, and the method was not investigated further.

Formation of **5** for use as a ligand for **3** for asymmetric hydrophosphination was unrealized due to a series of problematic deprotection steps. Despite significant problem-solving or problem-evading strategies, compound **5** was only isolated in small quantities. Installation of trimethylsilyl groups on **5** to form **6** provided the compound in quantities sufficient for NMR verification but not enough to be synthetically viable to form **3** (Figure 4.5).



**Figure 4.5:** A crude reaction forming compound **6** (eqn 4.4)

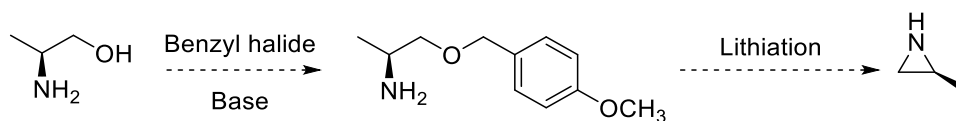
Reproduction of the deprotection step using sulfuric acid was not reproduced again, despite numerous attempts (eqn 4.6). This reproducibility is likely a result of the isolation procedure, as neutralization under aqueous conditions enlarges the reaction scale to such an extent that **5** is soluble in both aqueous and organic media.

### 4.3 Conclusions

Despite significant advances, isolation of **6** from **3** is still an ongoing challenge, owing from the deprotection step to form **5**. Protection methodologies that allow for enantioselective functionalization of the parent amino alcohol to form derivatives of **5** have problems due to poor selectivity of nucleophilic addition, challenging protecting group removal, or uncontrollable epimerization. Some synthetic methodologies that may avoid

these methods include diversification of the protecting group and functionalization at the aziridine.

For example, protection of the parent alaninol with a *p*-methoxybenzyl halide would result in protection of the alcohol with the chiral C–N bond intact.<sup>58</sup> The *p*-methoxybenzyl group is easily cleaved by hydrolysis, so analogous methods outlined above may not work. Instead, one option is to forgo protection at the amine and instead deprotonate it to facilitate nucleophilic attack at the electrophilic carbon adjacent to the benzyl ether to form the aziridine (Scheme 4.11). This reaction would liberate the (*S*)-2-methylaziridine, so the reaction should be run in a high-boiling, polar solvent in a distillation apparatus to collect the aziridine. This compound could then be protected with trimethylsilyl for ring-opening with anhydrous ammonia. The principal advantage in this method is that the benzyl group is not nearly as stable as the tosyl- or nosyl- derivatives. The issue of nucleophilic attack avoided as the deprotection step is folded in to the aziridination reaction. The success of this method relies heavily on the isolation of the product (*S*)-2-methylaziridine.



**Scheme 4.11:** Formation of (*S*)-2-methylaziridine by bypassing the problematic primary amine deprotection step

If this method were challenging, likely due to the poor nucleophilic substitution at either side of the benzyl ether, the next most promising tactic is deprotection at the tosyl aziridine **7**. This can be facilitated a variety of ways. Methods to deprotect a secondary tosyl amide to form a secondary amine are both more numerous and more auspicious than

those of their primary counterpart. More aggressive reductions, such as salt formation by metallic sodium or lithium, would result in the aziridinide. This species would be easily quenched by reaction with trimethylsilyl chloride, forming the precursor required for ring-opening with anhydrous ammonia. However, this method could result in epimerization concomitant with aziridinide formation.

If the influence of the methyl substituents on **3** were not enough to promote favorability of one phosphide isomer over another, an analogous ligand to **5** could be formed in which the methyl groups are replaced by isopropyl groups. Synthesis would start on the commercially available chiral valine or valinol to form the eventual analogue of **5**. Substitution of the methyl groups with the isopropyl groups would likely result in formation of a specific orientation of the trimethylsilyl substituent which would be cradled by the isopropyl group on the ligand backbone.

It is important to underscore that determination of chirality of the phosphorus products produced by asymmetric hydrophosphination with **3** is not a trivial feat. Determination of enantiomeric excesses of tertiary chiral phosphines often requires a crystal structure of the phosphine, either on its own or ligated to a metal center. Noncrystalline chiral tertiary phosphines can be attached to a chiral reporter<sup>59,60</sup> for determination of enantiomeric excess by NMR spectroscopy, which is the most plausible methodology to employ in this case. Other options include chiral columns or magnetic circular dichroism spectroscopy.

It is not clear if products will be formed in appreciable enantiomeric excesses, but formation of *rac* and *meso* isomers during catalytic dehydrocoupling with **3** suggests that

phosphide inversion is rapid on the NMR time scale. This would give rise to formation of phosphine products are enantioenriched at the phosphorus center. Catalytic routes to secondary phosphines via hydrophosphination are limited, and catalytic routes to *enantioenriched* secondary phosphines are unknown. Thus far the only reported hydrophosphination catalysts require precious metals. Utilization of an earth-abundant metal like zirconium would be highly attractive. Development of this methodology would be of immense value and tackle a significant hurdle in metal-catalyzed hydrophosphination.

## 4.4 Experimental methods

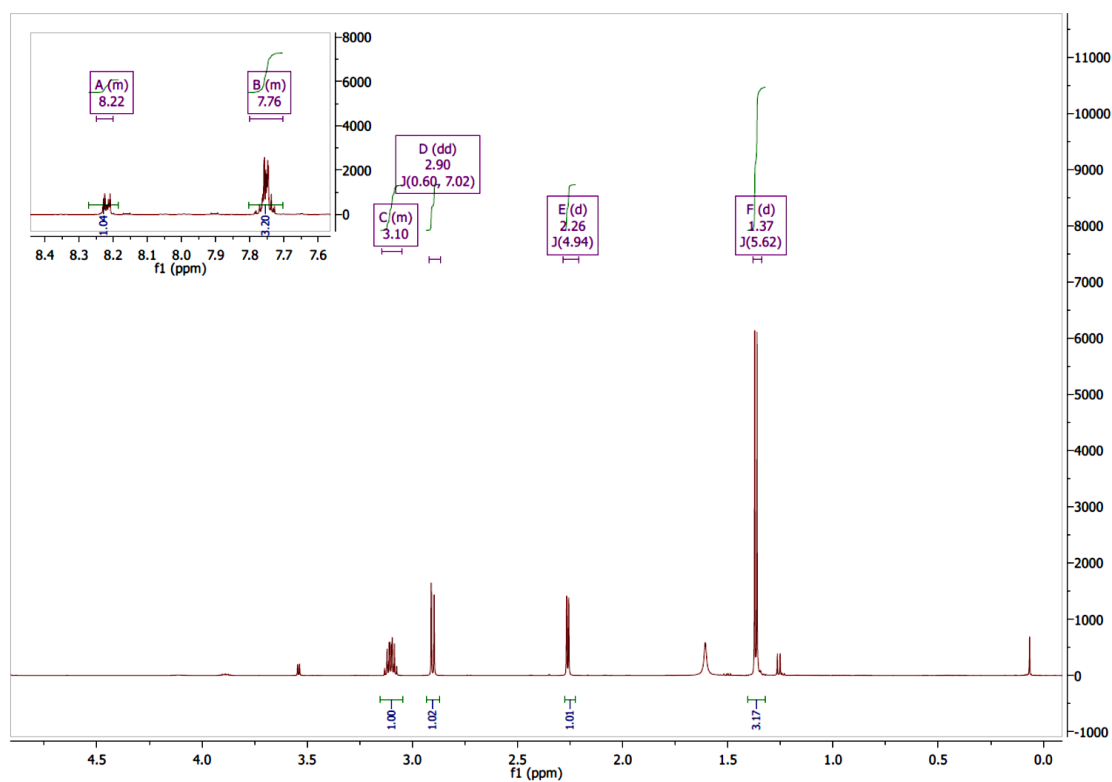
### 4.4.1 General methods

All manipulations, unless otherwise stated, were performed under an atmosphere of nitrogen using standard Schlenk line techniques. NMR spectra were recorded on a Bruker AXR 500 MHz spectrometer where  $^1\text{H}$  and  $^{13}\text{C}$  NMR spectra were referenced to residual solvent resonances.  $\text{CDCl}_3$  was purchased from Cambridge Isotope Laboratories and used as received. Diethyl ether and THF were dried over sodium before use. All other chemicals were purchased from either Sigma-Aldrich or Alfa Aesar and used as received. Compounds **1** and **2** were prepared as described in the literature.<sup>42</sup> Compounds **7**,<sup>46</sup> **8**,<sup>44,45</sup> **9**,<sup>52</sup> **10**,<sup>61</sup> and **12**,<sup>53</sup> were made following slight modifications on known literature procedures. All spectra agree with the literature.

### 4.4.2 Formation of compound 15

A solution of (*S*)-alaninol (2.73 g, 36.3 mmol) at 0 °C in *ca* 100 mL of water and 50 mL of pyridine was slowly given solid 2-nitrobenzenesulfonyl chloride (12.4 g, 78.6

mmol, 2.2 equiv) over the course of ten minutes. The reaction stirred overnight with gradual warming of the cold bath. The resulting bright yellow solution was recooled to 0 °C and given concentrated HCl slowly. This solution was washed with diethyl ether (4 x 50 mL), and concentrated to provide **14** as a yellow oil. Compound **14** was dissolved in diethyl ether and added to a suspension of 1.27 g (53.1 mmol) of NaH at 0 °C. After gas evolution ceased the cold bath was removed and the contents stirred overnight. Slow addition of ater to the crude reaction, followed by extraction with dichloromethane (3 x 50 mL) gave **15** (8.61 g, 35.6 mmol, 98%).<sup>62</sup> <sup>1</sup>H NMR (CDCl<sub>3</sub>): δ 8.22 (m, 1 H, C<sub>6</sub>H<sub>4</sub>NO<sub>2</sub>), 7.76 (m, 3 H, C<sub>6</sub>H<sub>4</sub>NO<sub>2</sub>), 3.10 (m, 1 H, CH), 2.90 (d, *J* = 7 Hz, 1 H, CH<sub>2</sub>), 2.26 (d, *J* = 5 Hz, 1 H, CH<sub>2</sub>), 1.37 (d, *J* = 6 Hz, 3 H).



**Figure 4.6:** <sup>1</sup>H NMR spectrum of **15**

#### 4.4.3 Formation of compound 16 (Figure 4.4)

This procedure follows a modification on known literature procedures.<sup>44,45</sup> A solution of **15** in methanol (0.211 g, 0.87 mmol) was given 0.10 mL of 1.9 M ammonia in methanol. The contents stirred at 55 °C for 2 h, then refluxed overnight. Volatiles were removed under reduced pressure to provide **16** as a colorless solid (0.127 g, 0.171 mmol, 59%). <sup>1</sup>H NMR (CDCl<sub>3</sub>): δ 8.35 (d, *J* = 7.5 Hz, 6 H, C<sub>6</sub>H<sub>4</sub>NO<sub>2</sub>), 7.81 (m, 2 H, 12 H, C<sub>6</sub>H<sub>4</sub>NO<sub>2</sub>), 7.70 (d, 8 Hz, 2 H, C<sub>6</sub>H<sub>4</sub>NO<sub>2</sub>), 4.81 (m, 3 H, CH), 4.01 (dd, *J* = 11 Hz, 7 Hz, CH<sub>2</sub>), 3.78 (dd, 11 Hz, 7 Hz, CH<sub>2</sub>), 1.60 (d, *J* = 7 Hz, 9 H, CH<sub>3</sub>).

#### 4.4.4 Deprotection of 8 with sulfuric acid to form 5 (Figure 4.3)

This procedure follows a literature report for a related compound.<sup>50</sup> A reaction tube containing 1.18 g (1.81 mmol) of **8** was slurried in concentrated sulfuric acid and heated to 90 °C for 2 days. The contents were cooled to 0 °C and given aqueous NaOH until the pH reached 14. The contents were extracted twice with DCM to give **5** (337.1 mg, 1.79 mmol, 93%).

#### 4.5 References

- (1) Lorke, D. E.; Stegmeier-Petroianu, A.; Petroianu, G. A. *J. Appl. Toxicol.* **2017**, 37, 13.
- (2) Galloway, T.; Handy, R. *Ecotoxicology* **2003**, 12, 345.
- (3) Butler, M. S.; Buss, A. D. *Biochem. Pharmacol.* **2006**, 71, 919.
- (4) Falagas, M. E.; Kastoris, A. C.; Kapaskelis, A. M.; Karageorgopoulos, D. E. *Lancet Infect. Dis.* **2010**, 10, 43.
- (5) Ji, H.-m.; Wei, L.-q. *Wujing Houqin Xueyuan Xuebao, Yixueban* **2015**, 24, 845.



- (6) Ogura, T.; Yoshida, K.; Yanagisawa, A.; Imamoto, T. *Org. Lett.* **2009**, *11*, 2245.
- (7) Mueller, G.; Brand, J. Z. *Anorg. Allg. Chem.* **2005**, *631*, 2820.
- (8) Lapprand, A.; Dutartre, M.; Khiri, N.; Levert, E.; Fortin, D.; Rousselin, Y.; Soldera, A.; Juge, S.; Harvey, P. D. *Inorg. Chem.* **2013**, *52*, 7958.
- (9) Rodriguez, L.-I.; Rossell, O.; Seco, M.; Muller, G. *J. Organomet. Chem.* **2007**, *692*, 851.
- (10) Rodriguez, L.-I.; Rossell, O.; Seco, M.; Orejon, A.; Masdeu-Bulto, A. M. *J. Organomet. Chem.* **2008**, *693*, 1857.
- (11) Rodriguez, L. I.; Rossell, O.; Seco, M.; Muller, G. *J. Organomet. Chem.* **2009**, *694*, 1938.
- (12) Rodriguez, L.-I.; Rossell, O.; Seco, M.; Orejon, A.; Masdeu-Bulto, A. M. *J. Supercrit. Fluids* **2011**, *55*, 1023.
- (13) Rodriguez, L.-I.; Rossell, O.; Seco, M.; Grabulosa, A.; Muller, G.; Rocamora, M. *Organometallics* **2006**, *25*, 1368.
- (14) Preetz, A.; Baumann, W.; Fischer, C.; Drexler, H.-J.; Schmidt, T.; Thede, R.; Heller, D. *Organometallics* **2009**, *28*, 3673.
- (15) Fryzuk, M. D.; Bosnich, B. *J. Am. Chem. Soc.* **1978**, *100*, 5491.
- (16) Glueck, D. S. *Chem. Eur. J.* **2008**, *14*, 7108.
- (17) Bartoli, G.; Bosco, M.; Sambri, L.; Marcantoni, E. *Tetrahedron Lett.* **1996**, *37*, 7421.
- (18) Gusarova, N. K.; Volkov, P. A.; Ivanova, N. I.; Khrapova, K. O.; Albanov, A. I.; Trofimov, B. A. *Russ. J. Gen. Chem.* **2016**, *86*, 731.

- (19) Sowa, S.; Stankevic, M.; Szmigielska, A.; Maluszynska, H.; Koziol, A. E.; Pietrusiewicz, K. M. *J. Org. Chem.* **2015**, *80*, 1672.
- (20) Dutartre, M.; Bayardon, J.; Juge, S. *Chem. Soc. Rev.* **2016**, *45*, 5771.
- (21) Glueck, D. S. *Chem. Eur. J.* **2008**, *14*, 7108.
- (22) Dubrovina, N. V.; Tararov, V. I.; Monsees, A.; Kadyrov, R.; Fischer, C.; Borner, A. *Tetrahedron: Asymmetry* **2003**, *14*, 2739.
- (23) Hayashi, T.; Niizuma, S.; Kamikawa, T.; Suzuki, N.; Uozumi, Y. *J. Am. Chem. Soc.* **1995**, *117*, 9101.
- (24) Rossen, K.; Pye, P. J.; Maliakal, A.; Volante, R. P. *J. Org. Chem.* **1997**, *62*, 6462.
- (25) Kagan, H. B.; Tahar, M.; Fiaud, J. C. *Tetrahedron Lett.* **1991**, *32*, 5959.
- (26) Shioji, K.; Ueno, Y.; Kurauchi, Y.; Okuma, K. *Tetrahedron Lett.* **2001**, *42*, 6569.
- (27) Wikteliu, D.; Johansson, M. J.; Luthman, K.; Kann, N. *Org. Lett.* **2005**, *7*, 4991.
- (28) Genet, C.; Canipa, S. J.; O'Brien, P.; Taylor, S. *J. Am. Chem. Soc.* **2006**, *128*, 9336.
- (29) Mislow, K.; Baechler, R. D. *J. Am. Chem. Soc.* **1971**, *93*, 773.
- (30) Pullarkat, S. A. *Synthesis* **2016**, *48*, 493.
- (31) Bange, C. A.; Waterman, R. *Chem. Eur. J.* **2016**, *22*, 12598.
- (32) Glueck, D. S. *Coord. Chem. Rev.* **2008**, *252*, 2171.
- (33) Rogers, J. R.; Wagner, T. P. S.; Marynick, D. S. *Inorg. Chem.* **1994**, *33*, 3104.
- (34) Malisch, W.; Maisch, R.; Meyer, A.; Greissinger, D.; Gross, E.; Colquhoun, I. J.; McFarlane, W. *Phosphorus, Sulfur Silicon Relat. Elem.* **1983**, *18*, 299.
- (35) Buhro, W. E.; Zwick, B. D.; Georgiou, S.; Hutchinson, J. P.; Gladysz, J. A. *J. Am. Chem. Soc.* **1988**, *110*, 2427.

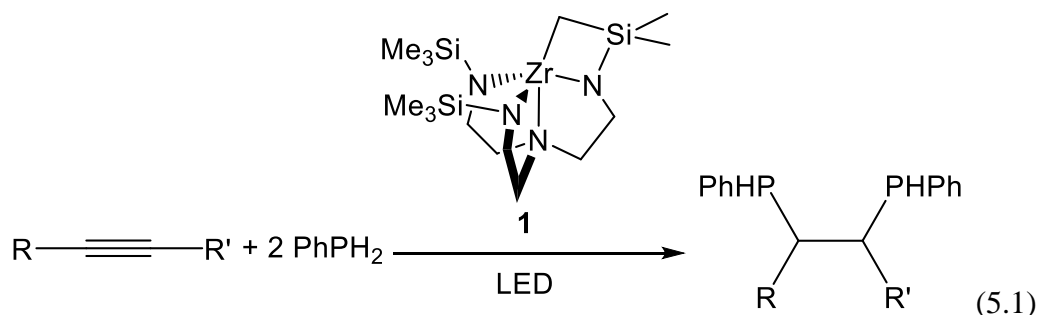
- (36) Buhro, W. E.; Gladysz, J. A. *Inorg. Chem.* **1985**, *24*, 3505.
- (37) Zwick, B. D.; Dewey, M. A.; Knight, D. A.; Buhro, W. E.; Arif, A. M.; Gladysz, J. A. *Organometallics* **1992**, *11*, 2673.
- (38) Baker, R. T.; Whitney, J. F.; Wreford, S. S. *Organometallics* **1983**, *2*, 1049.
- (39) Crisp, G. T.; Salem, G.; Stephens, F. S.; Wild, S. B. *J. Chem. Soc., Chem. Commun.* **1987**, 600.
- (40) Crisp, G. T.; Salem, G.; Wild, S. B.; Stephens, F. S. *Organometallics* **1989**, *8*, 2360.
- (41) Trost, B. M.; Bunt, R. C.; Lemoine, R. C.; Calkins, T. L. *J. Am. Chem. Soc.* **2000**, *122*, 5968.
- (42) Waterman, R. *Organometallics* **2007**, *26*, 2492.
- (43) Kovacic, I.; Wicht, D. K.; Grewal, N. S.; Glueck, D. S.; Incarvito, C. D.; Guzei, I. A.; Rheingold, A. L. *Organometallics* **2000**, *19*, 950.
- (44) Cernerud, M.; Adolfsson, H.; Moberg, C. *Tetrahedron: Asymmetry* **1997**, *8*, 2655.
- (45) Pei, Y.; Brade, K.; Brulé, E.; Hagberg, L.; Lake, F.; Moberg, C. *Eur. J. Org. Chem.* **2005**, *2005*, 2835.
- (46) Shintani, R.; Ikehata, K.; Hayashi, T. *J. O. C.* **2011**, *76*, 4776.
- (47) Wuts, P. G. M.; Greene, T. W. In *Greene's Protective Groups in Organic Synthesis*; John Wiley & Sons, Inc.: 2006, p 696.
- (48) Ramón, D. J.; Yus, M. *Eur. J. Org. Chem.* **2000**, *2000*, 225.
- (49) Vedejs, E.; Lin, S. *J. O. C.* **1994**, *59*, 1602.
- (50) Skinner, M. E. G.; Li, Y.; Mountford, P. *Inorg. Chem.* **2002**, *41*, 1110.

- (51) Shendage, D. M.; Fröhlich, R.; Haufe, G. *Org. Lett.* **2004**, *6*, 3675.
- (52) Gobbini, M.; Armaroli, S.; Banfi, L.; Benicchio, A.; Carzana, G.; Fedrizzi, G.; Ferrari, P.; Giacalone, G.; Giubileo, M.; Marazzi, G.; Micheletti, R.; Moro, B.; Pozzi, M.; Scotti, P. E.; Torri, M.; Cerri, A. *J. Med. Chem.* **2008**, *51*, 4601.
- (53) Hajela, S. P.; Johnson, A. R.; Xu, J.; Sunderland, C. J.; Cohen, S. M.; Caulder, D. L.; Raymond, K. N. *Inorg. Chem.* **2001**, *40*, 3208.
- (54) Sylla-Iyarreta Veitia, M.; Brun, P. L.; Jorda, P.; Falguieres, A.; Ferroud, C. *Tetrahedron: Asymmetry* **2009**, *20*, 2077.
- (55) Brown, A. C.; Carpino, L. A. *J. O. C.* **1985**, *50*, 1749.
- (56) Nyasse, B.; Grehn, L.; Ragnarsson, U. *Chem. Commun.* **1997**, 1017.
- (57) Hutchins, R. O.; Hutchins, M. K. In *Encyclopedia of Reagents for Organic Synthesis*; John Wiley & Sons, Ltd: 2001.
- (58) Yuan, J.; Huang, Y.; Chi, J.; Yuan, F.; BrightGene Bio-Medical Technology Suzhou Co., Ltd., Peop. Rep. China . 2017, p 12pp.
- (59) Albert, J.; Cadena, J. M.; Granell, J.; Muller, G.; Panyella, D.; Sanudo, C. *Eur. J. Inorg. Chem.* **2000**, 1283.
- (60) Otsuka, S.; Nakamura, A.; Kano, T.; Tani, K. *J. Am. Chem. Soc.* **1971**, *93*, 4301.
- (61) Rotstein, B. H.; Yudin, A. K. *Synthesis* **2012**, *44*, 2851.
- (62) Farras, J.; Ginesta, X.; Sutton, P. W.; Taltavull, J.; Egeler, F.; Romea, P.; Urpi, F.; Vilarrasa, J. *Tetrahedron* **2001**, *57*, 7665.

## CHAPTER 5: LIGHT-DEPENDENT ALKENE HYDROPHOSPHINATION: THE ROLE OF IRRADIATION

### 5.1 Introduction

The observed improvement in performance in the catalytic double hydrophosphination of alkynes<sup>1</sup> with primary phosphines under visible light irradiation with  $[\kappa^5-N',N',N',N',C-(Me_3SiNCH_2CH_2)_2NCH_2CH_2NSiMe_2CH_2]Zr$  (**1**) prompted an investigation into the role of light in general (eqn 5.1).



The observation that catalytic hydrophosphination of alkynes with **1** and PhPH<sub>2</sub> did not proceed in the absence of light strongly suggests that the mechanism by which **1** operates is by photoexcitation.<sup>1</sup>

Mechanistic reactivity of a variety of hydrophosphination metal catalysts has been discussed in depth.<sup>2</sup> The putative mechanism for many d<sup>0</sup> hydrophosphination catalysts is a form of insertion reactivity, like that noted for **1** (*vide infra*). The seminal report of terminal alkyne catalytic hydrophosphination with **1** identified an insertion-based mechanism.<sup>3</sup> However, previous studies on catalytic alkene and diene hydrophosphination with the same catalyst found that for primary phosphines internal competition experiments for styrenes with different electronic substituents showed preference for substrates with

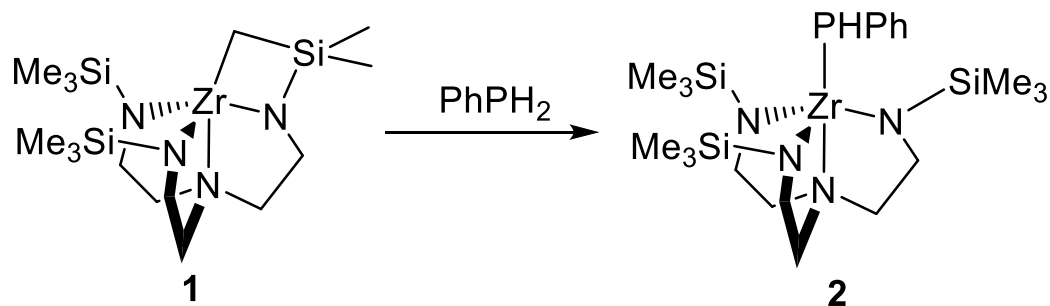
electron-withdrawing substituents.<sup>4</sup> This indicates some degree of nucleophilic attack from the zirconium–phosphide. In either of these studies there was found to be no light dependence on catalytic hydrophosphination with **1**, which is inconsistent with our current understanding for both alkene and alkyne hydrophosphination.

Very few hydrophosphination catalysts are known to be light-dependent,<sup>1, 5-8</sup> except for those which proceed through radical chemistry. The possibility of a radical in catalytic hydrophosphination with **1** is discounted by the instability of radical, and eliminated by radical clock experiments<sup>1</sup> and fluorescence lifetimes (*vide infra*). It should be underscored that absolutely no hydrophosphination happens in the absence of light for either alkenes or alkynes,<sup>1</sup> strongly suggesting that irradiation is crucial for catalysis with **1**. Furthermore, our system seems indifferent to heating for alkene substrates, unlike most reported hydrophosphination catalysts (*vide infra*). This catalyst is stimulated by light, rather than heat, making this system more environmentally friendly. This work aims to address the challenges in catalytic hydrophosphination by identifying and examining a system that operates under mild, photolytic conditions at substantially reduced reaction times.

## 5.2 Results and discussion

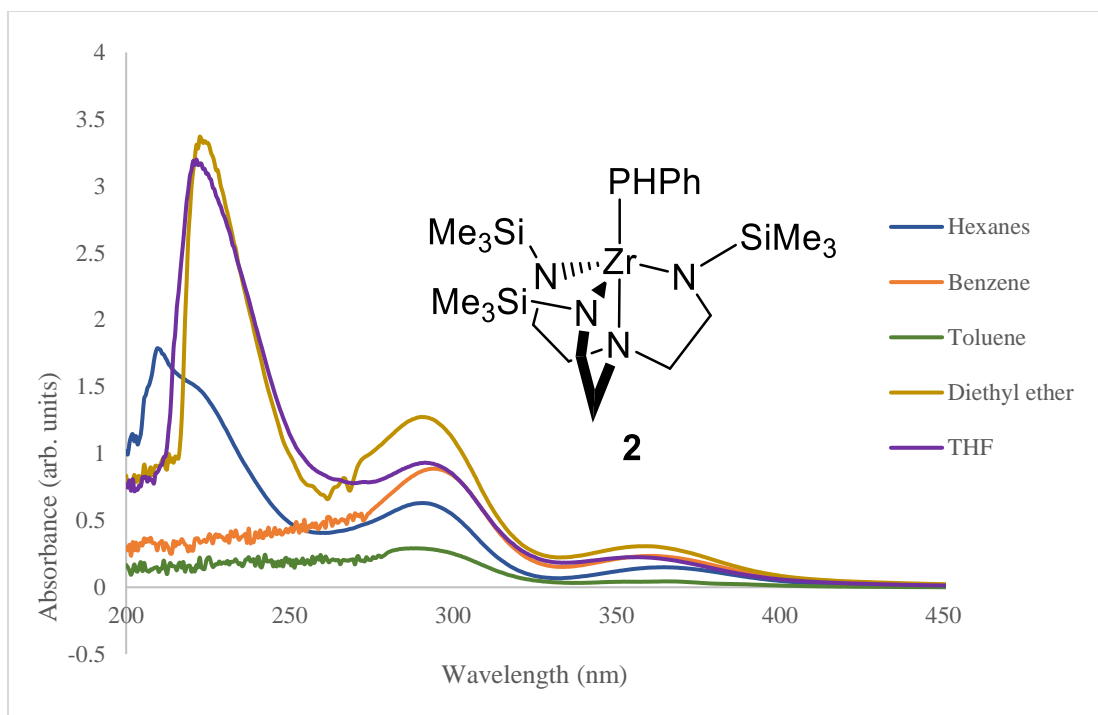
### 5.2.1: Ultraviolet-visible spectroscopy

The first attempts at consideration of the light dependence of **1** targeted understanding the photophysical properties of the active catalysts, **1** and **2**. While compound **1** is colorless, addition of PhPH<sub>2</sub> immediately forms the yellow zirconium phosphide **2** which is thought to be the resting state in catalysis<sup>9</sup> (Scheme 5.1).



**Scheme 5.1:** The two catalytically active zirconium species

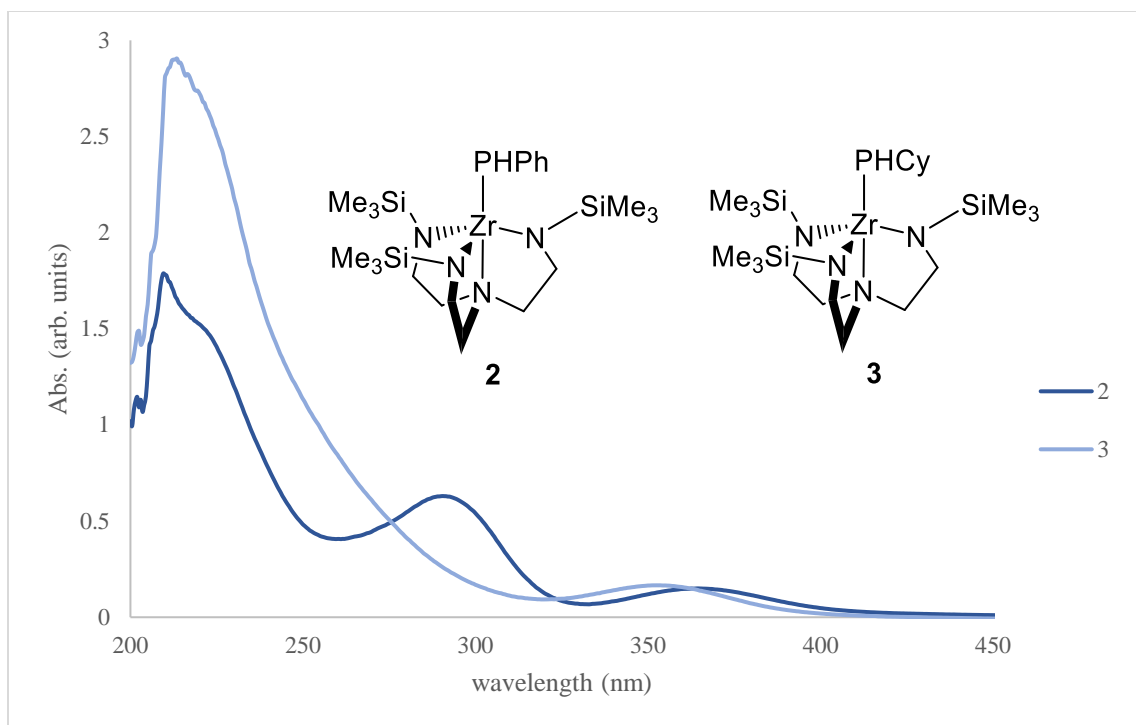
A working hypothesis in the alkyne hydrophosphination chemistry was that **2** is excited by visible light to allow for productive catalytic hydrophosphination.<sup>1</sup> Hydrophosphination in the absence of light failed to provide detectable levels of phosphine products, even after heating and extended reaction times.<sup>1</sup> Naturally, we were intrigued to investigate how derivatives of **1**, notably **2**, interacted with light. The UV-vis spectrum of **2** was collected to provide insight (Figure 5.1).



**Figure 5.1:** UV-vis spectra of **2** in various solvents

Three main transitions occur in UV/Vis spectrum of **2** at 364.5 nm, 290.5 nm, and a high-energy transition at roughly 209.5 nm, as shown for **2** in hexanes (Figure 5.1). The working hypothesis is that the visible transition (364.5 nm) is the Zr–P  $n \rightarrow d$  bond that is responsible for light-driven catalytic hydrophosphination with **1**. We speculated that the transition at 290 nm is in part due to the  $\pi \rightarrow \pi^*$  transition of the phenyl ring on the phosphide. This occurs in the typical region for  $\pi \rightarrow \pi^*$  for organic molecules,<sup>10</sup> and it is close to the  $\pi \rightarrow \pi^*$  transition for PhPH<sub>2</sub> (286 nm in benzene). This feature is absent for a related molecule, (N<sub>3</sub>N)Zr–PHCy (**3**, Cy = cyclohexyl, Figure 5.2).





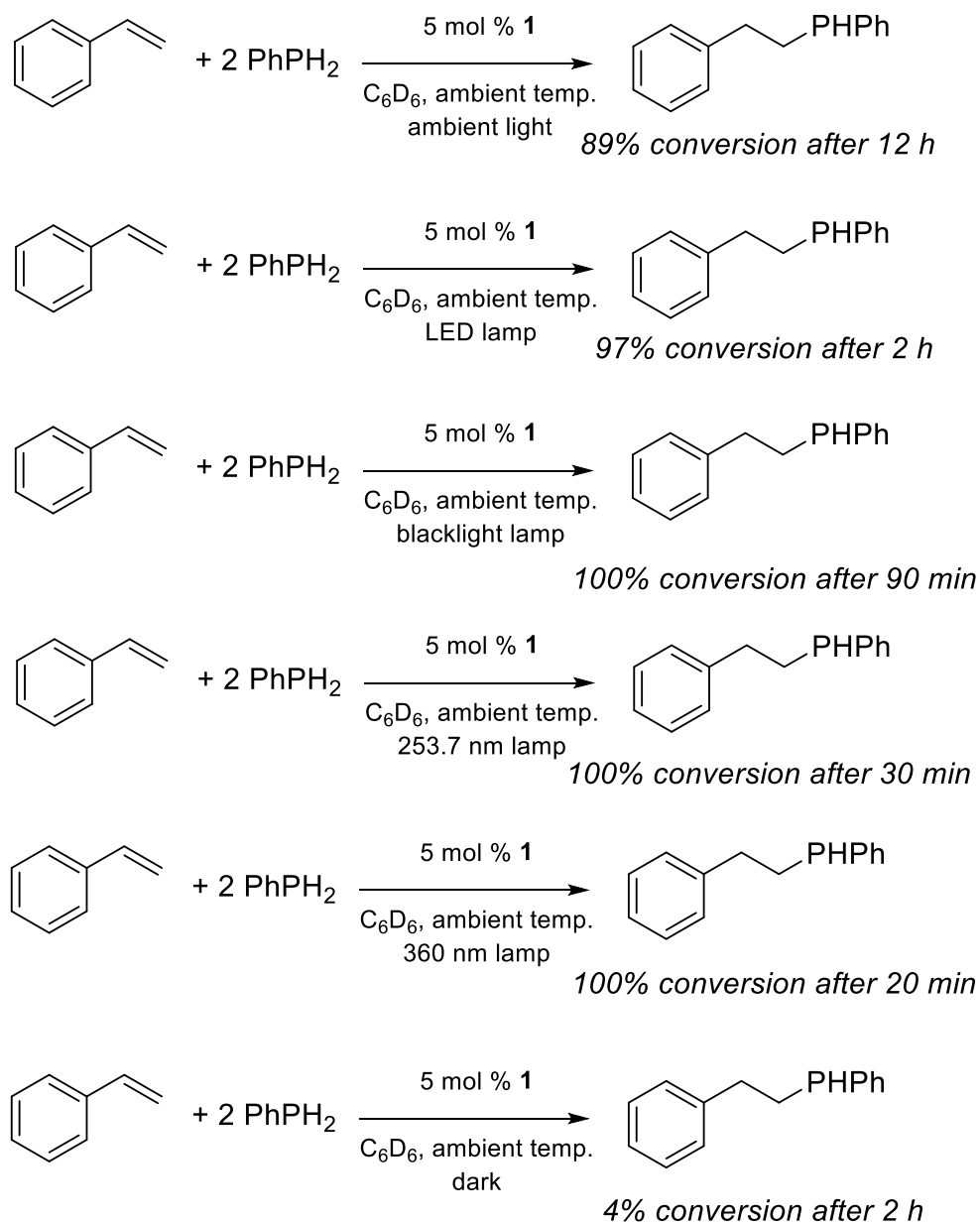
**Figure 5.2:** UV-vis spectra of **2** and **3** in hexanes

The observation that low-energy ultraviolet light activates catalytic hydrophosphination eliminates the 209.5 nm feature from governing hydrophosphination with **2** because this high-energy feature is not reached under irradiation with either the blacklight or the 253.7 nm lamps used for catalysis (*vide infra*). This supports the working hypothesis that the transition of interest is visible transition at 364.5 nm. This feature is mainly in the ultraviolet region but trickles into the visible, which explains the increased catalytic activity under LED irradiation over no irradiation, as observed for alkynes.<sup>1</sup>

### 5.2.2 Alkene hydrophosphination promoted by light

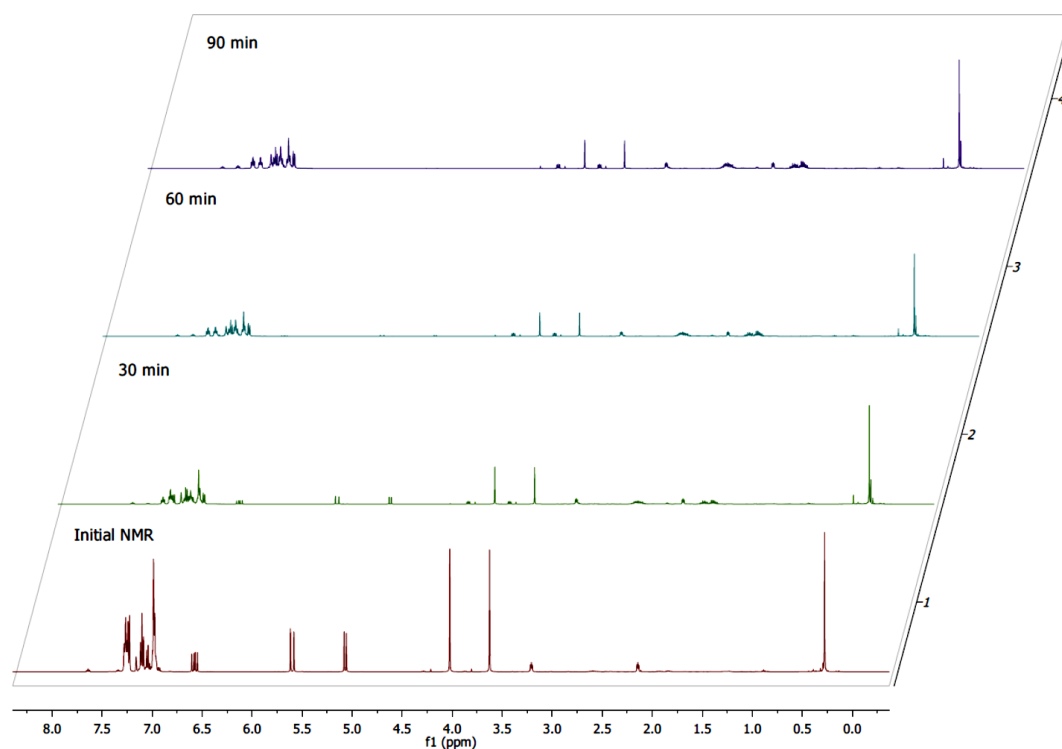
The working hypothesis that the visible transition is the 364.5 nm feature is the P–Zr  $n \rightarrow d$  electronic transition that is responsible for light-driven catalytic hydrophosphination. This thought launched an exploration into the photoexcitation of **2**

during catalysis. Direct irradiation of a mixture of styrene, PhPH<sub>2</sub> and catalytic amounts of **1** with the purpose of exciting into the transition at 364.5 nm resulted in productive hydrophosphination chemistry (Scheme 5.2).



**Scheme 5.2:** Catalytic hydrophosphination of styrene with **1** under different light sources

Catalytic hydrophosphination of styrene under irradiation with **1** provides the hydrophosphination products in drastically reduced time with the consistently high selectivity as previously reported.<sup>4</sup> Hydrophosphination products are detected after thirty minutes under blacklight irradiation, and quantitative conversion occurs after ninety minutes (Figure 5.3).

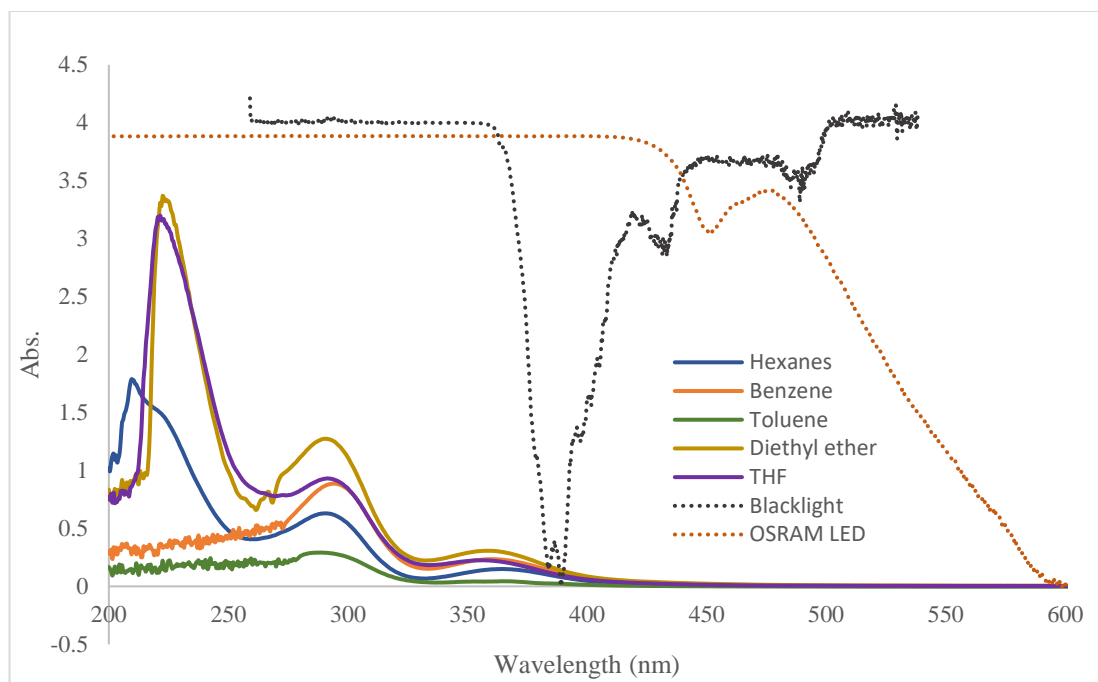


**Figure 5.3:** Stacked <sup>1</sup>H NMR spectra of the hydrophosphination of styrene under blacklight. Conditions: Two equivalents of PhPH<sub>2</sub> to styrene and 5 mol % **1**, ambient temperature, blacklight irradiation.

Styrene and its derivatives display absorbance features in the ultraviolet at around 280 nm.<sup>11</sup> The photochemistry of styrene derivatives is well-studied, particularly for styrene polymerizations.<sup>12-13</sup> The increased activity of these styrene derivatives under ultraviolet light could not be ignored as a potential source of the observed increased

hydrophosphination activity under backlight. However, the spectral energy distribution of any of the lamps shows no emission at these wavelengths (see experimental methods for details). Hydrophosphination of styrene in the absence of **1** showed less than 3% conversion under either backlight or 253.7 nm irradiation. Thus, these results strongly imply that the mechanism by which photocatalysis operates is by excitation of **1** rather than substrate activation under irradiation.

As explored previously,<sup>4</sup> hydrophosphination under ambient light provides 89% conversion of styrene to the product phosphine after 12 hours at ambient temperature (Scheme 5.2). However, as noted for the double alkyne hydrophosphination,<sup>1</sup> direct irradiation from an LED lamp increases catalytic activity such that the product PhCH<sub>2</sub>CH<sub>2</sub>PHPh is formed in nearly quantitative yields over two hours (Scheme 5.2, entry 2). These observations prompted a closer look at the spectroscopic features of **2** and the light source. Examination of the spectral energy distribution of the LED lamp reveals little overlap between the light output wavelength range and the absorbance of the proposed excited P  $n \rightarrow$  Zr  $d$  transition in the UV-vis spectrum (Figure 5.4).



**Figure 5.4:** Overlap of the spectral energy distribution of the OSRAM Sylvania Ultra LED A19 Lamp – generation 5, operating power of 6 W and output of 450 lumens (red dash), VEI UV Blacklight Party Lamp, operating power of 13 W (black dash), and UV-vis absorbance of **2**. Transmission spectra are scaled as a percentage of their maximum output.

The spectral energy distribution of the LED lamp scarcely overlaps with the shoulder of the anticipated 364.5 nm  $P\ n \rightarrow Zr\ d$  transition for **2** (Figure 5.4). While irradiation from the LED promotes catalytic hydrophosphination, we hypothesized that irradiation at wavelengths that align more closely with the proposed  $P\ n \rightarrow Zr\ d$  transition should promote catalysis to a greater extent. That turned out to be true. Irradiation from a commercially available blacklight bulb decreases the time to reach quantitative hydrophosphination of styrene from two hours to ninety minutes (Scheme 5.2, entry 3).

The 364.5 nm transition is the least intense of all three features ( $\epsilon = 290\ (6)\ M^{-1}\ cm^{-1}$  for hexanes at 364.5 nm). Therefore, excitation into a higher energy band remained

intriguing. Use of a series of monochromatic 253.7 nm UV/C mercury arc lamps provided quantitative consumption of styrene after thirty minutes (Scheme 5.2, entry 4).

It is clear from the manufacturer's specifications that this lamp generates significant power. The increased reactivity from the blacklight bulb to the 253.7 nm bulb could be explained by the dramatic increase in light intensity (photon density). The promotion of catalytic hydrophosphination by the 253.7 nm light source is probably from the increased light intensity reaching the reaction, followed by rapid relaxation to the emissive state, rather than chemistry from a higher-energy feature. To test the relative contribution from the light intensity, all but two of the sixteen lamps in the photoreactor were covered with aluminum foil. This resulted in a decrease in the consumption of styrene from 100% to 54% after 30 min. This result suggests that the light intensity from the 253.7 nm photoreactor, rather than this specific wavelength, results in increased catalytic turnover.

None of the spectral energy distributions of the lamps strongly align with the proposed  $P\ n \rightarrow Zr\ d$  transition of **2** (Figure 5.1), despite the obvious light dependence on catalytic hydrophosphination. A 9-W UV/A lamp that has a broad spectral energy from 320–400 nm and that is centered at 360 nm was acquired from Rexim and used for hydrophosphination (see experimental methods for details). Use of this lamp for catalytic hydrophosphination with **1** resulted in quantitative conversion after 20 minutes at ambient temperature (TON = 20 and TOF = 60 h<sup>-1</sup>) (Scheme 5.2, entry 5). Thus it seems that targeting this 364.5 nm feature directly provides higher turnover than is observed for the blacklight or the monochromatic 253.7 nm bulb, as anticipated (Scheme 5.2, entry 5). The

blacklight lamp and 253.7 nm lamps can excite to only a smaller fraction of this transition, and thus the discrepancy is observed (Scheme 5.2, entries 3-5).

Comparison of the lamps shown in Scheme 5.2 is made complicated because several factors are at play. For example, each lamp has a different wattage, surface area, wavelength, and operating temperature. Some values are outlined in Table 5.1.

**Table 5.1:** Lamp specifications. <sup>a</sup>Manufacturer's specifications. <sup>b</sup>Measured. <sup>c</sup>Calculated. Intensities are calculated by dividing the lamp wattage over the surface area of the bulb. Spherical light bulbs are approximated as perfect spheres and linear bulbs are approximated as perfect cylinders. The relative intensity integration is the product of the intensity and the overlap of the lamp transmission with the absorbance spectra of **2** (Figure 5.1).

	LED (Osram)	Blacklight (VEI party lamp)	360 nm (Rexim)	253.7 nm
Wavelength range	400-800 nm <sup>b</sup>	360-500 nm <sup>b</sup>	350-400 nm <sup>a</sup>	253.7 nm <sup>a</sup>
Wattage	9 Watts <sup>a</sup>	13 Watts <sup>a</sup>	9 Watts <sup>a</sup>	128 Watts <sup>a</sup>
Intensity (mW/cm <sup>2</sup> )	~2,000 <sup>c</sup>	~10,000 <sup>c</sup>	~100,000 <sup>c</sup>	12,800 <sup>a</sup>
Relative intensity integration over wavelength range (mW/cm <sup>2</sup> ) <sup>c</sup>	1.0 x 10 <sup>4</sup>	1.8 x 10 <sup>4</sup>	3.0 x 10 <sup>6</sup>	5.3 x 10 <sup>3</sup>

One way to relate these differences is by the light intensity, which is defined as the wattage output per surface area. Because not all of the lamp's spectral distribution will reach the  $P\ n \rightarrow Zr\ d$  feature of **2** (Figure 5.3), a comparison of the intensity to the absorbance region of the molecule was made. The integration of the UV-vis spectrum shown in Figure 5.3 over the active wavelengths per each bulb was calculated. This value was multiplied by the light intensity to provide the relative intensity integration over the wavelength range (Table 5.1, row 4).

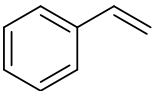
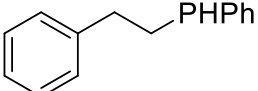
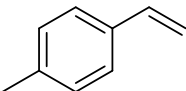
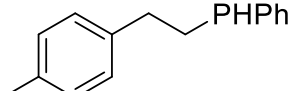
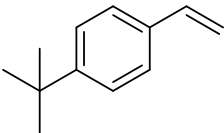
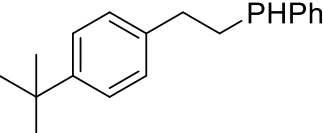
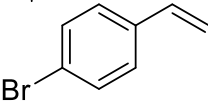
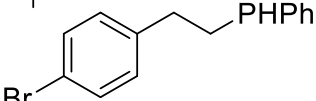
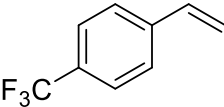
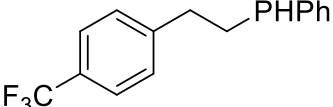
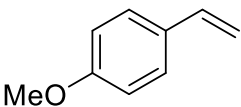
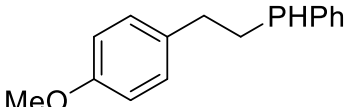
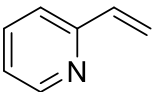
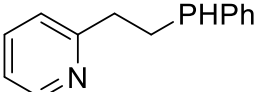
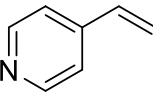
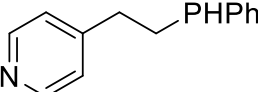
It is clear from Table 5.1 why the Rexim lamps provide the highest catalytic turnover. The relative intensity of the Rexim lamp over the feature at 360 nm is calculated to be significantly higher than that of any other lamp. These values also explain why the blacklight bulb is the second-best candidate for promoting catalytic hydrophosphination with **1**, and why the LED bulb can promote hydrophosphination, despite the relatively low overlap with the 364.5 nm, proposed  $P\ n \rightarrow Zr\ d$  feature. It is worth noting that the values outlined in Table 5.1 do not account for relaxation from higher-energy excited states to lower-energy excited states, as is probably the case for the 253.7 nm lamp. Instead, this lamp likely absorbs more photons (Figure 5.1), corresponding to enhanced reactivity.

### 5.2.3: Alkene hydrophosphination with **1**

The catalytic turnover of styrene under blacklight irradiation was not as impressive as turnovers from either the Rexim lamps or 253.7 nm irradiation (Table 5.2 entries 3-5). However, conversions reached under blacklight irradiation are still a dramatic improvement from that previously reported. For example, styrene hydrophosphination took 12 hours to provide 89% conversion,<sup>4</sup> whereas blacklight irradiation provides the same product in quantitative conversions in two hours. Furthermore, the blacklight lamps are inexpensive and commercially available, unlike either the Rexim lamp or 253.7 mercury arc lamps. Given the insight gained, a series of styrene derivatives were targeted for catalytic hydrophosphination with **1** under blacklight irradiation (Table 5.2).



**Table 5.2:** Catalytic hydrophosphination of styrene derivatives with **1** under blacklight. Conditions: 20 equiv. of styrene, 40 equiv. of PhPH<sub>2</sub>, 1 equiv. of **1** in ca 0.5 mL benzene-*d*<sub>6</sub>. <sup>1</sup>H NMR spectra were recorded before irradiation. Percent conversion was measured by integration of the <sup>1</sup>H NMR spectra.

$2 \text{ PhPH}_2 + \text{R-CH=CH}_2 \xrightarrow[\text{ambient temperature}]{\text{5 mol \% } \mathbf{1}, \text{C}_6\text{D}_6, \text{blacklight}} \text{R-CH}_2\text{CH}_2\text{P(Ph)}_2$				
Entry	Substrate	Time (min)	Product	Conversion (%)
a		90		100
b		90		100
c		90		100
d		90		100
e		90		98
f		90		100
g		120		84
h		120		85

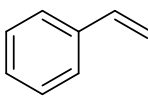
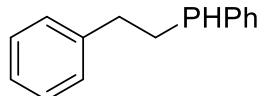
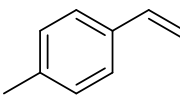
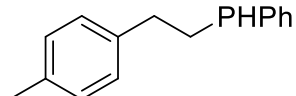
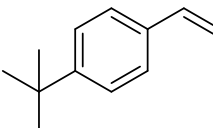
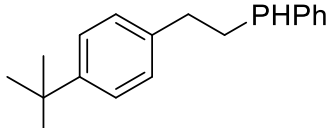
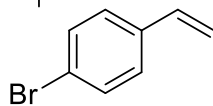
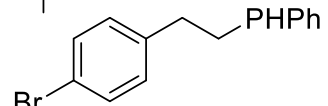
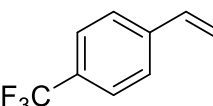
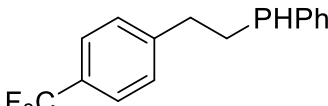
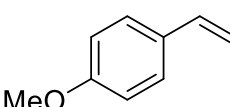
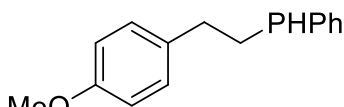
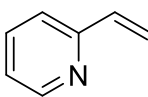
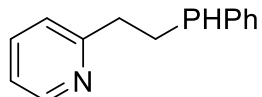
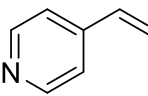
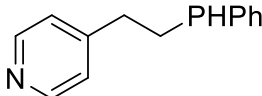
As expected from prior hydrophosphination investigations with **1** and primary phosphines,<sup>4, 14-15</sup> the secondary phosphine products were formed in high conversions. The

anticipated selectivity for secondary phosphine formation still remains and the catalysis tolerates a variety of functional groups.

Blacklight irradiation increases the turnover frequency compared to reactions run under ambient light. For example, hydrophosphination of *p*-trifluoromethylstyrene proceeded to nearly quantitative conversion of the secondary phosphine product after 90 min (Table 5.2, 1e), but previously reported hydrophosphination without irradiation provides 82% after 12 h under otherwise identical conditions.<sup>4</sup> Interestingly, reactions run under irradiation from either LED or blacklight lamps with heating from an oil bath at 55 °C result in a *lower* conversion to the products. For example, catalytic styrene hydrophosphination with **1** under blacklight irradiation results in 47% conversion at ambient temperature after 18 minutes, but 36% conversion at 55 °C after 18 minutes. It is worth noting that the light cannot penetrate the oil bath to the same extent, which results in the lower observed conversions.

The fastest conversions for styrene hydrophosphination are obtained under irradiation at 253.7 nm. The improvement is substantial. The conversions increase from 89% to quantitative, and the reaction time is decreased for 12 hours (TON = 18 and TOF = 1.5 h<sup>-1</sup>) to 30 minutes (TON = 20 and TOF = 40 h<sup>-1</sup>). For these reasons a variety of styrene derivatives were targeted for catalytic hydrophosphination with **1** under irradiation from the 253.7 nm photoreactor (Table 5.3).

**Table 5.3:** Catalytic hydrophosphination of styrenes under 253.7 nm. Conditions: 20 equiv. of unsaturated substrate, 40 equiv. of PhPH<sub>2</sub>, 1 equiv. of **1** in ca 0.5 mL benzene-*d*<sub>6</sub>. <sup>1</sup>H NMR spectra were recorded before blacklight irradiation. Percent conversion was measured by integration of the <sup>1</sup>H NMR spectra.

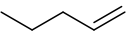
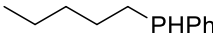
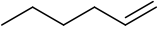
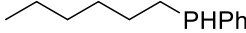
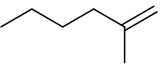
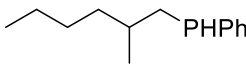
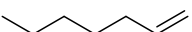
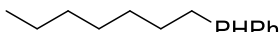
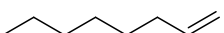
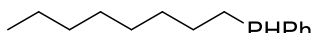
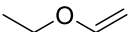
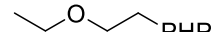
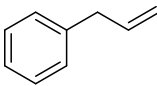
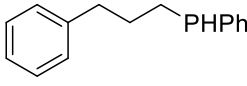
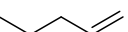
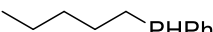
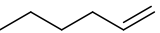
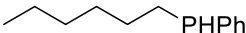
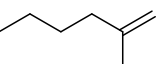
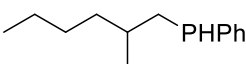

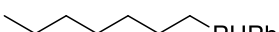
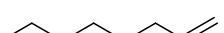
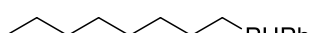
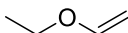
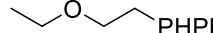
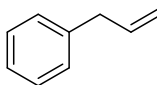
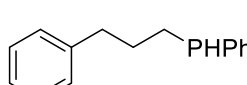
$2 \text{ PhPH}_2 + \text{R-CH=CH}_2 \xrightarrow[\text{ambient temperature}]{\text{C}_6\text{D}_6, 253.7 \text{ nm}, 5 \text{ mol } \% \text{ 1}} \text{R-CH}_2\text{CH}_2\text{P(Ph)}_2$				
Entry	Substrate	Time (min)	Product	Conversion (%)
a		30		100
b		30		100
c		30		100
d		30		82
e		30		100
f		30		100
g		120		100
h		120		100

The increased reactivity is consistent for every substrate (Table 5.3). The higher conversions under irradiation from the 253.7 nm photoreactor is a direct reflection of the

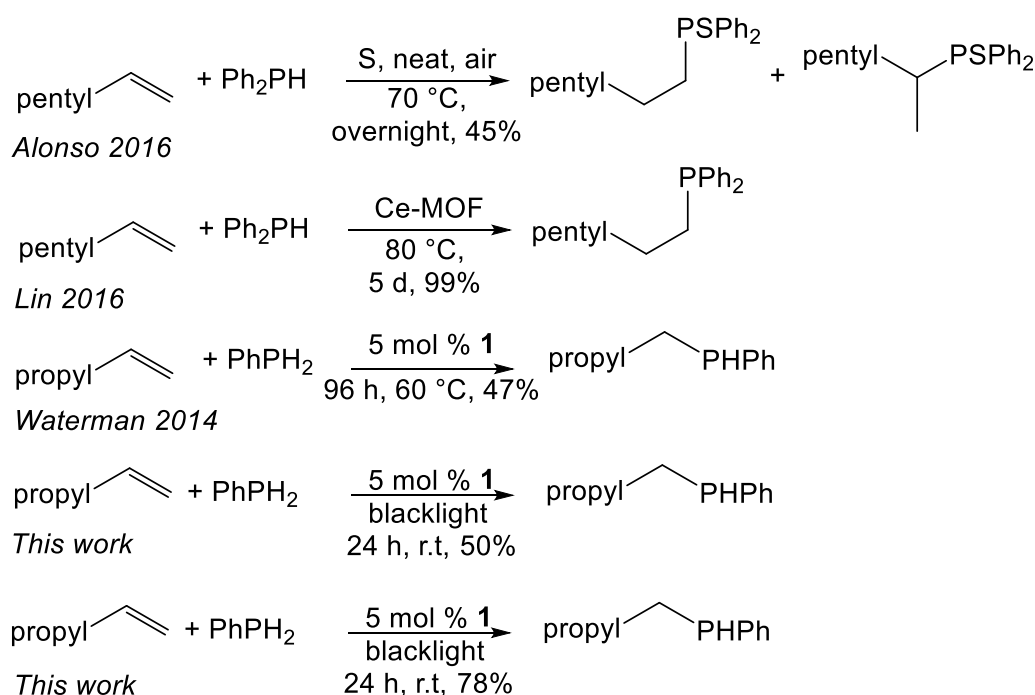
light intensity, rather than the specific wavelength (*vide supra*). Regardless, this represents substantial improvement in catalytic hydrophosphination. Only a handful can reach conversions higher than 90% for any phosphine even under more forcing conditions.<sup>16-19</sup>

Given the new implications a variety of unactivated alkene substrates were targeted (Table 5.4). These substrates are underreported in catalytic hydrophosphination.<sup>1</sup>

**Table 5.4:** Catalytic hydrophosphination of unactivated alkenes. Conditions: 20 equiv. of unsaturated substrate, 40 equiv. of PhPH<sub>2</sub>, 1 equiv. of **1** in ca 0.5 mL benzene-*d*<sub>6</sub>. <sup>1</sup>H NMR spectra were recorded before irradiation. Percent conversion was measured by integration of the <sup>1</sup>H NMR spectra.

$2 \text{ PhPH}_2 + \text{R}-\text{CH}=\text{CH}_2 \xrightarrow[\text{ambient temperature}]{\text{5 mol \% } \mathbf{1}, \text{C}_6\text{D}_6, \text{blacklight}} \text{R}-\text{CH}_2\text{CH}_2\text{P(Ph)}_2$					
Entry	Substrate	Time (h)	lamp	Product	Conversion (%)
a		24	blacklight		59
b		24	blacklight		50
c		24	blacklight		52
d		24	blacklight		60
e		24	blacklight		45
f		24	blacklight		63
g		24	blacklight		61
h		24	253.7 nm		81
i		24	253.7 nm		78
j		24	253.7 nm		70
k		24	253.7 nm		73
l		24	253.7 nm		74
m		24	253.7 nm		56
n		24	253.7 nm		81

Catalytic hydrophosphination of unactivated alkenes with **1** requires longer reaction times than those for styrene substrates and provides the secondary phosphine products in lower yields, as anticipated (Table 5.4). Despite the modest conversions, it is worth underscoring that the only two other hydrophosphination catalysts that report attempts of hydrophosphination with 1-hexene only form the products in trace amounts with either primary or secondary phosphines, despite more forcing conditions,<sup>20-21</sup> though two groups have reported *stoichiometric* hydrophosphination reactions with 1-hexene.<sup>22-23</sup> Only two other report managed to obtain detectable levels of hydrophosphination products using an unactivated linear alkene<sup>24-25</sup> (Scheme 5.3).



**Scheme 5.3:** Notable examples of unactivated alkene hydrophosphination

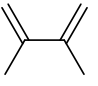
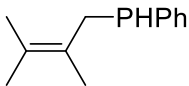
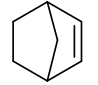
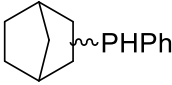
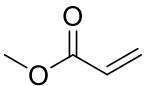
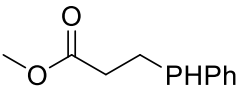
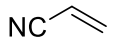
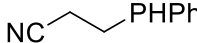
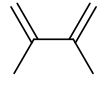
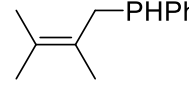
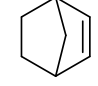
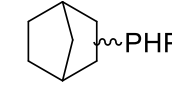
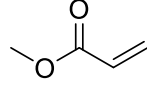
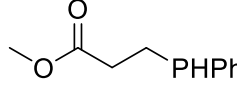
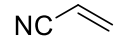
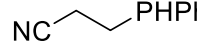
One report proceeded with Ph<sub>2</sub>PH to give limited conversions to the tertiary product as two isomers.<sup>24</sup> A separate example used a cerium-based metal-organic framework to achieve high conversions after several days at elevated temperatures.<sup>25</sup>

Clearly these are challenging substrates for this reaction. Our previous report using no irradiation required 96 hours at 60 °C for modest conversion (Scheme 5.3). This system offers the highest conversions to date of underreported, challenging substrates, and it does so with relatively low reaction times at ambient temperature. Now, the activity of unactivated alkenes rivals the reactivity of styrene derivatives under thermal conditions with **1**.

This scarcity of this transformation is not a reflection of the nature of unactivated alkene itself, as these should appear to be excellent candidates for hydrophosphination. The electronics of the unactivated alkene are concentrated at the double bond making them good candidates for insertion-based chemistry. The sterics of the unsaturated linear alkenes are minimal.<sup>10</sup> The degree of rotation along the carbon backbone is high enough that these ought to readily fold and contort in solution to properly interact with a metal catalyst. However, this underrepresentation can be understood because most late-metal hydrophosphination catalysts operate via nucleophilic attack of the metal phosphide to the substrate.<sup>2</sup> Substrates that possess electron-withdrawing groups are better suited for those catalysts. The observation that so few hydrophosphination catalysts can successfully add a phosphine across this bond presents a limitation in the field.<sup>26</sup> We hope that this work closes that substrate gap.

Given the high generality of catalytic hydrophosphination with **1** for a wide family of substrates, a series of Michael acceptors and uncommon alkenes and dienes were tested under blacklight irradiation (Table 5.5).

**Table 5.5:** Catalytic hydrophosphination of dienes substrates, unactivated substrates, and Michael acceptors. Conditions: 20 equiv. of unsaturated substrate, 40 equiv. of PhPH<sub>2</sub>, 1 equiv. of **1** in ca 0.5 mL benzene-*d*<sub>6</sub>. <sup>1</sup>H NMR spectra were recorded before irradiation. Percent conversion was measured by integration of the <sup>1</sup>H NMR spectra.

$2 \text{ PhPH}_2 + \text{R-CH=CH}_2 \xrightarrow[\text{ambient temperature}]{\text{5 mol \% } \mathbf{1}, \text{C}_6\text{D}_6, h\nu} \text{R-CH}_2\text{CH}_2\text{P(Ph)}_2$					
Entry	Substrate	Time (h)	light	Product	Conversion (%)
a		2	blacklight		100
b		4.5	blacklight		96
d		2	blacklight		85
e		3	blacklight		94
e		1	253.7 nm		100
f		3.5	253.7 nm		97
g		2	253.7 nm		100
h		2	253.7 nm		100

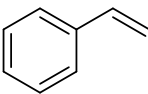
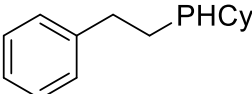
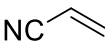
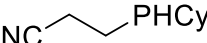
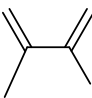
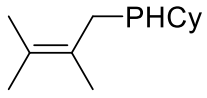
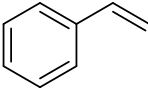
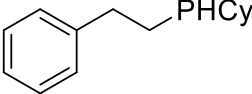
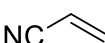
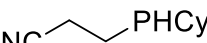
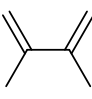
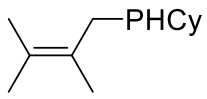
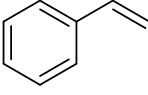
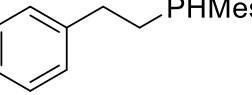
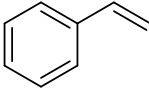
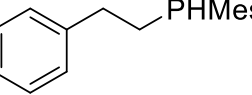
As is the case for styrene derivatives and unactivated alkenes, catalytic hydrophosphination with **1** offers the highest conversions to date of all substrates shown in Table 5.5. It is worth highlighting the remarkable substrate versatility in catalytic hydrophosphination with **1** (Table 5.4) as it lends credence to the working hypothesis that light irradiation excites the Zr *n* → P *d* transition in the catalyst responsible for product formation, rather than any direct irradiation of the substrate itself. Michael acceptors are



very common among late transition-metal catalysts because these substrates are better-suited for nucleophilic attack. Our photocatalytic system operates by substrate insertion, so it is understandable why the improvement of these substrates is not as substantial as that observed for unactivated alkene and styrene derivatives (Tables 5.2-5.4).

The impact of light on catalysis prompted an investigation into challenging primary phosphines for hydrophosphination with **1**. While **1** has been known to catalyze the hydrophosphination of bulky, air-stable primary phosphines,<sup>14-15</sup> hydrophosphination with CyPH<sub>2</sub> proved limited<sup>3</sup> and hydrophosphination with MesPH<sub>2</sub> failed (Mes = mesityl = 2,4,6-trimethylphenyl). We were curious to see if irradiation would promote hydrophosphination of both CyPH<sub>2</sub> and MesPH<sub>2</sub>. Hydrophosphination of substrates with CyPH<sub>2</sub> under irradiation from either the blacklight or 253.7 nm bulb shows substantially increased activity over previous reports<sup>4</sup> (Table 5.6).

**Table 5.6:** Catalytic hydrophosphination using CyPH<sub>2</sub> and MesPH<sub>2</sub>. Conditions: 20 equiv. of unsaturated substrate, 40 equiv. of RPH<sub>2</sub>, 1 equiv. of **1** in ca 0.5 mL benzene-*d*<sub>6</sub>. <sup>1</sup>H NMR spectra were recorded before irradiation. Percent conversion was measured by integration of the <sup>1</sup>H NMR spectra.

$2 \text{ R'PH}_2 + \text{R-CH=CH}_2 \xrightarrow[\text{ambient temperature}]{\text{5 mol \% } \mathbf{1}, \text{C}_6\text{D}_6, h\nu} \text{R-CH}_2\text{-CH}_2\text{-PHR'}$						
Entry	Substrate	R'PH <sub>2</sub>	Time (h)	lamp	Product	Conversion (%)
a		CyPH <sub>2</sub>	24	blacklight		90
b		CyPH <sub>2</sub>	24	blacklight		68
c		CyPH <sub>2</sub>	24	blacklight		53
d		CyPH <sub>2</sub>	5	253.7 nm		98
e		CyPH <sub>2</sub>	24	253.7 nm		98
f		CyPH <sub>2</sub>	24	253.7 nm		95
g		MesPH <sub>2</sub>	24	blacklight		83
h		MesPH <sub>2</sub>	24	253.7 nm		95

Catalytic hydrophosphination of CyPH<sub>2</sub> using **1** provides the secondary phosphine products in high conversions (Table 5.6). This is especially apparent for reactions run under 253.7 nm irradiation. For example, both styrene and 2,3-dimethyl-1,3-butadiene undergo the single hydrophosphination after hours at ambient temperature

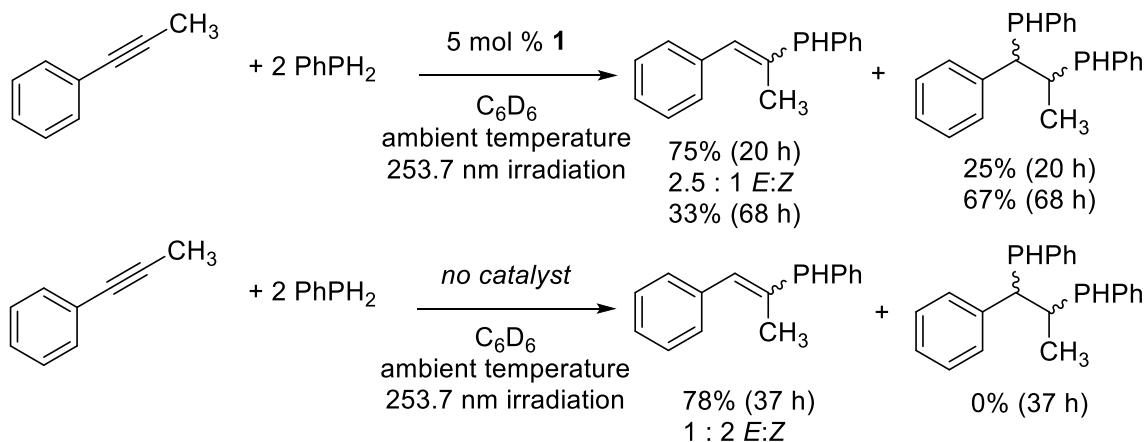
(Table 5.6, entries e-f). Previous studies required heating and extended reaction times to achieve appreciable yields for CyPH<sub>2</sub>.<sup>4</sup>

The turnover increased for both CyPH<sub>2</sub> and MesPH<sub>2</sub> under irradiation from 253.7 nm bulb from the blacklight bulb, as anticipated from hydrophosphination of PhPH<sub>2</sub>. It is worth noting that MesPH<sub>2</sub> is the largest primary phosphine for which productive catalysis can occur with **1**. Reactions run under LED give poor (ca 12%) conversion to the product, and reactions run in the absence of light fail to provide any detectable products. Like **2** and **3**, the zirconium mesityl phosphide **4** has an electronic feature at 372 nm in hexanes that is reached under irradiation from the blacklight and 253.7 nm lamps. The poor turnover (albeit an improvement!) from irradiation under LED is probably a reflection of the increased steric demands of the mesityl phosphine, rather than an electronic effect. Regardless, the hydrophosphination represented in Table 5.6 is the first example of a catalytic hydrophosphination with **1** and MesPH<sub>2</sub>. Control reactions under ambient light with MesPH<sub>2</sub> failed to provide reactivity. Furthermore, hydrophosphination under irradiation outperforms the previous proof-of-concept studies on hydrophosphination with CyPH<sub>2</sub>.<sup>4</sup>

These results go in tandem with the observed light dependence on hydrophosphination with **1** and its derivatives. The underlying theme is that light excites the zirconium–phosphides to do productive chemistry. Because the proposed P *n* → Zr *d* absorbance features of **3** and **4** are the only feature with energy that overlaps with that of the blacklight emission, it is entirely reasonable to see how excitation of this P *n* → Zr *d* transition drives catalysis with **1**.

#### 5.2.4: Light-driven alkyne hydrophosphination with **1**

Given the success of irradiation in alkene hydrophosphination with **1**, reinvestigation of *alkyne* substrates under photochemical conditions was enticing. Alkyne double hydrophosphination was limited by the long reaction times and elevated temperatures required for this transformation to proceed.<sup>1</sup>



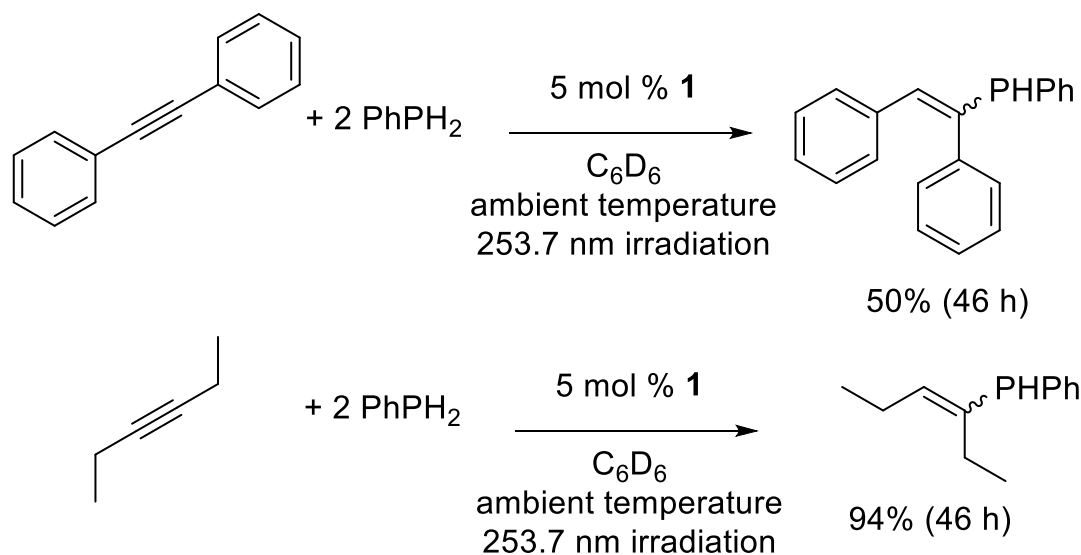
**Scheme 5.5:** Hydrophosphination of methylphenylacetylene under 253.7 nm irradiation

Catalytic hydrophosphination of methylphenylacetylene provided the vinyl phosphine at ambient temperature under 253.7 nm irradiation (Scheme 5.5). Hydrophosphination reactions run under blacklight irradiation either at ambient temperature or with heating underperform compared to previously reported conditions.<sup>1</sup> The relatively high conversion of methylphenylacetylene to the single hydrophosphination product without heating was encouraging, but the selectivity of this transformation was worse than previously reported under LED. The poor selectivity observed for either blacklight or 253.7 nm irradiation compared to the LED-driven reactions explored previously is likely an expression of the faster kinetics of the insertion process. It is

suspected that the light does not govern this second step as strongly as the initial hydrophosphination event as noted for alkyne hydrophosphination under LED irradiation.

The double hydrophosphination to the diphosphine occurred after approximately three days at ambient temperature under irradiation from the 253.7 nm lamp (Scheme 5.5). Previously reported hydrophosphination targeting this product required three days at 80 °C under LED irradiation to achieve a similar conversion. The inability of the photoreactor to improve upon the sluggish turnover in the double hydrophosphination catalysis was discouraging, but also highlights how difficult a double hydrophosphination reaction is.

The high-energy photoreactor used in these experiments is utilized among organic chemists for photoreactions. We were curious to see if the light irradiation were sufficient enough to drive hydrophosphination without a catalyst. A control reaction of methylphenylacetylene and  $\text{PhPH}_2$  in the absence of **1** run in the photoreactor provided the vinyl phosphine, but with longer reaction times, poorer conversions, and reversed selectivity (Scheme 5.5). More importantly, formation of the double hydrophosphination product did not occur under these conditions.



**Scheme 5.6:** Hydrophosphination of internal alkynes

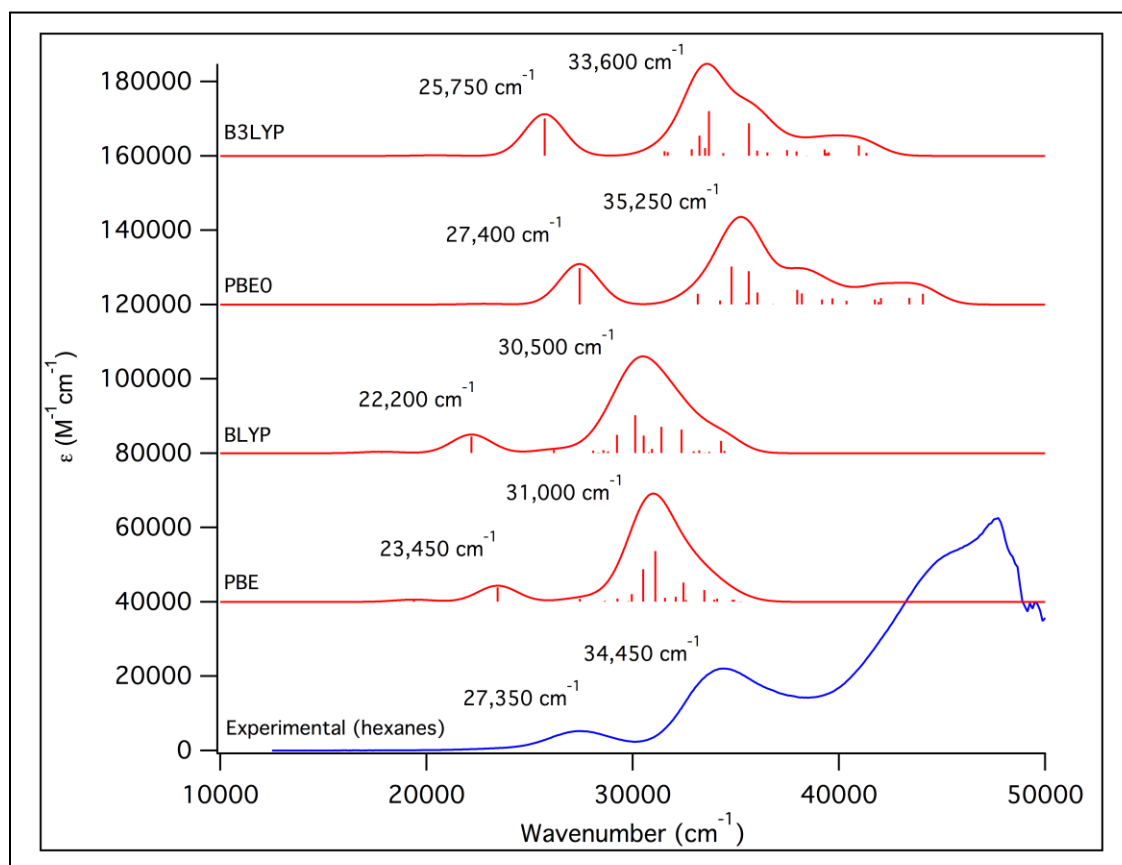
Catalytic hydrophosphination of 3-hexyne or diphenylacetylene gave the anticipated vinyl phosphines under 253.7 nm irradiation, but no double hydrophosphination products were detected under these conditions (Scheme 5.6). As excepted from the double hydrophosphination work,<sup>1</sup> catalytic formation of the diphosphine (i.e., double hydrophosphination) is a thermal process. Attempts to encourage catalysis to undergo the second hydrophosphination event under ultraviolet light were not as effective as heating.

### 5.2.5: TDDFT calculations

The working hypothesis in light-driven hydrophosphination with **1** is that the P  $n \rightarrow$  Zr  $d$  transition at 364.5 nm in hexanes is responsible for hydrophosphination (Figure 5.2). Because strong evidence exists that the next-lowest energy feature belongs in part to the  $\pi \rightarrow \pi^*$  transition in the phenyl ring (Figure 5.3), the 364.5 nm feature was thought to govern the photochemistry with **1** in accordance with Kasha's rule. The experimental

support for this working hypothesis launched an exploration into calculated energy of the ground and excited states of the molecule.

Investigation by Matthew Conger and Prof. Dr. Matthew Liptak using time-dependent density functional theory (TDDFT) of the ground- and excited-state profile of **2** supported this hypothesis. Calculation of the transition energies and absorbance intensities for the first twenty excited states within an expansion of 100 vectors for each optimized structure showed that the 364.5 nm ( $27,350\text{ cm}^{-1}$ ) feature predicted a low- and high-energy band consistent with the experiment (Figure 5.5).



**Figure 5.5:** TDDFT predicted absorbance spectra for **2**

Matthew Conger calculated the gas-phase structures using the generalized gradient approximation (GGA functionals PBE and BLYP or the hybrid functionals PBE0 and B3LYP with the TZVP-def2 basis set) which uses an extended core potential for Zr as implemented in ORCA 4.0. All four functionals accurately predicted the structure around Zr (Table 5.7), but the GGA functionals more accurately predicted the orientation of the phenyl ring. Geometry optimizations with a zeroth order regular approximation (ZORA) for relativistic effects did not have a significant effect on the optimized structures.

**Table 5.7:** Structure optimization around Zr as implemented in ORCA 4.0

	PBE	BLYP	PBE0	B3LYP
Average Bond Error (Å)	0.039	0.060	0.027	0.043
Dihedral Error (deg)	-14.2	-16.1	-49.7	-48.1

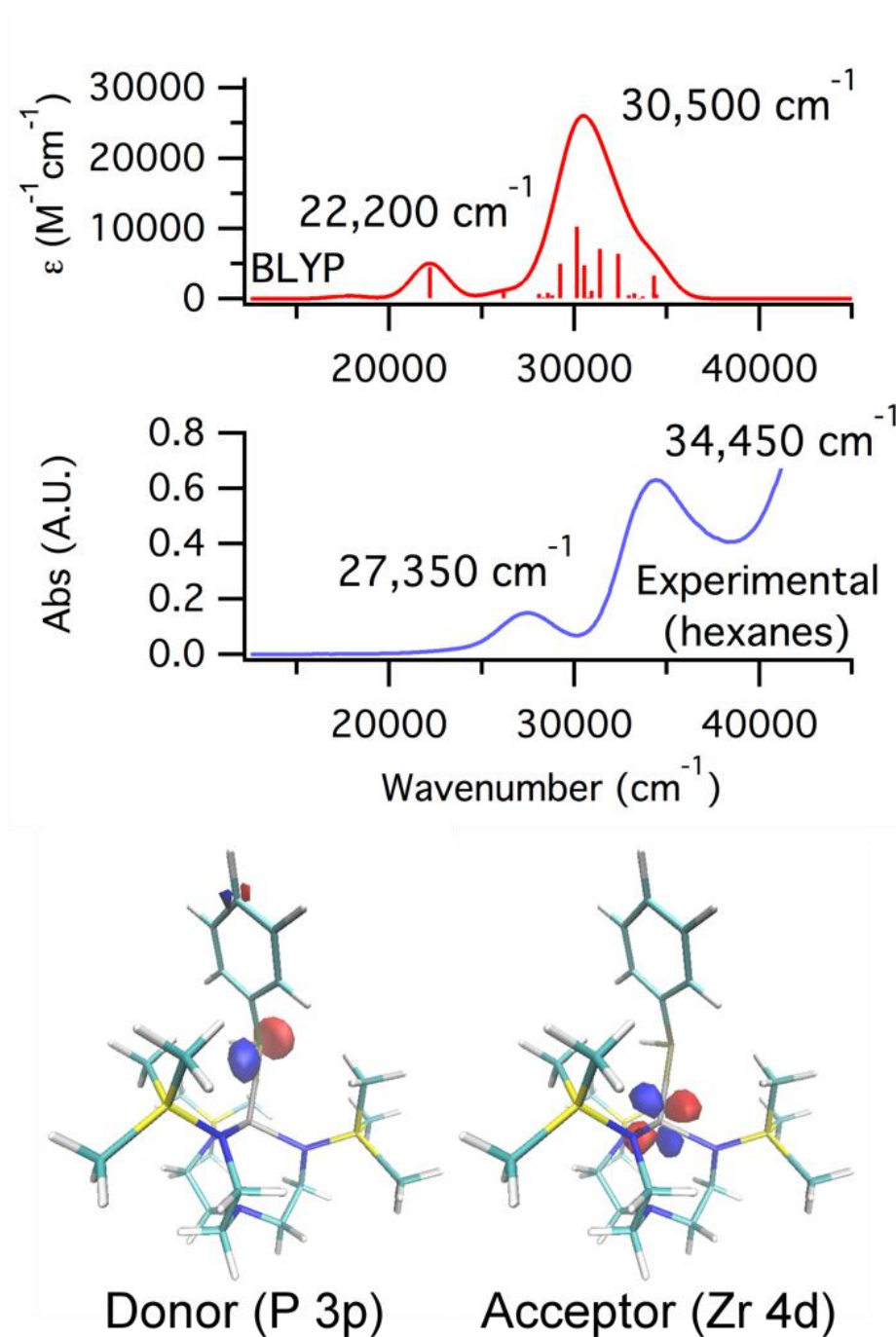
Comparison of the ratio of band intensities and the difference between the bands from the TDDFT data revealed that all four functionals predicted a low energy and high energy band, consistent with our observation. The GGA functionals overestimated the ratio of the high and low energy band intensities while the hybrid functionals underestimated the ratio. None of the four functionals gave exceptionally poor results; therefore, all four were used in the analysis (Table 5.8).



**Table 5.8:** Band intensity ratios and differences for GGA functionals

	Experimental	PBE	BLYP	PBE0	B3LYP
Band Intensity Ratio	4.2	6.7	5.2	2.2	2.2
Band Difference (cm <sup>-1</sup> )	7100	7550	8300	7850	7850

The band of interest occurs at 364.5 nm (27,350 cm<sup>-1</sup>), and each predicted absorption spectrum contains a similar low energy band composed of one transition. Orca\_plot was used to visualize the donor and acceptor MOs for the low energy band in each TDDFT predicted spectra (Figure 5.6).

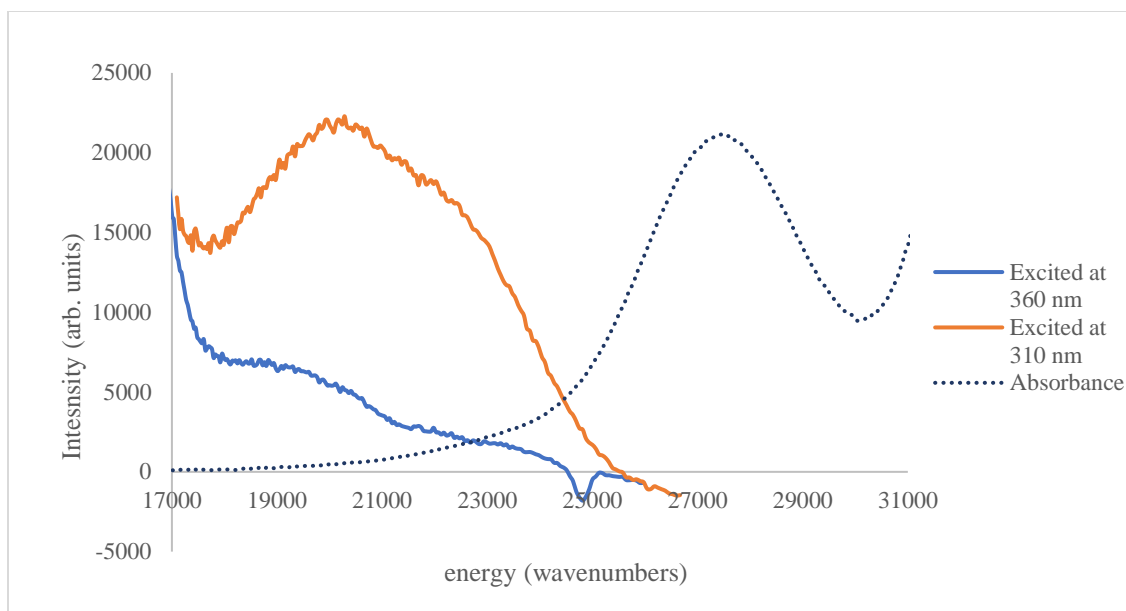


**Figure 5.6:** Donor and acceptor orbitals for the low energy band predicted in each spectrum

Analysis of the donor and acceptor orbitals reveals a P  $n \rightarrow$  Zr  $d$  charge transfer transition for the ground state structure of **2** (Figure 5.6). Calculated percent MO contributions show that the donor orbital is primarily phosphorus-based and the acceptor orbitals are *antibonding* between zirconium and phosphorus. Thus, the experimental band at 27.350 cm<sup>-1</sup> was assigned to a one-electron excitation from P  $n \rightarrow$  Zr  $d$ . Although efforts to calculate the excited state were unsuccessful, the identification of a one-electron excitation from P  $n \rightarrow$  Zr  $d$  strongly supports the working hypothesis that excitation from light irradiation weakens the Zr–P bonding orbital. That could promote faster insertion, as theorized for light-catalyzed hydrophosphination with **2**.

#### 5.2.6 Fluorescence spectroscopy on **2**

Photoluminescence was first observed under blacklight irradiation of NMR-scale reactions. After excitation from consumption of a photon in the ultraviolet region, **2** emits a photon of lower energy and relaxes back down to the ground state. The photoluminescence of **2** was measured spectroscopically by a fluorimeter, which plots the amount of light emitted by a sample as a function of the photon wavelength (Figure 5.7).

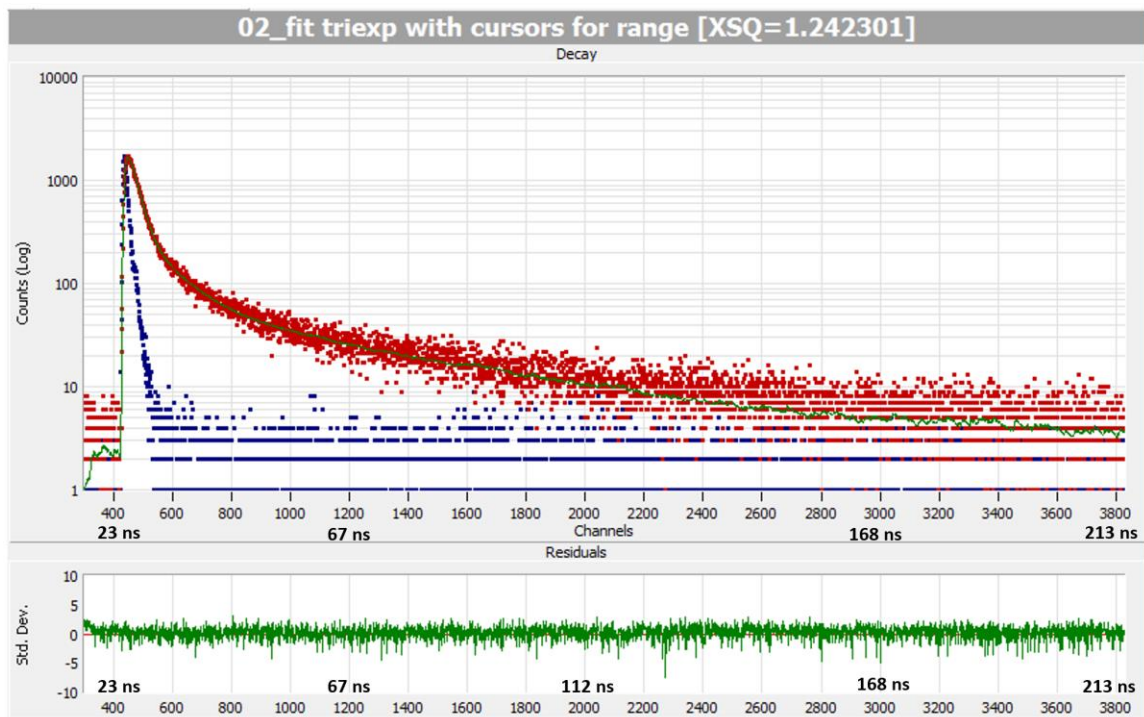


**Figure 5.7:** Overlay of fluorescence and UV-vis spectrum of **2** in hexanes. Light blue solid line: Fluorescence after excitation at 360 nm; orange solid line: fluorescence after excitation at 310 nm; dark blue dotted line: UV/Vis absorbance spectrum of **2**. Intensities are scaled to be relative to one another.

Excitation of **2** at 310 nm and 360 nm results in a fluorescence spectrum that is the mirror image of the absorbance but shifted to a lower energy since the emitting photons have less energy than the absorbed photons. The difference between the positions of the band maxima of the absorption and emission spectra is the Stoke's shift, calculated at 7300  $\text{cm}^{-1}$  for **2**. This energy difference is an anticipated reflection of an energy loss due to vibration or other solvent effects in the excited state. The excitation wavelength is at a lower energy than the intense band at 34000  $\text{cm}^{-1}$ . This indicates that fluorescence is emission from the band at 27350  $\text{cm}^{-1}$  that was assigned to a charge transfer (*vide supra*).

The emission spectrum in Figure 5.7 gives information about the energy difference of the excited state of **2** back to the ground state. However, two possible emission patterns are possible. Emission can go through either a singlet excited state,

corresponding to fluorescence, or through a triplet excited state, corresponding to phosphorescence. The former is an allowed transition and usually occurs on the nanosecond time scale, whereas the latter is a forbidden transition and occurs much more slowly. To test for either fluorescence or phosphorescence, time-resolved photoluminescence spectroscopy was employed for **2** (Figure 5.8).



**Figure 5.8:** Time-resolved photoluminescence spectrum of **2** with triexponential fit. Red: Time-resolved photoluminescence of **2** in toluene. Blue: Scattering prompt. Green: Residual fit of data.

The nanosecond lifetimes shown in Figure 5.8 indicate that relaxation occurs from a singlet excited state (fluorescence). Relaxation of the excited state of **2** to the ground state occurs through three different photoluminescent lifetimes (Table 5.9).

**Table 5.9:** Lifetimes of fluorescence decay in **2**

Lifetime	Fluorescence Lifetime (ns)	Relative amplitude (%)
1	1.30	47.1
2	6.31	23.6
3	37.7	29.2

The emission pathways decay with time according to equation 5.2:

$$I(t) = I_0 e^{-t/\tau} \quad (5.2)$$

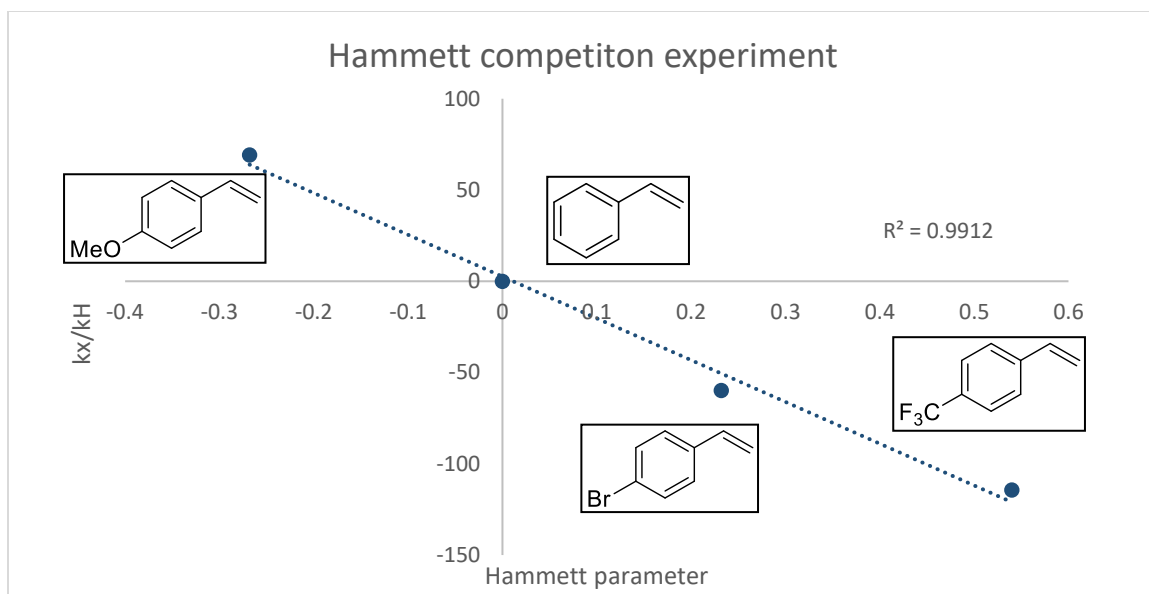
Where  $I$  is the measured fluorescence intensity at time  $t$ ,  $I_0$  is the initial fluorescence intensity,  $t$  is the time, and  $\tau$  is the fluorescence lifetime. The lifetime  $\tau$  is independent of the initial intensity and of the emitted light. Because **2** shows nanosecond lifetimes it is understood that photoluminescence occurs from a singlet excited state. This is an anticipated observation since it is understood that catalytic hydrophosphination with **1** does not proceed via a radical mechanism (*vide supra*).

### 5.2.7: Mechanistic insights

Because the conversions of styrene derivatives in Tables 5.2 and 5.4 are similar a Hammett analysis was carried out. Treatment of equimolar amounts of styrene and a substituted styrene derivative with a deficiency of  $\text{PhPH}_2$  allows for a relative rate measurement<sup>27-28</sup> (eqn 5.3).

$$\frac{k_x}{k_H} = \frac{\ln(\frac{s_x}{s_{x,0}})}{\ln(\frac{s_H}{s_{H,0}})} \quad (5.3)$$

Comparison of the rate of the consumption of the substituted styrene derivative versus styrene in a binary competition reaction will provide information about the free-energy relationship. This competition experiment was performed in an NMR experiment (Figure 5.9).

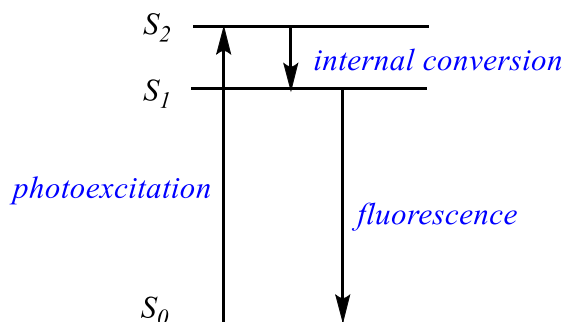


**Figure 5.9:** Relative rate constants of competition experiments after 15 min

It is clear from the data that the reaction is faster for electron-rich styrene derivatives, indicating an insertion-based mechanism. This is consistent with the mechanism proposed in the seminal hydrophosphination work with **1** on secondary phosphines.<sup>3</sup> Treatment of equimolar amounts of styrene and a styrene derivative with a deficiency of PhPH2 and 10 mol % of **1** under irradiation from a 360 nm lamp provided hydrophosphination products after fifteen minutes (see supplementary information for details).

Prior work from our group on the hydrophosphination of alkenes with PhPH2 found that there was no change between reactions run under ambient light and reactions run in the dark for hydrophosphination of alkene<sup>4</sup> or alkyne substrates.<sup>3</sup> Competition experiments in that report favored styrene substrates bearing electron-withdrawing substituents, which suggests some degree of nucleophilic attack on the phosphide.<sup>4</sup> The difference between these two preferences in primary phosphine hydrophosphination with **1** stems from the

light dependence. If catalytic hydrophosphination with **1** goes through an insertion-based mechanism then styrenes bearing electron-donating groups would be more favored. This corresponds to the relationship for this system outlined in Figure 5.10. The observation that the phosphide on **2** acts as a nucleophile in the absence of excitation is supported by previous DFT studies on **2**.<sup>29</sup> The Zr–P bond of **2** is relatively weak and polar, which would amplify the nucleophilicity of the phosphide of **2**. Thus it can be understood that hydrophosphination run under ambient light proceeds via some degree of nucleophilic attack from the phosphide, but reactions run under irradiation proceed through insertion. This is consistent with the hydrophosphination experiments on styrene substrates bearing electron-donating groups and unactivated alkenes. Comparison of the two mechanisms is thwarted by the turnover-limiting dependence on photoexcitation. Light irradiation promotes hydrophosphination by excitation into a charge transfer band between zirconium and phosphorus (*vide supra*). A simplified picture of this method is shown in Figure 5.10.



**Figure 5.10:** Jablonski diagram for photoexcitation of **2**

Photoexcitation takes electron density out of  $S_0$  and into the excited state ( $S_1$  and  $S_2$ ). Because the acceptor orbitals in the excited state are antibonding between zirconium and phosphorus, population of this state corresponds to a weakened Zr–P bond, which



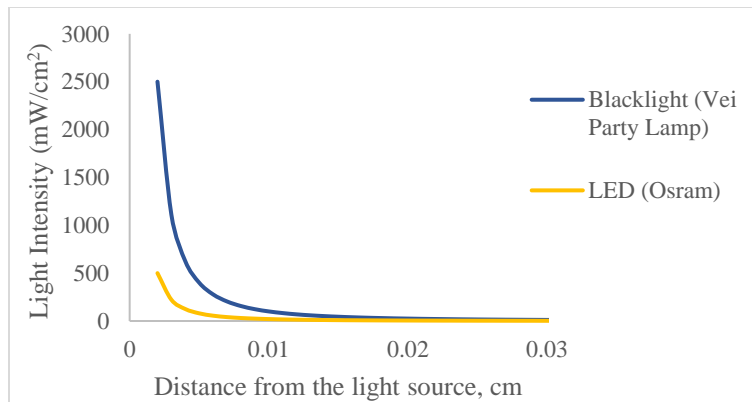
allows for more facile substrate insertion. It is clear from the fluorescence spectra that the chemistry occurs from the same singlet excited state, which by Kasha's rule must be the  $S_1$ . Although computational methods to calculate the excited state structure failed, it is clear from the TDDFT calculations that the photoexcitation is an  $n \rightarrow d$  charge transfer from the ground state of **2**. An increase in charge transfer by careful selection of the lamp used for irradiation allows for productive hydrophosphination chemistry to occur with **1**.

### 5.2.6 Optimization of photocatalytic hydrophosphination with **1**

Photoactivation raises a new consideration that is not routine in thermal catalysis. Namely, the consideration of the light intensity that reaches the reaction. Light intensity is inversely proportional to distance squared (eqn 5.4).

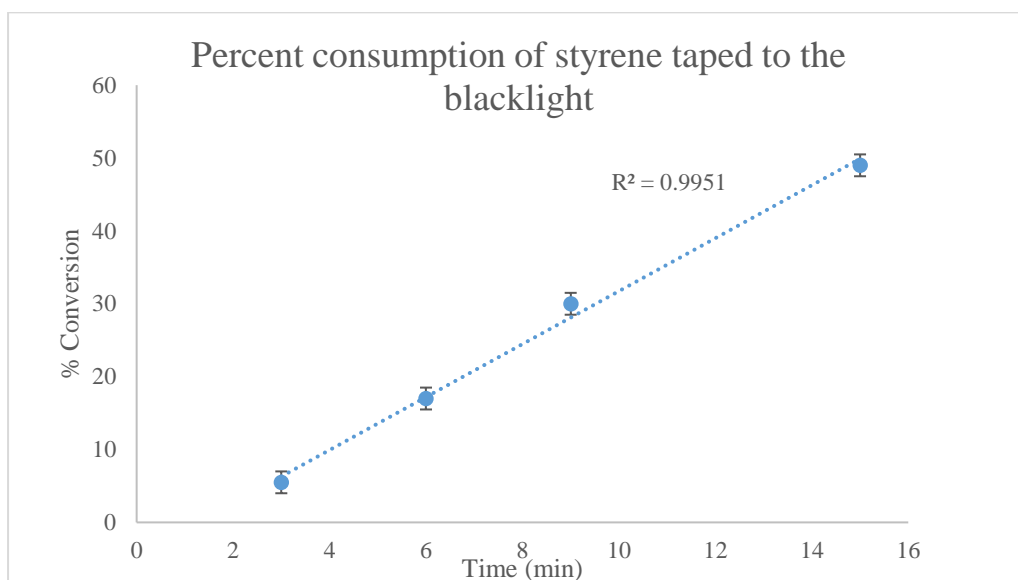
$$\frac{I_1}{I_2} = \frac{d_2^2}{d_1^2} \quad (5.4)$$

That is, light intensity from the light to the reaction contents depends on distance. Hydrophosphination reactions shown in Scheme 5.2 and Tables 5.2-5.5 were run in NMR tubes placed approximately six inches away from the light source. At these distances the amount of light reaching the reaction varies by an insignificant amount (Figure 5.11).



**Figure 5.11:** Light intensity as a function of distance from the lamp. The values are calculated with eqn 5.3 using the data from table 5.1.

As demonstrated in Figure 5.12, the light intensity reaching the lamp only varies significantly at very close distances to the light source. Because it is evident that hydrophosphination with **1** requires light to proceed, it was a natural to consider if the degree of light intensity could affect catalytic turnover. That turned out to be true. Reactions run in NMR tubes that were taped up to the surface of the bulb cut the reaction time from 90 to 20 minutes (Figure 5.12).



**Figure 5.12:** Percent consumption of styrene with 2 equiv of PhPH<sub>2</sub> and 5 mol % of **1** in an NMR tube taped to the surface of a VEi party lamp blacklight. The reaction was monitored by <sup>31</sup>P NMR spectroscopy. Error is determined by NMR integration.

The consumption of styrene in these experiments appears to be zero-order in substrate, indicating that the step *before* substrate insertion is turnover-limiting. This is consistent with a mechanism in which excitation of the zirconium–phosphide governs the reaction. Likely the catalysis is limited by reformation/excitation of **2** because those processes are dependent only on both the zirconium species and the phosphine, not the substrate.

However, the high degree of variation of light intensity during these taped experiments also has a caveat. Small fluctuations in the distance from the lamp return dramatically different hydrophosphination conversions (Figure 5.13).

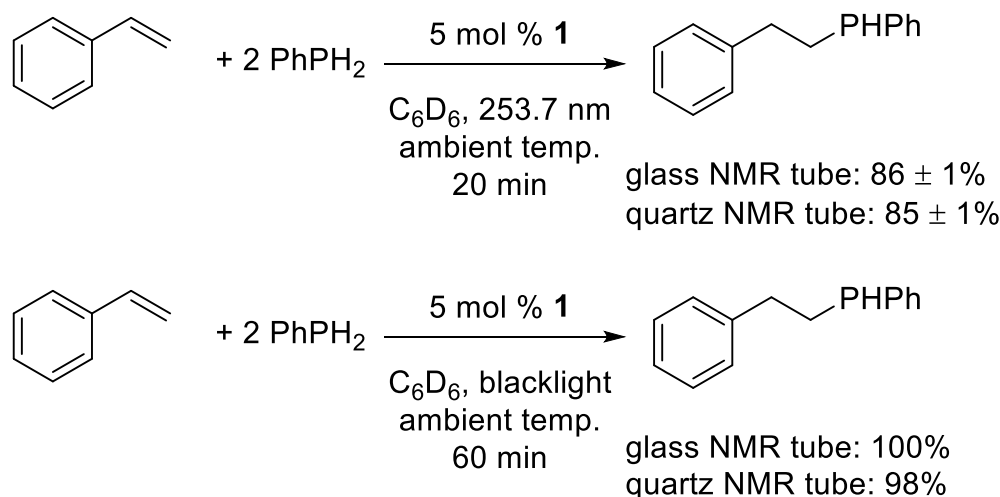


**Figure 5.13:** Hydrophosphination of styrene with 2 equiv of  $\text{PhPH}_2$  and 5 mol % of **1** in an NMR tube taped to the surface of a VEi party lamp blacklight. The reaction was halted after 12 min. Conversions were monitored by  $^{31}\text{P}$  NMR spectroscopy.

For example, taping an NMR tube directly to the center results in good conversions, whereas a tube taped to one inch away from the center of the lamp already shows a decrease

in the conversions from 63% to 48% (Figure 5.13). Reactions run on the outside of direct contact from the lamp give modest conversions, despite insignificant temperature fluctuations. This is an expected result from what is known about the light dependence on catalytic hydrophosphination with **1** and what is calculated from the light intensity as a function of distance (eqn 5.3, Figure 5.12).

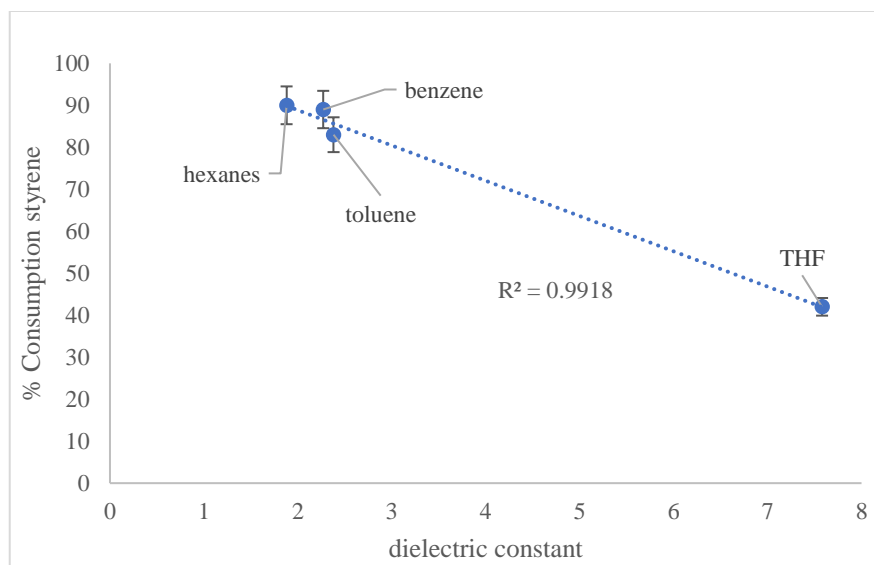
The stark requirement on light for catalytic hydrophosphination with **1** brought out an additional consideration that is common in photochemistry. All NMR reactions were performed in borosilicate NMR tubes that have some absorbance in the ultraviolet. This absorbance could limit how much light penetrates the NMR tube and the reaction.



**Scheme 5.10:** Hydrophosphination under standard conditions comparing glass and quartz NMR tubes.

However, no change was observed in the hydrophosphination of styrene run under either the 253.7 nm lamp or blacklight irradiation in either a quartz or a glass NMR tubes (Scheme 5.10).

One final consideration for the optimizations of the hydrophosphination reaction is the polarity of the solvent.



**Figure 5.14:** Effect of solvent on % consumption of styrene. Error is determined by NMR integration.

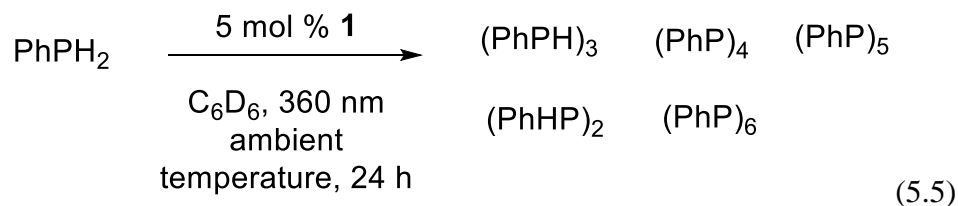
It appears that reactions run in low-polarity solvents such as hexanes, toluene and benzene outperform relatively polar solvents such as THF. The low hydrophosphination conversion of styrene in THF is possibly a reflection of coordination of THF to the zirconium metal center. Highly polar solvents were not tested in this system because many of them degraded **1**.

### 5.2.9: Excitation of **2** for catalytic dehydrocoupling of PhPH<sub>2</sub>

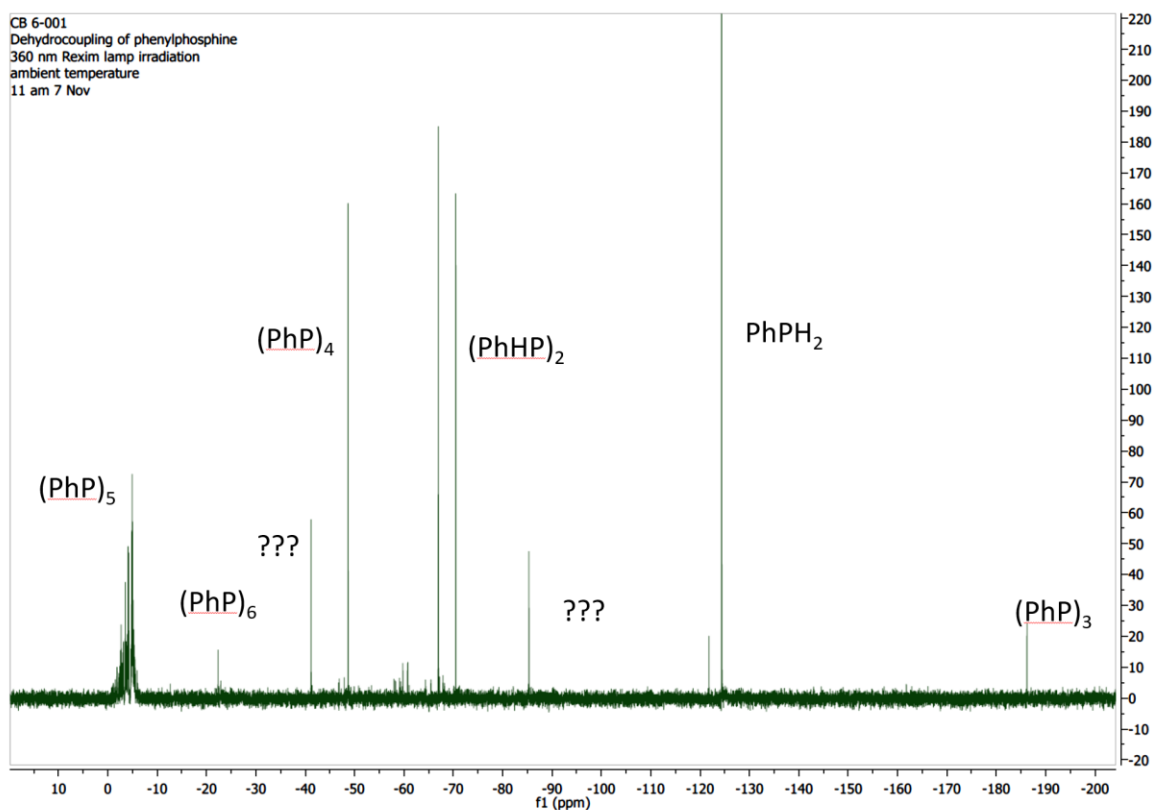
The newfound understanding of the relationship of **2** with light prompted reinvestigation of prior work in the Waterman group with catalytic phosphine dehydrocoupling. Reported early-transition metal catalysts capable of dehydrocoupling have historically been limited to (RPH)<sub>2</sub> and (RP)<sub>*n*</sub> (*n* = 4,5,6) for small phosphines. Moreover, these catalysts only convert at high temperatures and long reaction times.

A deeper understanding of the reactivity of **1** and its phosphide **2** from a photochemical perspective prompted reconsideration of the phosphine dehydrocoupling

work. Treatment of  $\text{PhPH}_2$  in the presence of catalytic amounts of **1** showed high dehydrocoupling reactivity at ambient temperature (eqn 5.5).



A mixture of dehydrocoupling products were observed, but not all were identified (Figure 5.15). For this reason it is not possible to quantify the product conversions.



**Figure 5.15:** Dehydrocoupling of  $\text{PhPH}_2$  at ambient temperature with **1**. Conditions: 20 equiv  $\text{PhPH}_2$ , 1 equiv **1**, benzene, degassed, ambient temperature, 24 h, 360 nm irradiation.

As demonstrated previously, (PhHP)<sub>2</sub> is formed under catalytic dehydrocoupling with **1**. This system selects for new products, (PhP)<sub>3</sub>, and two unknown species at  $\delta$  -87 ppm and -41 ppm. While the majority of products are not new, it is worth noting that this system gives good turnover at ambient temperature after only 24 h, in comparison to the aforementioned 7 d at 90 °C.

An interesting feature in this photo-driven dehydrocoupling reaction is the unexplained reactivity difference. While the argument for easier insertion into **2** upon irradiation can explain the drastic reactivity difference, P–P bond formation is proposed to proceed through  $\sigma$ -bond metathesis. One explanation is that excitation elongates the Zr–P bond, allowing for faster  $\sigma$ -bond metathesis, much like it allows for faster insertion. In this case the elongated Zr–P bond is weakened, allowing for a more facile electron rearrangement during the bond-forming step. This thought is supported by the apparent weakening of the Zr–P orbital by TDDFT calculations.

### 5.3 Conclusions

Light irradiation of **1** promotes catalytic alkene hydrophosphination for all substrates. TDDFT results suggest a weakening of the Zr–P bond upon photoexcitation, which may allow for faster substrate insertion. Free energy competition experiments between styrenes bearing different electronic groups under photocatalysis show a favoritism for styrenes bearing electron-donating groups, providing further support for insertion-based catalysis.

Photoirradiation of **1** allows for the fastest primary phosphine hydrophosphination to date for all substrates tested. For context, our previous report showed the catalytic

hydrophosphination of styrene after 12 h at ambient temperature with TON = 18 and TOF = 1.5 h<sup>-1</sup>. Direct irradiation makes this process substantially more efficient (TON = 20 and TOF = 60 h<sup>-1</sup>). Furthermore, light activation allows for increasingly larger primary phosphines to undergo catalytic hydrophosphination with **1**. All reactions are run at ambient temperature and provide excellent product conversion and selectivity. The short reaction times, earth-abundant catalyst, and increasingly large substrate scope are impressive. Furthermore, this system operates by photoexcitation, rather than heat, which makes it unique in catalytic hydrophosphination.

## 5.4: Experimental methods

### 5.4.1: General methods

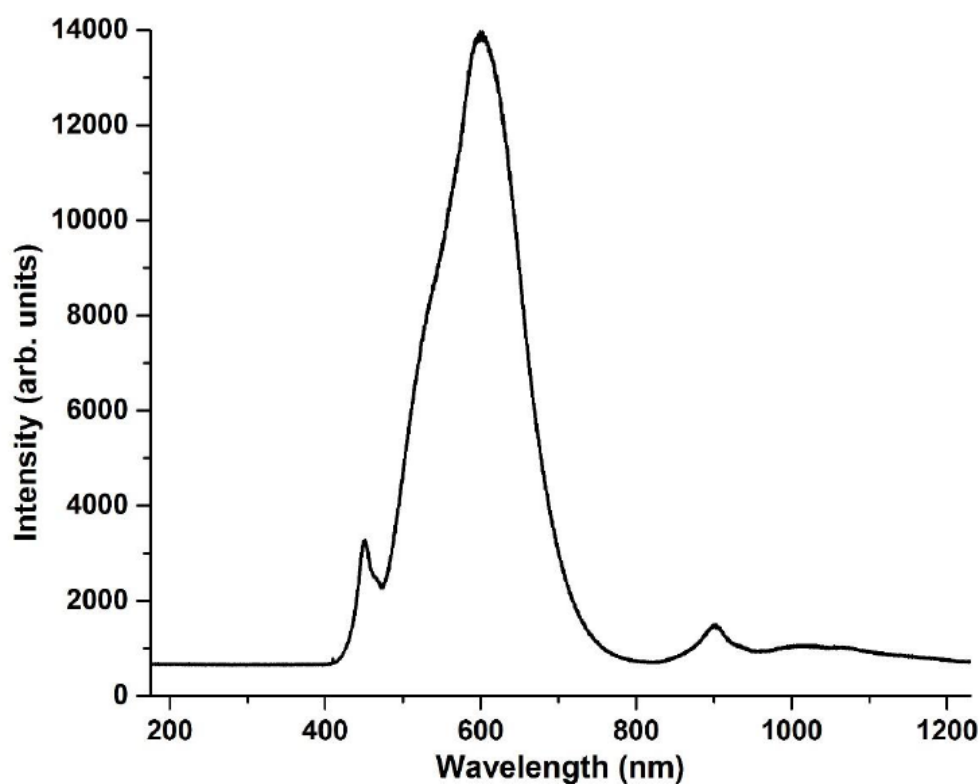
All air-sensitive manipulations were performed under a positive pressure of nitrogen using standard Schlenk line or in a M. Braun glove box. Dry, oxygen-free solvents were employed throughout. Benzene-*d*<sub>6</sub> was purchased then degassed and dried over NaK alloy and distilled under reduced pressure. NMR spectra were recorded with a Bruker AXR 500 MHz spectrometer in benzene-*d*<sub>6</sub> and are reported with reference to residual solvent signals (C<sub>6</sub>D<sub>6</sub>,  $\delta$  7.16 and 128.0) and to an external 85% H<sub>3</sub>PO<sub>4</sub> ( $\delta$  0.0) standard for <sup>31</sup>P NMR spectra. Compound **2** was excited at either 310 nm or 360 nm and excitation and emission slits were both set to 1 nm. PhPH<sub>2</sub> and CyPH<sub>2</sub> were purchased from Strem Chemicals and used without further purification. MesPH<sub>2</sub> was prepared by a modified literature procedure.<sup>30</sup> Compound [K<sup>5</sup> -N,N,N,N,C-(Me<sub>3</sub>SiNCH<sub>2</sub>CH<sub>2</sub>)<sub>2</sub>NCH<sub>2</sub>CH<sub>2</sub>NSiMe<sub>2</sub>CH<sub>2</sub>]Zr (**1**) was prepared according to the literature



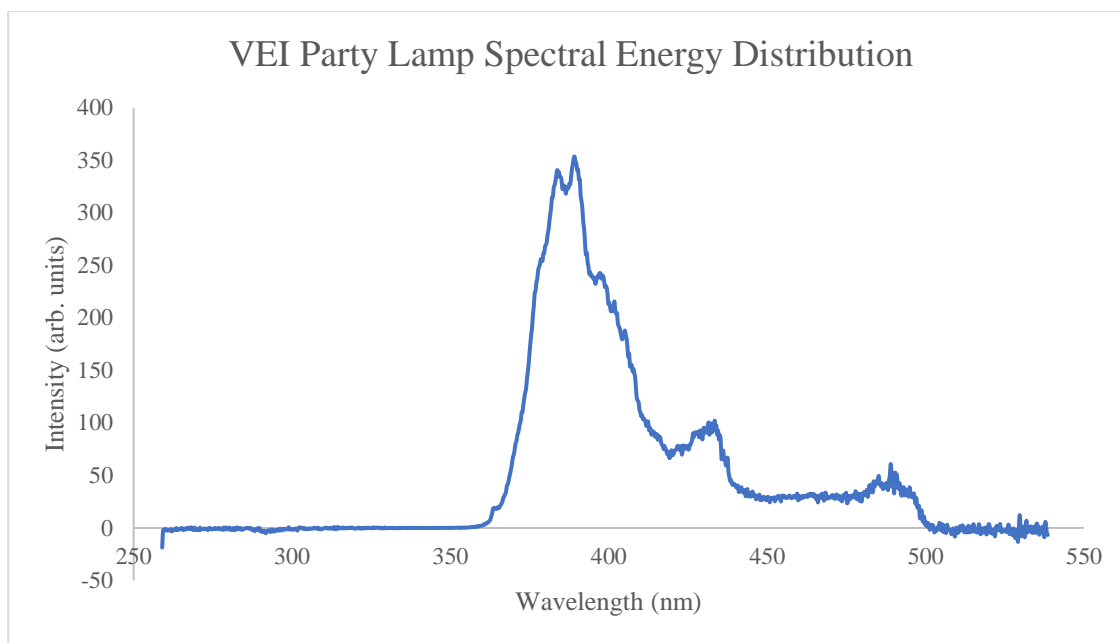
procedure.<sup>9</sup> All other chemicals were obtained from commercial suppliers and dried by appropriate means.

#### 5.4.2: Spectral energy distributions of the lamps

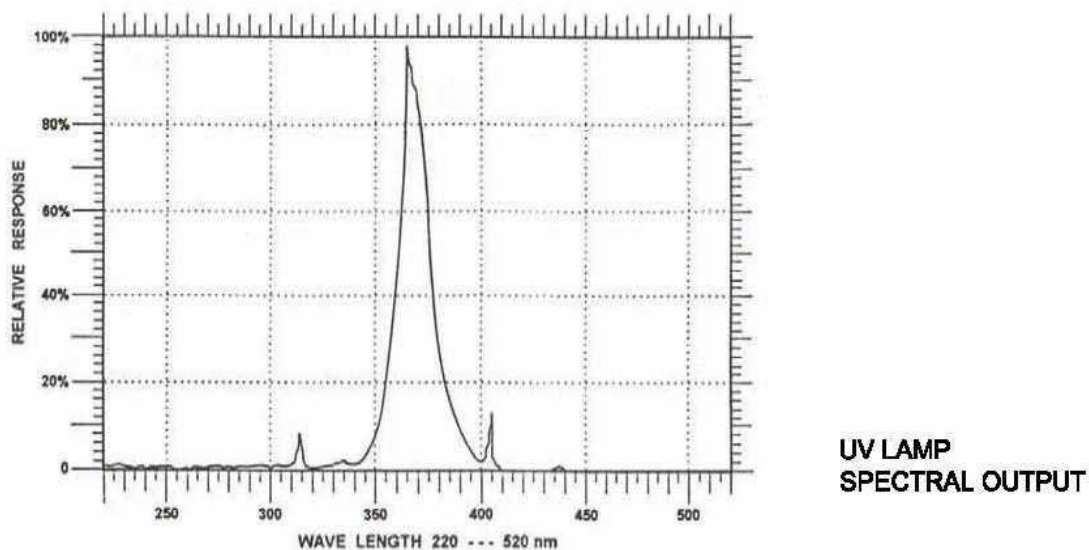
Spectral energy distributions of the lamps were either measured or obtained from the manufacturer. The 253.7 nm mercury arc lamp is monochromatic.



**Figure 5.16:** Spectral energy distribution of an OSRAM Sylvania Ultra LED A19 Lamp – generation 5, operating power of 6 W and output of 450 lumens.<sup>31</sup>



**Figure 5.17:** Spectral energy distribution of VEI UV Blacklight Party Lamp, operating power of 13 W. Spectrum was measured with assistance from Prof. Dr. Madalina Furis.



**Figure 5.18:** Spectral energy distribution of a Rexim G23 UV-A 360 nm Lamp, operating power of 9 W. Spectrum is provided by the manufacturer.

### 5.4.3: General procedure for hydrophosphination reactions

A borosilicate NMR tube was charged with 0.1 mmol primary phosphine and 0.05 mmol alkene or diene in the presence of 5 mol % of **1** in benzene-*d*<sub>6</sub> solvent. The mixture

solutions were stirred at ambient temperature for noted time period. The consumption of substrate to product was monitored by  $^{31}\text{P}$  and  $^1\text{H}$  NMR spectroscopy. Yields were determined from integration of the substrate converted by  $^1\text{H}$  NMR and  $^{31}\text{P}$  NMR spectra.<sup>32</sup> Reactions run in brand-new NMR tubes showed identical conversions as reactions run using standard reaction tubes.

#### 5.4.4: Procedure for Hammett plot generation

An NMR tube was charged with equimolar amounts of the heterosubstituted styrene derivative and styrene (Table S5.1). To this NMR tube was added 0.80 equiv of  $\text{PhPH}_2$  and 0.10 equivalents of **1**. An initial  $^1\text{H}$  NMR spectrum was recorded. The reaction was irradiated at 360 nm and monitored after fifteen minutes by  $^1\text{H}$  NMR spectroscopy.

**Table 5.10:** Initial concentrations of reactants in hydrophosphination competition experiments

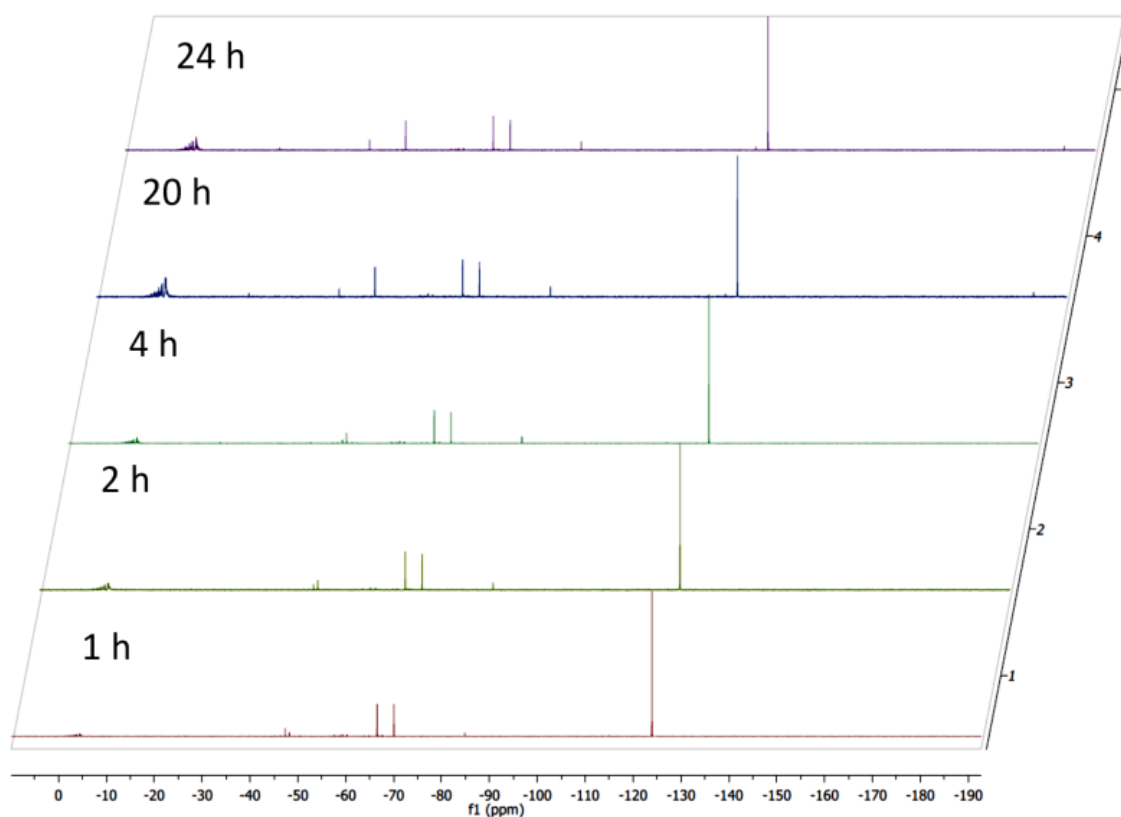
Substituted styrene	[substituted styrene]	[styrene]	[ $\text{PhPH}_2$ ]	[ <b>1</b> ]
<i>p</i> -bromostyrene	0.100 M	0.105 M	0.081 M	0.011 M
<i>p</i> -trifluoromethyl styrene	0.100 M	0.100 M	0.080 M	0.010 M
<i>p</i> -methoxystyrene	0.100 M	0.102 M	0.080 M	0.010 M

**Table 5.11:**  $^1\text{H}$  integration ratios of styrene and styrene derivatives in hydrophosphination competition experiments. The initial ratio of substituted styrene derivative to styrene was measured by integration of the vinyl  $^1\text{H}$  resonances by NMR spectroscopy.

Styrene derivative	$\sigma$ -parameter	Rel. int. styrene, initial	Rel. int. derivative, initial	Rel. int. styrene, final	Rel. int. derivative, final
<i>p</i> -bromostyrene	0.232	5.00	3.55	5.01	3.15
<i>p</i> - $\text{CF}_3$ styrene	0.54	5.00	4.11	5.01	3.27
<i>p</i> -methoxystyrene	-0.268	5.00	4.05	5.01	4.65

#### 5.4.5: Procedure for dehydrocoupling of PhPH<sub>2</sub>

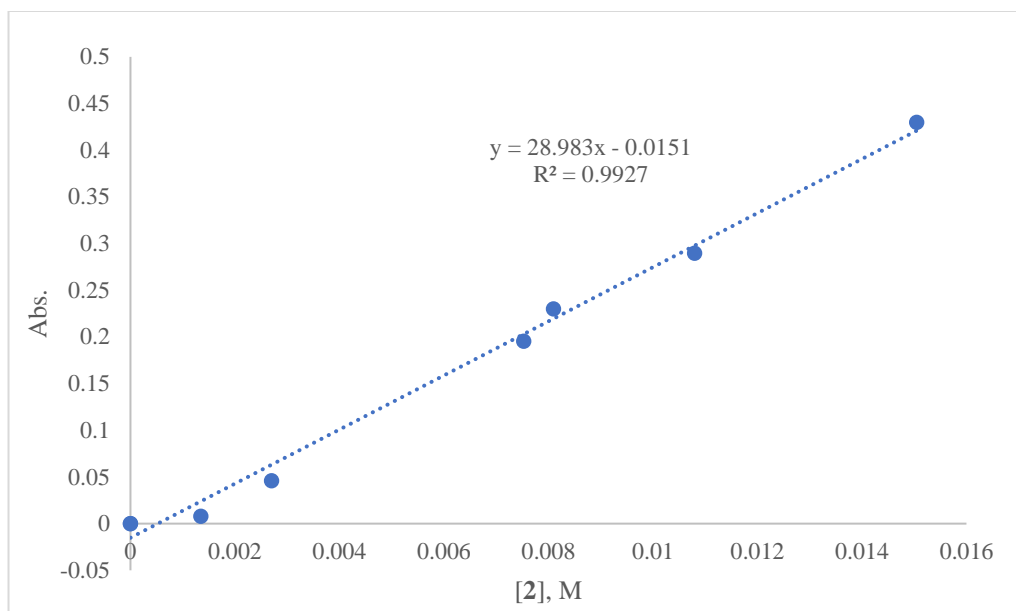
A J-Young NMR tube was charged with 20.0 mg (0.182 mmol) of PhPH<sub>2</sub> and 0.12 mL of a 0.0778 M solution of **1** in benzene-*d*<sub>6</sub> (0.009<sub>3</sub> mmol, 5.1 mol %). An additional 0.40 mL of benzene-*d*<sub>6</sub> was added. The J-Young NMR tube was freeze-pump-thawed twice before irradiation at 360 nm. The reaction was monitored by <sup>31</sup>P NMR spectroscopy over the course of 24 h (Figure 5.15).



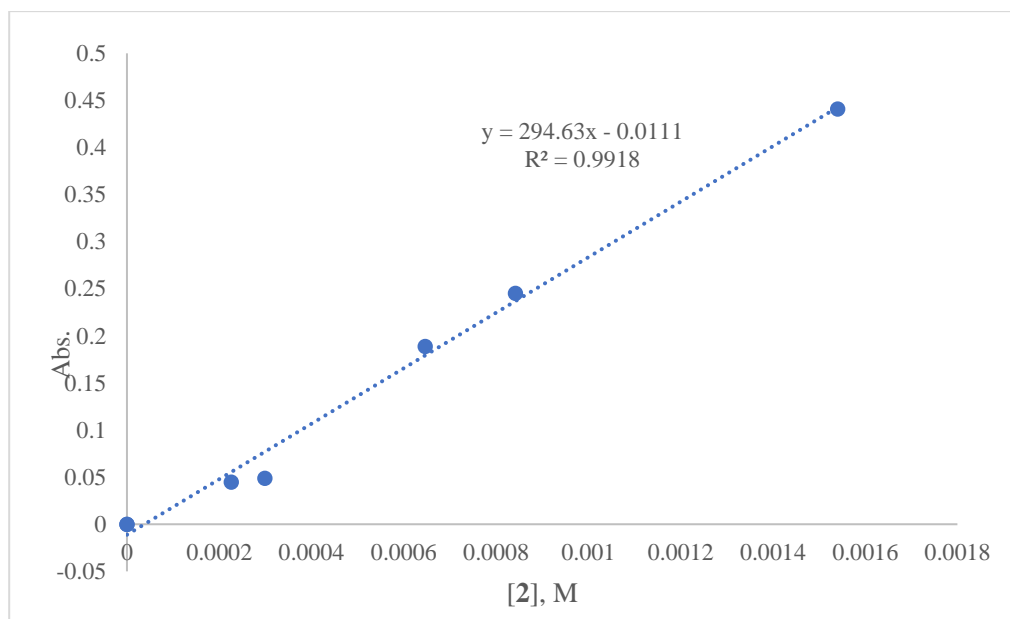
**Figure 5.20:** Stacked <sup>31</sup>P{<sup>1</sup>H} NMR spectra of the dehydrocoupling of PhPH<sub>2</sub> with **1** at ambient temperature

#### 5.4.6: Determination of extinction coefficient for **2**

The extinction coefficient for **2** was found to be 290 M<sup>-1</sup> cm<sup>-1</sup> at 364.5 nm in hexanes (Figure 5.16), 295 M<sup>-1</sup> cm<sup>-1</sup> at 360.0 nm in benzene (Figure 5.21).



**Figure 5.20:** Determination of the extinction coefficient of **2** in hexanes measured at 364.5 nm in a 1.0 mm cuvette



**Figure 5.21:** Determination of the extinction coefficient of **2** in benzene measured at 360.0 nm in a 1.0 cm cuvette

## 5.5: References

- (1) Bange, C. A.; Waterman, R., *ACS Catal.* **2016**, *6*, 6413-6416.

- (2) Rosenberg, L., *ACS Catal.* **2013**, 3, 2845-2855.
- (3) Roering, A. J.; Leshinski, S. E.; Chan, S. M.; Shalumova, T.; MacMillan, S. N.; Tanski, J. M.; Waterman, R., *Organometallics* **2010**, 29, 2557-2565.
- (4) Ghebreab, M. B.; Bange, C. A.; Waterman, R., *J. Am. Chem. Soc.* **2014**, 136, 9240-9243.
- (5) Jimenez, M. V.; Perez-Torrente, J. J.; Bartolome, M. I.; Oro, L. A., *Synthesis* **2009**, 1916-1922.
- (6) Kenaree, A. R.; Cuthbert, T. J.; Barbon, S. M.; Boyle, P. D.; Gillies, E. R.; Ragnogna, P. J.; Gilroy, J. B., *Organometallics* **2015**, 34, 4272-4280.
- (7) Otomura, N.; Okugawa, Y.; Hirano, K.; Miura, M., *Org. Lett.* **2017**, 19, 4802-4805.
- (8) Pagano, J. K.; Bange, C. A.; Farmiloe, S. E.; Waterman, R., *Organometallics* **2017**, 36, 3891-3895.
- (9) Waterman, R., *Organometallics* **2007**, 26, 2492-2494.
- (10) Eric V. Anslyn, D. A. D., *Modern Physical Organic Chemistry*. University Science Books: 2006.
- (11) Mairena, M. A.; Urbano, J.; Carbajo, J.; Maraver, J. J.; Alvarez, E.; Diaz-Requejo, M. M.; Perez, P. J., *Inorg. Chem.* **2007**, 46, 7428-7435.
- (12) Lewis, F. D.; Zuo, X., *Spectrum (Bowling Green, OH, U. S.)* **2003**, 16, 8-15.
- (13) Mori, T.; Inoue, Y., *Mol. Supramol. Photochem.* **2005**, 12, 417-452.
- (14) Bange, C.; Mucha, N.; Cousins, M.; Gehsmann, A.; Singer, A.; Truax, T.; Higham, L.; Waterman, R., *Inorganics* **2016**, 4, 26.

- (15) Bange, C. A.; Ghebreab, M. B.; Ficks, A.; Mucha, N. T.; Higham, L.; Waterman, R., *Dalton Trans.* **2016**, 45, 1863-1867.
- (16) Gallagher, K. J.; Espinal-Viguri, M.; Mahon, M. F.; Webster, R. L., *Adv. Synth. Catal.* **2016**, 358, 2460-2468.
- (17) Zhang, Y.; Qu, L.; Wang, Y.; Yuan, D.; Yao, Y.; Shen, Q., *Inorg. Chem.* **2018**, 57, 139-149.
- (18) Yuan, J.; Hu, H.; Cui, C., *Chem. Eur. J.* **2016**, 22, 5778-5785.
- (19) Basalov, I. V.; Yurova, O. S.; Cherkasov, A. V.; Fukin, G. K.; Trifonov, A. A., *Inorg. Chem.* **2016**, 55, 1236-1244.
- (20) Belli, R. G.; Burton, K. M. E.; Rufh, S. A.; McDonald, R.; Rosenberg, L., *Organometallics* **2015**, 34, 5637-5646.
- (21) King, A. K.; Buchard, A.; Mahon, M. F.; Webster, R. L., *Chem. Eur. J.* **2015**, 21, 15960-15963.
- (22) Ganushevich, Y. S.; Miluykov, V. A.; Polyancev, F. M.; Latypov, S. K.; Lönnecke, P.; Hey-Hawkins, E.; Yakhvarov, D. G.; Sinyashin, O. G., *Organometallics* **2013**, 32, 3914-3919.
- (23) Guterman, R.; Gillies, E. R.; Ragogna, P. J., *Dalton Trans.* **2015**, 44, 15664-15670.
- (24) Moglie, Y.; Gonzalez-Soria, M. J.; Martin-Garcia, I.; Radivoy, G.; Alonso, F., *Green Chem.* **2016**, 18, 4896-4907.
- (25) Ji, P.; Sawano, T.; Lin, Z.; Urban, A.; Boures, D.; Lin, W., *J. Am. Chem. Soc.* **2016**, 138, 14860-14863.

- (26) Bange, C. A.; Waterman, R., *Chem. Eur. J.* **2016**, 22, 12598-12605.
- (27) Yau, H. M.; Croft, A. K.; Harper, J. B., *Chem. Commun.* **2012**, 48, 8937-8939.
- (28) Ingold, C. K.; Shaw, F. R., *J. Chem. Soc.* **1927**, 2918-2926.
- (29) Roering, A. J.; Maddox, A. F.; Elrod, L. T.; Chan, S. M.; Ghebreab, M. B.;  
Donovan, K. L.; Davidson, J. J.; Hughes, R. P.; Shalumova, T.; MacMillan, S. N.;  
Tanski, J. M.; Waterman, R., *Organometallics* **2009**, 28, 573-581.
- (30) Masuda, J. D.; Jantunen, K. C.; Ozerov, O. V.; Noonan, K. J. T.; Gates, D. P.;  
Scott, B. L.; Kiplinger, J. L., *J. Am. Chem. Soc.* **2008**, 130, 2408-2409.
- (31) Pagano, J. K.; Bange, C. A.; Farmiloe, S. E.; Waterman, R., *Organometallics*  
**2017**, 36, 3891-3895.
- (32) Fluck, E.; Issleib, K., *Chem. Ber.* **1965**, 98, 2674-2680.

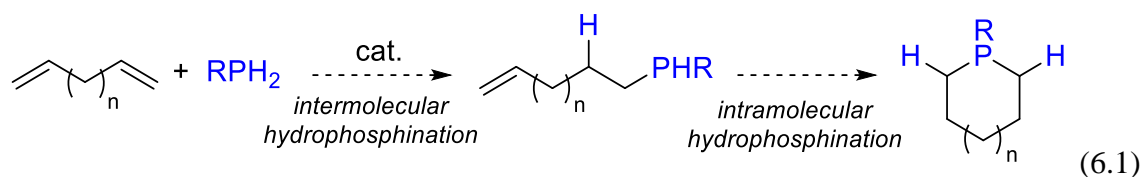


## CHAPTER 6: SEQUENTIAL CATALYTIC INTERMOLECULAR AND INTRAMOLECULAR HYDROPHOSPHINATION OF DIENES TARGETING PHOSPHORUS-CONTAINING RINGS

### 6.1 Introduction

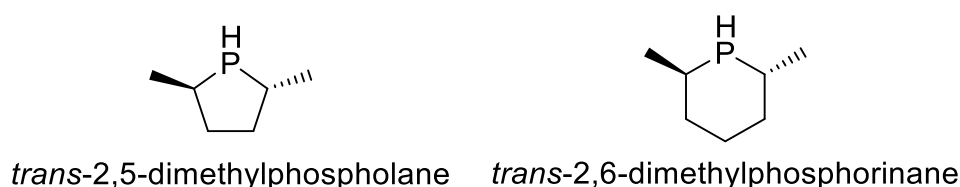
Hydrophosphination has enormous potential to provide tailor-made phosphine products because the only prerequisites are an unsaturated fragment and a non-tertiary phosphine.<sup>1</sup> While examples of metal catalysts capable of hydrophosphination have grown in recent years, Waterman's catalyst [ $\kappa^5$ -N,N,N,N,C-(Me<sub>3</sub>SiNCH<sub>2</sub>CH<sub>2</sub>)<sub>2</sub>NCH<sub>2</sub>CH<sub>2</sub>NSiMe<sub>2</sub>CH<sub>2</sub>]<sub>2</sub>Zr (**1**) stands out for operating under mild reaction conditions and encompassing a broad substrate scope, particularly unactivated alkenes.<sup>2</sup>

Because hydrophosphination is not yet mature, there are promising advancements but notable gaps. For example, intramolecular hydrophosphination is less common than intermolecular hydrophosphination. Although examples of intramolecular hydrophosphination were among the first to be reported for this reaction,<sup>3-5</sup> the field has remained stagnant in recent years. Examples of intermolecular hydrophosphination have grown increasingly popular.<sup>1, 6-7</sup> However, a combination of an inter- and intramolecular hydrophosphination to product a phosphacycle remains unreported. One example of this process is outlined in eqn 6.1.



While some reports of isolated phosphacycles have surfaced, little is known compared to carbon- and nitrogen-based ring systems.<sup>8-9</sup> Some phosphacycles are of

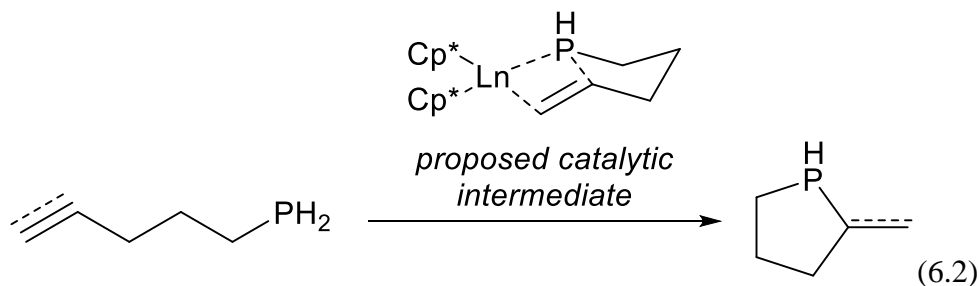
interest as alkaloid mimics and as building blocks in asymmetric chemistry.<sup>4, 10-11</sup> Cyclic phosphines such as DuPhos are widely used as ligands in asymmetric catalysis.<sup>12</sup> Studies of simple phosphacycles have not yet matured to the levels that the privileged ligands have, but preliminary studies suggest that these products already display desirable reactivity. For example, *trans*-2,5-dimethylphospholane and *trans*-2,6-dimethylphosphorinane have been shown to be effective as ligands in a variety of asymmetric hydrogenations (Figure 6.1).<sup>13-15</sup> Related phospholanes have proposed to be good ligands for catalytic hydrovinylation,<sup>16</sup> and an example of a self-assembled copper-phospholane metallamacrocycle recently emerged.<sup>17</sup> Such products could be made from a combinational intermolecular/intramolecular hydrophosphination of dienes.



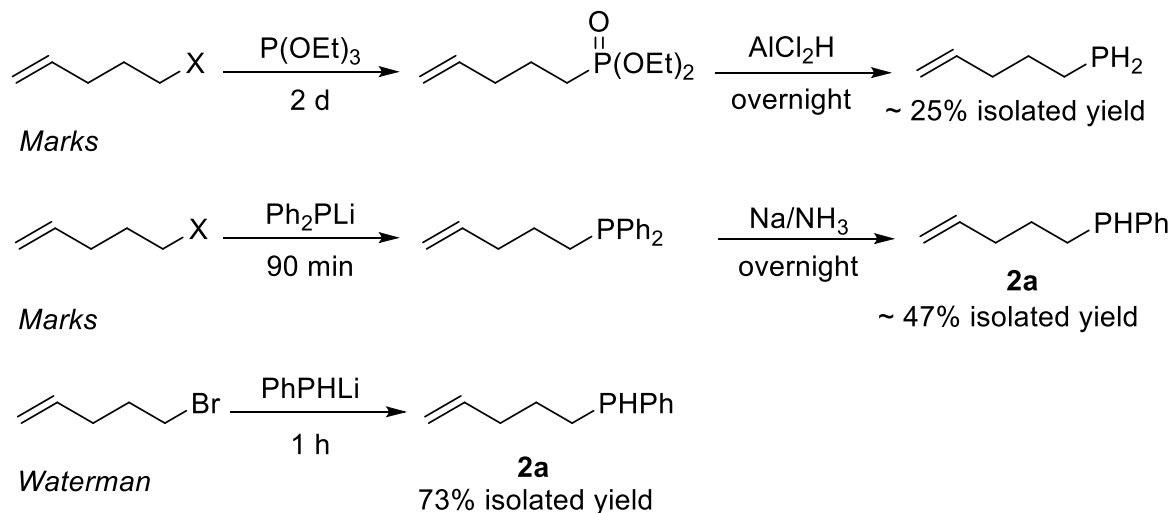
**Figure 6.1:** Cyclic phosphines as ligands for asymmetric catalysis

Catalytic hydrophosphination targeting phosphacycle formation has been reported by both Marks<sup>4, 10-11</sup> and Webster.<sup>18</sup> These reports closed primary or secondary alkenyl phosphines catalytically to make secondary or tertiary rings. In both cases, multiple cyclic isomers were formed and the products were primarily five- and six-membered rings. The proposed mechanisms account for the selectivity of the ring sizes. For example, the alkenyl phosphine in Mark's system is proposed to interact with the metal to form a seven-membered phosphametallacycle before formation of the five-membered product (eqn 6.2).<sup>4</sup>

Computational work on this system using a simplified catalyst identified that C=C insertion is turnover-limiting, though the origin of selectivity was not discussed.<sup>11</sup>



The syntheses of the primary phosphinoalkene and phosphinoalkyne hydrophosphination substrates in these reports are not trivial. The requirement for a prefunctionalized substrate limits these transformations to only reactants that can be readily synthesized from multistep processes (Scheme 6.1). For example, all primary phosphinoalkenes and phosphinoalkynes were synthesized by reaction of a commercially available alkenyl or alkynyl halide via an Arbuzov reaction to make a phosphate, followed by reduction to make the primary phosphine.<sup>4, 10-11, 18</sup> This multistep process requires several reagents, long reaction times, and provides the product in modest yields. Secondary phosphinoalkenes tested in these systems displayed similar reactivity to their primary counterparts, suggesting that catalysis is not substantially limited to phosphine identity. We found that the secondary alkenyl phosphine **2a** can be synthesized in good yields by treatment of a cold, ethereal solution of PhPHLi with an alkenyl bromide.



**Scheme 6.1:** Synthesis of alkenyl phosphines

Direct functionalization via hydrophosphination of a commercially available starting material to make the phosphinoalkene or phosphinoalkyne would circumvent the synthetic difficulties noted. That is, hydrophosphination of a diene with  $\text{PH}_3$  or a primary phosphine would make the primary or secondary alkenyl phosphine, respectively. The rare reactivity of unactivated alkenes in our system<sup>2</sup> led us to examine if dienes could undergo catalytic hydrophosphination with **1**. This product could, in theory, undergo an intramolecular ring-closure to form a phosphacycle with **1** in the same reaction (eqn 6.1). This reactivity could offer an unprecedented route to phosphacycles and demonstrate the power of catalytic hydrophosphination, thus closing a reactivity gap in catalytic hydrophosphination.

## 6.2 Results and discussion

Substrate 1,4-pentadiene was chosen for initial work targeting intermolecular and subsequent intramolecular hydrophosphination (Table 6.1).

**Table 6.1:** Catalytic hydrophosphination of 1,4-pentadiene with PhPH<sub>2</sub> to form vinyl phosphine **2a** and phosphacycle **2b**. \*Reaction heated to 60 °C.

$\text{PhPH}_2 + \text{CH}_2=\text{CH}-\text{CH}=\text{CH}-\text{CH}_3 \xrightarrow[\text{ambient temp.}]{\text{5 mol \% 1, C}_6\text{D}_6, 20-22 \text{ h}}$ 
 $\text{CH}_2=\text{CH}-\text{CH}_2-\text{CH}_2-\text{CH}_2-\text{P}(\text{Ph})_2$  (**2a**)
  $\longrightarrow$ 
 $\text{Cyclohexyl-P(Ph)}_2$  (**2b**)
  $\text{Cyclopentyl-P(Ph)}_2$  (**2c**, not observed)

Entry	Equiv PhPH <sub>2</sub>	Light	Conversion to <b>2a</b>	Conversion to <b>2b</b>
1	2	blacklight	8	29
2	2	LED	9	34
3	2	253.7 nm	5	23
4	4	blacklight	7	27
5	4	LED	9	32
6	4	253.7 nm	8	33
7	1	LED	7	42
8	1	253.7 nm	15	61
9	1	LED*	3	30
10	1	dark	0	0
11	1	dark*	0	0

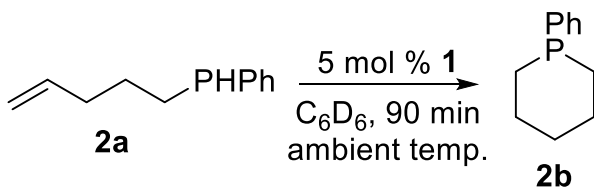
Catalytic hydrophosphination of 1,4-pentadiene installs a new P–C bond on the diene to make the vinyl phosphine **2a** before forming 1-phenylphosphinane **2b** (Table 6.1). The two products appear at the characteristic <sup>31</sup>P chemical shifts of -52 ppm for secondary phosphine **2a** and -34 ppm for the dominate ring isomer.<sup>3, 8</sup> Product **2b** forms as a mixture of axial and equatorial isomers with a 20:1 preference for the axial isomer for all cases. The barrier to ring flip between axial and equatorial isomers is relatively low, but the formation of the axial isomer is consistent with known thermodynamic parameters **2b**.<sup>8</sup> That is, compound **2b** flips between axial and equatorial isomers independently of **1**.

As anticipated, reactions run in the dark fail to provide hydrophosphination products, even with heating (Table 6.1, entries 10 and 11). Reactions run under irradiation at elevated temperatures provide lower conversions than ones run under irradiation without heating (Table 6.1, entries 7 and 9). A working hypothesis is that the light requirement for catalytic hydrophosphination with **1** is so strong that catalytic turnover diminishes when heating a sample due to the decrease in light intensity penetrating the oil bath during catalysis, as noted for alkenes. Catalytic hydrophosphination of these substrates with **1** is a photochemical, rather than thermal process.

The limited conversions in Table 6.1 arise from two different inherent problems. First, the substrates are essentially unactivated alkenes, which are known to be challenging substrates for hydrophosphination.<sup>1</sup> Second, the initial hydrophosphination step is relatively slow. Addition of excess PhPH<sub>2</sub> in an attempt to increase the turnover to the vinyl phosphine resulted in a new problem. The increased amount of PhPH<sub>2</sub> impeded the second ring-closing step by competing for coordination to **1**. PhPH<sub>2</sub> attaches more favorably to zirconium than the alkyl phosphide, resulting in the poor conversions to **2b**, because P–H activation of **2a** to **1** is a prerequisite for formation of **2b**. Use of one equivalent of PhPH<sub>2</sub> to thwart this problem gave poor conversions arising from even a more sluggish initial hydrophosphination event to form **2a**. Conversions using just one equivalent of PhPH<sub>2</sub> were still the greatest because less PhPH<sub>2</sub> was competing for the metal center (Table 6.1, entries 7 and 8).

To investigate the second step in hydrophosphination compound **2b** was synthesized independently and reacted with 5 mol % of **1** (Scheme 6.2).

**Table 6.2:** Catalytic hydrophosphination of **2a** to form **2b**. <sup>a</sup>Reaction run in the absence of **1**. <sup>b</sup>Reaction ran for 19 h.



**2a**  $\xrightarrow[\text{C}_6\text{D}_6, 90 \text{ min, ambient temp.}]{5 \text{ mol } \% \text{ 1}}$  **2b**

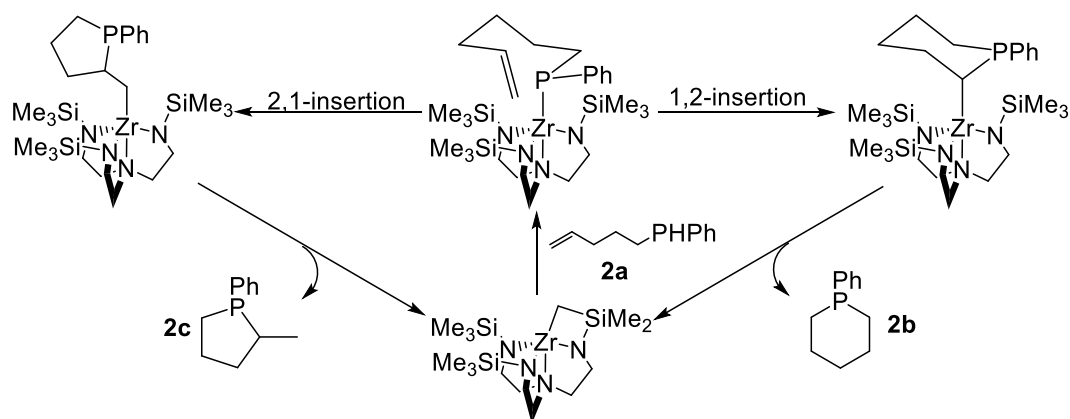
Entry	Light	Conversion to <b>2b</b>
1	blacklight	35
2	LED	20
3	253.7 nm	85
4 <sup>a</sup>	blacklight	7
5 <sup>a</sup>	LED	4
6 <sup>a</sup>	253.7 nm	35
7 <sup>b</sup>	dark	4

While **2b** can also be formed spontaneously by cyclization of **2a** under photolysis, control reactions run in the absence of **1** failed to provide significant conversion (Table 6.2, entries 4-6). Reactions run in the exclusion of light provide minimal conversion, even after extended reaction times (Table 6.2, entry 7). It should be noted that appreciable conversions of **2b** can be achieved without **1** under 253.7 nm irradiation, but this is not as fast as catalysis (Table 6.2, entries 3 and 6).

Intramolecular hydrophosphination of **2a** to form **2b** represents an advancement over the current art. Webster's intramolecular cyclization achieved quantitative yields after 14 h at 90 °C (TON = 0.72 h<sup>-1</sup>), and Mark's returns a 75% conversion at 40 °C (TON = 0.25 h<sup>-1</sup>). Our optimal conditions provide 85% conversion at ambient temperature after 90 min (TON = 11.3 h<sup>-1</sup>, Table 6.2, entry 3).

The selectivity in catalytic hydrophosphination with 1,4-pentadiene is exceptional. Compound **1** is the first hydrophosphination catalyst that selects for formation of the six-membered phosphorninane **2b** over the five-membered ring **2c**. Mark's lanthanide catalysts achieves 75% conversion of **2a** to **2c** with 5-20% formation of **2b**.<sup>3</sup> Webster's iron one select for **2c** with 100% conversion and complete selectivity.<sup>18</sup> Formation of the five-membered ring **2c** is surprising because this is the Markovnikov-addition product. Most metal hydrophosphination catalysts are *anti*-Markovnikov selective. Both mechanisms forming **2c** are proposed to proceed through phosphide coordination, then coordination and insertion of the olefin. Formation of the major product in Mark's system is the apparent 2,1-insertion product, although the authors do not suggest where the selectivity comes from (eqn 6.2). Such a suggestion would be difficult because multiple isomers are formed in that system.

Catalytic hydrophosphination with **1** to form the six-membered product **2b** is different. Compound **2b** is the product of the 1,2-insertion, whereas the phospholane **2c** is the product of the 2,1-insertion (Scheme 6.2).



**Scheme 6.2:** Possible 1,2- and 2,1-insertion routes to make products **2b** and **2c**



We were curious to see if the apparent selectivity of **1** for the 1,2-insertion was consistent between substrates. Treatment of 1,5-hexadiene with PhPH<sub>2</sub> under standard conditions gave both the six-membered ring and the 1,2-insertion product among other products (Table 6.3).

**Table 6.3:** Catalytic hydrophosphination of 1,5-hexadiene with PhPH<sub>2</sub> to form alkenyl phosphine **3a**, phosphacycles **3b** and **3c**, and diphosphine **3d**.

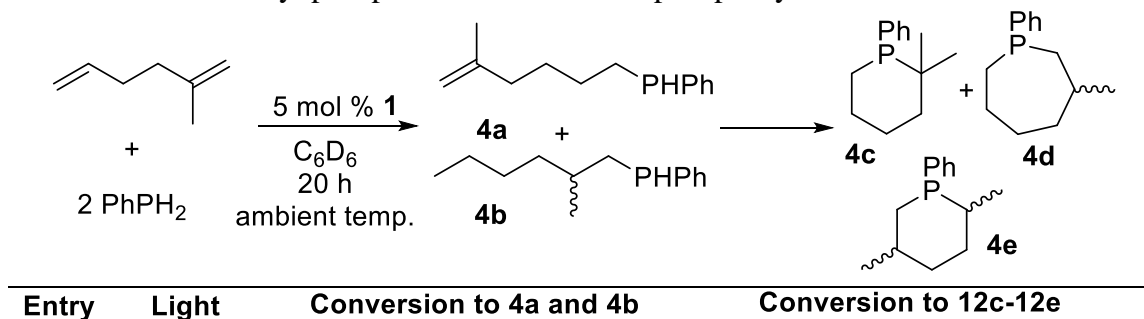
Entry	Equiv PhPH <sub>2</sub>	Light	Conv. to <b>3a</b>	Conv. to <b>3b</b>	Conv. to <b>3c</b>	Conv. to <b>3d</b>
1	2	blacklight	7	21	7	26
2	2	LED	2	26	4	36
3	2	253.7 nm	6	21	4	25
4	1	blacklight	5	15	3	18
5	1	LED	5	36	9	33
6	1	253.7 nm	4	14	3	17

In all cases the formation of the vinyl phosphine is modest, and only about half undergoes the second step to make **3b** and **3c**. Unlike hydrophosphination of 1,4-pentadiene (Table 6.1), the secondary vinyl phosphine builds up in solution to a greater degree, but conversion to the ring products **3b** and **3c** is limited and product **3d** formed instead. Extended reaction times without the problematic excess of PhPH<sub>2</sub> did not increase formation of **3b** and **3c**.

Regardless, formation of a mixture of six- and seven-membered rings from the hydrophosphination of 1,5-hexadiene suggests that insertion into the Zr–P bond is not as discriminatory as previously thought because products from both a 1,2-insertion and a 2,1-insertion were identified (Table 6.3).

The probability of asymmetric products arising from a  $C_{3v}$ -symmetric catalyst is relatively low, but the idea remained intriguing. Treatment of a prochiral diene 2-methyl-1,5-hexadiene under standard conditions gave a variety of products with no obvious preference, as anticipated (Table 6.4).

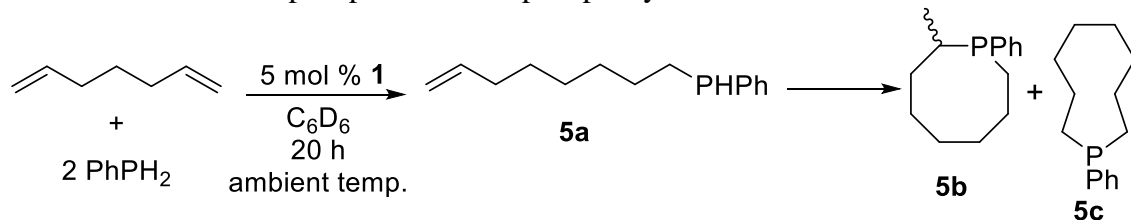
**Table 6.4:** Catalytic hydrophosphination of 2-methyl-1,5-hexadiene with  $\text{PhPH}_2$  to form vinyl phosphines **4a** and **4b** and phosphacycles **4c-4e**



Products **4b**, **4d** and **4e** have the possibility to be chiral. However, catalytic hydrophosphination with the prochiral diene produced mixtures of diastereomers for both products in addition to other achiral isomers **4a**, **4c**, and **4e**. It is worth noting that the anti-Markovnikov selectivity remains throughout, so the formation of variety of products as shown in Table 6.4 is only a fraction of the possible outcomes. A total of thirteen hydrophosphination products are possible, excluding side products arising from dehydrocoupling. Regardless, the selectivity was minimal and the conversions to the desired ring-closing products were poor.

Formation of larger eight- and nine-membered rings proved possible but of poor efficiency from the hydrophosphination of 1,7-octadiene (Table 6.5).

**Table 6.5:** Catalytic hydrophosphination of 1,7-octadiene with PhPH<sub>2</sub> to form vinyl phosphine **5a** and phosphacycles **5b** and **5c**



Entry	Light	Conv. to <b>5a</b>	Conv. to <b>5b</b>	Conv. to <b>5c</b>
1	blacklight	57	5	0
2	LED	64	9	0
3	253.7 nm	75	14	2

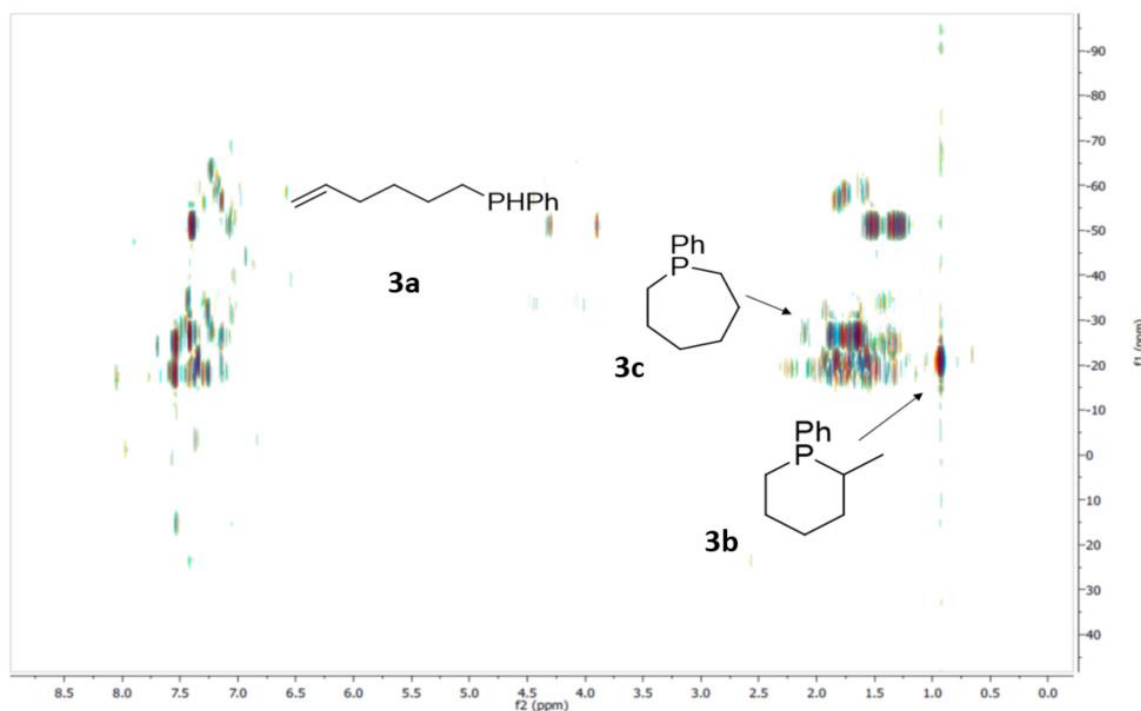
Formation of phosphacycles larger than seven is unprecedented catalytically.

However, the conversions were limited, as anticipated. Hydrophosphination to form the alkenyl phosphine **5a** proceeded relatively easily to allow for significant buildup, but intramolecular hydrophosphination to form **5b** and **5c** is sluggish. Formation of **5b** suggests that 2,1-insertion is more favorable than 1,2-insertion. This change in selectivity is more pronounced than in the hydrophosphination of the shorter-chain 1,5-hexadiene (Table 6.3).

Characterization of these phosphorus-containing cycles is not trivial. Only a handful of the many vinyl phosphines and rings were known. A variety of NMR spectroscopic methods were employed to identify vinyl phosphines, rings, and their isomers. The inherently high atom-economy of this transformation provides products that have identical molecular weights, so identification of isomers by mass spectrometry is often poorly informative.

The hydrophosphination of 1,5-hexadiene undergoes the expected initial hydrophosphination reaction to form **3a**, but has the potential to make either the six-membered ring **3b** or the seven-membered ring **3c**. While the methyl group of **3b** would

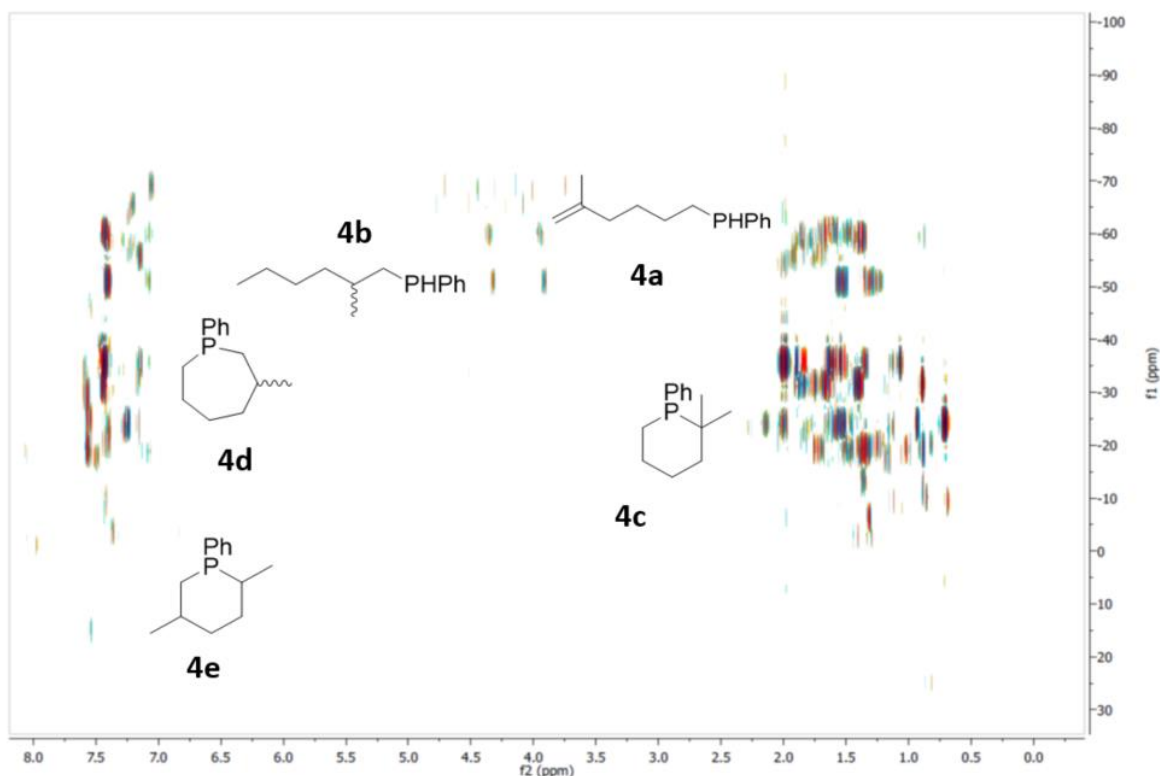
be diagnostic, the alkyl region of the  $^1\text{H}$  NMR spectrum has several overlapping peaks, making identification difficult. Investigation of the  $^{31}\text{P}$  NMR spectra can clearly show secondary and tertiary products apart, but the resolution on the multiplicity was too poor to distinguish between **3b** and **3c**. Two-dimensional Heteronuclear Multiple-Bond Coupling (HMBC) NMR spectroscopy was used to elucidate the assignments. The major isomers of the seven-membered ring and six-membered ring were identified by the coupling of the methyl group of **3b** to the  $^{31}\text{P}$  resonance of -26 ppm and -21 ppm, respectively (Figure 6.2).



**Figure 6.2:** Assignment of the isomers **3b** and **3c** by  $^{31}\text{P}$ - $^1\text{H}$  HMBC. At the time this spectrum was taken product **3d** had not formed in significant amounts.

This technique was used as the basis for the assignments for compounds arising from the hydrophosphination of 2-methyl-1,5-hexadiene and 1,7-octadiene. In the former

case two products, **4a** and **4b**, are observed in the initial hydrophosphination event. A  $^{31}\text{P}$ - $^1\text{H}$  HMBC spectrum distinguished the isomers on the basis of the diastereotopic methyl group of **4b** because the vinyl  $^1\text{H}$  resonances overlapped (Figure 6.3).

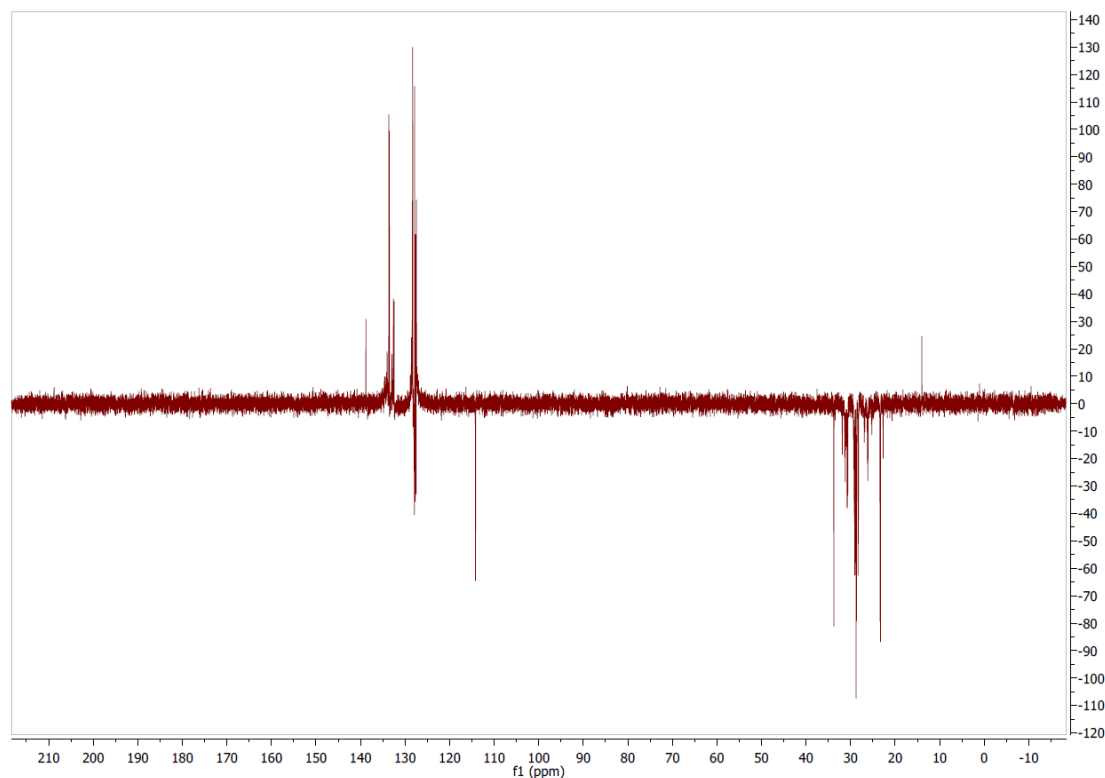


**Figure 6.3:** Assignment of the isomers **4a-4e** by  $^{31}\text{P}$ - $^1\text{H}$  HMBC

Assignments for rings **4c-4e** were made by consideration of the methyl resonances from the product phosphacycles. As anticipated, integration of the  $^1\text{H}$  NMR spectrum or consideration of the  $^{31}\text{P}$ - $^1\text{H}$  coupling were not enough to distinguish between isomers due to poor conversions, overlap, and similarity.

In some cases Distortionless Enhancement by Polarization Transfer (DEPT) was required for further structural confirmation. This  $^{13}\text{C}$  program uses a pulse angle of  $135^\circ$  such that only CH and  $\text{CH}_3$ - groups will be positive;  $\text{CH}_2$  groups will be negative.<sup>19</sup> This

is especially useful in cases where integration of  $^1\text{H}$  NMR spectra is difficult. Identification of **5b** was made possible by this method because the only methyl group in the reaction mixture appeared at 14 ppm (Figure 6.4).



**Figure 6.4:** DEPT-135 NMR spectrum of a reaction mixture of **5a-5c**

A common theme in this chemistry is that the secondary alkenyl phosphines formed from the first diene hydrophosphination give rise to several products (with the exception of 1,4-pentadiene). It is understood that **1** is an excellent hydrophosphination catalyst for primary<sup>1-2, 20-21</sup> but not secondary<sup>22</sup> phosphines. One hypothesis is that the secondary alkenyl phosphines make such poor phosphides on the metal center such that the diene will orient itself in any way to relieve this bond. Intramolecular hydrophosphination occurs with such poor selectivity for the 1,2- or the 2,1-insertion.

Still, catalytic turnover was thwarted by product inhibition. Unconjugated dienes are modest substrates for hydrophosphination even under photolysis and catalytic secondary phosphine hydrophosphination with **1** is limited. The accessibility of unactivated alkenes in catalytic hydrophosphination with **1** is somewhat restricted in turnover, despite the uniqueness and rarity of this transformation. The challenges of these substrates carry over to unactivated alkenes, but with an additional constraint. After sluggish hydrophosphination with **1** to form the alkenyl phosphine in modest conversions, the ring-closure step is slow and provides the product in even smaller conversions.

However, few catalytic routes to cyclic phosphines exist, and none exist for seven- eight- and nine-membered rings. Hydrophosphination of unactivated substrates is an ongoing challenge, and this system offers unprecedented access to a variety of phosphacycles from diene hydrophosphination with  $\text{PhPH}_2$ .

The consistent light requirement for hydrophosphination remains intriguing with these substrates. This observation blends well with the working hypothesis that catalytic hydrophosphination with **1** operates via insertion-based mechanism, which is aided by photoexcitation of the catalyst. This suggests that catalytic hydrophosphination with **1** proceeds through photoexcitation, even for secondary phosphines to make the tertiary products. While it cannot be determined if the light requirement is as strong for the second, intramolecular hydrophosphination event, preliminary results with **2a** indicate that photoexcitation of derivatives of **1** is a prerequisite for catalysis.

### 6.3: Conclusions

This investigation was a valid proof-of concept in many regards. Formation of seven-, eight-, and nine-membered rings is interesting in its own right, and this study showed that phosphacycles can be produced in a one-pot reaction from one of several dienes and PhPH<sub>2</sub> at ambient temperature. The scarcity of the number of catalytic transformations to make phosphacycles suggests that this transformation could be of value. Unactivated alkenes are still challenging substrates for hydrophosphination, as are primary phosphines. Joining both primary phosphine and diene chemistry allows for a simplified route to phosphacycles from a room temperature, catalytic intermolecular and intramolecular hydrophosphination that previous systems did not offer. The only comparable substrate, **2a**, cyclizes to **2b** at ambient temperature with significantly shorter reaction times, making it an improvement over known systems. Further studies to identify higher turnovers or more selective product formation could improve upon these preliminary results and further optimize a closed reactivity gap in catalytic hydrophosphination.

### 6.4 Experimental methods

#### 6.4.1 General methods

All air-sensitive manipulations were performed under a positive pressure of nitrogen using standard Schlenk line or in a M. Braun glove box. Dry, oxygen-free solvents were employed throughout. Benzene-*d*<sub>6</sub> was purchased then degassed and dried over NaK alloy and distilled under reduced pressure. NMR spectra were recorded with a Bruker AXR 500 MHz spectrometer in benzene-*d*<sub>6</sub> and are reported with reference to residual solvent signals (C<sub>6</sub>D<sub>6</sub>, δ 7.16 and 128.0) and to an external 85% H<sub>3</sub>PO<sub>4</sub> (δ 0.0) standard for <sup>31</sup>P



NMR spectra. PhPH<sub>2</sub> was purchased from Strem Chemicals and used without further purification. Compound [*K*<sup>5</sup>–*N,N,N,N,C*–(Me<sub>3</sub>SiNCH<sub>2</sub>CH<sub>2</sub>)<sub>2</sub>NCH<sub>2</sub>CH<sub>2</sub>NSiMe<sub>2</sub>CH<sub>2</sub>]Zr (**1**) was prepared according to the literature procedure.<sup>23</sup> All other chemicals were obtained from commercial suppliers and dried by appropriate means.

The LED bulb used for photoirradiation is an OSRAM Sylvania Ultra LED A19 Lamp – generation 5, operating power of 6 W and output of 450 lumens. The blacklight bulb used for photoirradiation is a VEi Party Lamp. The 253.7 nm photoreactor was purchased from the Southern New England Ultraviolet Company and uses Rayonet lamps. All reactions were run at ambient temperature with minimal additional heat from the lamps, as measured.

#### 6.4.2 Synthesis of **2a**

A scintillation vial containing 391.1 mg (3.55 mmol) of PhPH<sub>2</sub> in ca 8 mL of diethyl ether at -30 °C was dropwise given 2.20 mL of a 1.6 M butyllithium solution in hexanes (3.52 mmol). The contents stirred at ambient temperature for 15 minutes. The contents were cooled to -30 °C and given 0.45 mL (3.80 mmol) of 5-bromo-pent-1-ene. The contents were stirred for 1 hour at ambient temperature. Volatiles were removed under reduced pressure. The crude reaction mixture was dissolved in hexanes, filtered, and concentrated. Distillation (70-75 °C) under reduced pressure gave **2a** as a colorless oil (481 mg, 2.58 mmol, 73%). Spectra match those previously reported.<sup>3</sup>

#### 6.4.3 General procedure for hydrophosphination reactions with PhPH<sub>2</sub> targeting phosphacycles

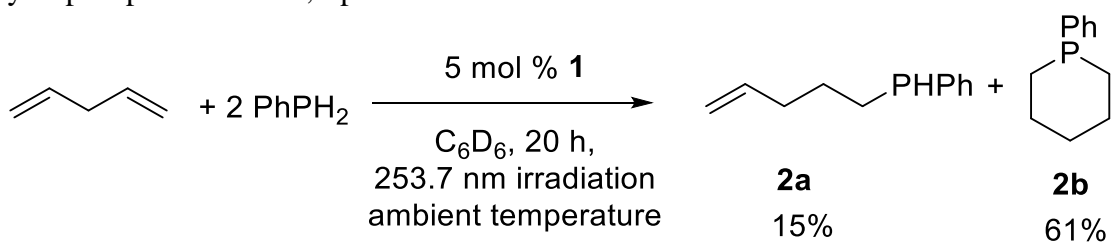
A scintillation vial was charged with 0.50 mmol PhPH<sub>2</sub> and 0.25 mmol alkene or diene in the presence of 5 mol % of **1** in benzene-*d*<sub>6</sub> solvent for reactions with two

equivalents of PhPH<sub>2</sub>. The reaction mixture was divided between three NMR tubes. Each NMR tube was placed in a different photochamber. The consumption of substrate to product was monitored by <sup>31</sup>P and <sup>1</sup>H NMR spectroscopy. Yields were determined from integration of the substrate converted by <sup>1</sup>H and <sup>31</sup>P NMR spectra.<sup>24</sup>

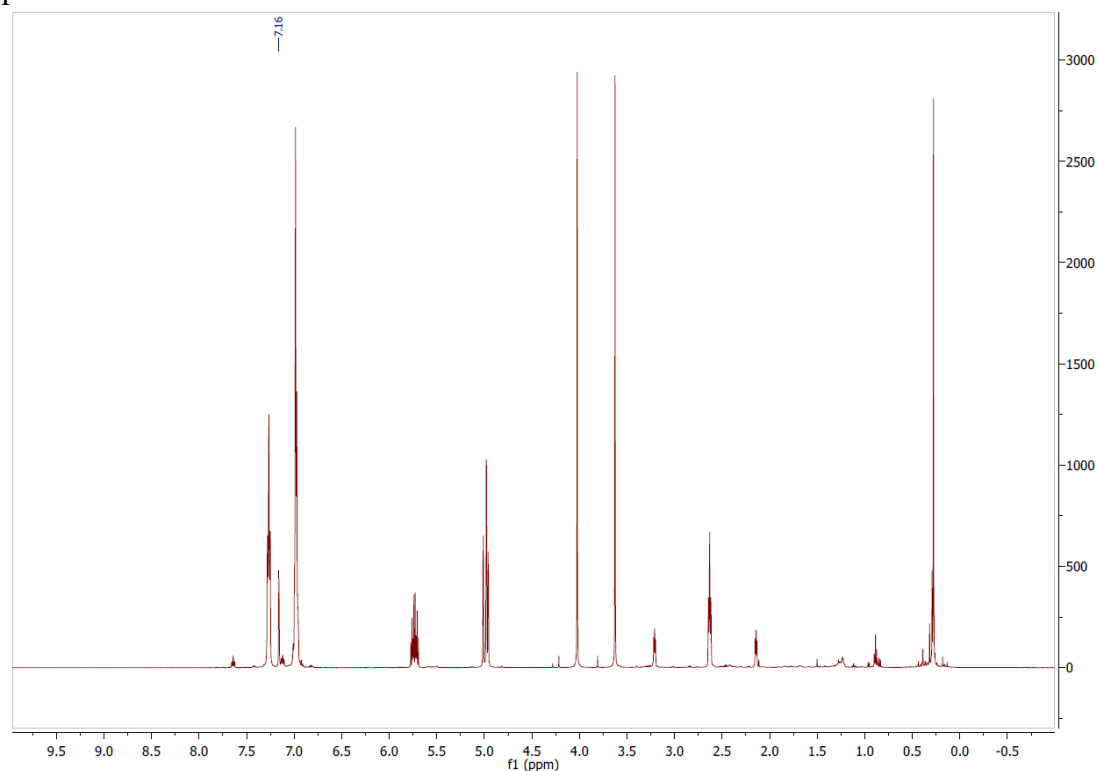
Spectroscopic data is consistent to that reported in the literature for known products.

#### 6.4.4 Representative NMR spectra

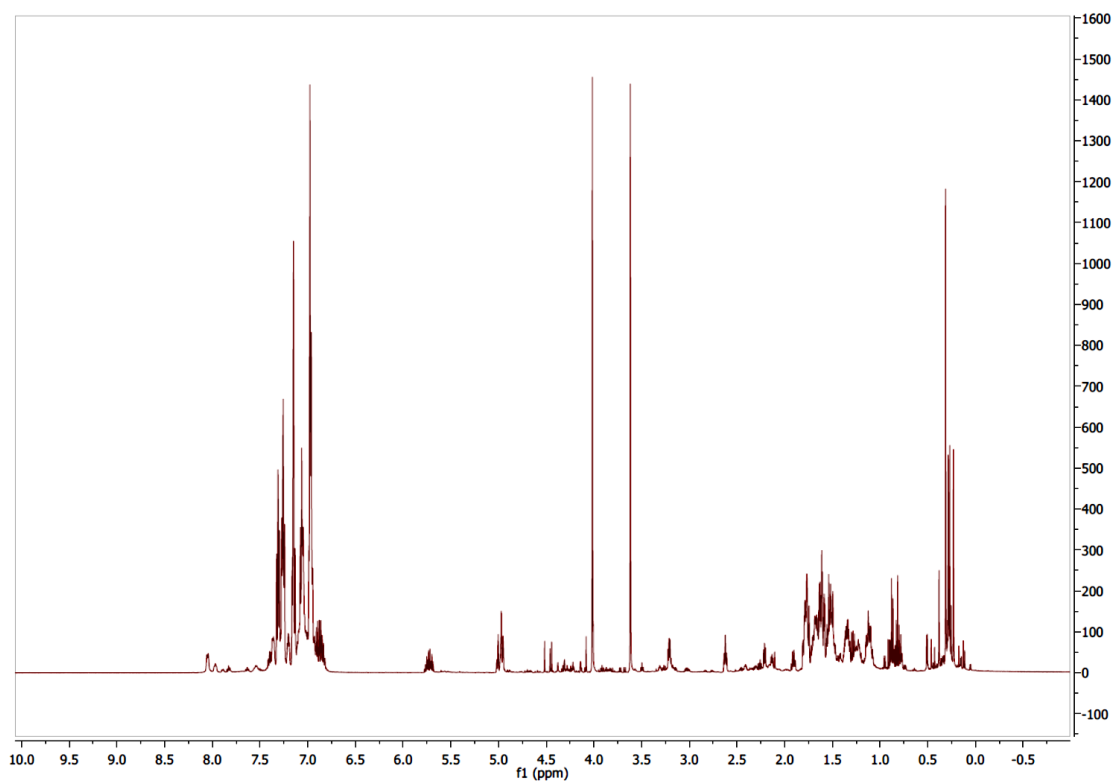
Hydrophosphination of 1,4-pentadiene to make **2a-2b**



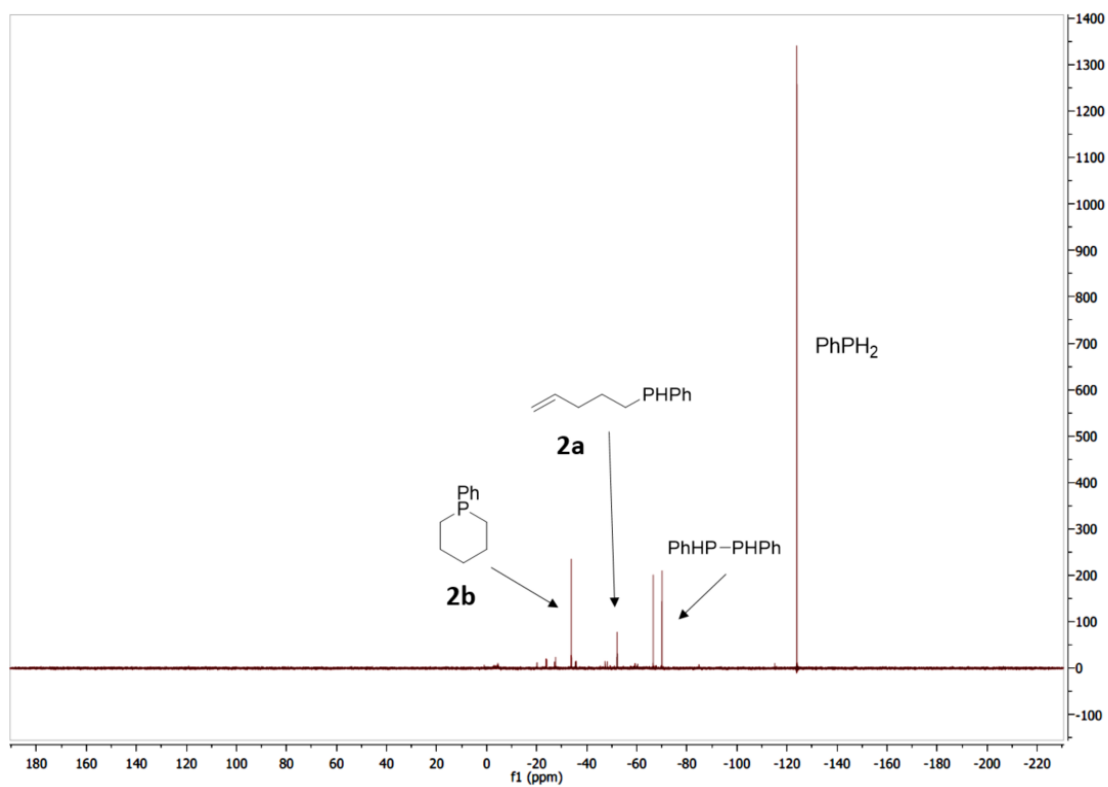
Spectra are consistent with the literature.<sup>9</sup>



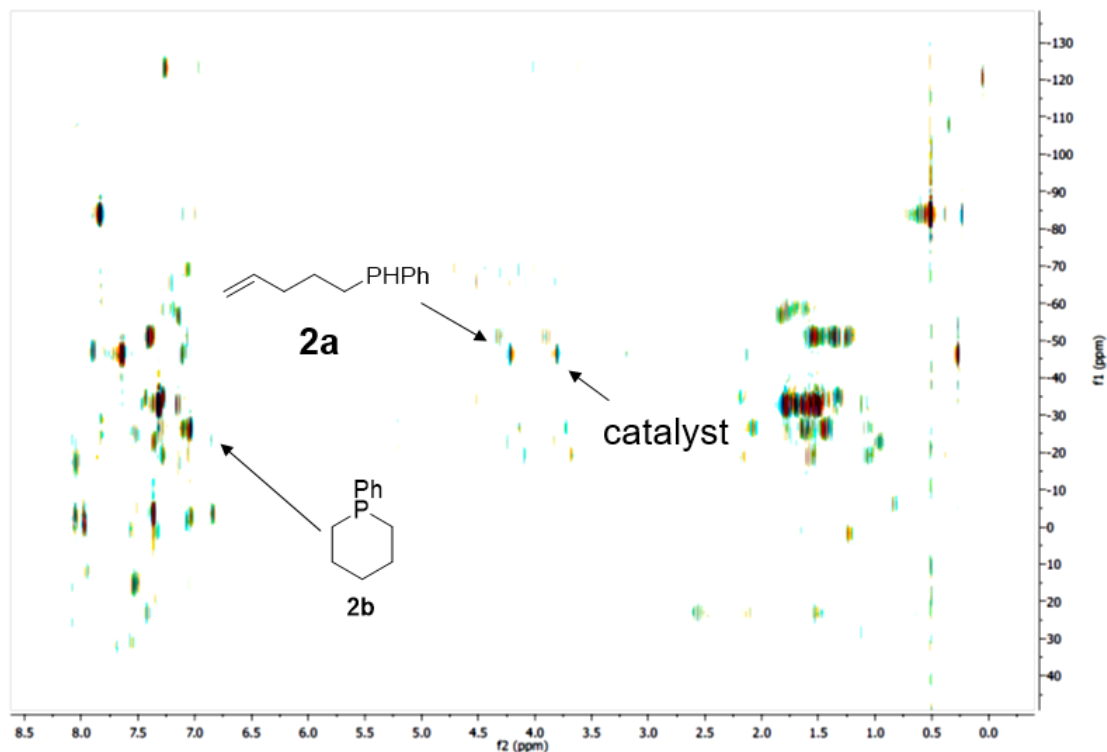
**Figure 6.5:** Representative initial <sup>1</sup>H NMR spectrum of the hydrophosphination of 1,4-pentadiene



**Figure 6.6:** Representative final  $^1\text{H}$  NMR spectrum of the hydrophosphination of 1,4-pentadiene

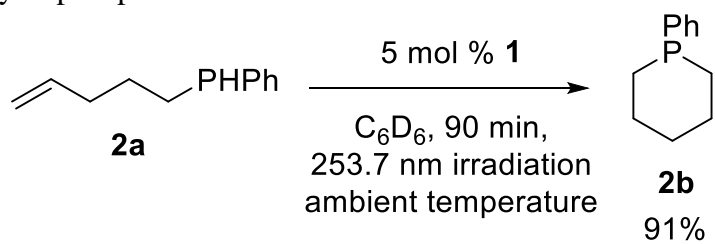


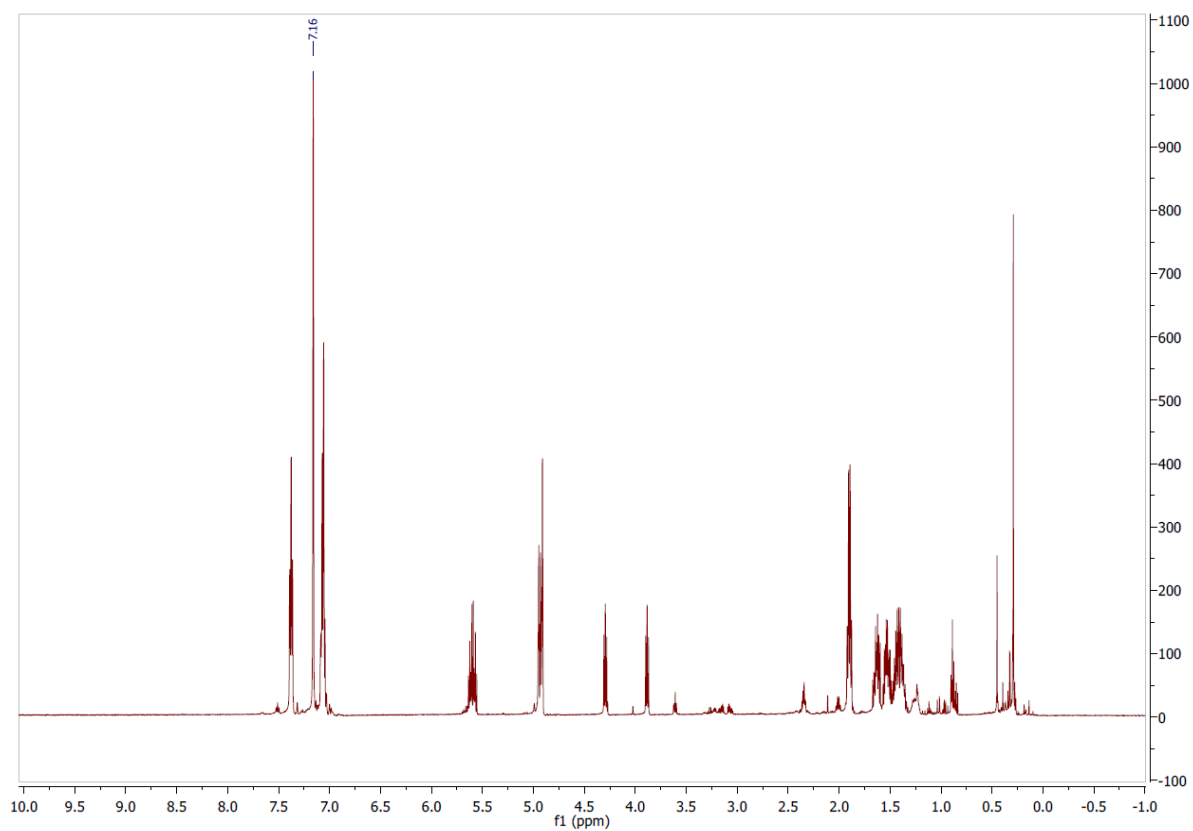
**Figure 6.7:** Representative  $^{31}\text{P}\{^1\text{H}\}$  NMR spectrum of the hydrophosphination of 1,4-pentadiene



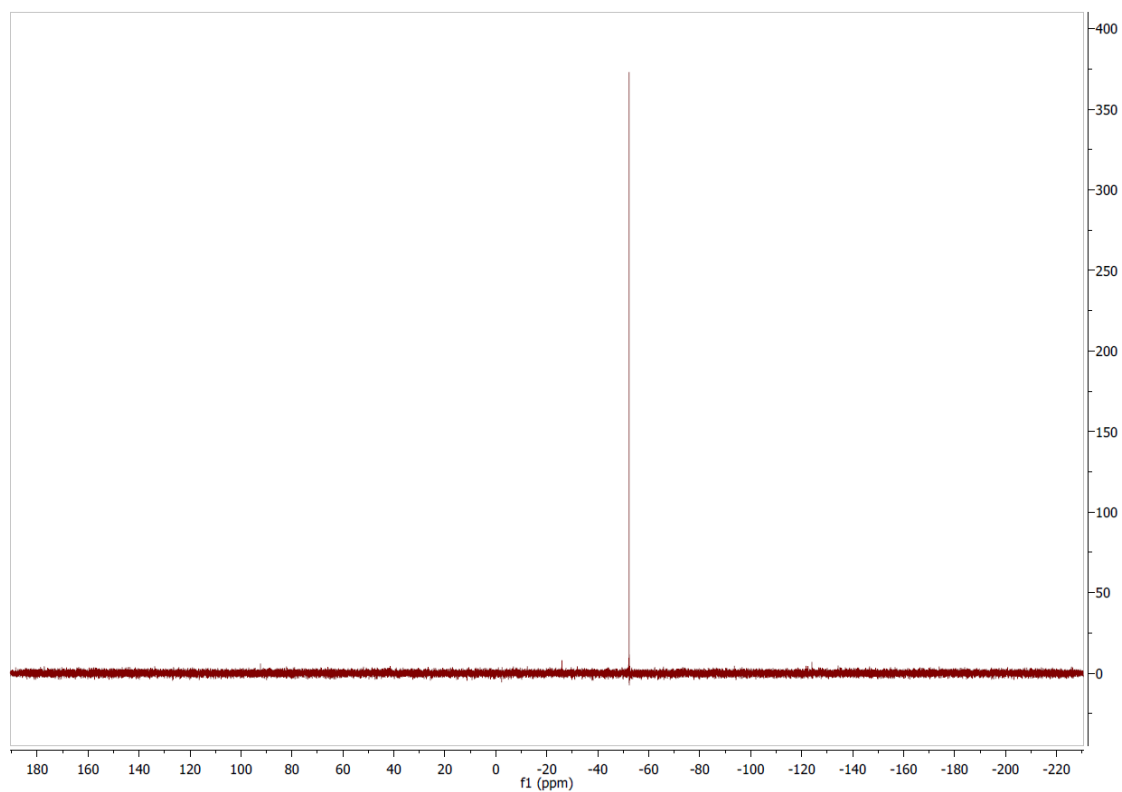
**Figure 6.8:** Representative  $^{31}\text{P}$ - $^1\text{H}$  HMBC NMR spectrum of the hydrophosphination of 1,4-pentadiene

Intramolecular hydrophosphination of **2a** to make **2b**

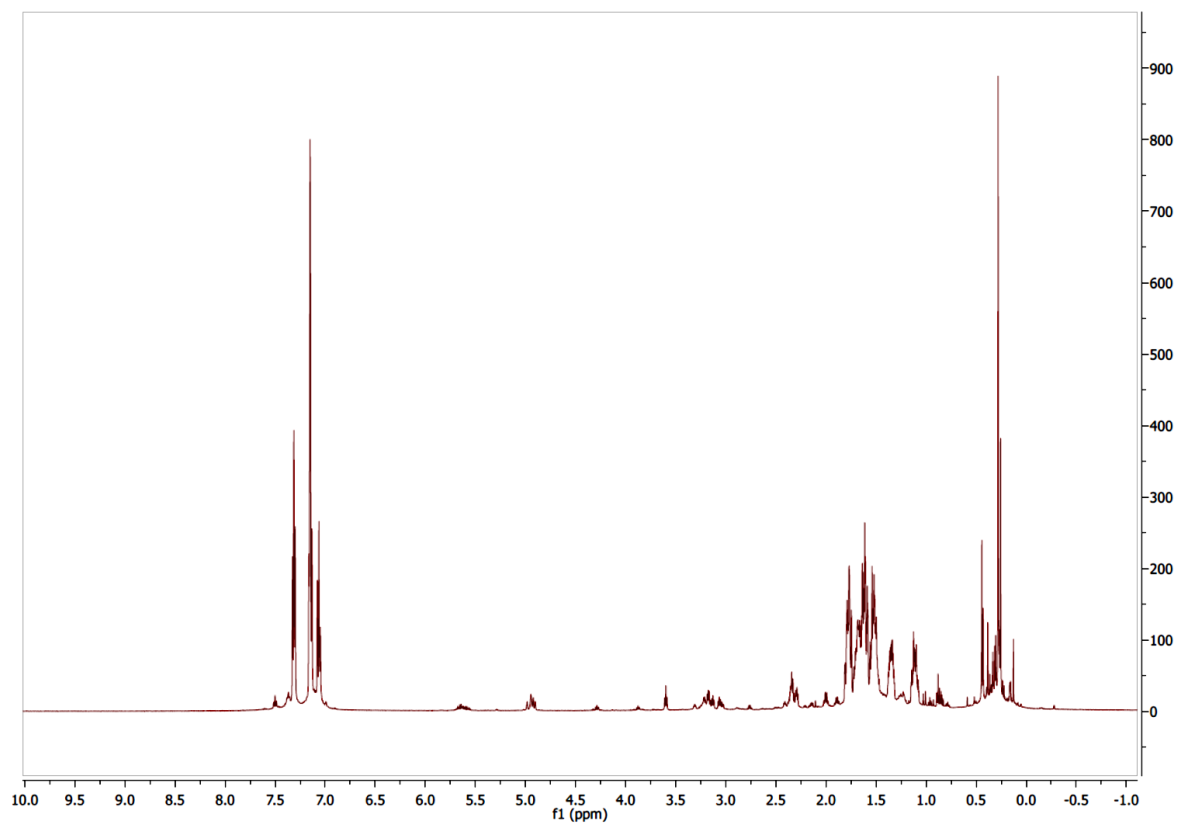




**Figure 6.9:** Representative initial  $^1\text{H}$  NMR spectrum of the ring closure of **2a** to make **2b**

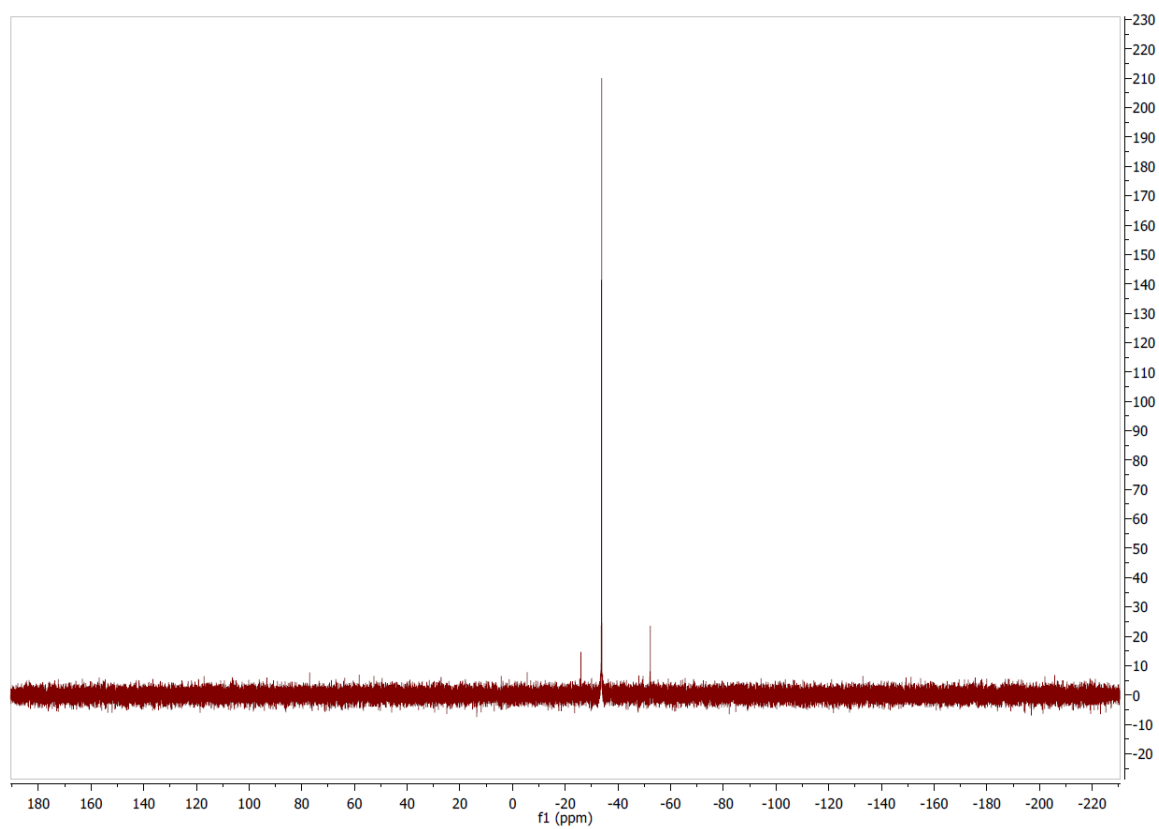


**Figure 6.10:** Representative initial  $^{31}\text{P}\{^1\text{H}\}$  NMR spectrum of the ring closure of **2a** to make **2b**

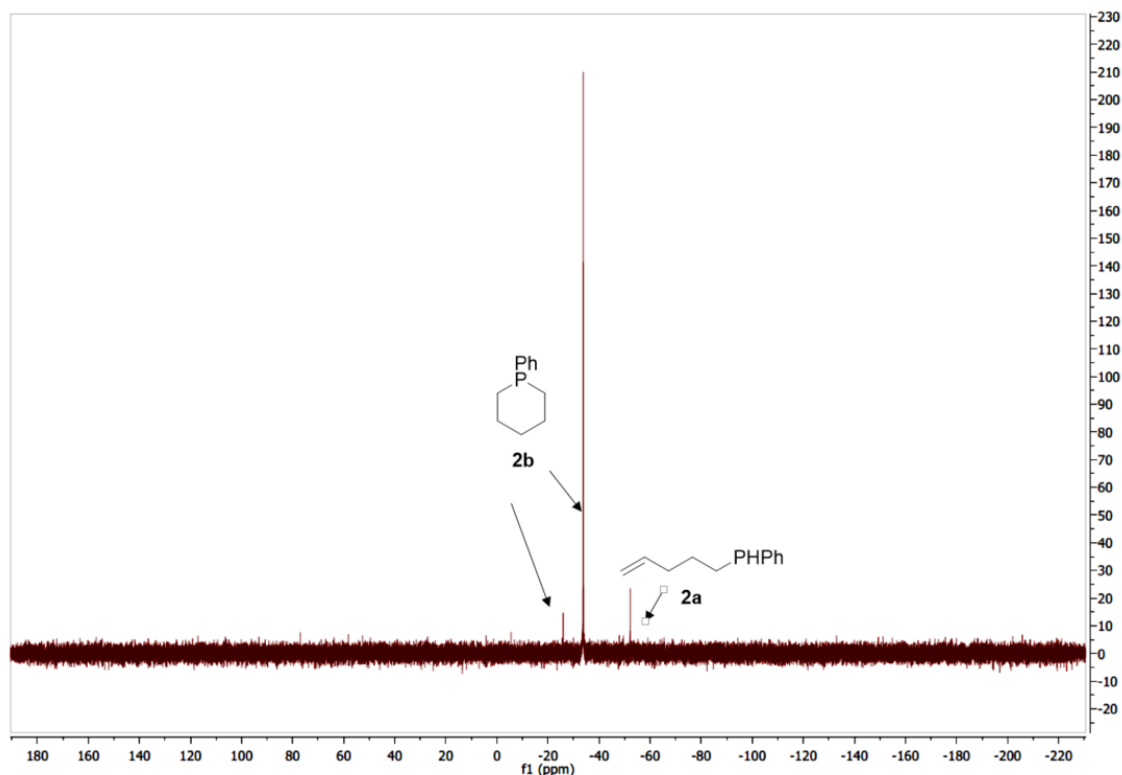


**Figure 6.11:** Representative final  $^1\text{H}$  NMR spectrum of the ring closure of **2a** to make **2b**





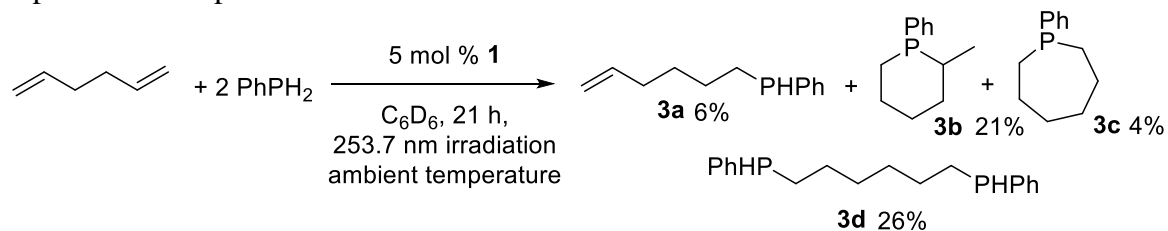
**Figure 6.12:** Representative final  $^{31}\text{P}\{^1\text{H}\}$  NMR spectrum of the ring closure of **2a** to make **2b**

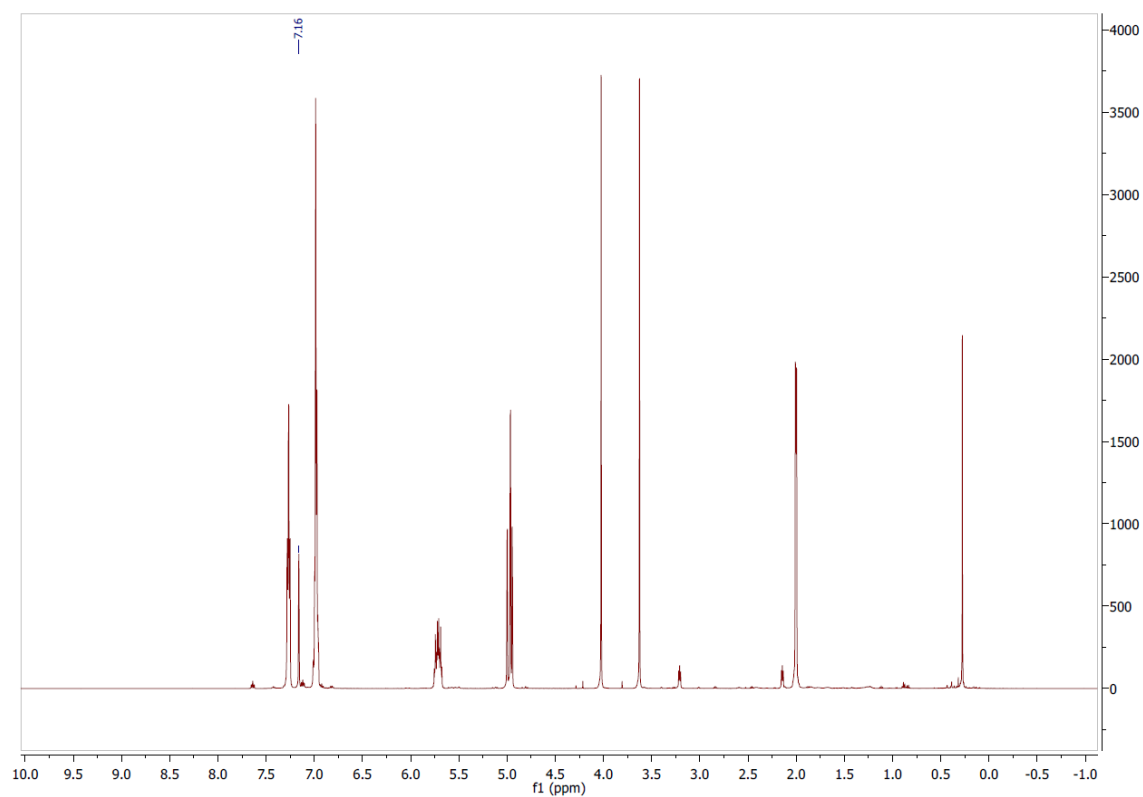


**Figure 6.13:** Representative  $^{31}\text{P}\{^1\text{H}\}$  NMR spectrum of the ring closure of **2a** to make **2b**

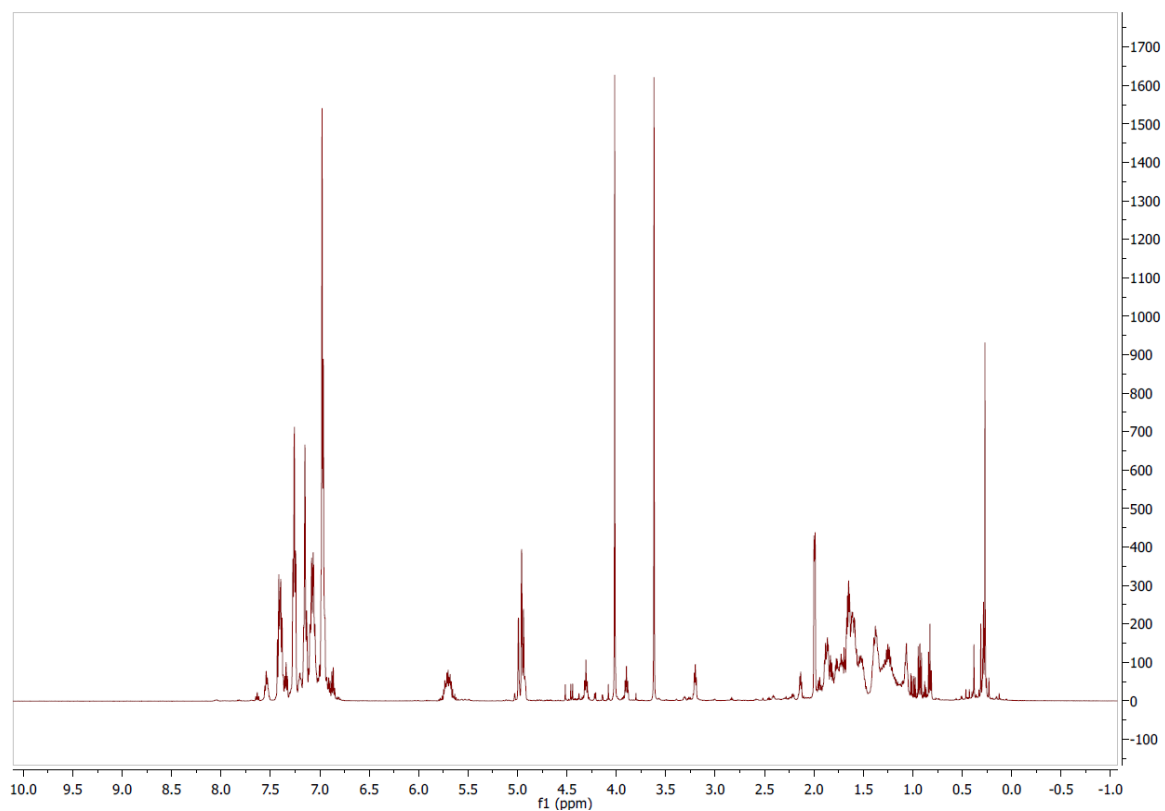
Hydrophosphination of 1,5-hexadiene to make **3a-3c**

Compound **3a** is a known compound for which additional characterization data is reported.<sup>25</sup> Compound **3c** is consistent with the literature.<sup>26</sup>

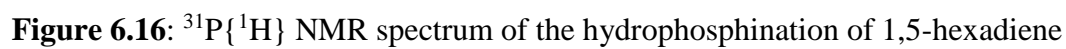


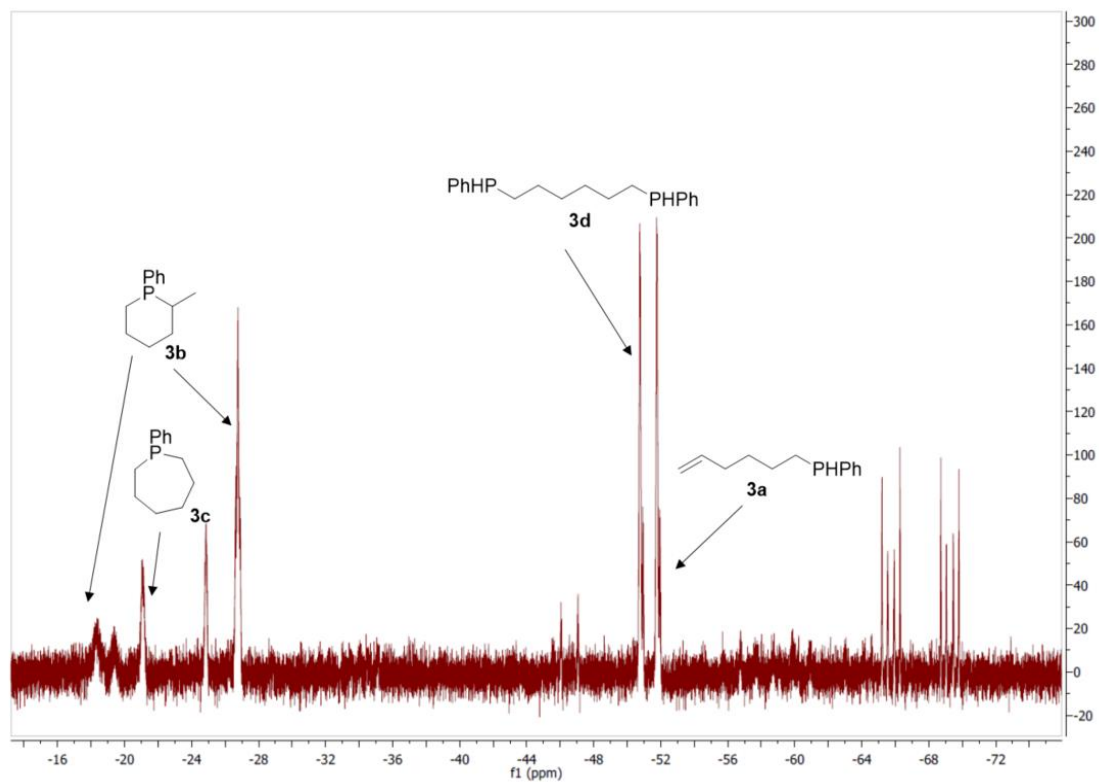


**Figure 6.14:** Representative initial  $^1\text{H}$  NMR spectrum of the hydrophosphination of 1,5-hexadiene

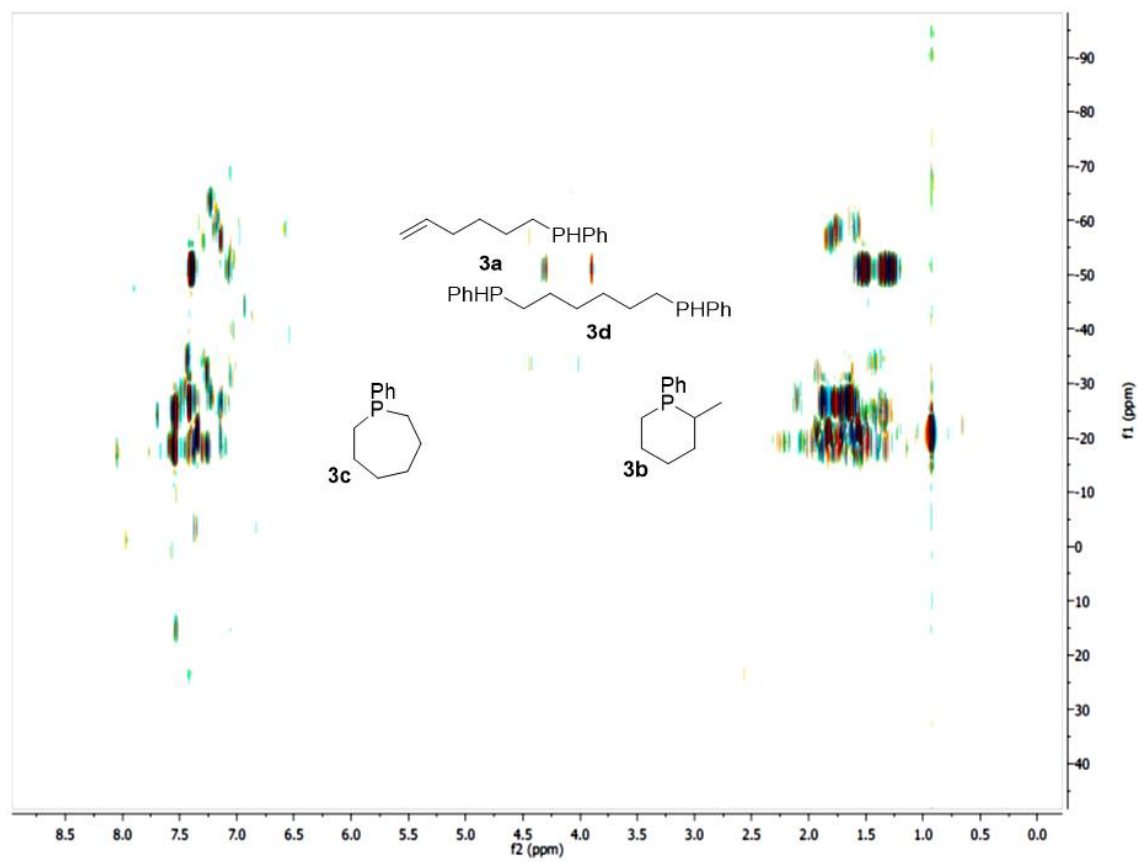


**Figure 6.15:** Representative final  $^1\text{H}$  NMR spectrum of the hydrophosphination of 1,5-hexadiene

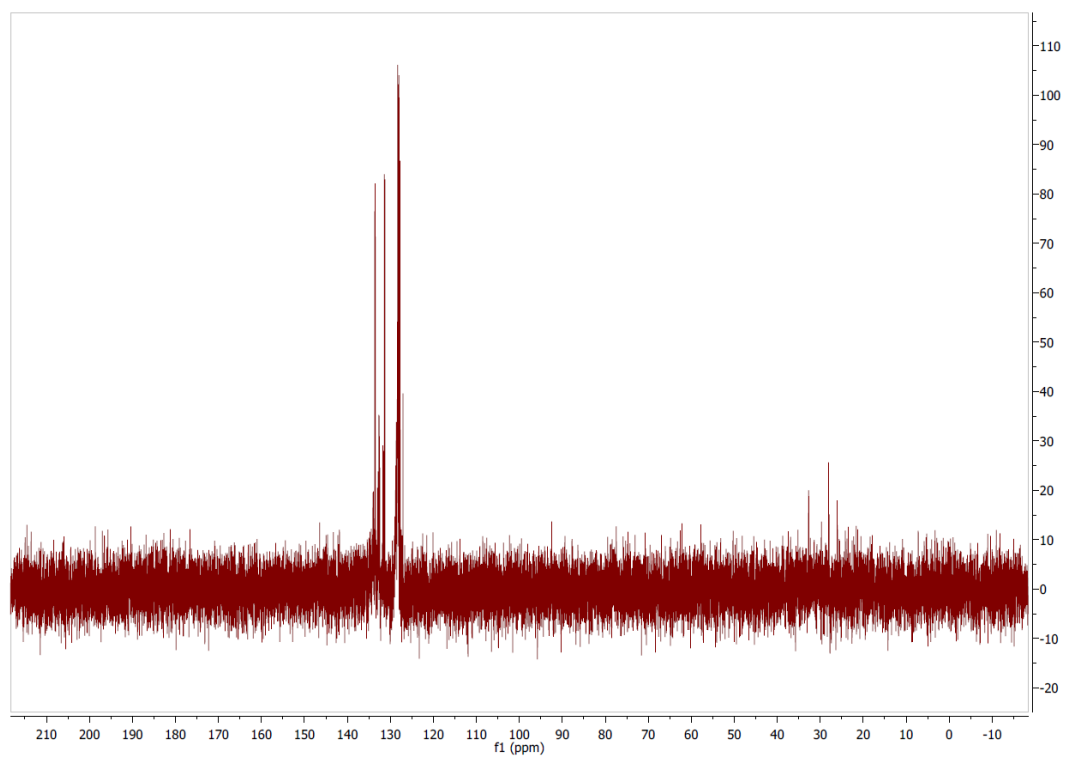




**Figure 6.17:**  $^{31}\text{P}$  NMR spectrum of the hydrophosphination of 1,5-hexadiene



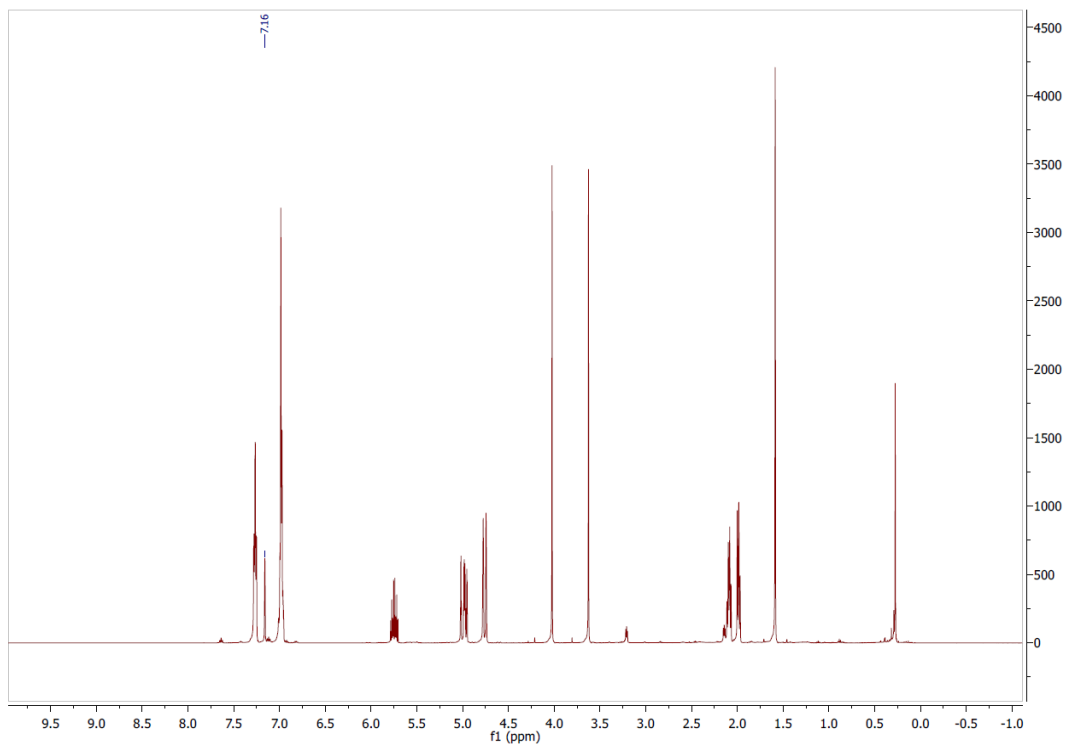
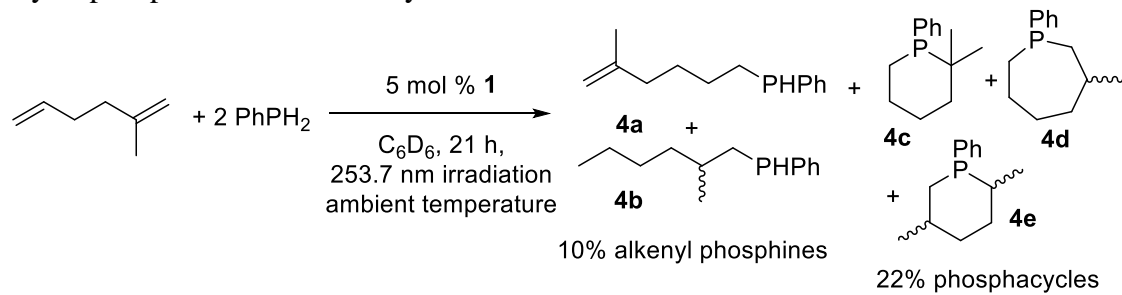
**Figure 6.18:**  $^{31}\text{P}$ - $^1\text{H}$  HMBC NMR spectrum of the hydrophosphination of 1,5-hexadiene



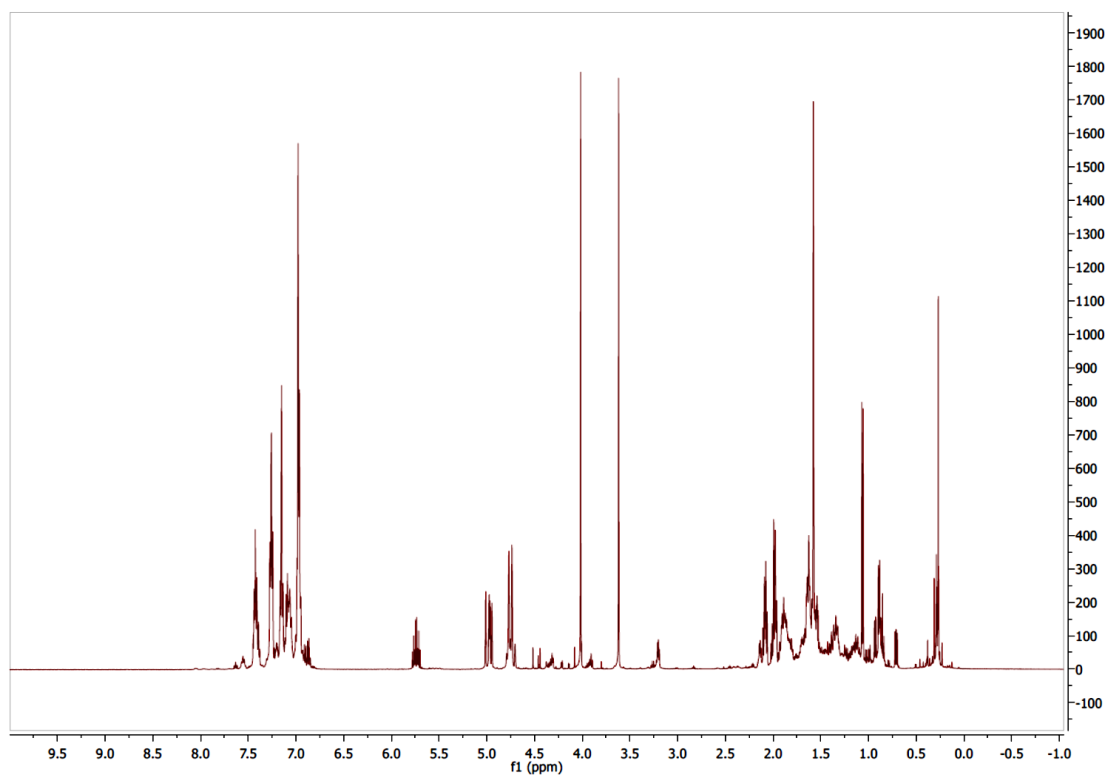
**Figure 6.19:**  $^{31}\text{P}\{^1\text{H}\}$  NMR spectrum of the hydrophosphination of 1,5-hexadiene



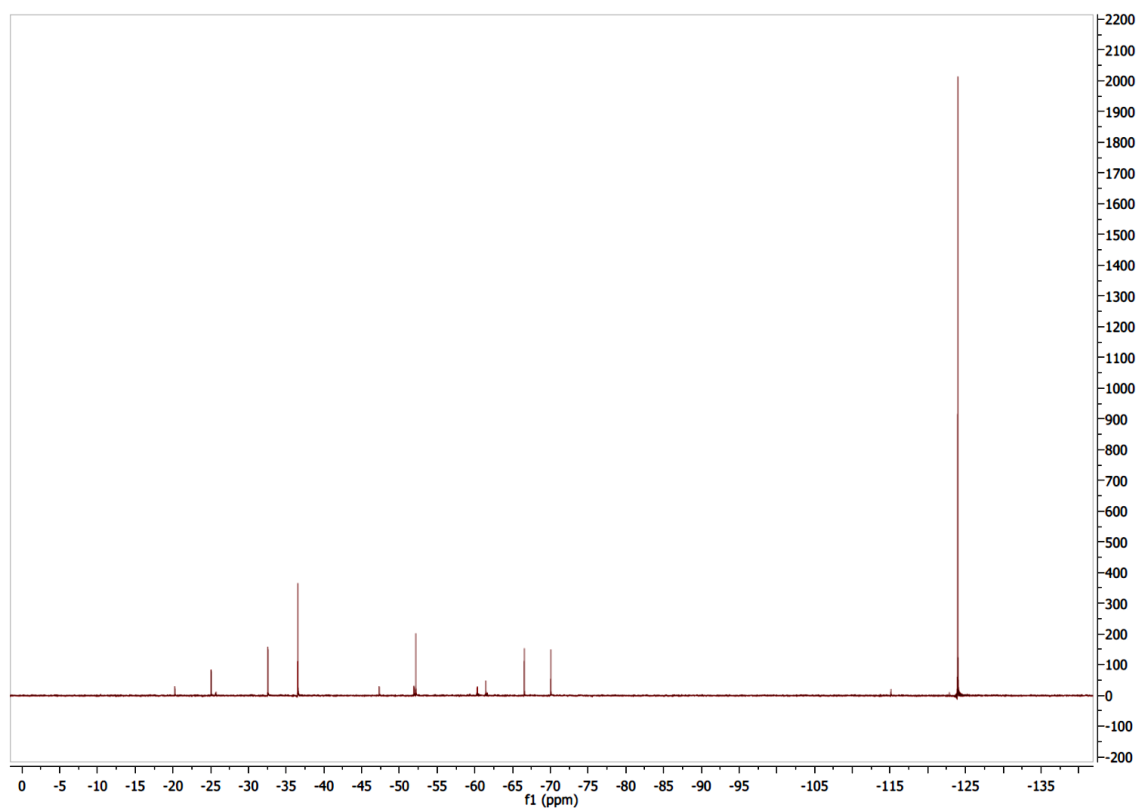
Hydrophosphination of 2-methyl-hex-1-ene to make **4a-4e**.



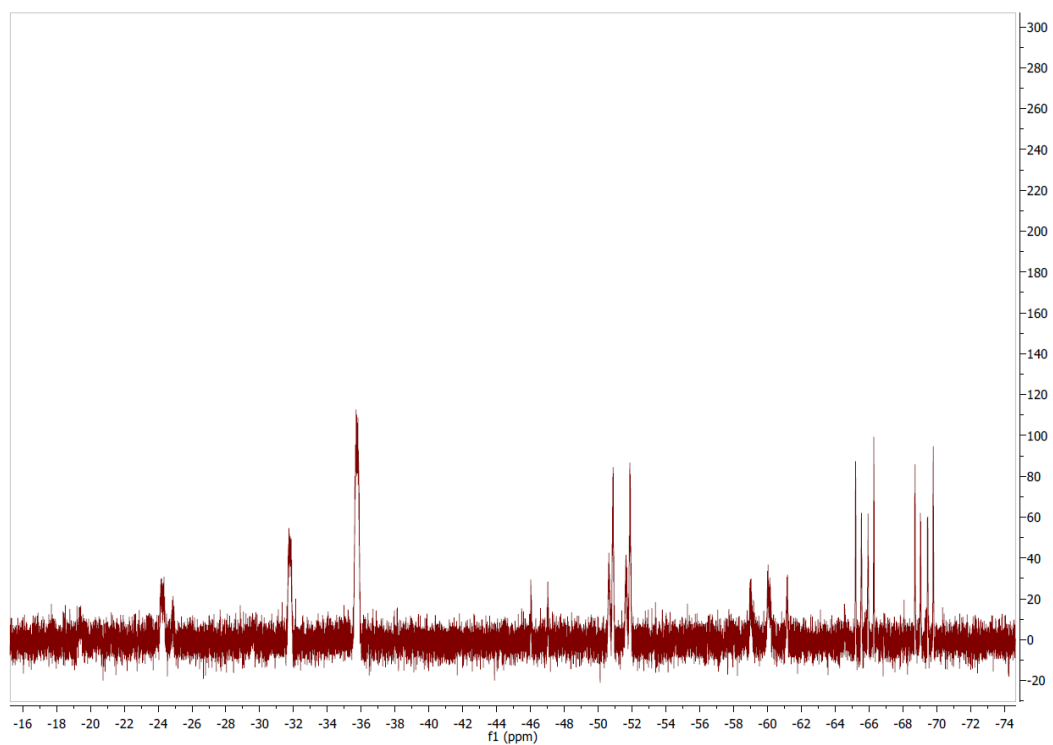
**Figure 6.20:** Representative initial <sup>1</sup>H NMR spectrum of the hydrophosphination of 2-methyl-hex-1-ene



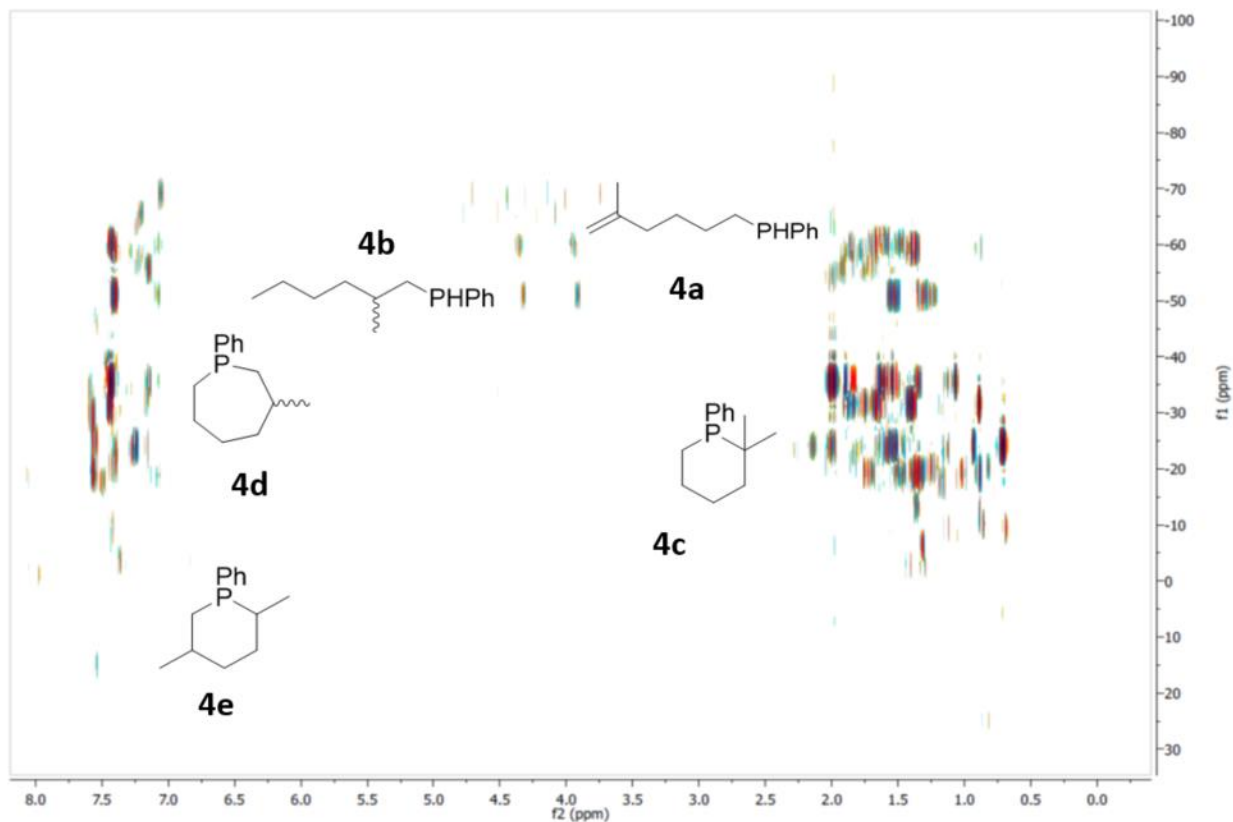
**Figure 6.21:** Representative final  $^1\text{H}$  NMR spectrum of the hydrophosphination of 2-methyl-hex-1-ene



**Figure 6.22:** Representative  $^{31}\text{P}\{^1\text{H}\}$  NMR spectrum of the hydrophosphination of 2-methyl-hex-1-ene

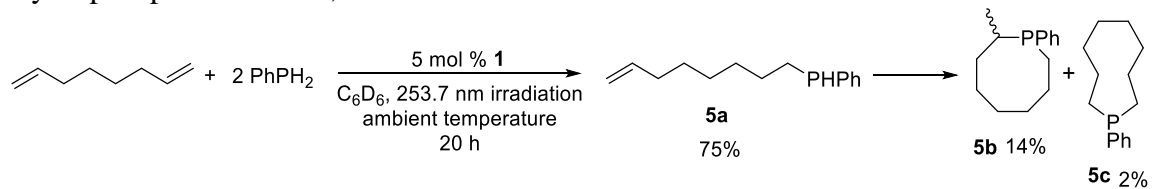


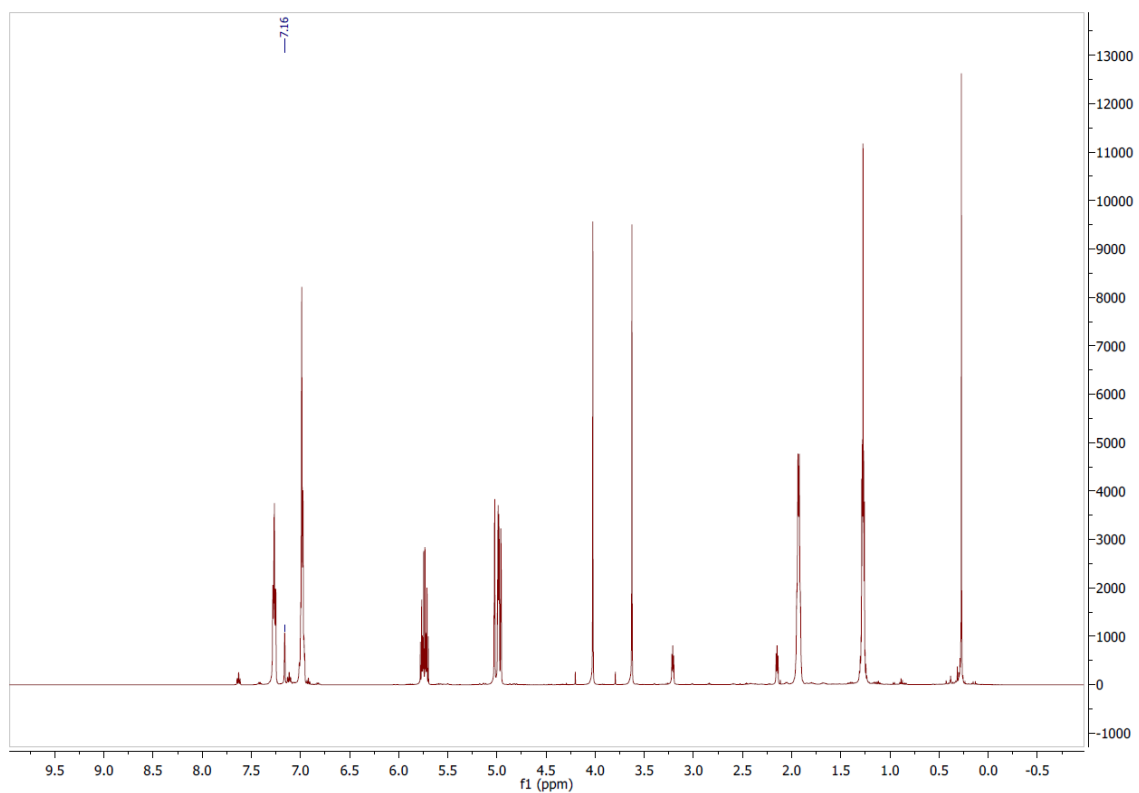
**Figure 6.23:** Representative  $^{31}\text{P}$  NMR spectrum of the hydrophosphination of 2-methylhex-1-ene



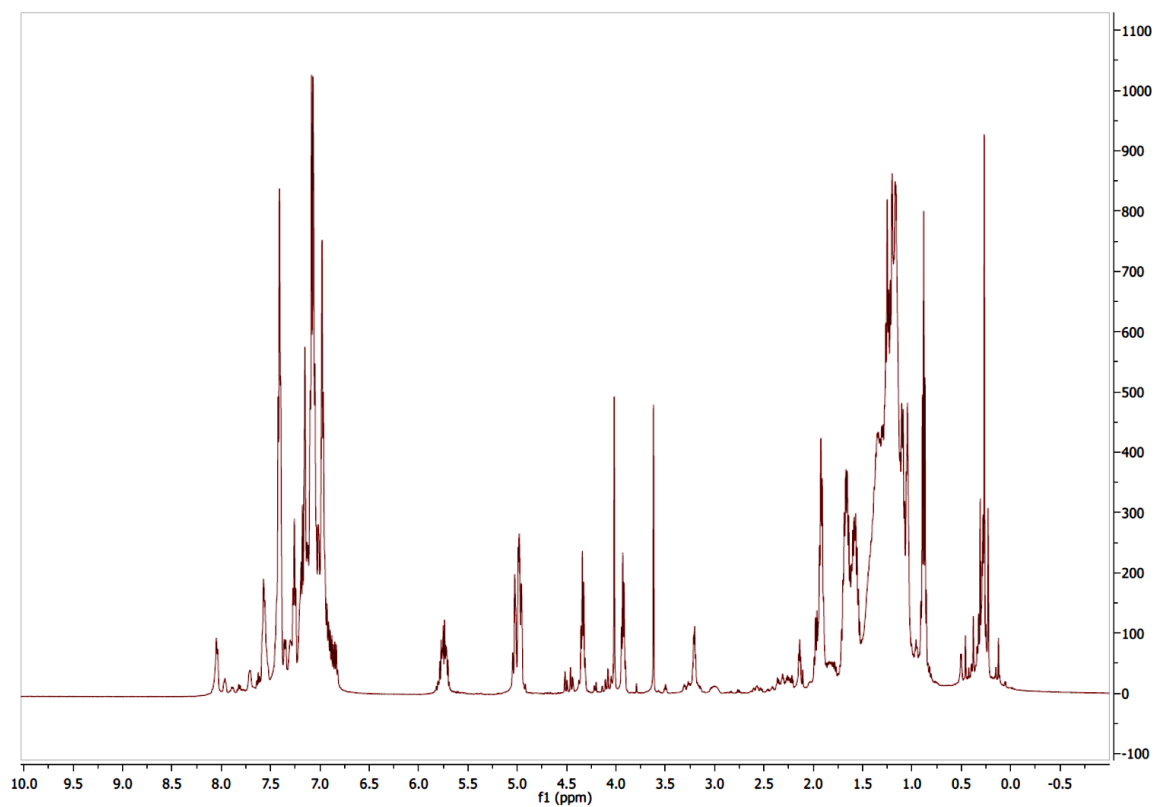
**Figure 6.24:** Representative  $^{31}\text{P}$ - $^1\text{H}$  HMBC NMR spectrum of the hydrophosphination of 2-methyl-hex-1-ene

Hydrophosphination of 1,7-octadiene to make **5a-5c**

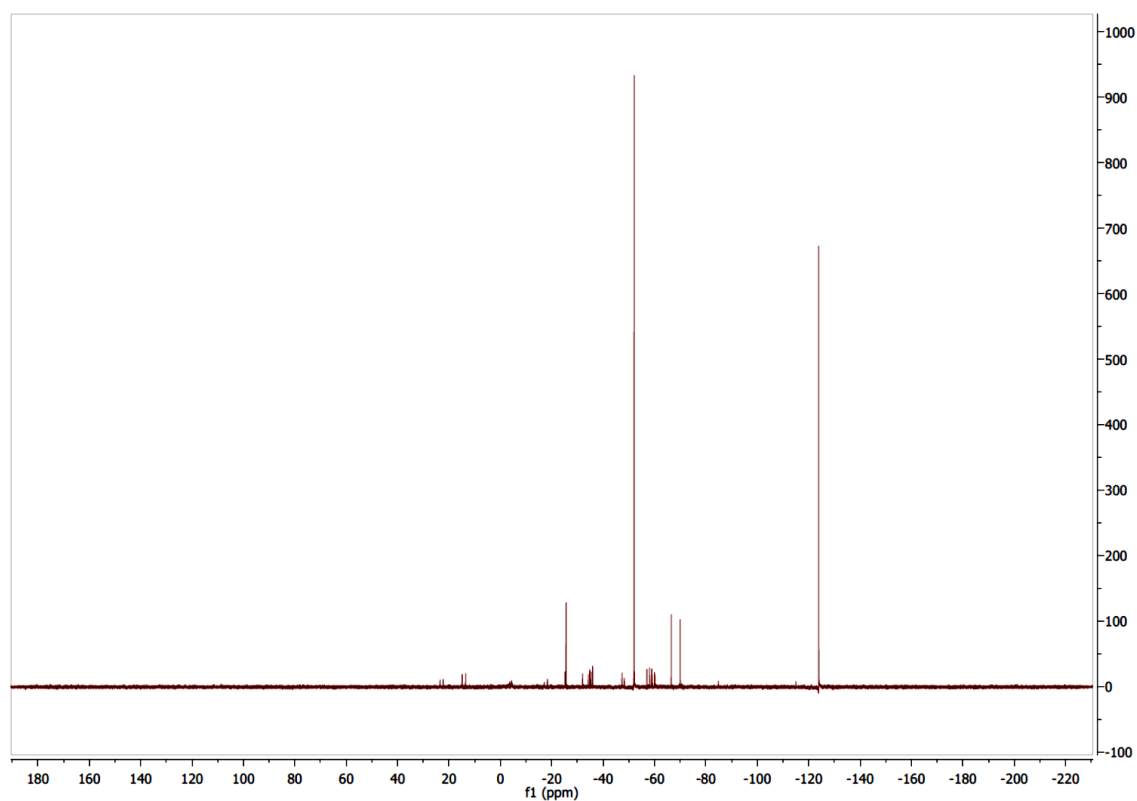




**Figure 6.25:** Representative initial  $^1\text{H}$  NMR spectrum of the hydrophosphination of 1,7-octadiene

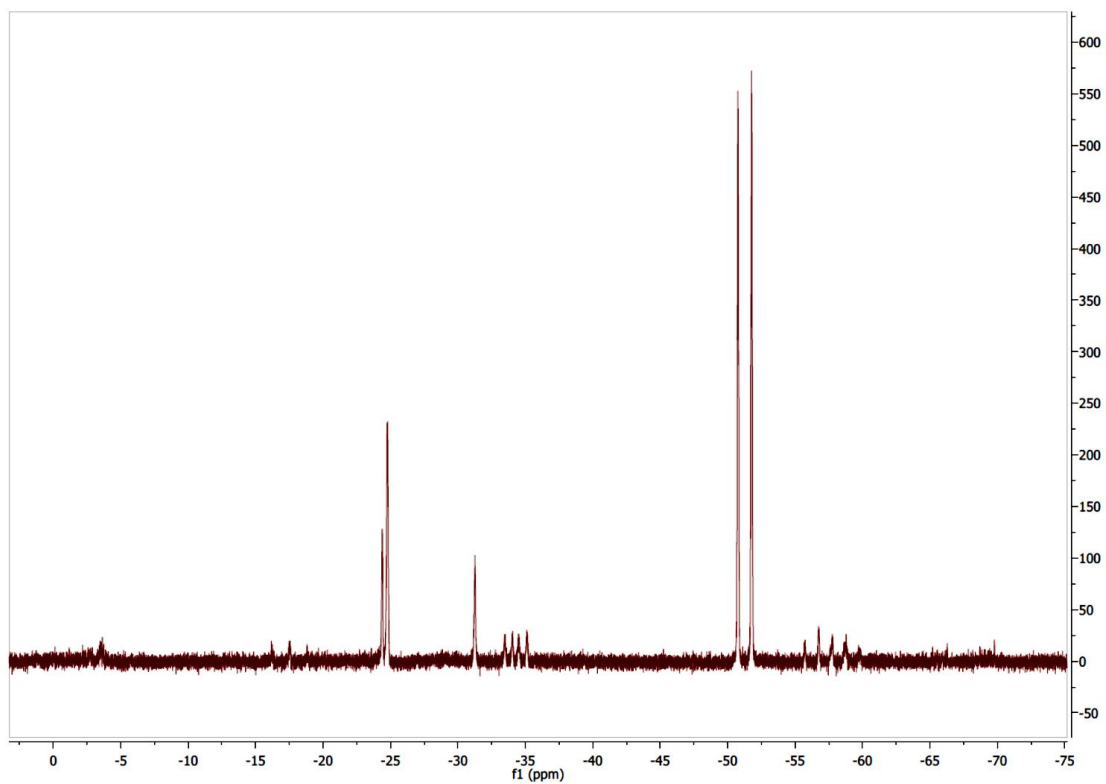


**Figure 6.26:** Representative final  $^1\text{H}$  NMR spectrum of the hydrophosphination of 1,7-octadiene

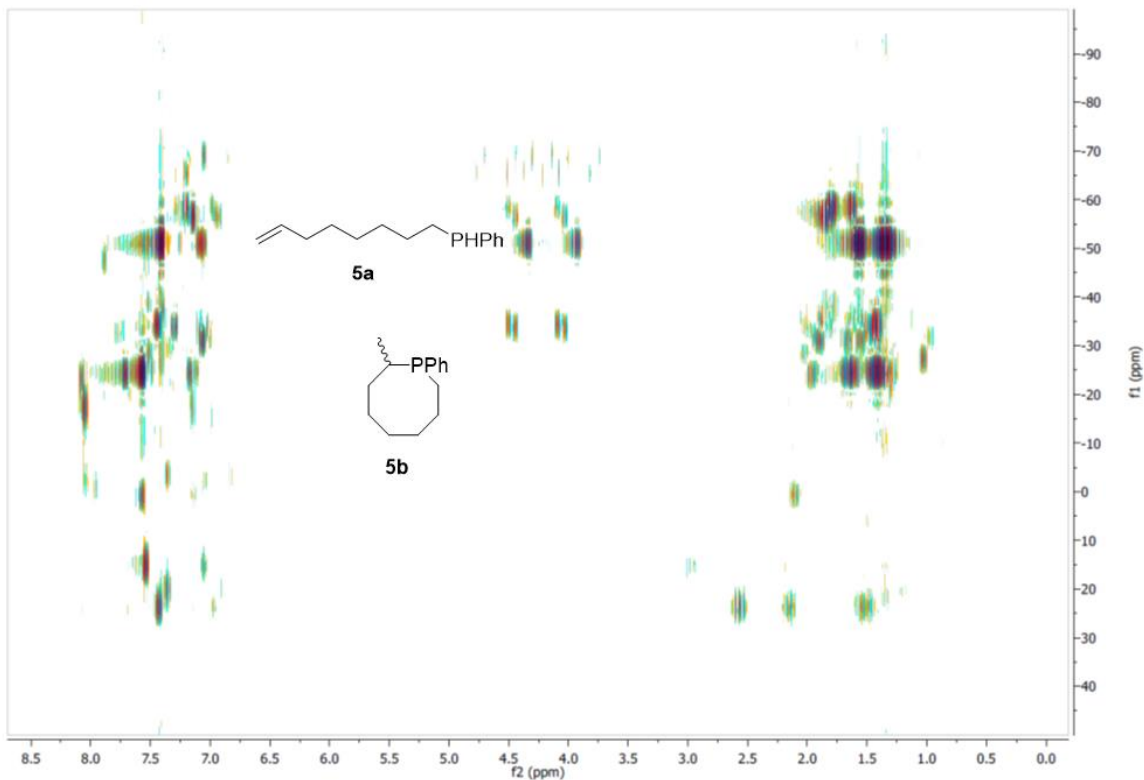


**Figure 6.27:** Representative  $^{31}\text{P}\{^1\text{H}\}$  NMR spectrum of the hydrophosphination of 1,7-octadiene





**Figure 6.28:** Representative  $^{31}\text{P}$  NMR spectrum of the hydrophosphination of 1,7-octadiene



**Figure 6.29:** Representative  $^{31}\text{P}$ - $^1\text{H}$  HMBC NMR spectrum of the hydrophosphination of 1,7-octadiene

## 6.5: References

- (1) Bange, C. A.; Waterman, R. *Chem. Eur. J.* **2016**, *22*, 12598-12605.
- (2) Ghebreab, M. B.; Bange, C. A.; Waterman, R. *J. Am. Chem. Soc.* **2014**, *136*, 9240-9243.
- (3) Douglass, M. R.; Marks, T. J. *J. Am. Chem. Soc.* **2000**, *122*, 1824-1825.
- (4) Douglass, M. R.; Stern, C. L.; Marks, T. J. *J. Am. Chem. Soc.* **2001**, *123*, 10221-10238.
- (5) Kawaoka, A. M.; Douglass, M. R.; Marks, T. J. *Organometallics* **2003**, *22*, 4630-4632.
- (6) Rosenberg, L. *ACS Catal.* **2013**, *3*, 2845-2855.

- (7) Koshti, V.; Gaikwad, S.; Chikkali, S. H. *Coord. Chem. Rev.* **2014**, 265, 52-73.
- (8) Featherman, S. I.; Quin, L. D. *J. Am. Chem. Soc.* **1975**, 97, 4349-4356.
- (9) Quin, L. D., *A Guide to Organophosphorus Chemistry*. John Wiley & Sons: New York, 2000.
- (10) Douglass, M. R.; Ogasawara, M.; Hong, S.; Metz, M. V.; Marks, T. J. *Organometallics* **2002**, 21, 283-292.
- (11) Motta, A.; Fragala, I. L.; Marks, T. J. *Organometallics* **2005**, 24, 4995-5003.
- (12) Zhang, W.; Zhang, X. In *Bisphosphacycles - from DuPhos and BPE to a diverse set of broadly applied ligands*, Wiley-VCH Verlag GmbH & Co. KGaA: 2011; pp 55-91.
- (13) Burk, M. J. *Acc. Chem. Res.* **2000**, 33, 363-372.
- (14) Burk, M. J.; Gross, M. F.; Martinez, J. P. *J. Am. Chem. Soc.* **1995**, 117, 9375-9376.
- (15) Burk, M. J.; Harper, T. G. P.; Kalberg, C. S. *J. Am. Chem. Soc.* **1995**, 117, 4423-4424.
- (16) Joseph, J.; RajanBabu, T. V.; Jemmis, E. D. *Organometallics* **2009**, 28, 3552-3566.
- (17) Boar, P.; Streitberger, M.; Lönnecke, P.; Hey-Hawkins, E. *Inorg. Chem.* **2017**, 56, 7285-7291.
- (18) Espinal-Viguri, M.; King, A. K.; Lowe, J. P.; Mahon, M. F.; Webster, R. L. *ACS Catal.* **2016**, 6, 7892-7897.
- (19) Claridge, T. D. w., *High-Resolution NMR Techniques in Organic Chemistry*. Elsevier: 2009; Vol. 27.

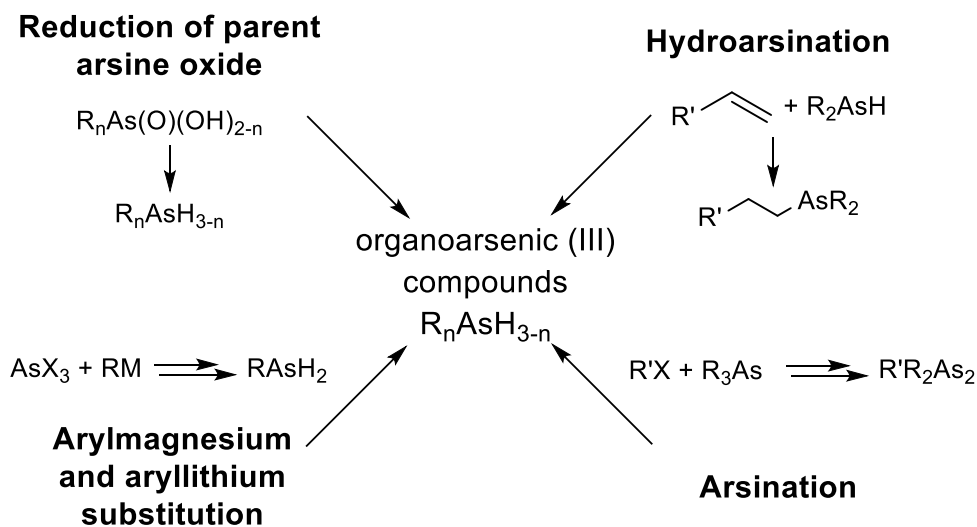
- (20) Bange, C.; Mucha, N.; Cousins, M.; Gehsmann, A.; Singer, A.; Truax, T.; Higham, L.; Waterman, R. *Inorganics* **2016**, *4*, 26.
- (21) Bange, C. A.; Ghebreab, M. B.; Ficks, A.; Mucha, N. T.; Higham, L.; Waterman, R. *Dalton Trans.* **2016**, *45*, 1863-1867.
- (22) Roering, A. J.; Leshinski, S. E.; Chan, S. M.; Shalumova, T.; MacMillan, S. N.; Tanski, J. M.; Waterman, R. *Organometallics* **2010**, *29*, 2557-2565.
- (23) Waterman, R. *Organometallics* **2007**, *26*, 2492-2494.
- (24) Fluck, E.; Issleib, K. *Chem. Ber.* **1965**, *98*, 2674-2680.
- (25) Davies, J. H.; Downer, J. D.; Kirby, P. *J. Chem. Soc. C* **1966**, 245-247.
- (26) Baber, R. A.; Haddow, M. F.; Middleton, A. J.; Orpen, A. G.; Pringle, P. G.; Haynes, A.; Williams, G. L.; Papp, R. *Organometallics* **2007**, *26*, 713-725.

## CHAPTER 7: ZIRCONIUM-CATALYZED HYDROARSINATION WITH PRIMARY ARSINES

### 7.1: Introduction

Organoarsine compounds have found applications in a vast number of transformations, including chemistry,<sup>1-5</sup> materials science,<sup>6</sup> and anti-cancer agents.<sup>7</sup> Arsenic chemistry is far from developed,<sup>1</sup> but a notable achievement is arsenic-based ligands. Some triarylarsine ligands have outperformed phosphorus analogues.<sup>7-10</sup>

The handful of methods used to prepare organoarsine compounds are mostly limited to classical nucleophilic substitution methods (Scheme 7.1). In general, substitution methods to generate organoarsenic compounds are compatible only with select functional groups and require protection of the reactive arsenic center.



**Scheme 7.1:** Synthetic methods to form organoarsine compounds

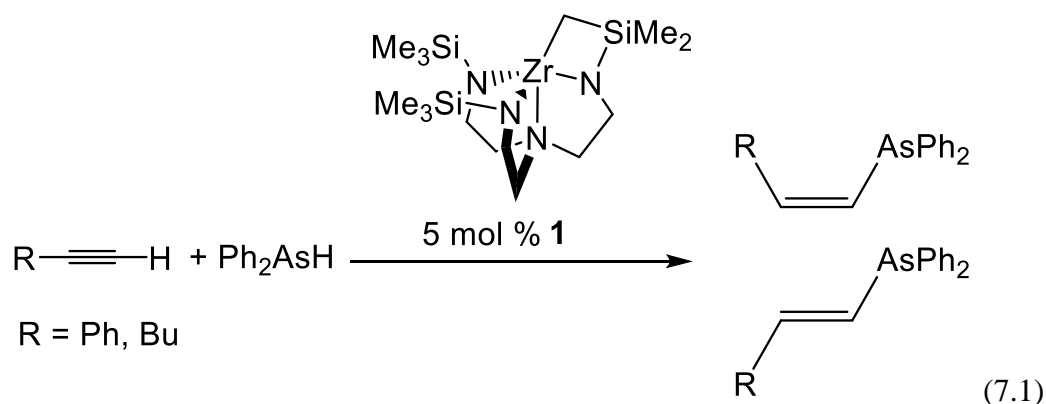
An attractive route to organoarsines is the direct reduction of the parent arsenic compound (Scheme 7.1, top left). This method requires that the pendant group in the starting material be the same as the desired product, which severely limits this method to

the handful of arsenic compounds that are commercially available. Furthermore, the only reported reductant to generate primary arsines from arsine oxides is zinc amalgam, which greatly increases the difficulty and toxicity of the transformation. Methods to generate secondary arsines from reduction of secondary arsine oxides are milder, but are also limited in scope. Broadening the class of available substrates, arsines, and conditions for synthesis of organoarsines is of ongoing interest.

Development of catalytic routes to novel arsines has lagged behind those of stoichiometric methods. While catalytic arsination has garnered some interest and development, the catalytic hydroarsination, the addition of As–H bonds across unsaturated fragments, has not seen much action.<sup>2-3, 5, 11-17</sup> All transformations functionalize either secondary arsines, or in one case an arsenylborane.<sup>13</sup>

Arsenic has a well-deserved historical reputation for its toxicity, particularly arsine oxides and compounds with As–Cl bonds.<sup>1</sup> Development of arsenic chemistry that circumvents usage of As–Cl compounds would be of significant interest. Organoarsines are significantly less toxic than arsine oxides.<sup>18</sup> Catalytic hydroarsination would provide direct accesses to these molecules, broaden the substrate scope to arsenic compounds that are not commercially available, and increase the atom-economy of the transformation.

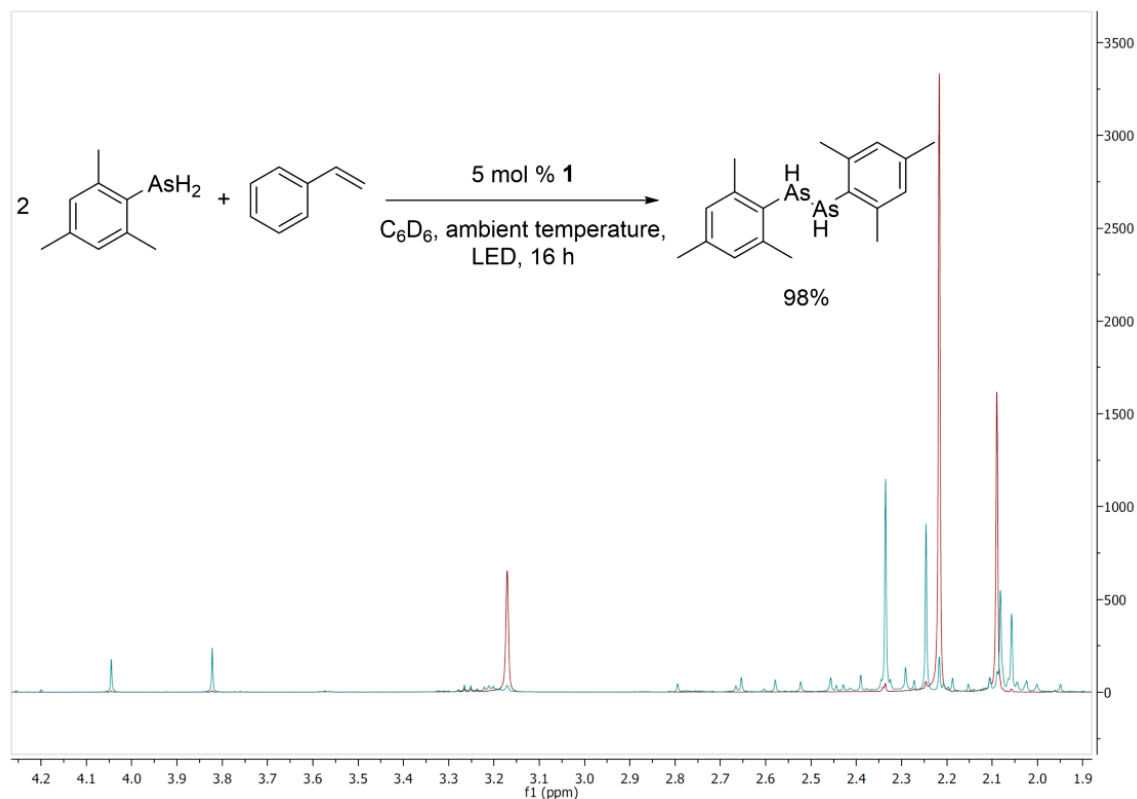
Previous work in the Waterman group on catalytic hydroarsination with [ $\kappa^5$  – *N,N,N,N,C*–(Me<sub>3</sub>SiNCH<sub>2</sub>CH<sub>2</sub>)<sub>2</sub>NCH<sub>2</sub>CH<sub>2</sub>–NSiMe<sub>2</sub>CH<sub>2</sub>]Zr (**1**) has targeted bond-forming reactions of terminal alkynes and secondary arsines to provide tertiary arsines (eqn 7.1).<sup>14</sup>



Given the advancement of **1** in hydrophosphination and its newfound photoexcitation behavior, further consideration of catalytic hydroarsination under photolysis is warranted. Hydroarsination of primary arsines to selectively generate *secondary* arsines would be of interest. Thus far catalytic hydroarsination has been able to make only tertiary products. Secondary arsines formed from primary arsine hydroarsination could be further functionalized, which gives them an added value over tertiary arsines.

## 7.2: Results and discussion

Previous work with **1** and  $\text{MesAsH}_2$  ( $\text{Mes}$  = mesityl = 2,4,6-trimethylphenyl) demonstrated the ease of isocyanide insertion into the zirconium–arsenido bond.<sup>14</sup> However, catalytic hydroarsination with **1** was never explored. Initial attempts of catalytic hydroarsination with  $\text{MesAsH}_2$  failed to provide hydroarsination products and instead dehydrocoupled the arsine (Figure 7.1).



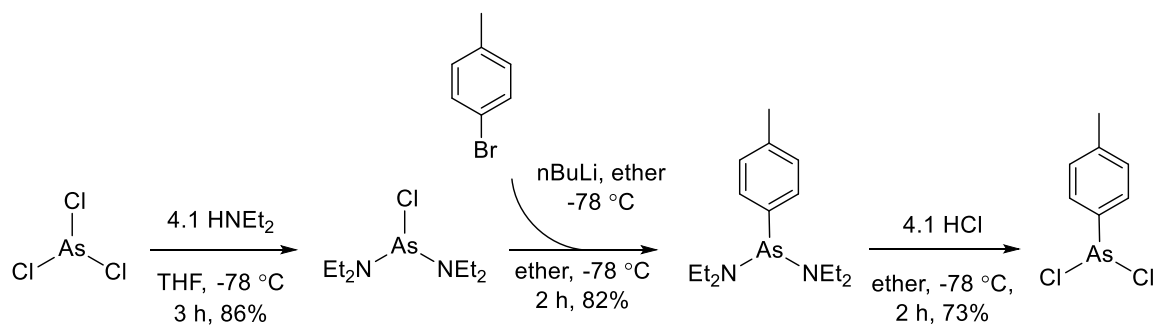
**Figure 7.1:** Attempted hydroarsination with **1** and MesAsH<sub>2</sub>. Red: Initial <sup>1</sup>H NMR spectrum. Teal: Final <sup>1</sup>H NMR spectrum showing (MesAsH)<sub>2</sub>

Products belonging to the hydroarsination product PhCH<sub>2</sub>CH<sub>2</sub>AsHMe<sub>3</sub> were not detected and styrene was preserved. Attempted hydroarsination reactions with MesAsH<sub>2</sub> ran in the dark showed limited product conversion, as anticipated from photochemistry with **1**. However, the preference of MesAsH<sub>2</sub> for catalytic dehydrocoupling over hydroarsination with **1** came as a surprise. The ability of phenylisocyanide to insert into the Zr–As bond showed that insertion, the prerequisite for C–As bond formation, is possible.<sup>14</sup> The apparent preference for dehydrocoupling over hydroarsination remained intriguing because it deviated significantly from catalytic hydrophosphination with **1**.

Regardless, a separate arsine was sought for hydroarsination. *p*-Tolylarsine was chosen for its NMR handle and postulated ease of synthesis. The precursor *p*-



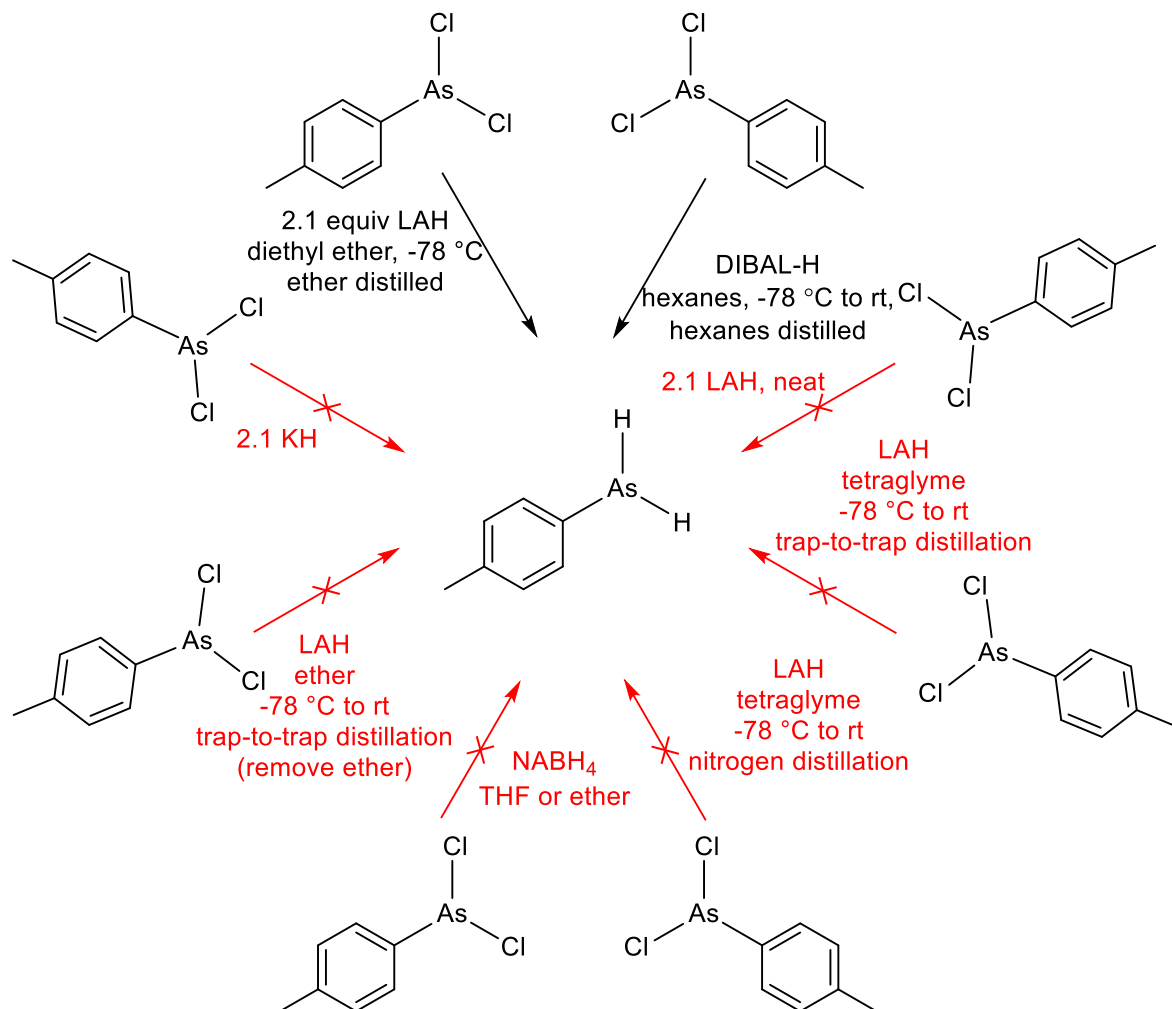
*p*-tolylchloroarsine was synthesized through modifications of known literature procedures.<sup>14, 22</sup>



**Scheme 7.2:** Synthesis of precursor *p*-tolylAsCl<sub>2</sub>

Protection of the arsenic species with Et<sub>2</sub>NH is required to prevent multiple additions of the nucleophilic aryl group to the electropositive arsenic center, which would result in formation of secondary and tertiary arsine products. Halogenation of the intermediate *p*-tolylbis(diethylamido)arsine with HCl in ether resulted in formation of the desired precursor *p*-tolylchloroarsine as colorless crystals.

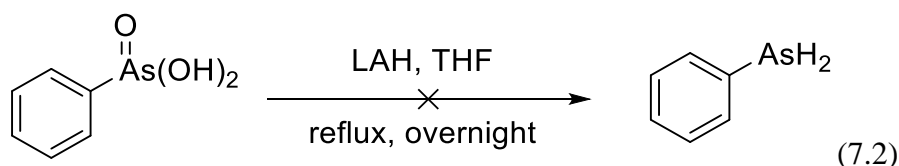
Reduction of *p*-tolylchloroarsine to the desired *p*-tolylarsine proved more difficult than anticipated (Scheme 7.3).



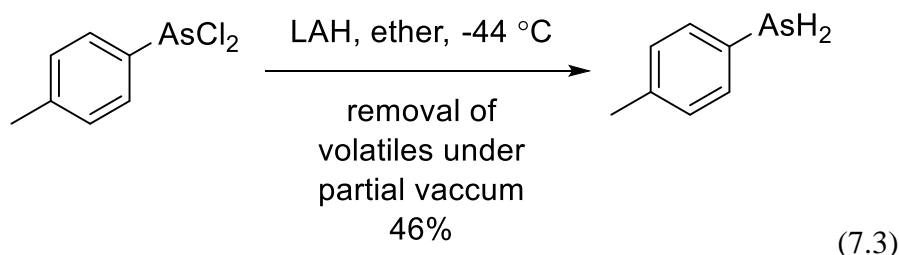
**Scheme 7.3:** Attempts at reduction of *p*-tolylchloroarsine

The high volatility of the product arsine made isolation more challenging than anticipated (Scheme 7.3). Removal of volatile solvents such as ether also concomitantly removed the product. Attempts to isolate *p*-tolylarsine by use of a nonvolatile solvent (i.e., tetraglyme) did not provide the product in satisfactory yields. It is unclear if that is due to incomplete reduction or improper isolation. Reactions run neat overreduced to provide  $\text{AsH}_3$ , as noted by formation of a red gas. Relatively mild reducing agents (e.g.,  $\text{NaBH}_4$  or  $\text{KH}$ ) did not reduce *p*-tolylchloroarsine.

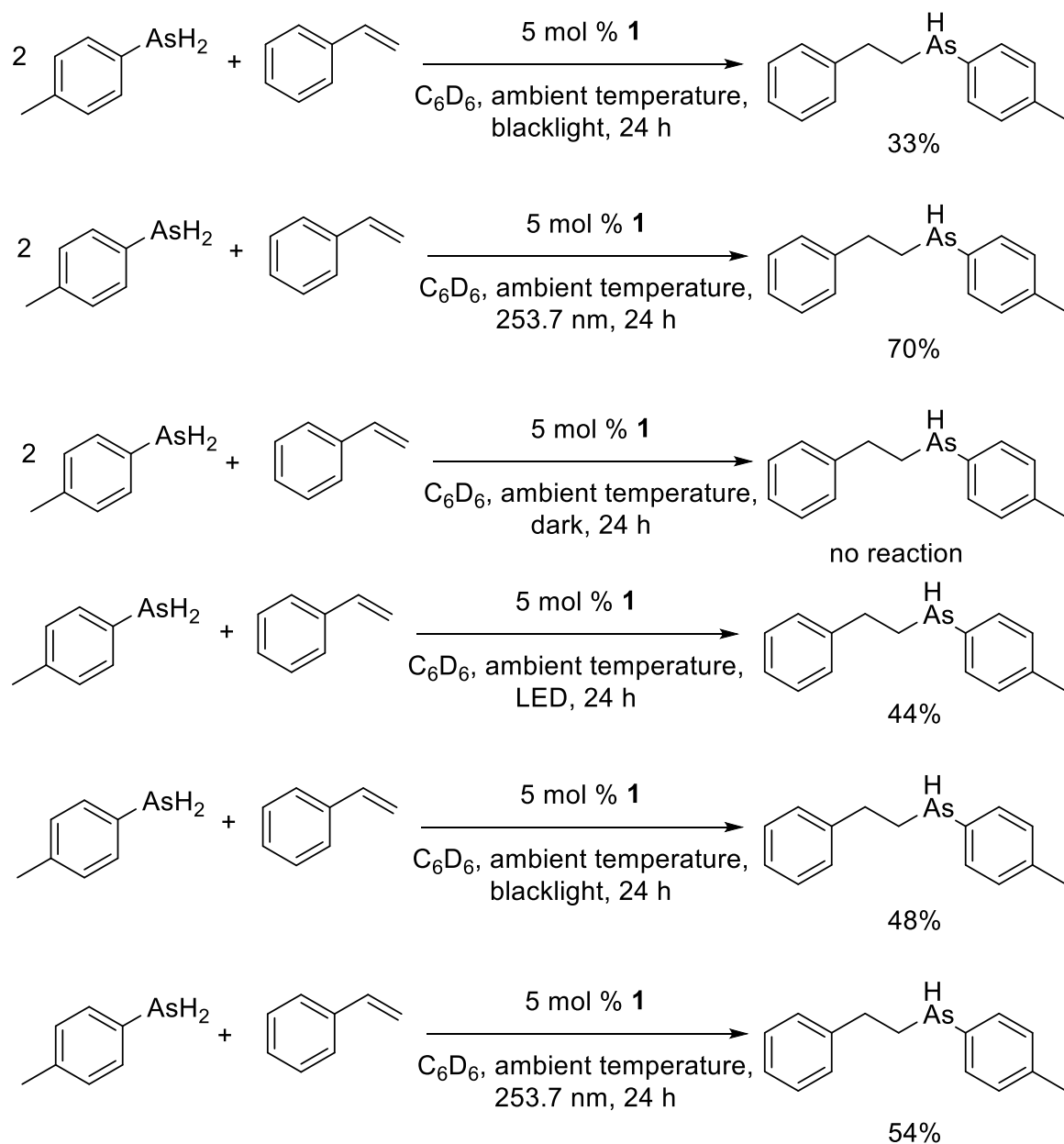
Isolation of a primary arsine from reduction of an arsine oxide may prove more facile and straightforward. However, reduction of phenylarsonic acid by LAH was unsuccessful and only returned unreacted phenylarsonic acid (eqn 7.2). Attempts to reduce this by zinc amalgam were unsuccessful.



Only two reduction methods provided the desired primary arsine (Scheme 7.3). Reduction of *p*-tolylldichloroarsine with DIBAL-H (DIBAL-H = diisobutyl aluminum hydride) in hexanes was successful. Removal of the hexanes by distillation under nitrogen was required so that the product *p*-tolylarsine would also not be removed. However, the more practical approach was reduction of *p*-tolylldichloroarsine with LAH in ether, followed by removal of the ether under a partial vacuum. This returned the product arsine in poor isolated yields presumably due to the high volatility of the product arsine (eqn 7.3).



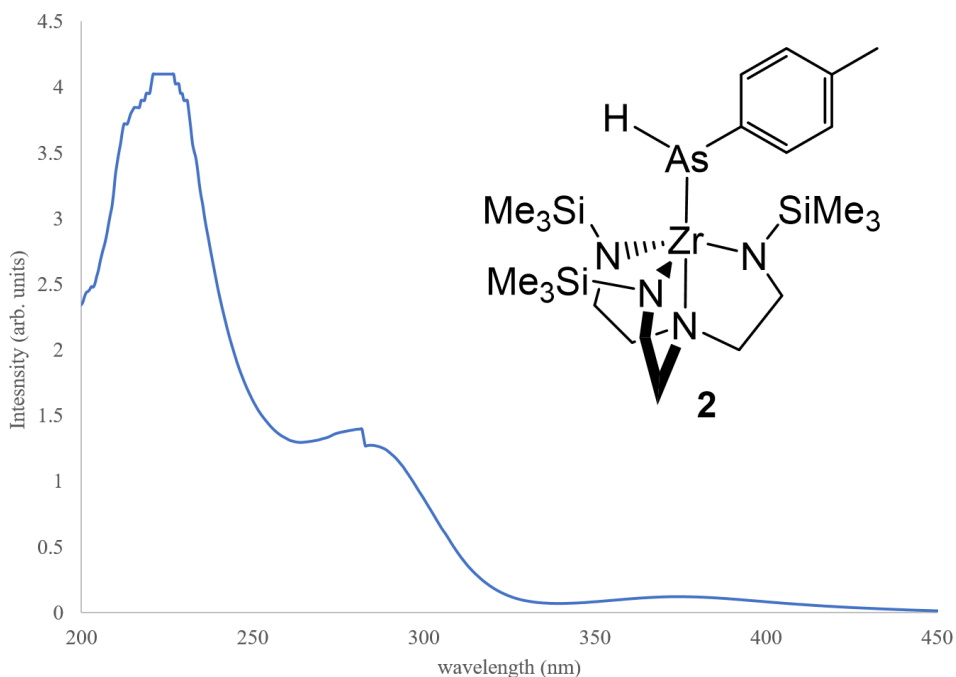
Regardless, the yield was high enough to move forward for initial catalytic hydroarsination work with **1**. As anticipated from catalytic hydrophosphination with **1**, irradiation promotes catalytic hydroarsination (Scheme 7.4).



**Scheme 7.4:** Initial hydroarsination work with styrene

Use of two equivalents of *p*-tolylarsine to prohibit formation of tertiary arsines was unnecessary because only secondary arsine products were detected (Scheme 7.1, entries 1-3). Use of only one equivalent of *p*-tolylarsine provided the products in lower, albeit satisfactory, conversions (Scheme 7.1, entries 4-6). As anticipated, reactions run in the dark

failed to provide any catalytic turnover. Reactions run under irradiation from the 253.7 nm mercury arc lamp provided the highest conversions when using two equivalents of arsine. However, use of only one equivalent of arsine provided comparable conversions for all lamps, unlike catalytic hydrophosphination with **1**. The UV-vis absorbance spectrum of the arsenido derivative of **1**, (N<sub>3</sub>N)Zr–AsH(*p*-tolyl) (**2**) in hexanes included a band at 375 nm (Figure 7.2). This band is assigned to the As *n* → Zr *d* charge transfer, as noted for phosphido derivatives of **1**.

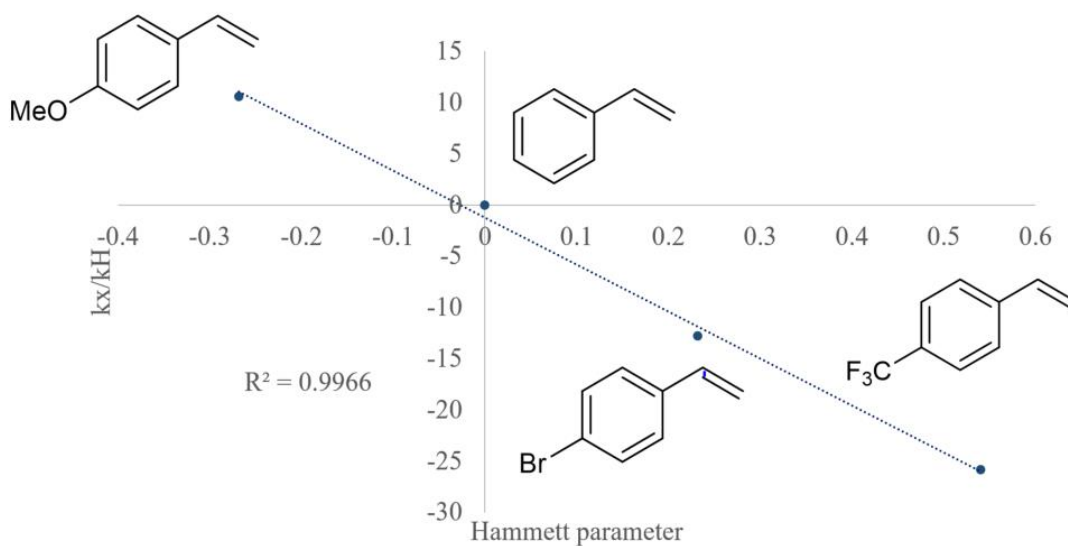


**Figure 7.2:** UV-vis absorbance spectrum of **2** in hexanes

Unlike catalytic hydrophosphination with phosphido derivatives of **1**, hydroarsination with **1** and **2** is not as light-dependent. The extinction coefficient for **2** is calculated to be 367 (9) M<sup>-1</sup> cm<sup>-1</sup> at 375 nm in hexanes, which makes it comparable to that

of the phosphide derivatives ( $290 (6) \text{ M}^{-1} \text{ cm}^{-1}$  at 364.5 nm for  $(\text{N}_3\text{N})\text{Zr-PHPh}$  in hexanes). However, the higher value for the extinction coefficient for **2** indicates that the absorbance of the proposed As  $n \rightarrow \text{Zr } d$  band absorbs more photons. This is *inconsistent* with the observation that catalysis is both less light-dependent and more sluggish than photocatalytic hydrophosphination with **1**.

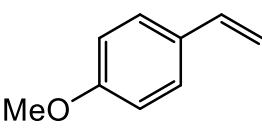
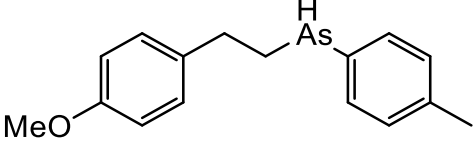
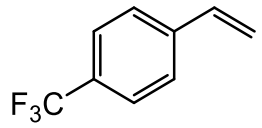
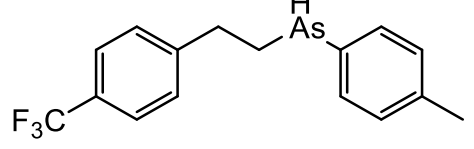
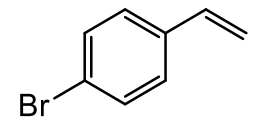
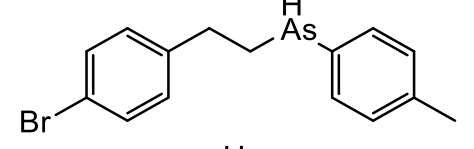
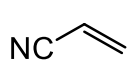
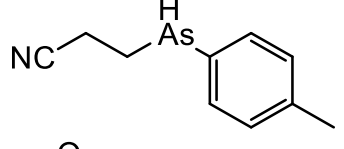
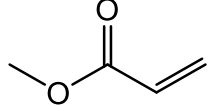
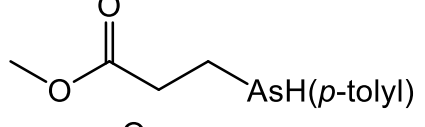
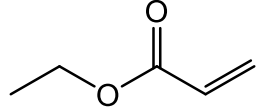
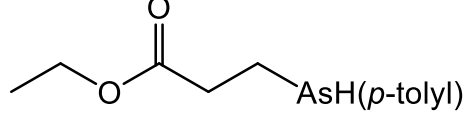
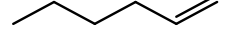
Consideration of similarities between catalytic hydrophosphination and hydroarsination with **1** may be useful. Competition experiments between styrene derivatives showed preference for styrenes bearing electron-donating groups, indicating that like hydrophosphination, hydroarsination occurs via insertion (Figure 7. 3).



**Figure 7.3:** Hammett competition experiment for hydroarsination

With this knowledge in hand, a variety of styrene derivatives were considered for catalytic hydroarsination with **1**. Hydroarsination of styrene derivatives shows comparable conversions for all styrene substrates (Table 7.1).

**Table 7.1:** Catalytic hydroarsination with **1**. Conditions: Twenty equiv. of *p*-tolylarsine, twenty equiv. of substrate, one equiv. of **1**, blacklight irradiation, ambient temperature. Percent conversions are measured by <sup>1</sup>H NMR spectroscopy.

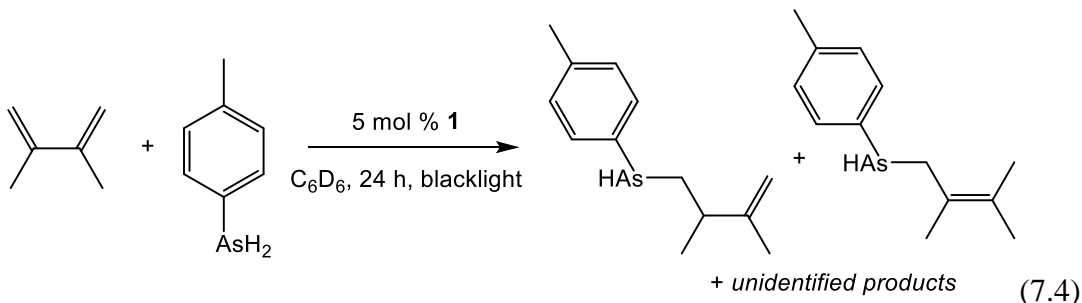
Entry	Product	% Conversion
		50% (24 h) 62% (48 h)
		44% (24 h) 51% (48 h)
		46% (24 h) 58% (48 h)
		100% (1 h)
		100 % (1 h)
		100% (1 h)
	—	No conversion

The NMR conversions for the hydroarsination reactions of styrene derivatives are poor, but consistent among all styrenes tested (Table 7.1). Extended reaction times did little to improve the catalytic conversions. Heating the reactions under irradiation did not substantially impact catalysis, as expected from alkene hydrophosphination reactivity.

Unlike hydrophosphination, catalysis with styrene derivatives is sluggish. All NMR-scale reactions were run at comparable concentrations of substrate, pnictine, and **1**, although hydrophosphination outperforms hydroarsination in all cases. Additionally, it appears that hydroarsination is significantly more limited by substrate identity. For

example, catalytic hydroarsination of 1-hexene failed to provide detectable levels of products after 48 hours, whereas catalytic hydrophosphination of 1-hexene with **1** and  $\text{PhPH}_2$  provides 50% conversion to the product after 24 hours.

In addition to the decreased light dependence, there is emerging evidence that catalytic hydroarsination with **1** is not entirely analogous to catalytic hydrophosphination. For example, the increased catalytic activity of Michael acceptors over more styrene derivatives is different than that observed for catalytic hydrophosphination. In those studies styrenes outperformed Michael acceptors, which is consistent with an insertion-based mechanism. Furthermore, catalytic hydroarsination of 2,3-dimethyl-1,3-butadiene does not return the anticipated [1,4]-addition product as observed for catalytic hydrophosphination (eqn 7.4). Instead, catalytic hydroarsination with this substrate returns a mixture of products, including the [1,2]-addition, [1,4]-addition, and other unidentified side products.



It is possible that the arsenide of **2** is acting as a nucleophile for certain substrates. Although the Hammett experiments identified an insertion-based mechanism, it is important to underscore that the insertion-based chemistry is only observed with styrene derivatives. Deviations from this mechanism, as noted for 2,3-dimethyl-1,3-butadiene and acrylonitrile, do not indicate that insertion precedes over nucleophilic attack.



Because reactions performed in the dark do not provide catalytic turnover, it is clear that light is necessary for catalysis. Hydroarsination may be operative through a triplet excited state rather than a singlet excited state reached by photoexcitation. This may introduce a radical species that is not present in hydrophosphination with **1**. Although the product selectivity for the *anti*-Markovnikov arsine is high for styrene derivatives, the poor selectivity in the hydroarsination of 2,3-dimethyl-1,3-butadiene suggests that a radical may be involved. It is possible that a long-lived excited state may be responsible for sluggish catalysis, because relaxation to the ground state may be slower for arsenido derivatives than phosphido derivatives. This would be consistent with the observed sluggish catalytic hydroarsination and poor product selectivity. Fluorescence lifetime experiments may be needed to detect a triplet excited state in catalysis.

Computational studies on the realted (N<sub>3</sub>N)Zr-PHPPh revealed that the donor orbitals were mainly phosphorus-based, while the acceptor orbitals were primarily zirconium-based. Photoexcitation of this molecule appeared to weaken the Zr-P bond, resulting in more facile insertion, and thus faster catalysis. However, one thought may be that the acceptor orbitals may have more arsenic character in **2**. This would result in a more covalent-type bond during photoexcitation, which would not promote substrate insertion to the same extent. This hypothesis is consistent with the observed light-dependence and the relatively sluggish catalysis. The possibility that the excited state has more arsenic character would also explain the apparent nucleophilic attack for Michael acceptors. Further computational studies would identify the nature of this transition.

It is worth stating that the *p*-tolylarsine used in catalysis is only 97% pure. However, it is important to underscore that purity alone is not responsible for the limited catalysis. For example, the MesAsH<sub>2</sub> used for catalysis was of high purity, but catalytic hydroarsination failed even under irradiation and/or heating. Additionally, compound **2** was observed spectroscopically in all catalytic hydroarsination NMR samples, as well as in its isolated form. Impurities do not account for the limited product selectivity for 2,3-dimethyl-1,3-butadiene or the speculated mechanistic inconsistencies. The origin of the underachieving catalytic activity may be identified by fluorescence lifetimes targeting identification of a triplet excited state, computational studies targeting percent contributions of the acceptor orbitals, or by system optimization, rather than tedious improvement of the purity of *p*-tolylarsine.

Regardless, this work represents the first example of a catalytic hydroarsination of a primary arsine. All products are formed exclusively as the secondary arsines. Although the initial demonstration of this work provided limited catalytic turnover, there is still room for improvement. For example, harnessing the potential nucleophilicity of the arsenide could offer access to secondary arsines from a broader family of Michael acceptors. These substrates were the best in preliminary catalytic hydroarsination work with **1**, and their reactivity merits further study.

### 7.3: Conclusions

While the origin of the reactivity difference is not clear, it is important to restate that many systems observe reactivity differences between hydrophosphination and hydroarsination.<sup>13, 16, 23</sup> Identification of the reaction mechanism may explain the

inconsistent results between catalytic hydrophosphination and hydroarsination. This may identify the internal inconsistencies in the preliminary studies on catalytic hydroarsination. For example, there is conflicting evidence that catalytic hydroarsination with **1** operates by an insertion-based mechanism and that it operates by a nucleophilic attack of the arsenide. Further study is warranted to elucidate the origin of this reactivity and to optimize the system.

## 7.4 Experimental methods

### 7.4.1 General methods

All air-sensitive manipulations were performed under a positive pressure of nitrogen using standard Schlenk line or in a M. Braun glove box. Dry, oxygen-free solvents were employed throughout. Benzene- $d_6$  was purchased then degassed and dried over NaK alloy and distilled under reduced pressure. NMR spectra were recorded with a Bruker AXR 500 MHz spectrometer in benzene- $d_6$  and are reported with reference to residual solvent signals ( $C_6D_6$ ,  $\delta$  7.16 and 128.0). Compound [ $\kappa^5$ - $N,N,N,N,C$ -( $Me_3SiNCH_2CH_2$ ) $_2NCH_2CH_2NSiMe_2CH_2$ ]Zr (**1**) was prepared according to the literature procedure.<sup>24</sup> *p*-Tolyldichloroarsine was prepared by modified literature procedures.<sup>14, 22</sup> All other chemicals were obtained from commercial suppliers and dried by appropriate means.

### 7.4.2 General procedure for catalytic hydroarsination with **1**

A borosilicate NMR tube was charged with 0.05 mmol *p*-tolylarsine and 0.05 mmol alkene or diene in the presence of 5 mol % of **1** in benzene- $d_6$  solvent. The mixture solutions were irradiated under light. The consumption of substrate to product was monitored by  $^1H$  NMR spectroscopy.

### 7.4.3 Procedure for Hammett plot generation

An NMR tube was charged with equimolar amounts of the heterosubstituted styrene derivative and styrene in benzene- $d_6$  (Table 7.2) To this NMR tube was added 0.80 equiv of *p*-tolylarsine and 0.10 equivalents of **1**. An initial  $^1H$  NMR spectrum was recorded. The reaction was irradiated at 360 nm and monitored after fifteen minutes by  $^1H$  NMR spectroscopy.

**Table 7.2:** Initial concentrations of reactants in hydroarsination competition experiments

Substituted styrene	[substituted styrene]	[styrene]	[ <i>p</i> -tolylarsine]	[ <b>1</b> ]
<i>p</i> -bromostyrene	0.0808 M	0.0814 M	0.066 M	0.0086 M
<i>p</i> -trifluoromethyl styrene	0.0780 M	0.0780 M	0.0610 M	0.0089 M
<i>p</i> -methoxystyrene	0.0813 M	0.0807 M	0.0670 M	0.0084 M

**Table 7.3:** <sup>1</sup>H integration ratios of styrene and styrene derivatives in hydroarsination competition experiments

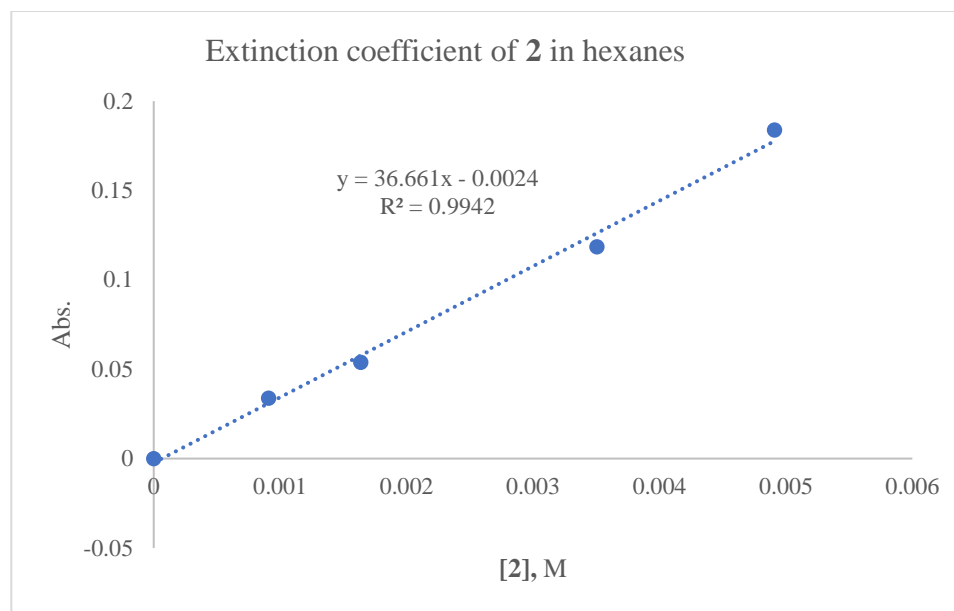
Styrene derivative	σ-parameter	Rel. int. styrene, initial	Rel. int. derivative, initial	Rel. int. styrene, final	Rel. int. derivative, final
<i>p</i> -bromostyrene	0.232	5.00	5.17	5.01	5.04
<i>p</i> -CF <sub>3</sub> styrene	0.54	5.00	3.78	5.01	3.59
<i>p</i> -methoxystyrene	-0.268	5.00	3.73	5.01	3.81

Comparison of the rate of consumption of the substituted styrene derivative versus styrene in a binary competition reaction by eqn 7.5 produces the linear free-energy relationship shown in Figure 7.3.

$$\frac{k_x}{k_H} = \frac{\ln(\frac{s_x}{s_{x,0}})}{\ln(\frac{s_H}{s_{H,0}})} \quad (7.5)$$

#### 7.4.4 Determination of extinction coefficient

The extinction coefficient for **2** in hexanes was measured at different concentrations of **2** in hexanes using a 1.0 mm cuvette and found to be 367 (9) M<sup>-1</sup> cm<sup>-1</sup> at 375.0 nm (Figure 7.4).



**Figure 7.4:** Calculation of extinction coefficient for 2

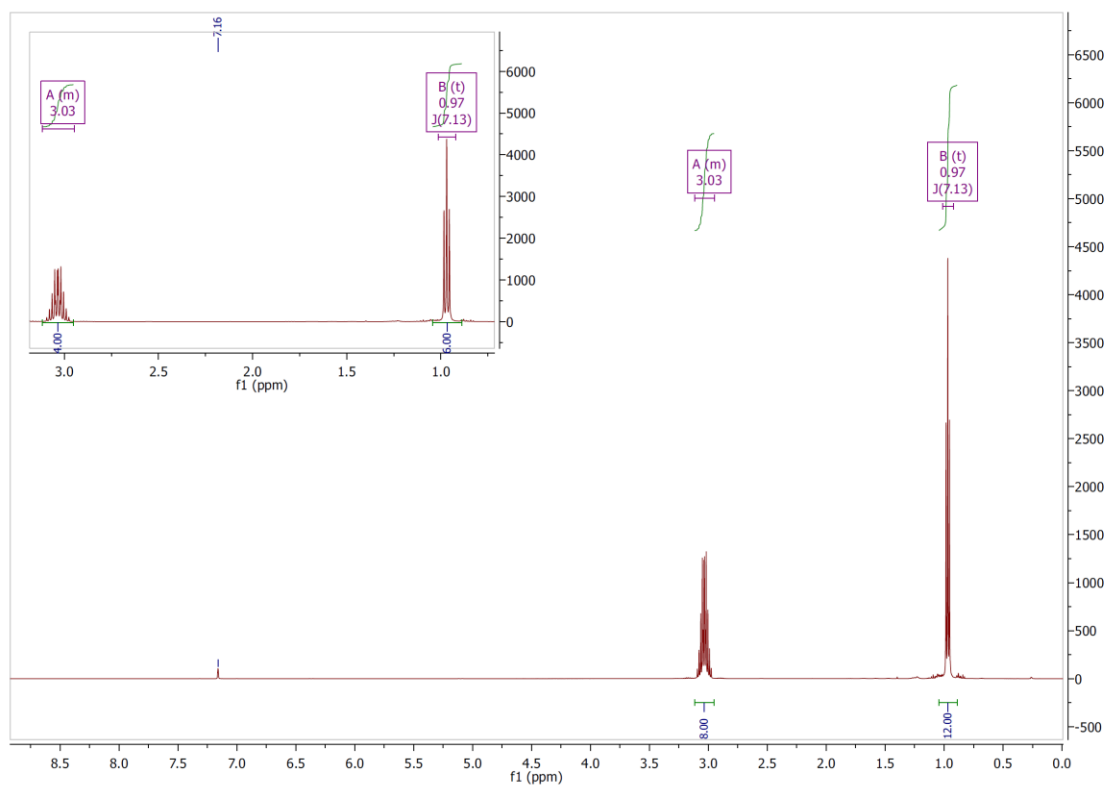
#### 7.4.4 Synthesis of arsenic precursors



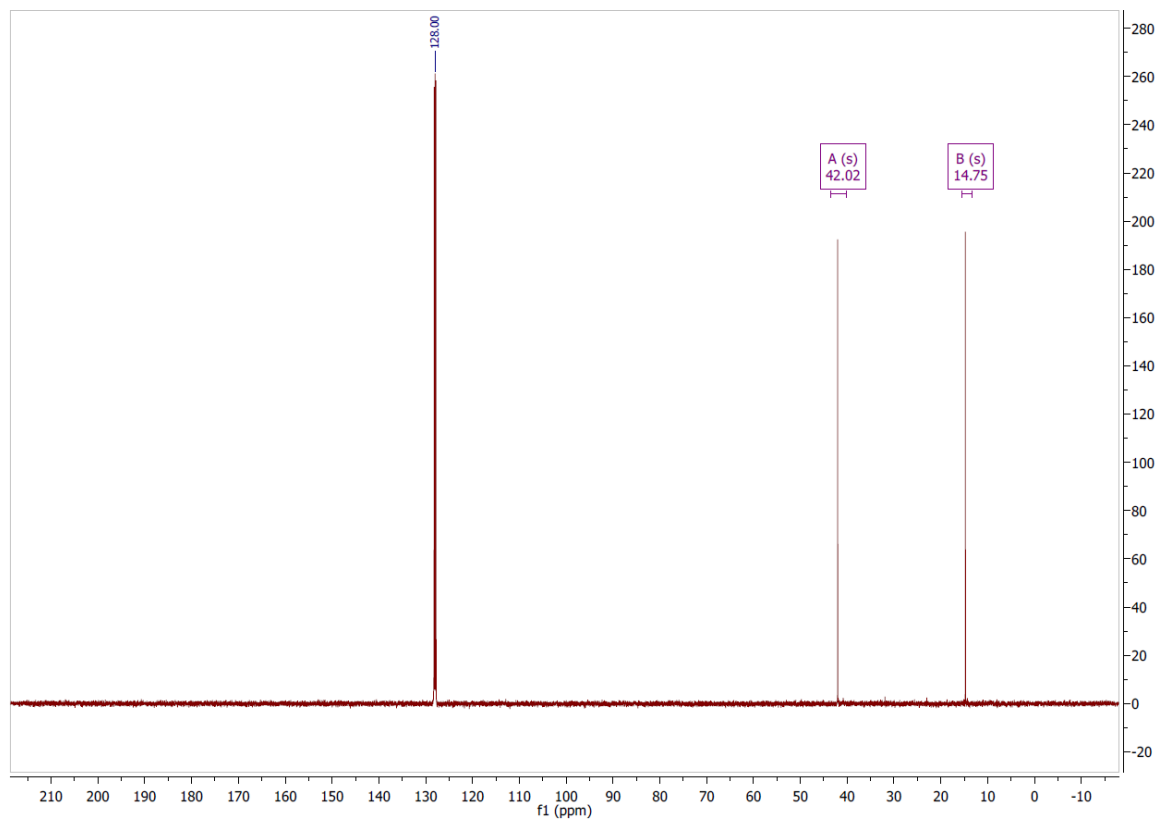
A 500-mL Schlenk flask was charged with 5.0 mL (10.8 g, 59.6 mmol) of trichloroarsine, ca 400 mL of diethyl ether, and cooled to -78 °C. Dropwise, via addition funnel, 27.0 mL of diethylamine (19.1 g, 261 mmol, 4.4 equiv) was added, resulting in a cloudy suspension. The contents were stirred cold for 15 minutes, then allowed to warm to ambient temperature and stirred for 18 hours. Volatile materials were removed under reduced pressure. The contents were dissolved in hexanes, filtered, and concentrated to provide bis(diethylamino)chloroarsine as a yellow oil. This was used without further purification. Yield: 13.114 g (51.6 mmol, 86%). <sup>1</sup>H NMR: δ 3.03 (m, 8 H, CH<sub>2</sub>CH<sub>3</sub>), 0.97 (t, *J* = 7 Hz, 12 H, CH<sub>2</sub>CH<sub>3</sub>). <sup>13</sup>C{<sup>1</sup>H}: δ 42.0 (s, CH<sub>2</sub>CH<sub>3</sub>), 14.8 (s, CH<sub>2</sub>CH<sub>3</sub>). IR (neat):

2966 s, 1447 m, 1375 s, 1289 m, 1176 s, 1054 m, 1002 s, 880 s, 783 s, 599 s, 468 m  $\text{cm}^{-1}$ .

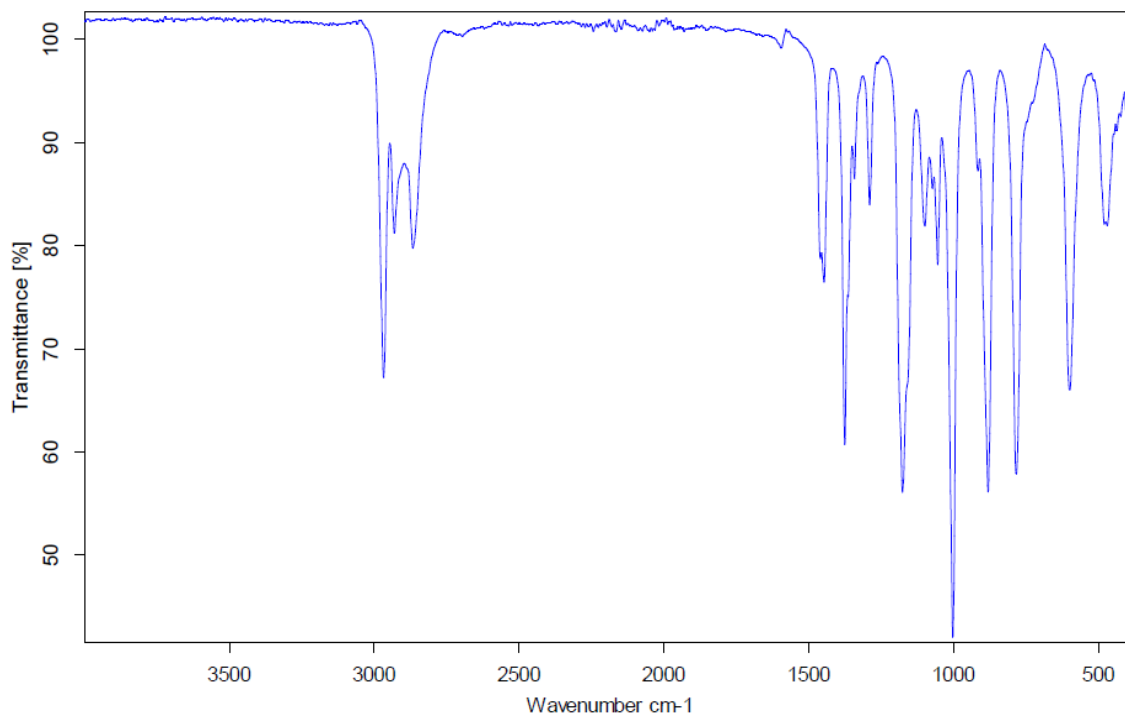
MS calcd for  $\text{C}_8\text{H}_{20}\text{AsClN}_2$ :  $m/z$  254.1. Found: 253.1.



**Figure 7.5:**  $^1\text{H}$  NMR spectrum of bis(diethylamino)chloroarsine

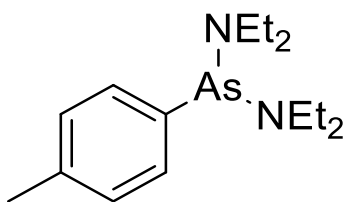


**Figure 7.6:**  $^{13}\text{C}\{^1\text{H}\}$  NMR spectrum of bis(diethylamino)chloroarsine



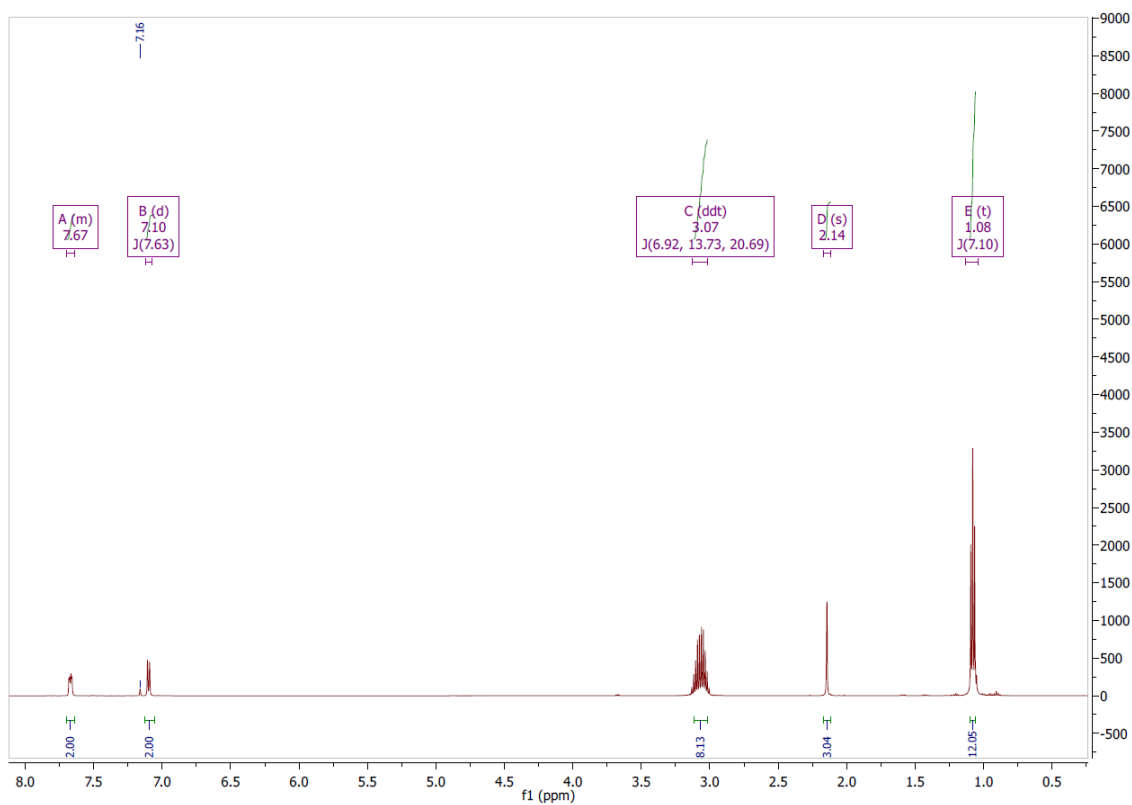
**Figure 7.7:** IR spectrum of bis(diethylamino)chloroarsine



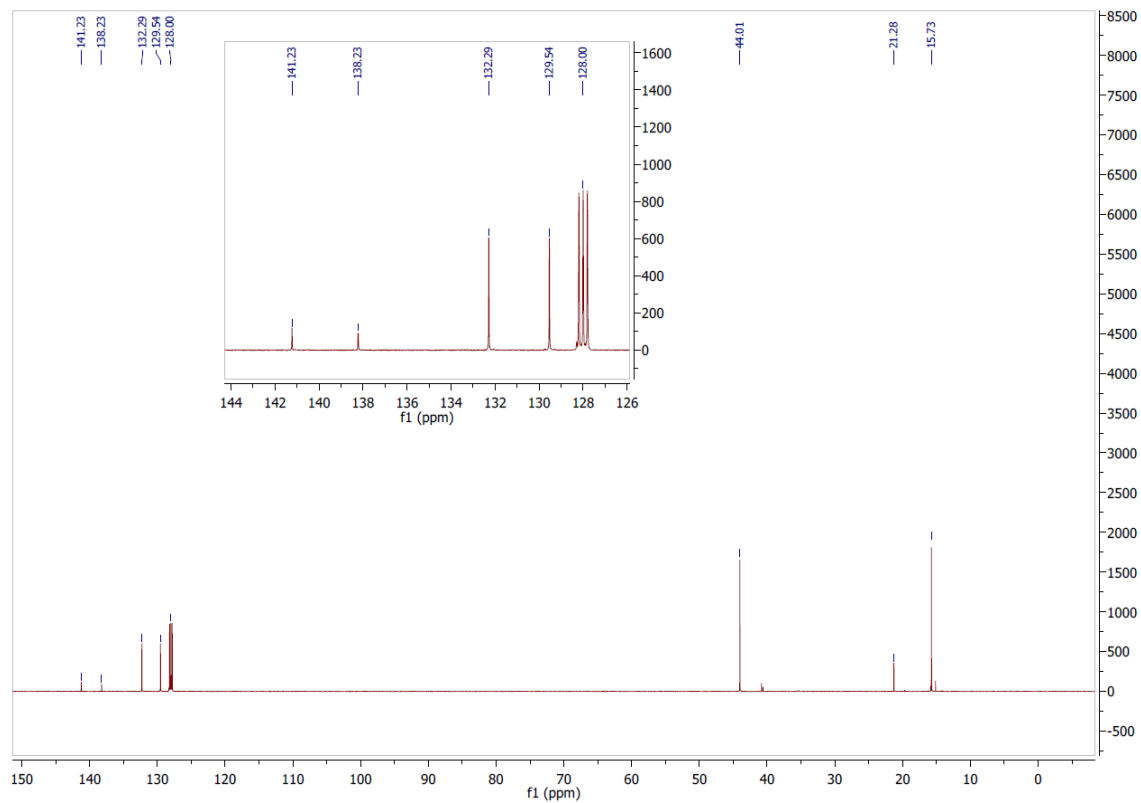


***N,N,N',N'*-tetraethyl-1-(*p*-tolyl)arsinediamine.**

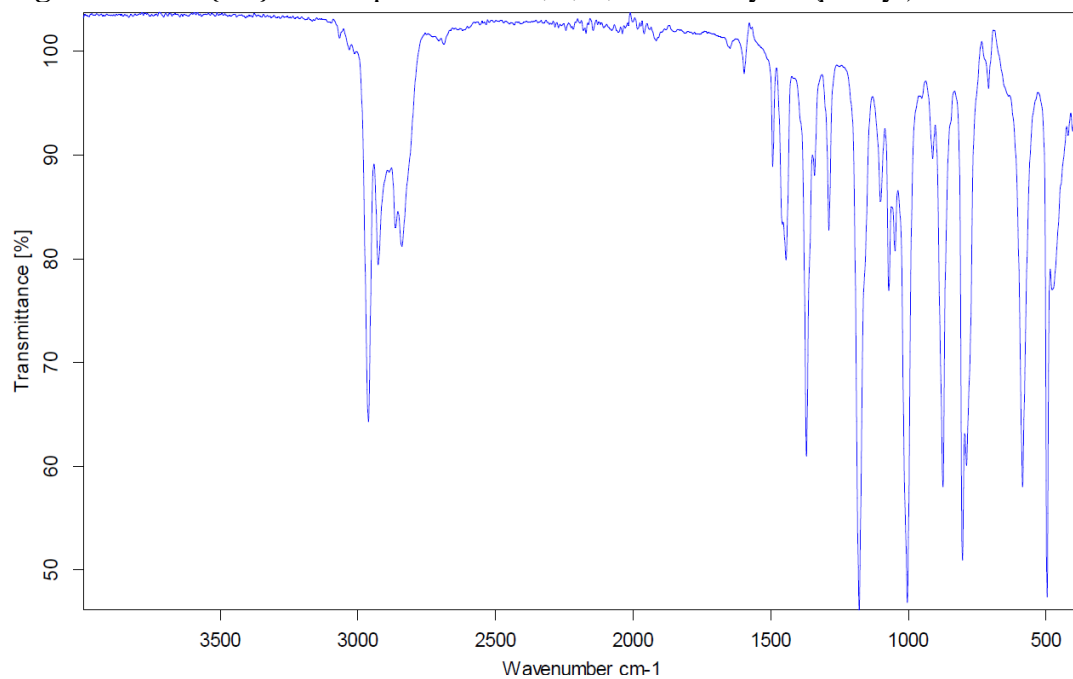
A 250 mL Schlenk flask was charged with 5.8 mL of 4-bromotoluene (47.1 mmol) and *ca* 100 mL of diethyl ether. The contents of the flask were cooled to -78 °C with an acetone/dry ice cold bath. Dropwise, 30 mL of a 1.6 M *n*BuLi solution in hexanes was added via addition funnel (56 mmol). The reaction was stirred at ambient temperature for 20 minutes, then cooled down to -78 °C and given 10.05 g (39.47 mmol) of bis(diethylamino)chloroarsine dissolved in 50 mL of diethyl ether. The reaction stirred cold for 10 minutes, and at ambient temperature for 2 h. Volatile materials were removed under reduced pressure. The crude mixture was dissolved in hexanes, filtered, and concentrated to provide a yellow oil. The product was distilled at 140 °C under reduced pressure to provide *N,N,N',N'*-tetraethyl-1-(*p*-tolyl)arsinediamine as a colorless oil. Isolated 10.03 g (32.3 mmol, 82%). <sup>1</sup>H NMR: δ 7.67 (m, 2 H, C<sub>6</sub>H<sub>4</sub>CH<sub>3</sub>), 7.10 (d, *J* = 8 Hz, 2 H, C<sub>6</sub>H<sub>4</sub>CH<sub>3</sub>), 3.07 (ddt, *J* = 21 Hz, 14 Hz, 7 Hz, 8 H, CH<sub>2</sub>CH<sub>3</sub>), 2.14 (s, 3 H, CH<sub>3</sub>), 1.08 (t, *J* = 7 Hz, 12 H, CH<sub>2</sub>CH<sub>3</sub>). <sup>13</sup>C{<sup>1</sup>H}: δ 141.2 (s, C<sub>6</sub>H<sub>4</sub>CH<sub>3</sub>), 138.2 (s, C<sub>6</sub>H<sub>4</sub>CH<sub>3</sub>), 132.3 (s, C<sub>6</sub>H<sub>4</sub>CH<sub>3</sub>), 129.5 (s, C<sub>6</sub>H<sub>4</sub>CH<sub>3</sub>), 44.0 (s, CH<sub>2</sub>CH<sub>3</sub>), 21.3 (s, C<sub>6</sub>H<sub>4</sub>CH<sub>3</sub>), 15.7 (s, CH<sub>2</sub>CH<sub>3</sub>). IR (neat): 2962 s, 1445 m, 1370s, 1289 m, 1170 s, 1004 s, 874 s, 804 s, 585 s, 496 s cm<sup>-1</sup>. MS calcd for C<sub>15</sub>H<sub>27</sub>AsN<sub>2</sub>: *m/z* 310.1. Found: 312.5.



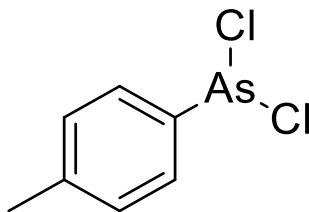
**Figure 7.8:**  $^1\text{H}$  NMR spectrum of  $N,N,N',N'$ -tetraethyl-1-(*p*-tolyl)arsinediamine



**Figure 7.9:**  $^{13}\text{C}\{^1\text{H}\}$  NMR spectrum of *N,N,N',N'*-tetraethyl-1-(*p*-tolyl)arsinediamine

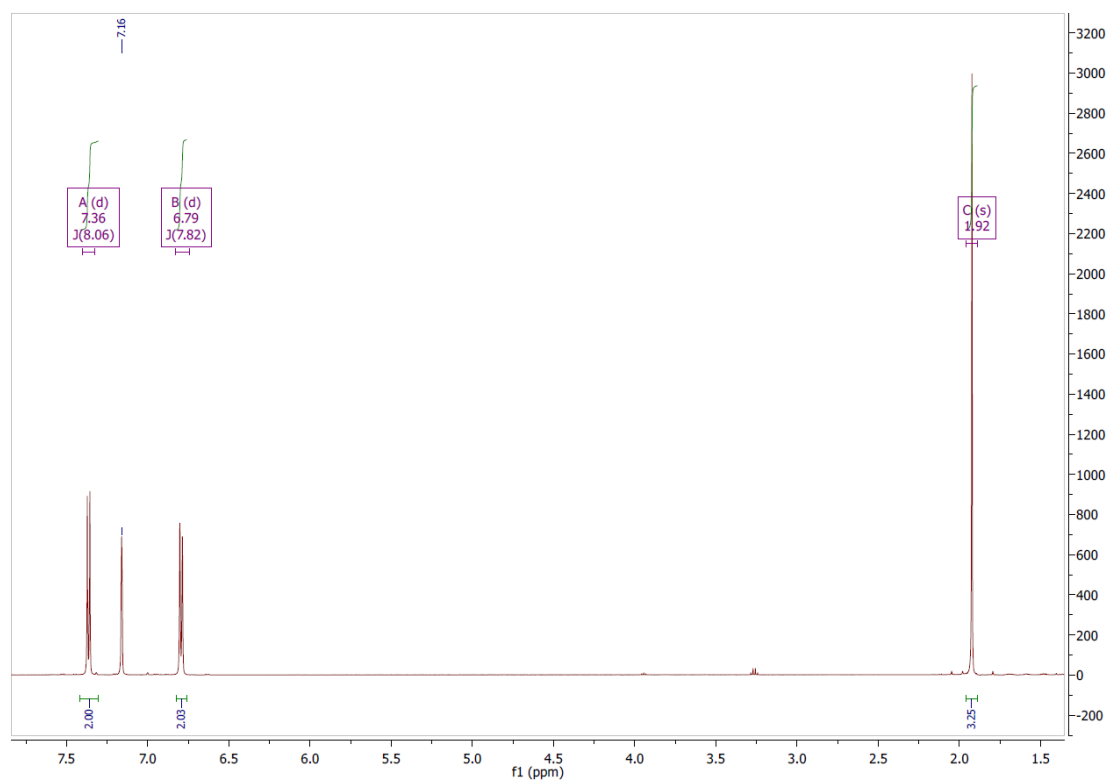


**Figure 7.10:** IR spectrum of *N,N,N',N'*-tetraethyl-1-(*p*-tolyl)arsinediamine

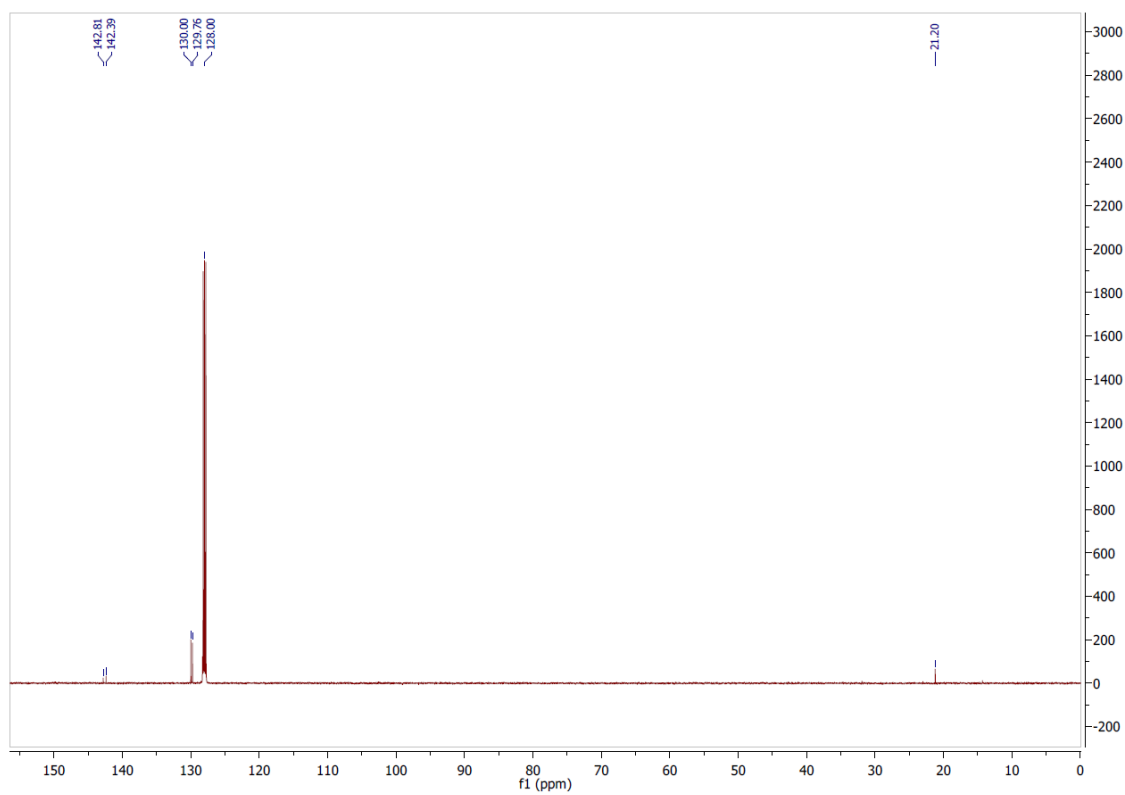


**Dichloro-*p*-tolylarsine.**

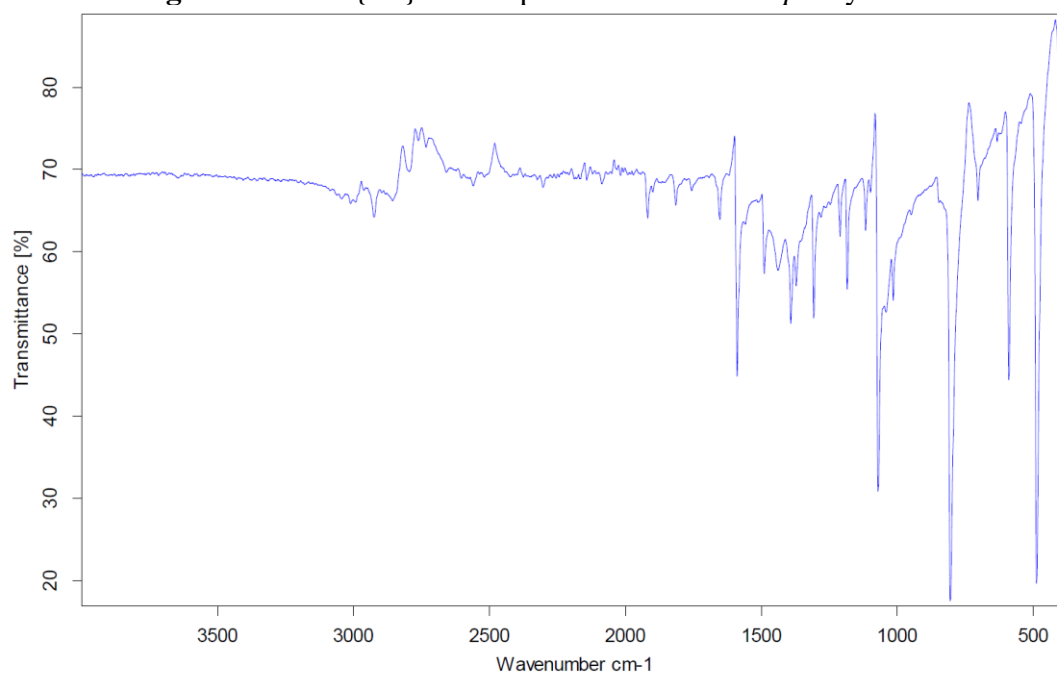
A 250-mL Schlenk flask was charged with 10.16 g (32.8 mmol) of *N,N,N,N*-tetraethyl-1-(*p*-tolyl)arsinediamine and ca 100 mL of diethyl ether. The contents of the flask were cooled to -78 °C with an acetone/dry ice cold bath. Dropwise, 70 mL of a 2 N solution of HCl in diethyl ether was added via addition funnel over a period of 20 minutes. The cold bath was removed and the reaction stirred at ambient temperature for 2 h. Volatile materials were removed under reduced pressure and the crude reaction mixture was dissolved in hexanes, filtered, and concentrated until incipient crystallization. The reaction mixture was allowed to warm to ambient temperature to redissolve the solid material, then cooled to -20 °C to provide off-white crystals after 15 minutes. Yield: 5.707 g (24.1 mmol, 73%). <sup>1</sup>H NMR: δ 7.36 (d, *J* = 8 Hz, 2 H, C<sub>6</sub>H<sub>4</sub>CH<sub>3</sub>), 6.79 (d, *J* = 8 Hz, 2 H, C<sub>6</sub>H<sub>4</sub>CH<sub>3</sub>), 1.92 (s, 3 H, C<sub>6</sub>H<sub>4</sub>CH<sub>3</sub>). <sup>13</sup>C{<sup>1</sup>H}: δ 142.8 (s, C<sub>6</sub>H<sub>4</sub>CH<sub>3</sub>), 142.4 (s, C<sub>6</sub>H<sub>4</sub>CH<sub>3</sub>), 130.0 (s, C<sub>6</sub>H<sub>4</sub>CH<sub>3</sub>), 129.8 (s, C<sub>6</sub>H<sub>4</sub>CH<sub>3</sub>), 21.2 (s, C<sub>6</sub>H<sub>4</sub>CH<sub>3</sub>). IR (neat): 1589 s, 1391 s, 1307 m, 1070 s, 805 s, 590 s, 488 s cm<sup>-1</sup>. MS calcd for C<sub>7</sub>H<sub>7</sub>AsCl<sub>2</sub>: *m/z* 235.9. Found: 236.5.



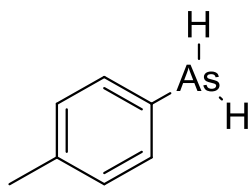
**Figure 7.11:**  $^1\text{H}$  NMR spectrum of dichloro-*p*-tolylarsine



**Figure 7.12:**  $^{13}\text{C}\{^1\text{H}\}$  NMR spectrum of dichloro-*p*-tolylarsine

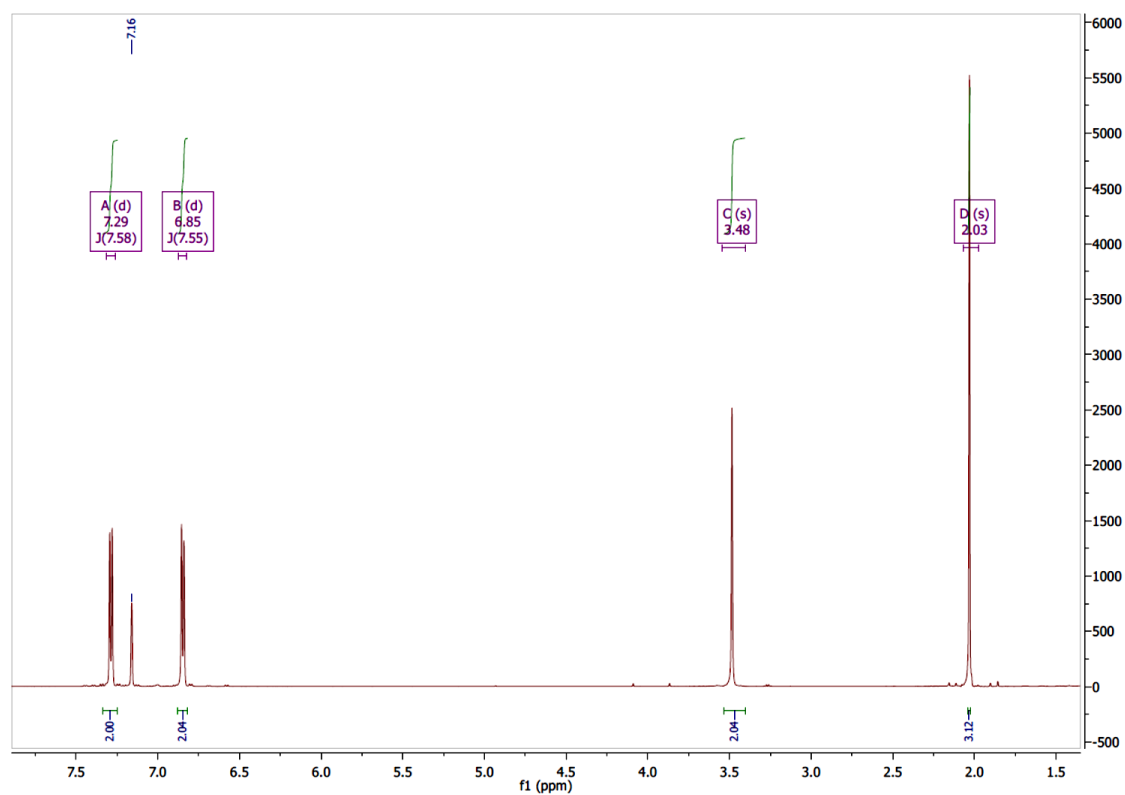


**Figure 7.13:** IR spectrum of dichloro-*p*-tolylarsine



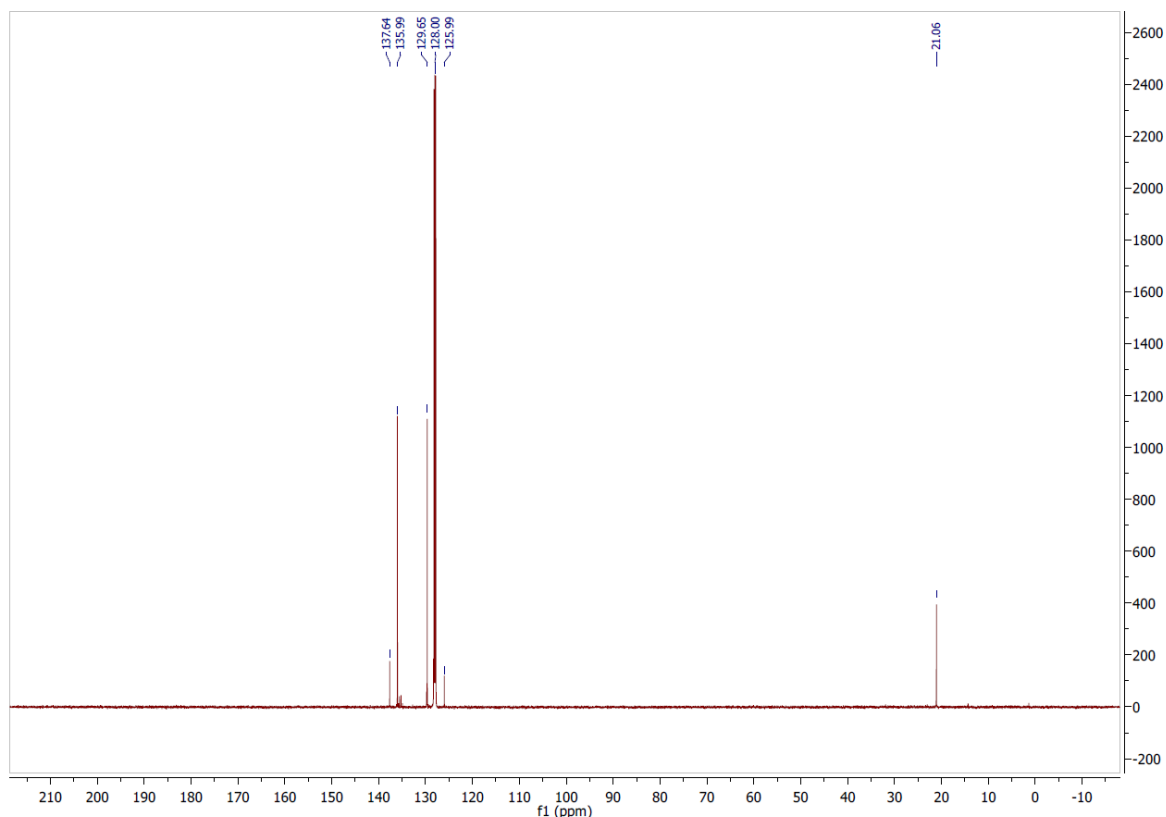
***p*-Tolylarsine.**

A Schlenk flask containing 247 mg (6.05 mmol, 2.1 equiv) of lithium aluminum hydride was suspended in diethyl ether and cooled to -78 °C. Slowly, via cannula, a solution of 686.7 mg (2.90 mmol) of *p*-tolylchloroarsine in diethyl ether was added. The reaction stirred cold for 1 h, then gradually warmed to ambient temperature and stirred overnight. The crude mixture was quenched with degassed water and filtered via cannula. Diethyl ether was removed by distillation under nitrogen. The crude reaction mixture was dissolved in hexanes, filtered, and concentrated to provide the product as a colorless oil (224.8 mg, 1.34 mmol, 46%).  $^1\text{H}$  NMR:  $\delta$  7.28 (d,  $J = 8$  Hz, 2 H,  $\text{C}_6\text{H}_4\text{CH}_3$ ), 6.85 (d, 8 Hz, 2 H,  $\text{C}_6\text{H}_4\text{CH}_3$ ), 3.49 (s, 2 H,  $\text{AsH}_2$ ), 2.03 (s, 3 H,  $\text{C}_6\text{H}_4\text{CH}_3$ ).  $^{13}\text{C}\{^1\text{H}\}$ :  $\delta$  137.7 (s,  $\text{C}_6\text{H}_4\text{CH}_3$ ), 136.0 (s,  $\text{C}_6\text{H}_4\text{CH}_3$ ), 129.7 (s,  $\text{C}_6\text{H}_4\text{CH}_3$ ), 126.0 (s,  $\text{C}_6\text{H}_4\text{CH}_3$ ), 21.0 (s,  $\text{C}_6\text{H}_4\text{CH}_3$ ). MS calcd for  $\text{C}_7\text{H}_9\text{As}$ :  $m/z$  168.1. Found: 168.8.

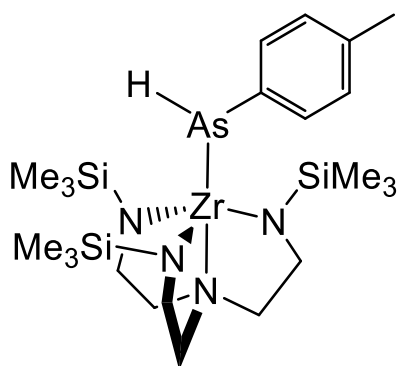


**Figure 7.14:**  $^1\text{H}$  NMR spectrum of *p*-tolylarsine





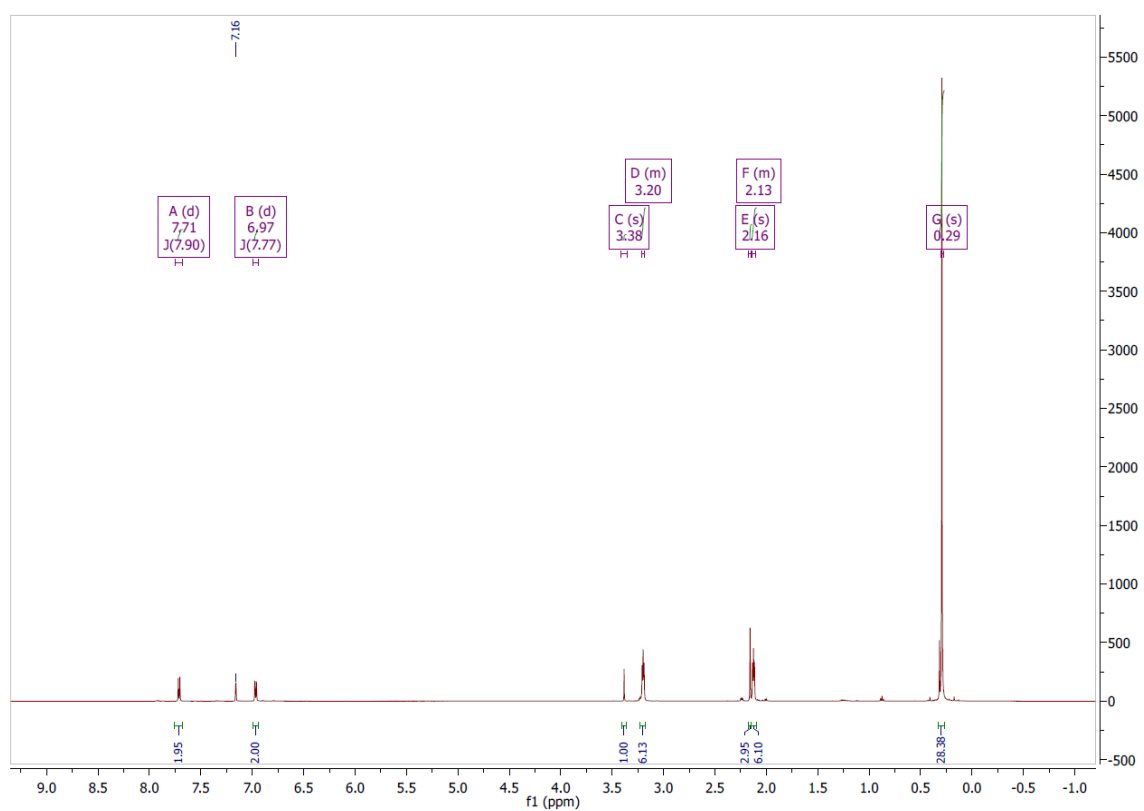
**Figure 7.15:**  $^{13}\text{C}\{^1\text{H}\}$  NMR spectrum of *p*-tolylarsine  
**7.4.6 Formation of 2**



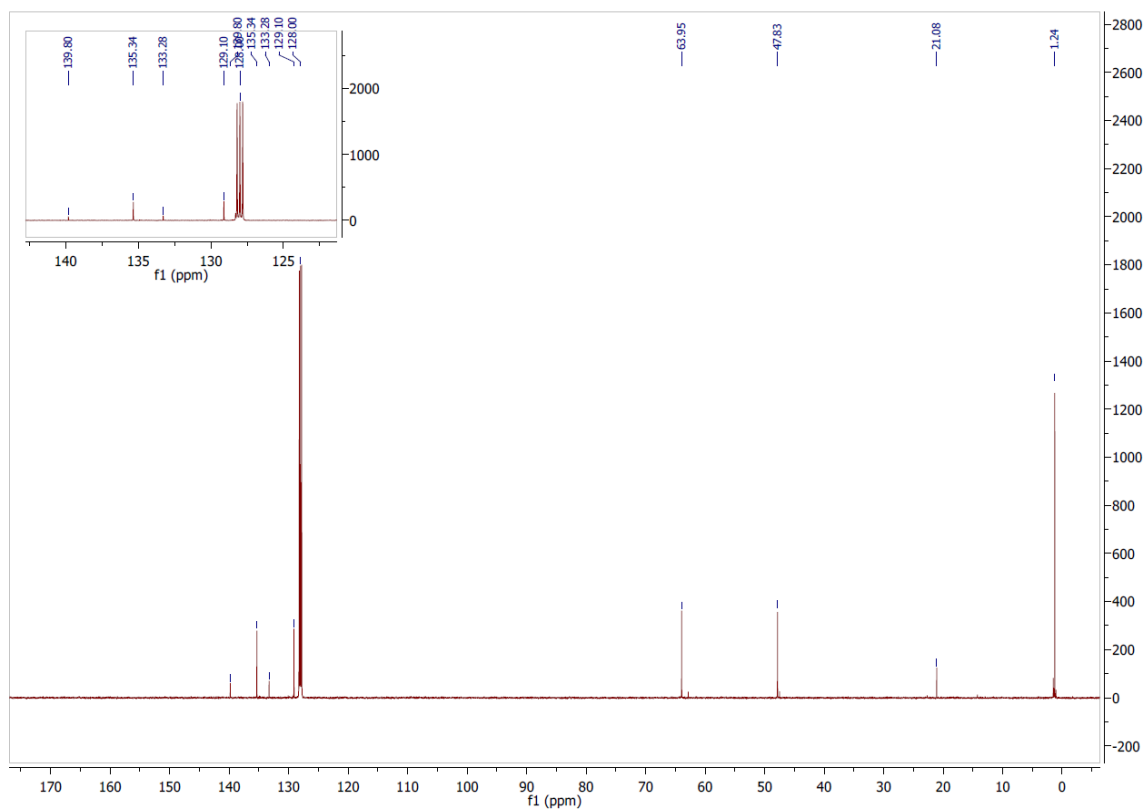
**(N<sub>3</sub>N)Zr(*p*-tolyl)AsH (2).**

A scintillation vial was charged with 41.4 mg (0.246 mmol) of *p*-tolylarsine, 112.1 mg (0.247 mmol) of **1**, and ca 4 mL of toluene to give a deep golden-orange solution. This stirred for twenty minutes, and then the toluene was removed under reduced pressure. The crude reaction mixture was dissolved in pentanes and cooled to -20 °C to afford orange crystals after 3 d.  $^1\text{H}$  NMR:  $\delta$  7.71 (d, 8 Hz, 2 H,  $\text{C}_6\text{H}_4\text{CH}_3$ ), 6.97 (d, 8 Hz, 2 H,  $\text{C}_6\text{H}_4\text{CH}_3$ ),

3.38 (s, 1 H,  $AsH$ ), 3.20 (t,  $J = 5$  Hz, 6 H,  $CH_2$ ), 2.16 (s, 3 H,  $CH_3$ ), 2.13 (t,  $J = 5$  Hz, 6 H,  $CH_2$ ), 0.29 (s, 27 H,  $Si(CH_3)_3$ ).  $^{13}C\{^1H\}$ :  $\delta$  139.8 (s,  $C_6H_4CH_3$ ), 135.3 (s,  $C_6H_4CH_3$ ), 133.3 (s,  $C_6H_4CH_3$ ), 129.1 (s,  $C_6H_4CH_3$ ), 64.0 (s,  $CH_2$ ), 47.8 (s,  $CH_2$ ), 21.1 (s,  $C_6H_4CH_3$ ), 1.2 (s,  $Si(CH_3)_3$ ).

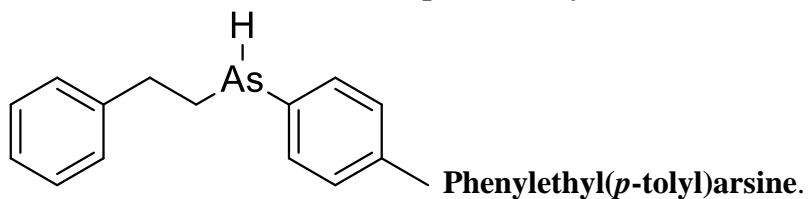


**Figure 7.16:**  $^1H$  NMR spectrum of **2**

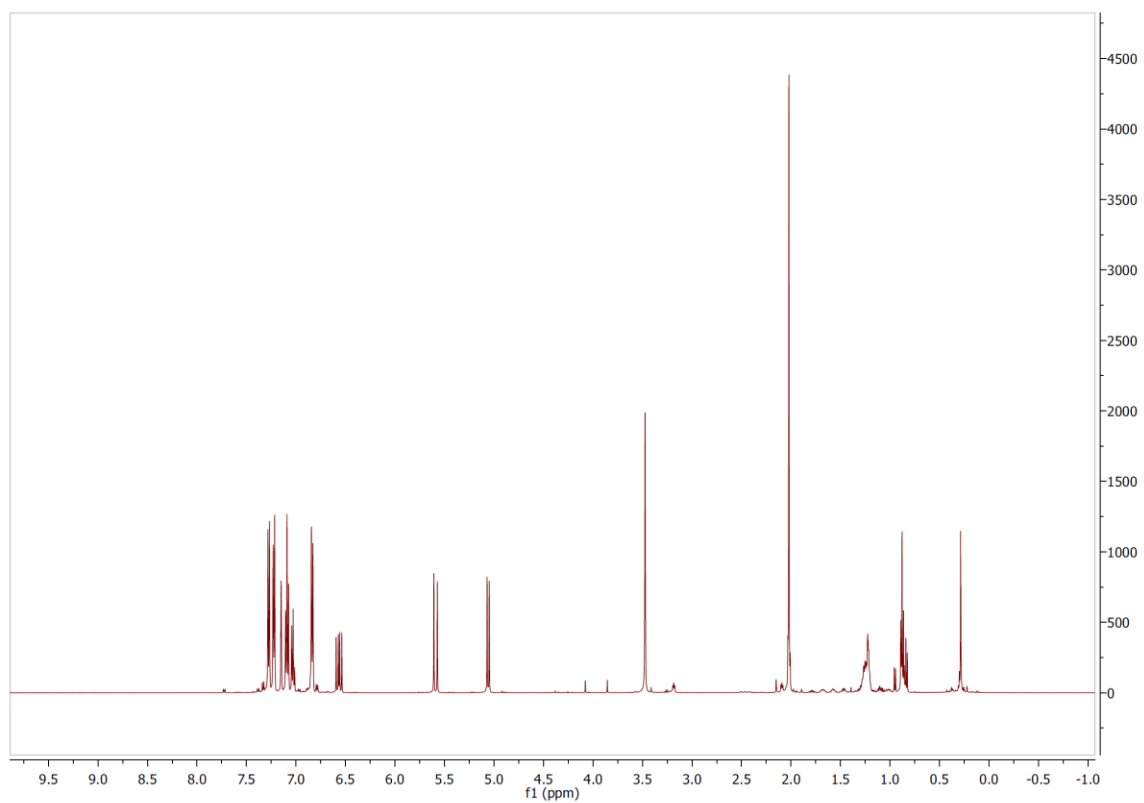


**Figure 7.17:**  $^{13}\text{C}\{^1\text{H}\}$  NMR spectrum of **2**

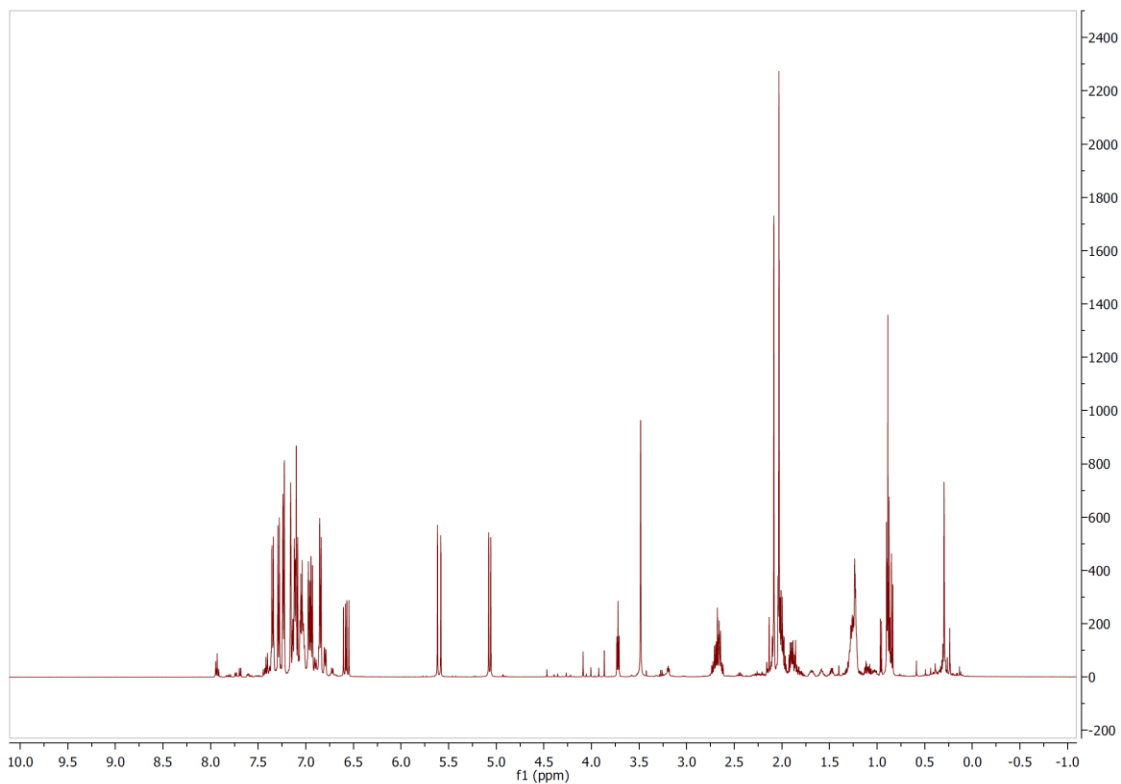
#### 7.4.5 NMR spectra of hydroarsination reactions



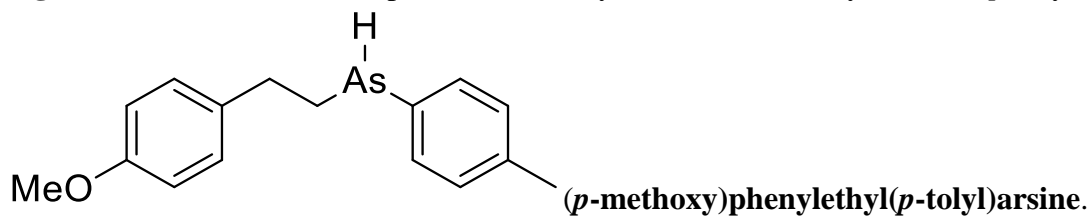
Reaction goes to completion in 24 hours under irradiation from a blacklight lamp with 48% consumption of styrene as measured by  $^1\text{H}$  NMR spectroscopy.



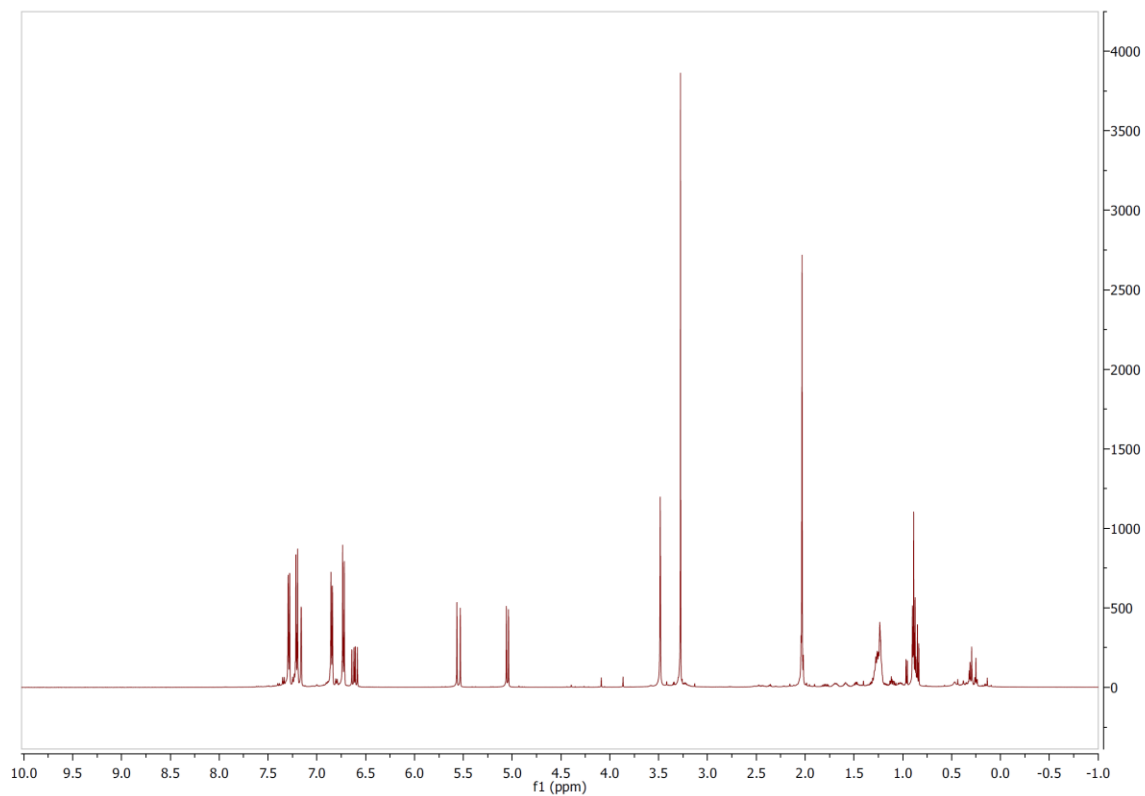
**Figure 7.18:** Initial  $^1\text{H}$  NMR spectrum of the hydroarsination of styrene with *p*-tolylarsine



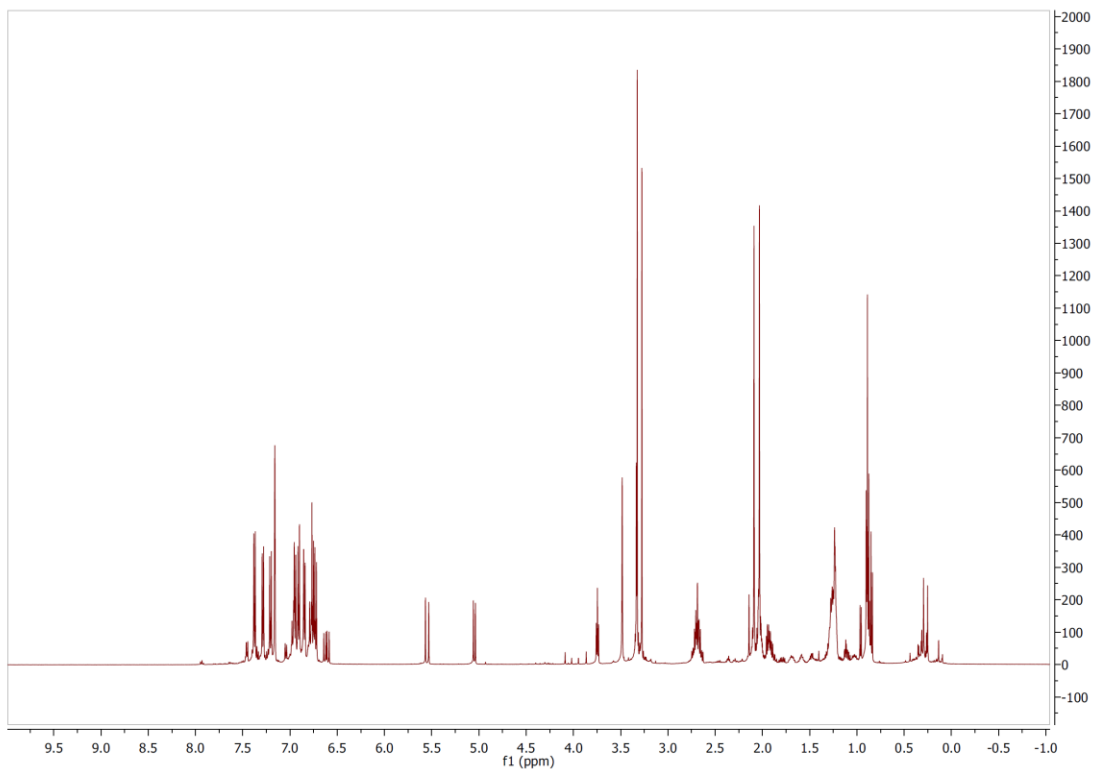
**Figure 7.19:** Final  $^1\text{H}$  NMR spectrum of the hydroarsination of styrene with *p*-tolylarsine



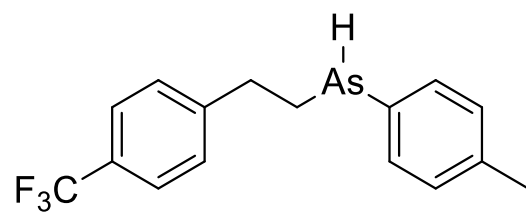
Reaction goes to completion in 24 hours under irradiation from a blacklight lamp with 50% consumption of *p*-methoxystyrene as measured by  $^1\text{H}$  NMR spectroscopy.



**Figure 7.20:** Initial  $^1\text{H}$  NMR spectrum of the hydroarsination of *p*-methoxystyrene with *p*-tolylarsine

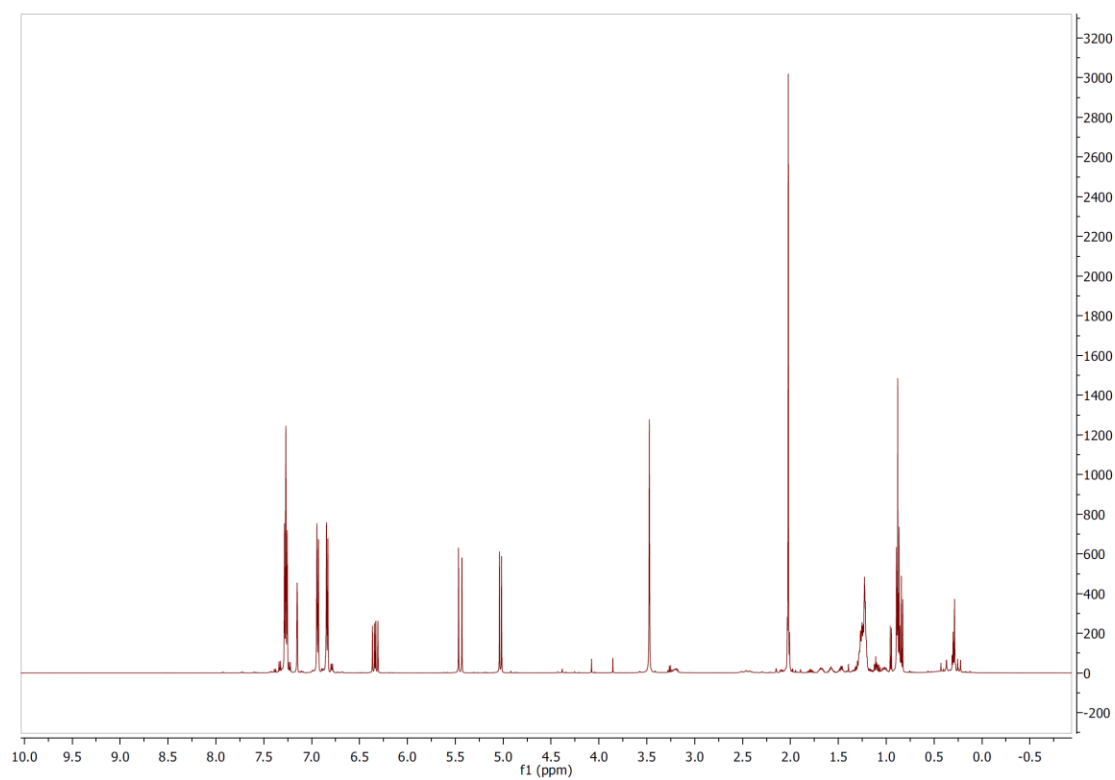


**Figure 7.21:** Final  $^1\text{H}$  NMR spectrum of the hydroarsination of *p*-methoxystyrene with *p*-tolylarsine



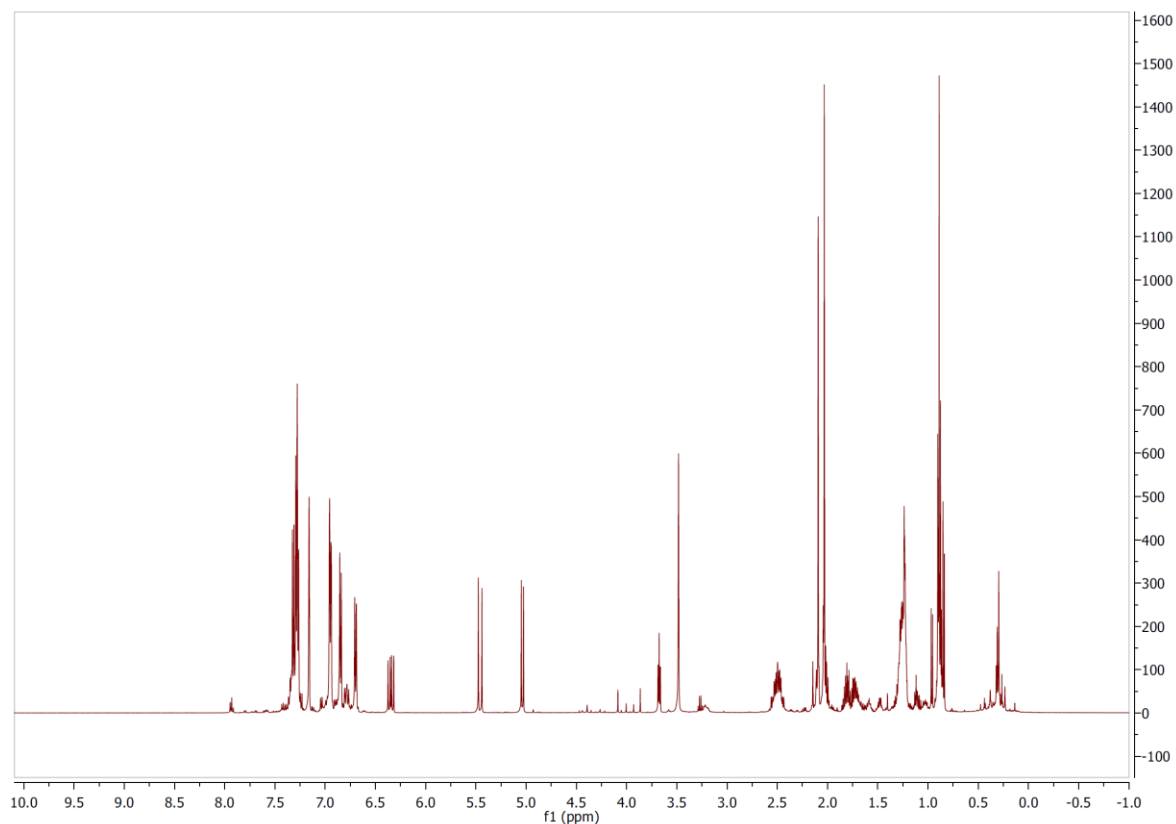
**(*p*-trifluoromethyl)phenylethyl(*p*-tolyl)arsine.**

Reaction goes to completion in 24 hours under irradiation from a blacklight lamp with 44% consumption of *p*-trifluoromethylstyrene as measured by  $^1\text{H}$  NMR spectroscopy.

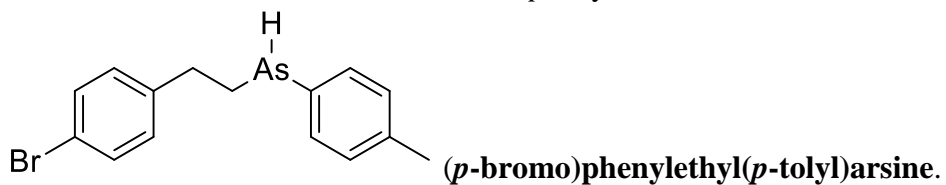


**Figure 7.22:** Initial  $^1\text{H}$  NMR spectrum of the hydroarsination of *p*-trifluoromethylstyrene with *p*-tolylarsine

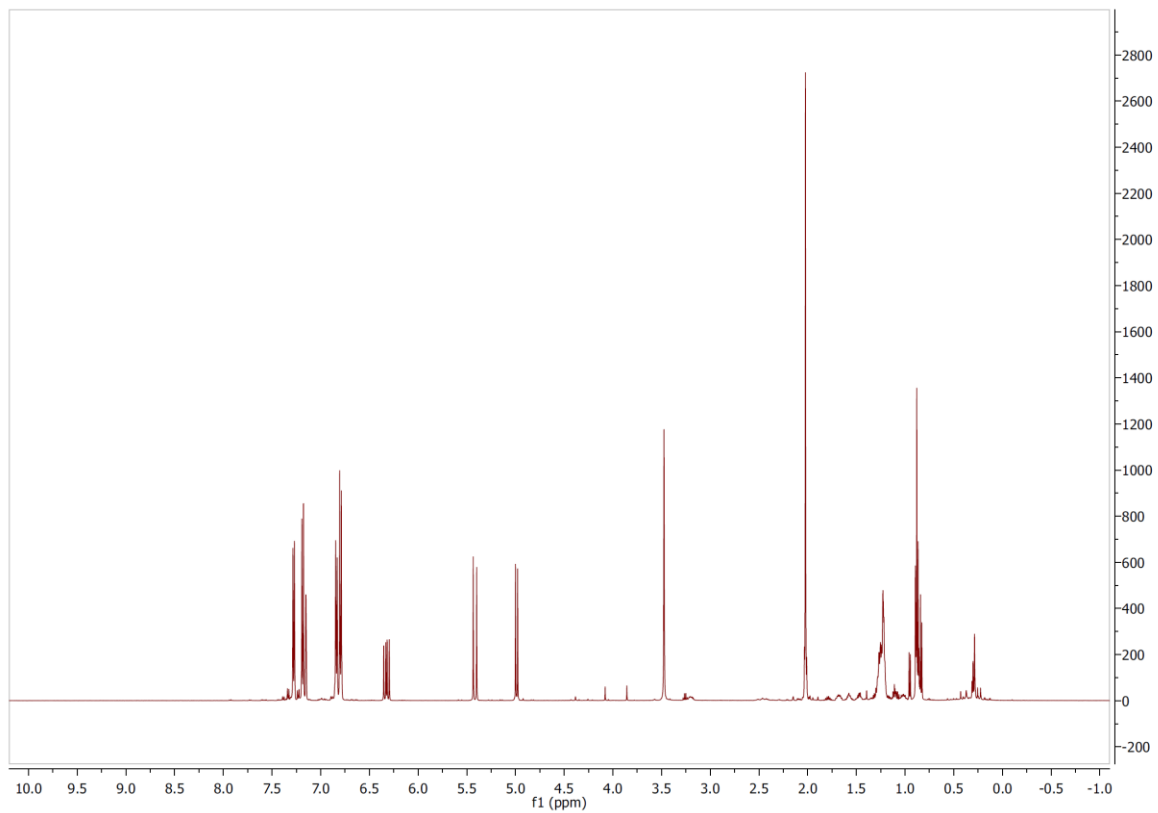




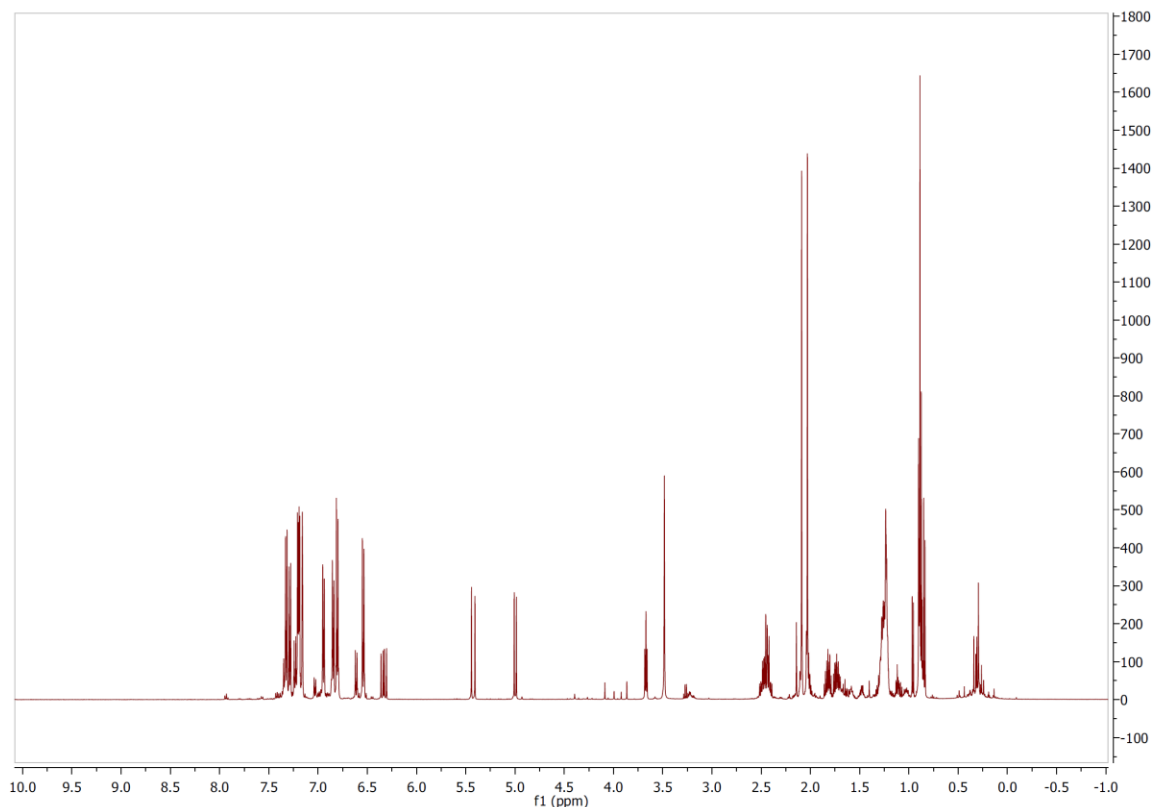
**Figure 7.23:** Final  $^1\text{H}$  NMR spectrum of the hydroarsination of *p*-trifluoromethylstyrene with *p*-tolylarsine



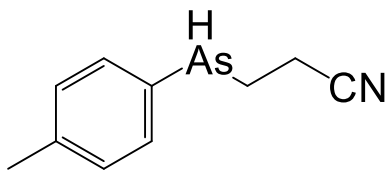
Reaction goes to completion in 24 hours under irradiation from a blacklight lamp with 44% consumption of *p*-bromostyrene as measured by  $^1\text{H}$  NMR spectroscopy.



**Figure 7.24:** Initial  $^1\text{H}$  NMR spectrum of the hydroarsination of *p*-bromostyrene with *p*-tolylarsine

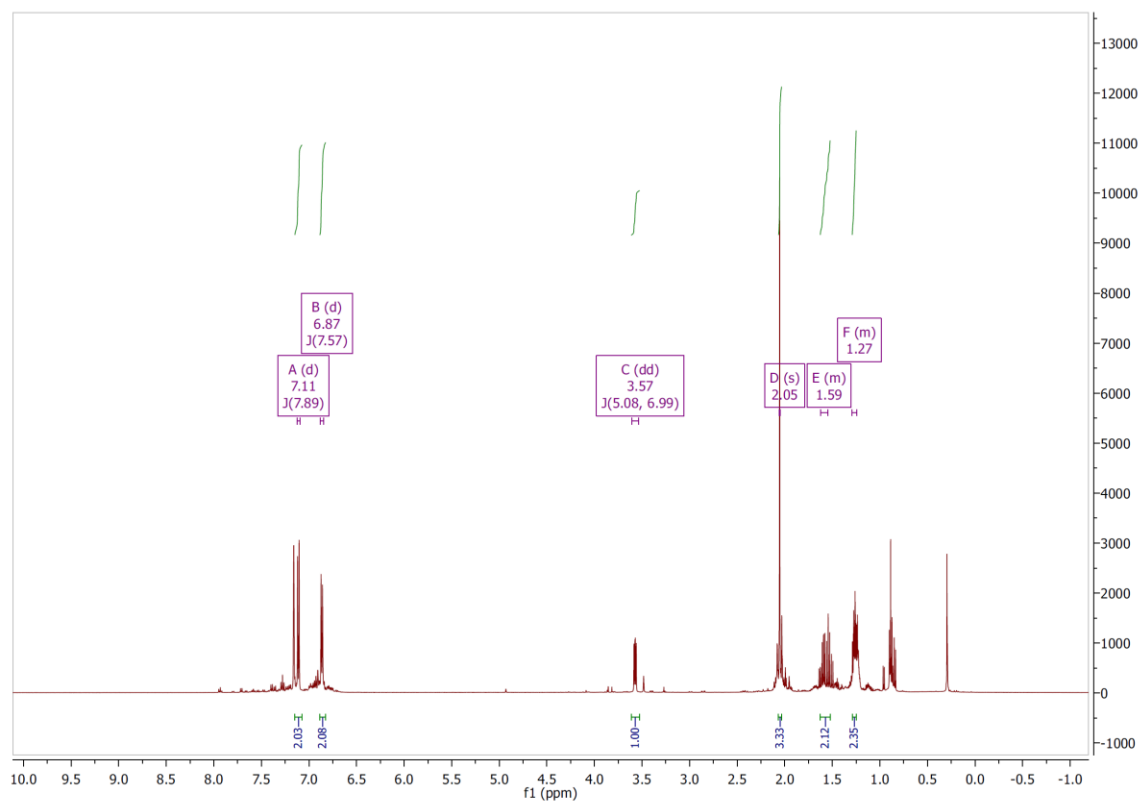


**Figure 7.25:** Final  $^1\text{H}$  NMR spectrum of the hydroarsination of *p*-bromostyrene with *p*-tolylarsine

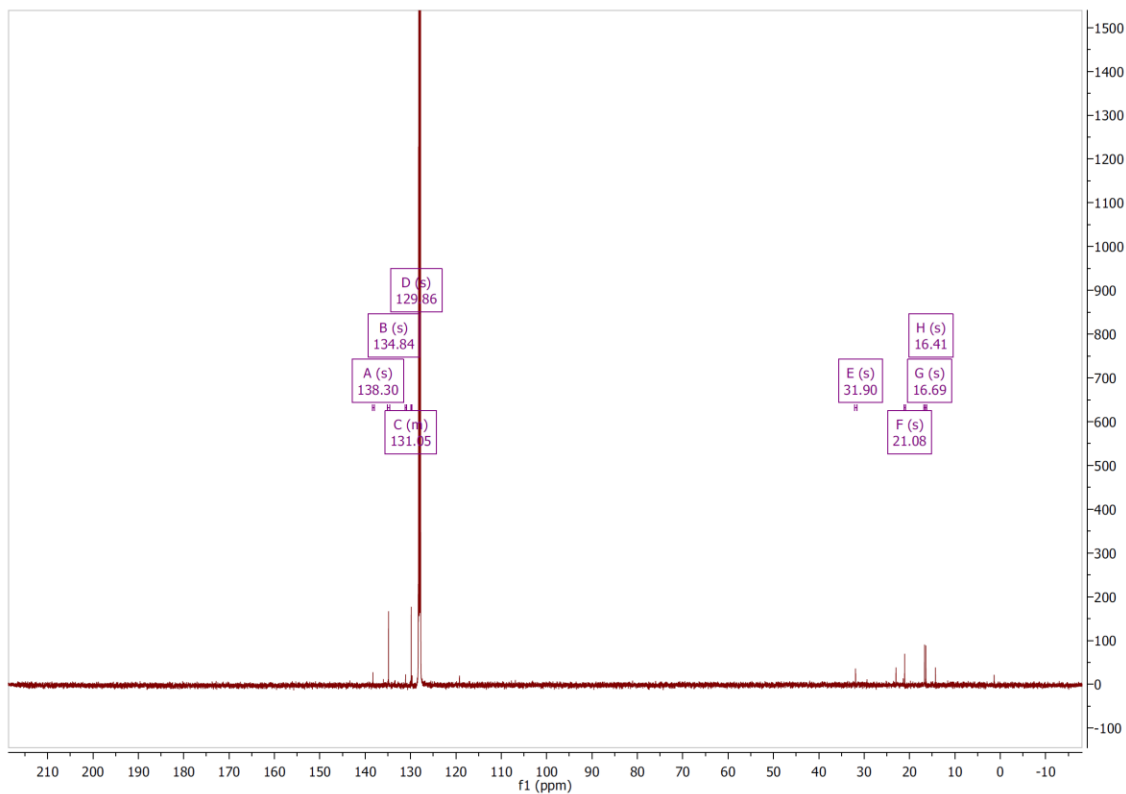


**(*p*-tolyl)As(H)CH<sub>2</sub>CH<sub>2</sub>CN**

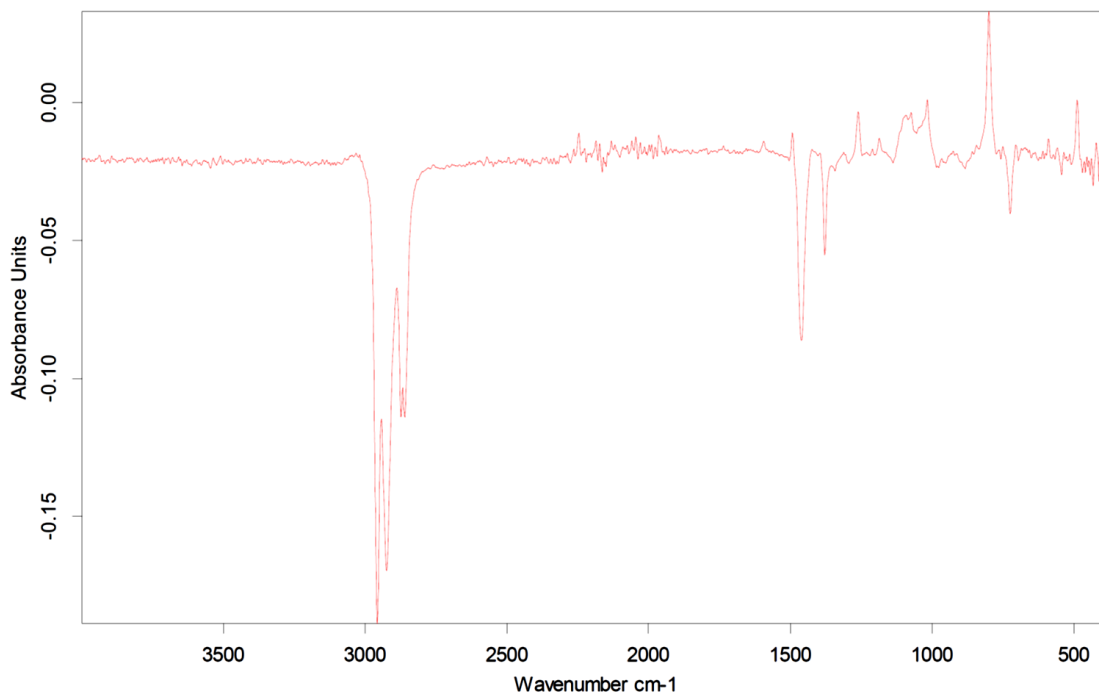
$^1\text{H}$ :  $\delta$  7.11 (d,  $J = 8$  Hz, 2 H,  $\text{C}_6\text{H}_4\text{CH}_3$ ), 6.87 (d,  $J = 8$  Hz, 2 H,  $\text{C}_6\text{H}_4\text{CH}_3$ ), 3.57 (dd,  $J = 7$  Hz, 5 Hz, 1 H, AsH), 2.05 (s, 3 H,  $\text{CH}_3$ ), 1.59 (m, 2 H,  $\text{CH}_2$ ), 1.27 (m, 2 H,  $\text{CH}_2$ ).  $^{13}\text{C}\{^1\text{H}\}$ :  $\delta$  138.3 (s), 134.8 (s), 135.1 (s), 129.9 (s), 31.9 (s), 21.1 (s), 16.7 (s), 16.4 (s). MS calcd for  $\text{C}_{11}\text{H}_{15}\text{AsO}_2$ :  $m/z$  221.0. Found: 222.8. Formed under blacklight irradiation for 1 h at ambient temperature with 100% consumption of methyl acrylate as measured by  $^1\text{H}$  NMR spectroscopy.



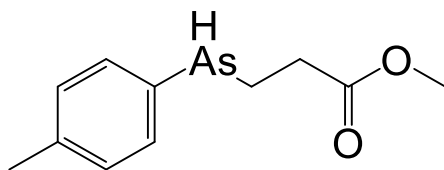
**Figure 7.26:** Crude  $^1\text{H}$  NMR spectrum  $(p\text{-tolyl})\text{As}(\text{H})\text{CH}_2\text{CH}_2\text{CN}$



**Figure 7.27:** Crude  $^{13}\text{C}\{^1\text{H}\}$  NMR spectrum of  $(p\text{-tolyl})\text{As}(\text{H})\text{CH}_2\text{CH}_2\text{CN}$

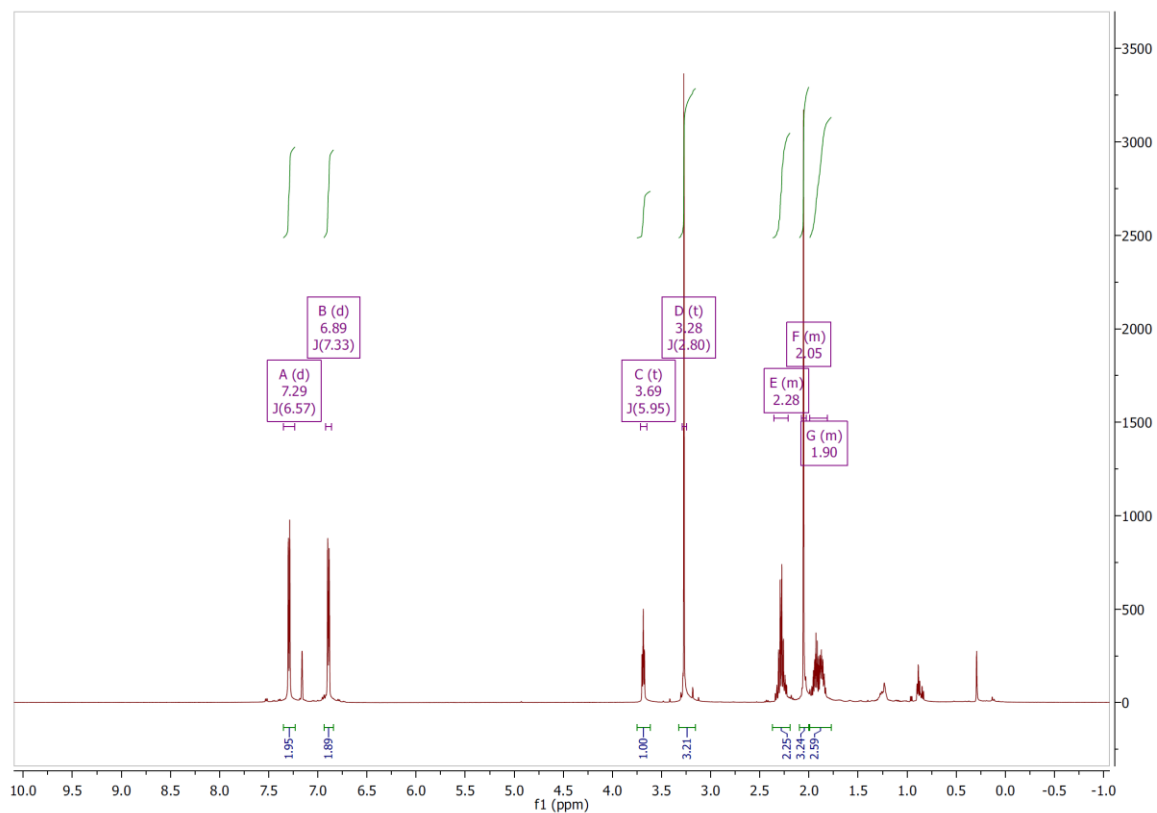


**Figure 7.28:** Crude IR spectrum of  $(p\text{-tolyl})\text{As}(\text{H})\text{CH}_2\text{CH}_2\text{CN}$

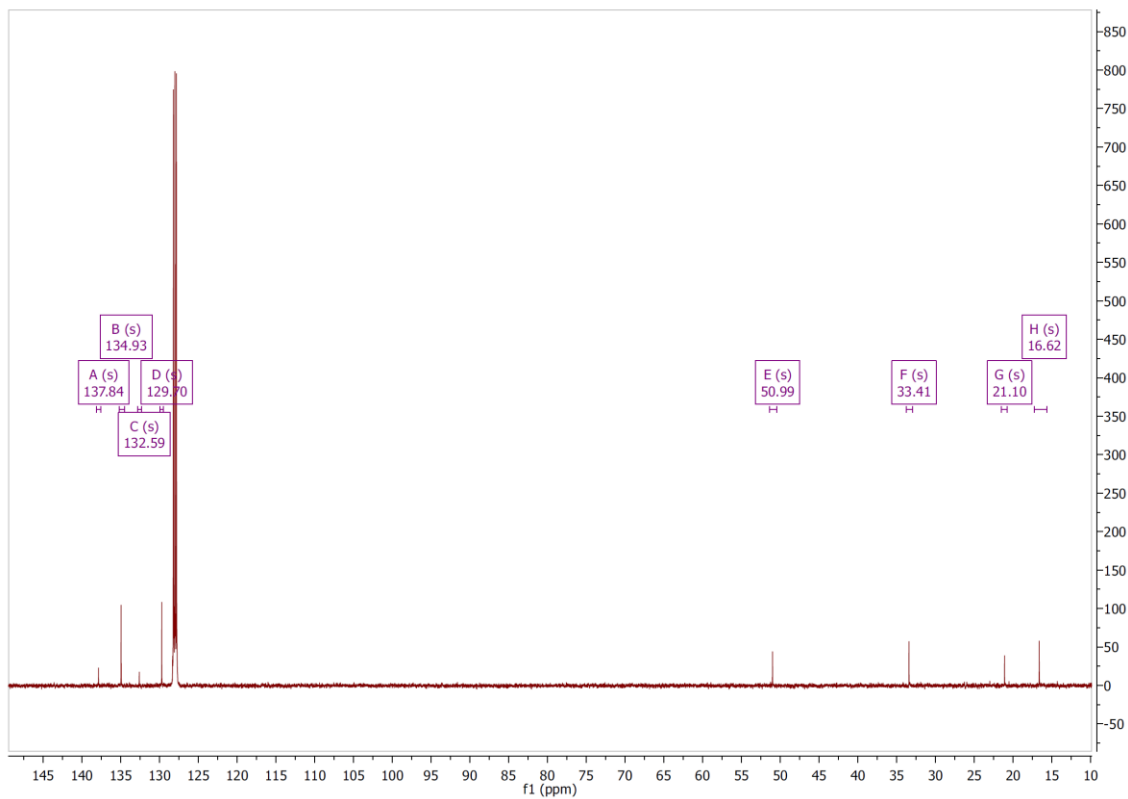


(*p*-tolyl)As(H)CH<sub>2</sub>CH<sub>2</sub>C(O)OMe

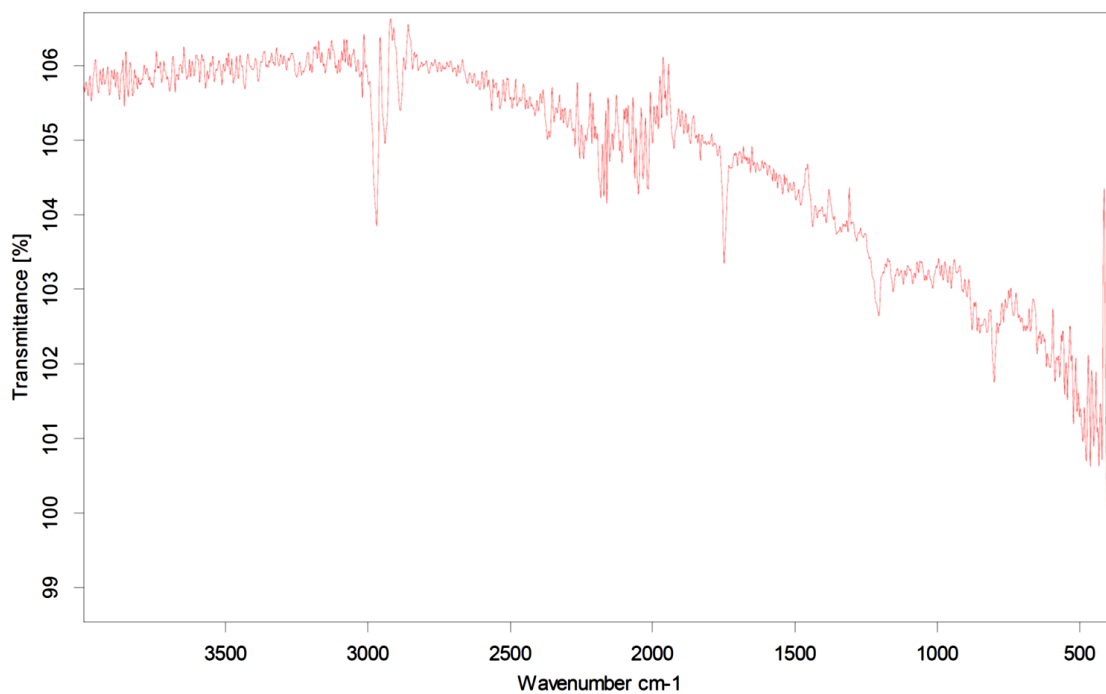
<sup>1</sup>H: δ 7.29 (d, *J* = 8 Hz, 2 H, C<sub>6</sub>H<sub>4</sub>CH<sub>3</sub>), 6.89 (d, *J* = 8 Hz, 2 H, C<sub>6</sub>H<sub>4</sub>CH<sub>3</sub>), 3.69 (dd, *J* = 7 Hz, 5 Hz, 1 H, AsH), 3.28 (s, 3 H, CH<sub>3</sub>), 2.28 (m, 2 H, CH<sub>2</sub>), 2.05 (s, 3 H, CH<sub>3</sub>), 1.90 (m, 2 H, CH<sub>2</sub>). <sup>13</sup>C{<sup>1</sup>H}: δ 137.8 (s), 135.0 (s), 132.6 (s), 129.7 (s), 51.0 (s), 33.4 (s), 21.1 (s), 16.6 (s). MS calcd for C<sub>11</sub>H<sub>15</sub>AsO<sub>2</sub>: *m/z* 254.0. Found: 253.2. Formed under blacklight irradiation for 1 h at ambient temperature with 100% consumption of methyl acrylate as measured by <sup>1</sup>H NMR spectroscopy. Isolated 73% yield as a colorless oil.



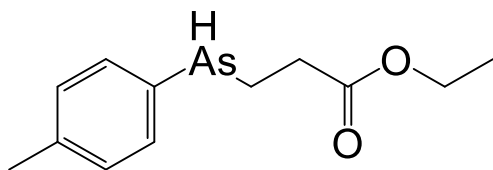
**Figure 7.29:** <sup>1</sup>H NMR spectrum (*p*-tolyl)As(H)CH<sub>2</sub>CH<sub>2</sub>C(O)OMe



**Figure 7.30:**  $^{13}\text{C}\{^1\text{H}\}$  NMR spectrum of  $(p\text{-tolyl})\text{As}(\text{H})\text{CH}_2\text{CH}_2\text{C}(\text{O})\text{OMe}$

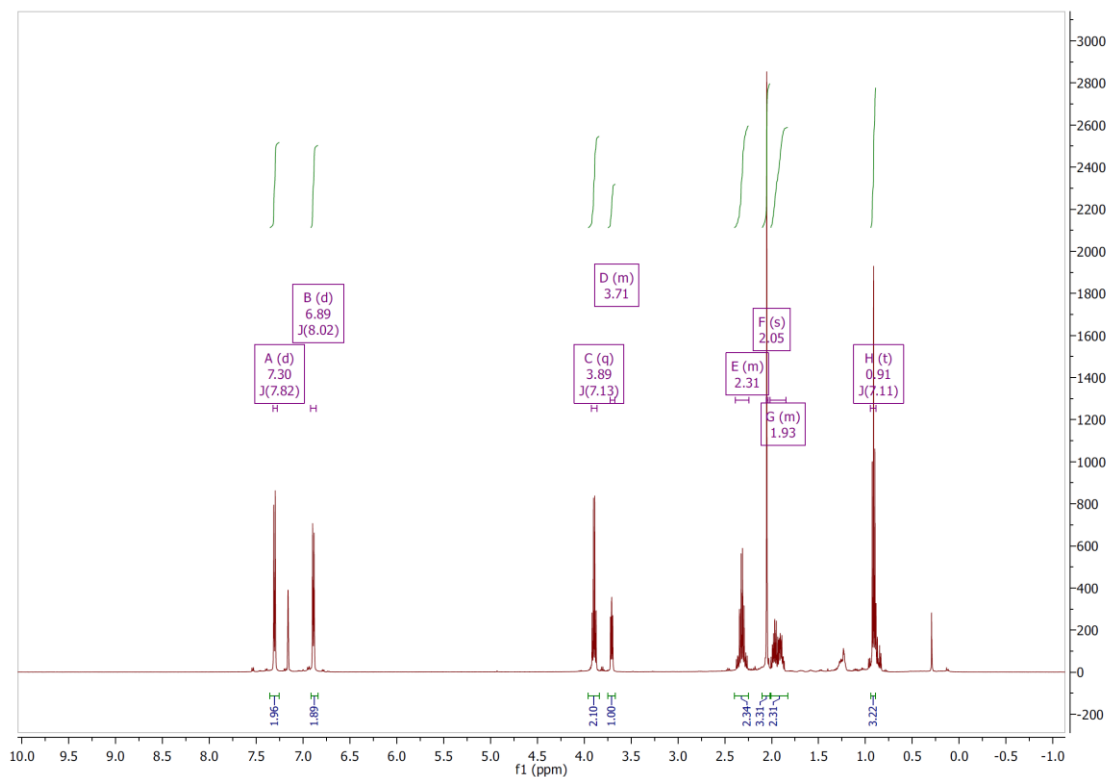


**Figure 7.31:** IR spectrum of  $(p\text{-tolyl})\text{As}(\text{H})\text{CH}_2\text{CH}_2\text{C}(\text{O})\text{OMe}$



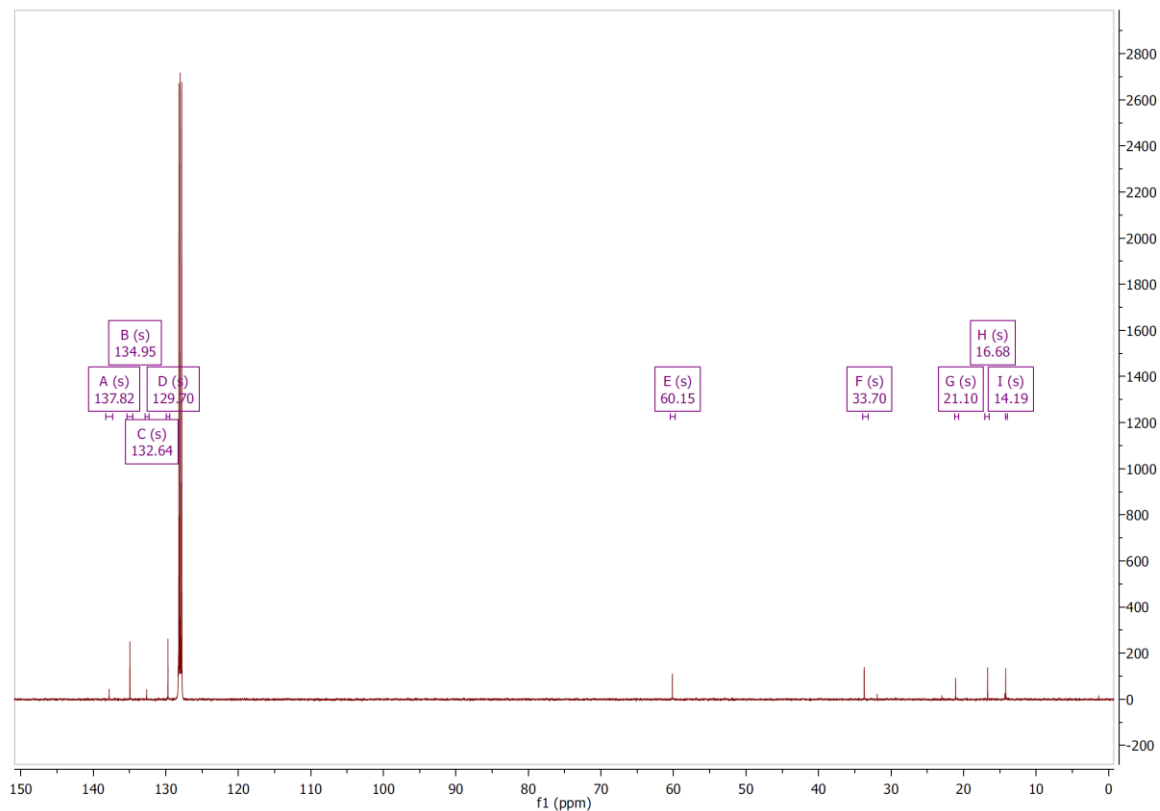
(*p*-tolyl)As(H)CH<sub>2</sub>CH<sub>2</sub>C(O)OEt

<sup>1</sup>H: δ 7.30 (d, *J* = 8 Hz, 2 H, C<sub>6</sub>H<sub>4</sub>CH<sub>3</sub>), 6.89 (d, *J* = 8 Hz, 2 H, C<sub>6</sub>H<sub>4</sub>CH<sub>3</sub>), 3.89 (q, *J* = 7 Hz, 2 H, CH<sub>2</sub>), 3.71 (m, 1 H, AsH), 2.31 (m, 2 H, CH<sub>2</sub>), 2.05 (s, 3 H, CH<sub>3</sub>), 1.93 (m, 2 H, CH<sub>2</sub>), 0.91 (t, 3 H, CH<sub>3</sub>). <sup>13</sup>C{<sup>1</sup>H}: δ 137.8 (s), 135.0 (s), 132.6 (s), 129.7 (s), 60.2 (s), 33.7 (s), 21.1 (s), 16.7 (s), 14.2 (s). MS calcd for C<sub>12</sub>H<sub>17</sub>AsO<sub>2</sub>: *m/z* 268.2. Found: 269.7. Formed under blacklight irradiation for 1 h at ambient temperature with 100% consumption of ethyl acrylate as measured by <sup>1</sup>H NMR spectroscopy. Isolated 69% yield as a colorless oil.

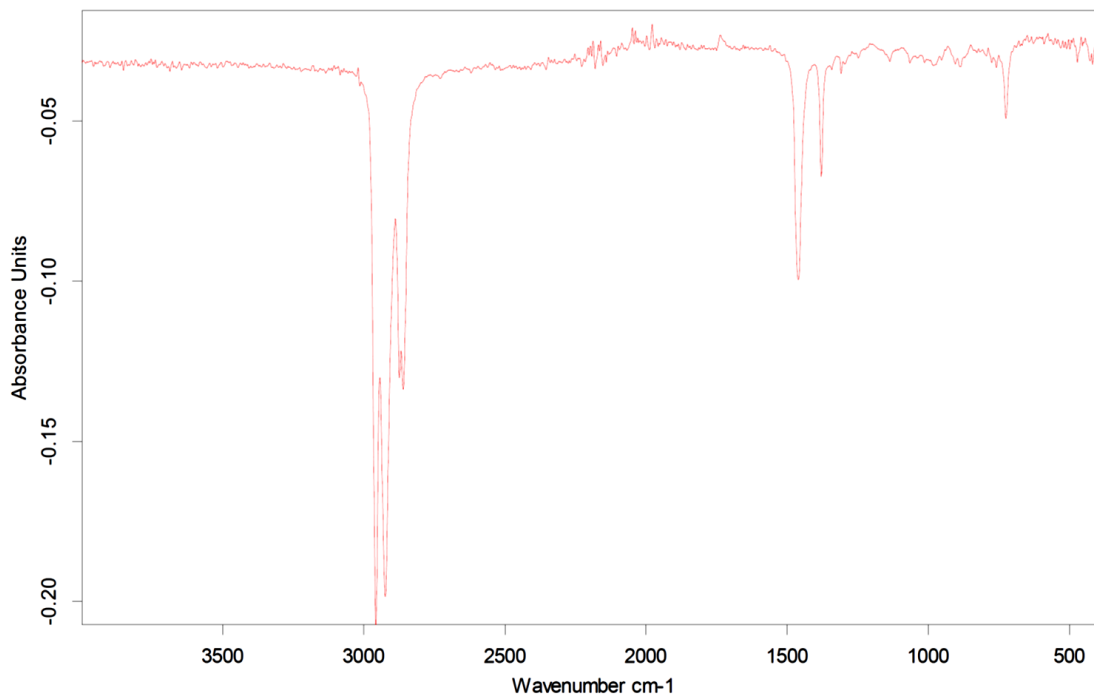


**Figure 7.32:** <sup>1</sup>H NMR spectrum (*p*-tolyl)As(H)CH<sub>2</sub>CH<sub>2</sub>C(O)OEt





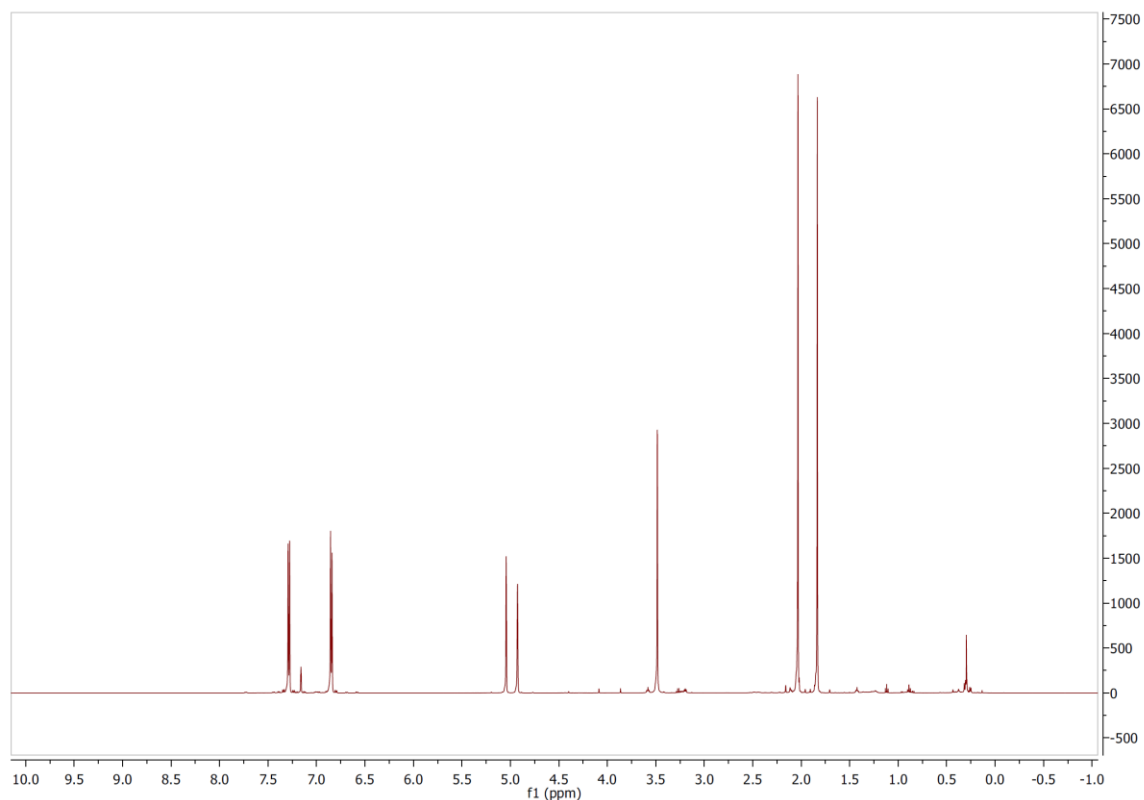
**Figure 7.33:** <sup>13</sup>C{<sup>1</sup>H} NMR spectrum of (p-tolyl)As(H)CH<sub>2</sub>CH<sub>2</sub>C(O)OEt



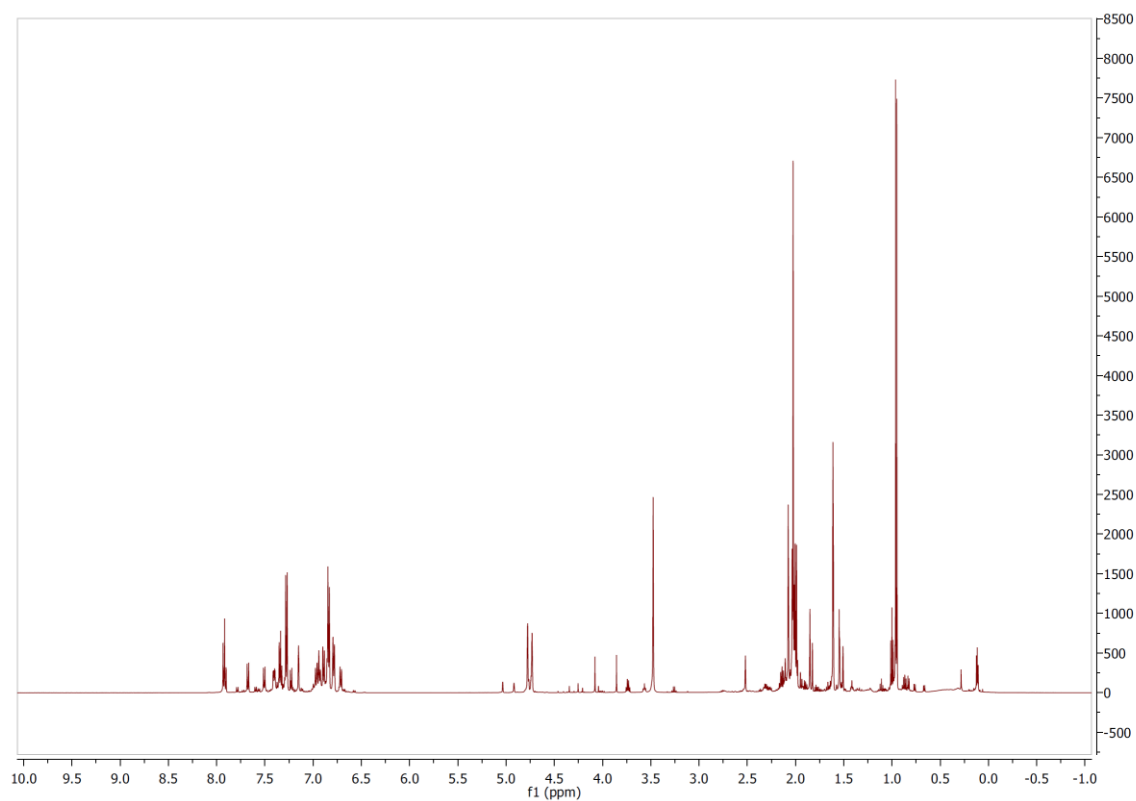
**Figure 7.34:** IR spectrum of (p-tolyl)As(H)CH<sub>2</sub>CH<sub>2</sub>C(O)OEt

### Hydrophosphination of 2,3-dimethyl-1,3-butadiene

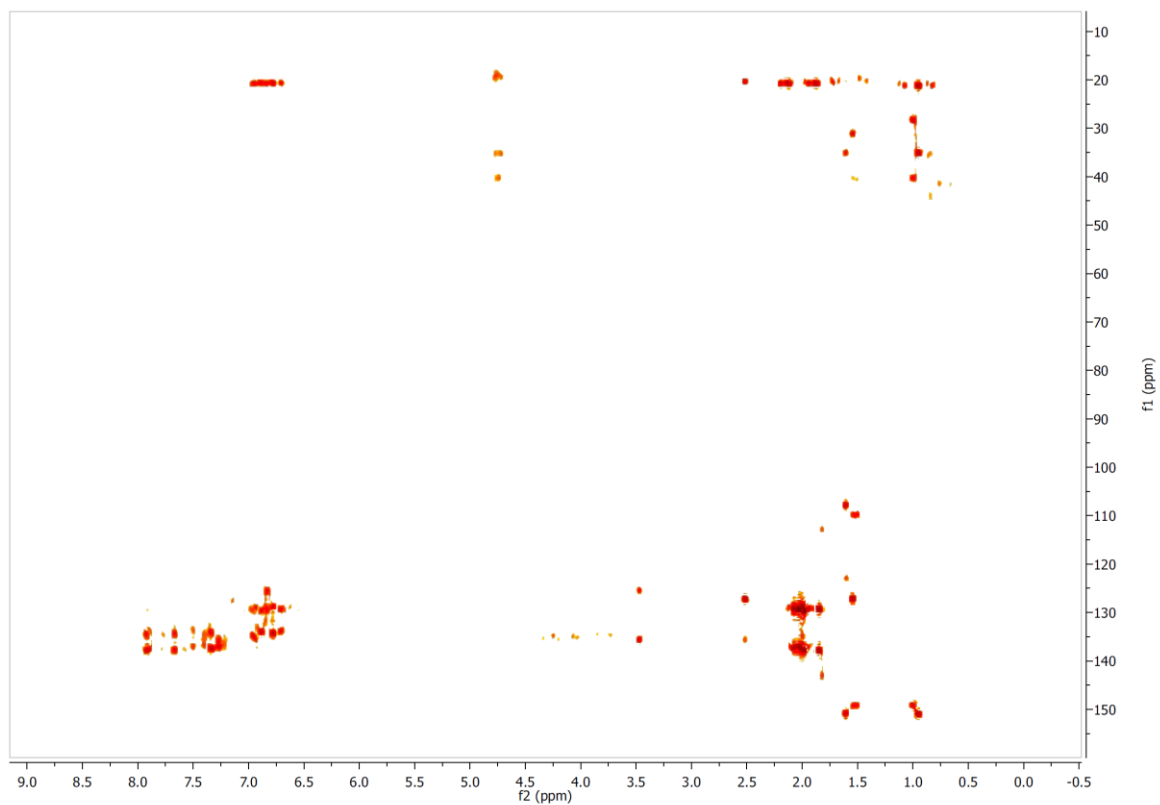
Conditions: 0.165 mmol *p*-tolylarsine, 0.084 mmol 2,3-dimethyl-1,3-butadiene, 0.0044 mmol **1**. Reaction goes to completion in 24 hours under irradiation from 253.7 nm lamps. Several products are unidentified.



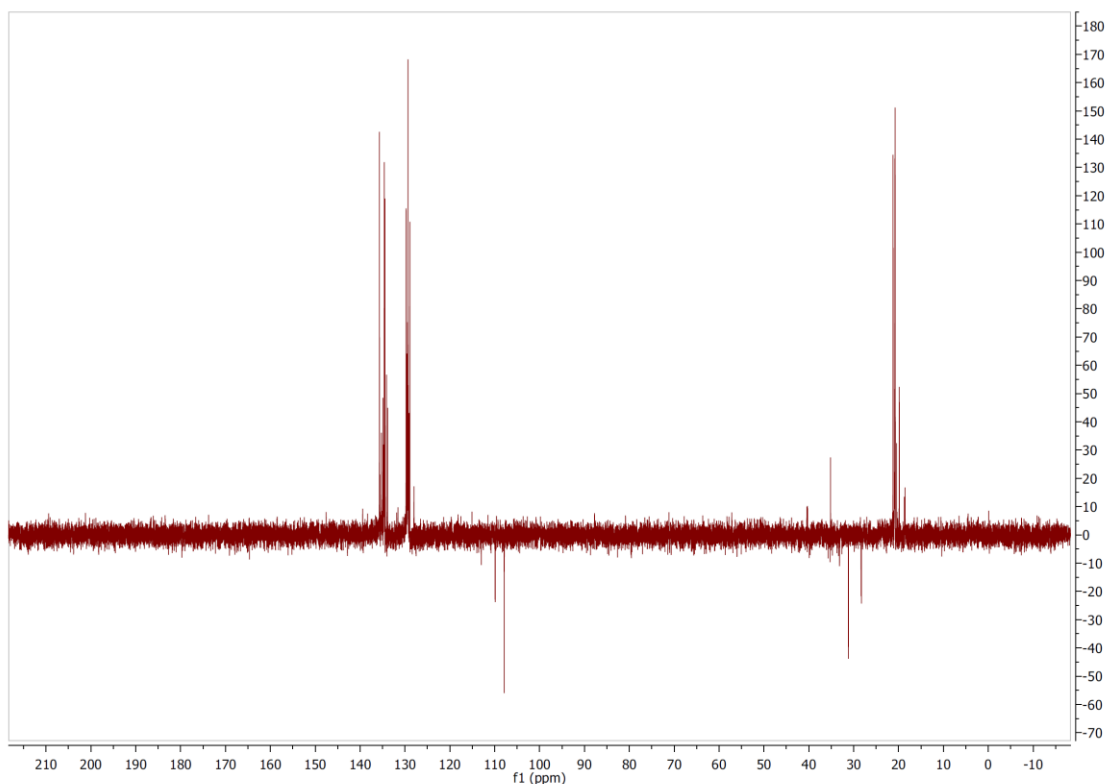
**Figure 7.35:** Initial <sup>1</sup>H NMR spectrum of the hydroarsination of 2,3-dimethyl-1,3-butadiene with *p*-tolylarsine



**Figure 7.36:** Final  $^1\text{H}$  NMR spectrum of the hydroarsination of 2,3-dimethyl-1,3-butadiene with *p*-tolylarsine



**Figure 7.37:**  $^{13}\text{C}$ – $^1\text{H}$  HMBC NMR spectrum of the hydroarsination of 2,3-dimethyl-1,3-butadiene with *p*-tolylarsine



**Figure 7.38:**  $^{13}\text{C}$  DEPT-135 NMR spectrum of the hydroarsination of 2,3-dimethyl-1,3-butadiene with *p*-tolylarsine

## 7.5 References

- (1) Gregson, A. M.; Wales, S. M.; Bailey, S. J.; Keller, P. A., *J. Organomet. Chem.* **2015**, 785, 77-83.
- (2) Berger, H. O.; Noeth, H., *J. Organomet. Chem.* **1983**, 250, 33-48.
- (3) Bungabong, M. L.; Tan, K. W.; Li, Y.; Selvaratnam, S. V.; Dongol, K. G.; Leung, P.-H., *Inorg. Chem.* **2007**, 46, 4733-4736.
- (4) Burt, J.; Levason, W.; Reid, G., *Coord. Chem. Rev.* **2014**, 260, 65-115.
- (5) Cheow, Y. L.; Pullarkat, S. A.; Li, Y.; Leung, P.-H., *J. Organomet. Chem.* **2012**, 696, 4215-4220.

- (6) Williams, J. O., *Angew. Chem. Int. Ed.* **1989**, 28, 1110-1120.
- (7) Lu, D.; Coote, M. L.; Ho, J.; Kilah, N. L.; Lin, C.-Y.; Salem, G.; Weir, M. L.; Willis, A. C.; Wild, S. B.; Dilda, P. J., *Organometallics* **2012**, 31, 1808-1816.
- (8) Denmark, S. E.; Ober, M. H., *Adv. Synth. Catal.* **2004**, 346, 1703-1714.
- (9) Kojima, A.; Boden, C. D. J.; Shibasaki, M., *Tetrahedron Lett.* **1997**, 38, 3459-3460.
- (10) Kojima, A.; Honzawa, S.; Boden, C. D. J.; Shibasaki, M., *Tetrahedron Lett.* **1997**, 38, 3455-3458.
- (11) Liu, F.; Pullarkat, S. A.; Li, Y.; Chen, S.; Leung, P.-H., *Eur. J. Inorg. Chem.* **2009**, 4134-4140.
- (12) Maitra, K.; Catalano, V. J.; Clark, J., III; Nelson, J. H., *Inorg. Chem.* **1998**, 37, 1105-1111.
- (13) Marquardt, C.; Balazs, G.; Baumann, J.; Virovets, A. V.; Scheer, M., *Chem. Eur. J.* **2017**, 23, 11423-11429.
- (14) Roering, A. J.; Davidson, J. J.; MacMillan, S. N.; Tanski, J. M.; Waterman, R., *Dalton Trans.* **2008**, 4488-4498.
- (15) Stubenhofer, M.; Lassandro, G.; Balazs, G.; Timoshkin, A. Y.; Scheer, M., *Chem. Commun.* **2012**, 48, 7262-7264.
- (16) Tay, W. S.; Yang, X.-Y.; Li, Y.; Pullarkat, S. A.; Leung, P.-H., *Chem. Commun.* **2017**, 53, 6307-6310.
- (17) Turbervill, R. S. P.; Goicoechea, J. M., *Eur. J. Inorg. Chem.* **2014**, 2014, 1660-1668.

- (18) Henke, K. R.; Hutchison, A. In *Arsenic chemistry*, John Wiley & Sons Ltd.: 2009; pp 9-68.
- (19) Kojima, A.; Boden, C. D. J.; Shibasaki, M., *Tetrahedron Lett.* **1997**, 38, 3459-3460.
- (20) Uberman, P. M.; Caira, M. R.; Martin, S. E., *Organometallics* **2013**, 32, 3220-3226.
- (21) Yambushev, F. D.; Usmanov, Z. I.; Shagidullin, R. R.; Khalitov, F. G.; Galeev, A. M.; Tenisheva, N. K., *Zh. Obshch. Khim.* **1978**, 48, 1766-1771.
- (22) Contrella, N. D.; Sampson, J. R.; Jordan, R. F., *Organometallics* **2014**, 33, 3546-3555.
- (23) Roering, A. J.; Davidson, J. J.; MacMillan, S. N.; Tanski, J. M.; Waterman, R., *Dalton Trans.* **2008**, 4488-4498.
- (24) Waterman, R., *Organometallics* **2007**, 26, 2492-2494.

## CHAPTER 8: GENERAL CONCLUSION

This work addresses challenges in metal-catalyzed hydrophosphination with a metal catalyst,  $[\kappa^5\text{-}N,N,N,N,C\text{-(Me}_3\text{SiNCH}_2\text{CH}_2)_2\text{NCH}_2\text{CH}_2\text{-NSiMe}_2\text{CH}_2]\text{Zr}$  (**1**). Catalytic hydrophosphination with **1** displays remarkable precision for generating a variety of hydrophosphination products. For example, secondary phosphines can be isolated exclusively over tertiary phosphines, or vice versa, merely by modification of the reaction stoichiometry. This allows for increasingly high product selectivity under relatively mild conditions. Elaboration of this chemistry to a chiral, air-stable primary phosphine returned chiral phosphine products.

Catalytic hydrophosphination with **1** resulted in the first report of double hydrophosphination of internal alkynes with primary phosphines. That hydrophosphination generated isolable vinyl phosphines or isolable double hydrophosphination products, depending on reaction conditions. This photocatalytic reaction proceeds with high selectivity for secondary phosphine product formation; no tertiary phosphine products were detected.

Reactions run under photolysis substantially enhanced the activity of the catalyst such that quantitative amounts of reaction products could be isolated in as little as twenty minutes at ambient temperature. Photocatalytic hydrophosphination allows for a broadened substrate scope such that a variety of unactivated alkenes, almost entirely absent from this reaction, became viable candidates. Furthermore, an unprecedented tandem intermolecular and intramolecular hydrophosphination with a diene to make a phosphacycle was realized under photolysis. Computational and spectroscopic data indicate that photoexcitation at a



variety of wavelengths results in a charge transfer in the active catalyst. This excitation appears to accelerate catalysis by promoting substrate insertion based on a linear free-energy relationship.

Catalytic hydroarsination with primary arsines to form secondary arsines was realized for the first time with **1**. This transformation requires light to proceed, although the light dependence is not as strong and the turnover numbers are modest. It may be the case that the identity of the excited state reached by photoexcitation may have more arsenic character, which makes the charge-transfer event necessary, although not as turnover-limiting as that understood for catalytic hydroarsination.

Attempts at making a chiral ligand for catalytic hydrophosphination to form *P*-chiral phosphines is discussed, but as yet, unrealized. Development of this methodology would address key challenges in catalytic hydrophosphination, given the unusual and attractive behavior of **1**. Catalytic hydrophosphination with primary phosphines to selectively generate secondary phosphines under fast reaction times, with high selectivity, and amenability to a broad substrate class would be highly attractive. This would close the gap on metal catalysts and substrates for this reaction. Currently only a handful of precious metal catalysts are capable of this transformation and are substantially limited by substrate identity.

## CHAPTER 9: COMPREHENSIVE BIBLIOGRAPHY

- (1) Albert, J.; Cadena, J. M.; Granell, J.; Muller, G.; Panyella, D.; Sanudo, C., *Eur. J. Inorg. Chem.* **2000**, 1283-1286.
- (2) Al-Shboul, T. M. A.; Goerls, H.; Westerhausen, M., *Inorg. Chem. Commun.* **2008**, *11*, 1419-1421.
- (3) Al-Shboul, T. M. A.; Palfi, V. K.; Yu, L.; Kretschmer, R.; Wimmer, K.; Fischer, R.; Goerls, H.; Reiher, M.; Westerhausen, M., *J. Organomet. Chem.* **2010**, *696*, 216-227.
- (4) Ananikov, V. P.; Beletskaya, I. P., *Chem. Asian J.* **2011**, *6*, 1423-1430.
- (5) Andrushko, N.; Boerner, A. In *Phosphine-boranes and related P-compounds as intermediates in the syntheses of chiral ligands and organocatalysts*, Wiley-VCH Verlag GmbH & Co. KGaA: 2008; pp 1275-1347.
- (6) Baber, R. A.; Haddow, M. F.; Middleton, A. J.; Orpen, A. G.; Pringle, P. G.; Haynes, A.; Williams, G. L.; Papp, R., *Organometallics* **2007**, *26*, 713-725.
- (7) Baker, R. T.; Whitney, J. F.; Wreford, S. S., *Organometallics* **1983**, *2*, 1049-1051.
- (8) Bange, C.; Mucha, N.; Cousins, M.; Gehsmann, A.; Singer, A.; Truax, T.; Higham, L.; Waterman, R., *Inorganics* **2016**, *4*, 26.
- (9) Bange, C. A.; Ghebreab, M. B.; Ficks, A.; Mucha, N. T.; Higham, L.; Waterman, R., *Dalton Trans.* **2016**, *45*, 1863-1867.
- (10) Bange, C. A.; Waterman, R., *ACS Catal.* **2016**, *6*, 6413-6416.
- (11) Bange, C. A.; Waterman, R., *Chem. Eur. J.* **2016**, *22*, 12598-12605.
- (12) Barre, C.; Boudot, P.; Kubicki, M. M.; Moiese, C., *Inorg. Chem.* **1995**, *34*, 284-291.
- (13) Bartoli, G.; Bosco, M.; Sambri, L.; Marcantoni, E., *Tetrahedron Lett.* **1996**, *37*, 7421-7424.
- (14) Basalov, I. V.; Dorcet, V.; Fukin, G. K.; Carpentier, J.-F.; Sarazin, Y.; Trifonov, A. A., *Chem. Eur. J.* **2015**, *21*, 6033-6036.
- (15) Basalov, I. V.; Rosca, S. C.; Lyubov, D. M.; Selikhov, A. N.; Fukin, G. K.; Sarazin, Y.; Carpentier, J.-F.; Trifonov, A. A., *Inorg. Chem.* **2014**, *53*, 1654-1661.
- (16) Basalov, I. V.; Yurova, O. S.; Cherkasov, A. V.; Fukin, G. K.; Trifonov, A. A., *Inorg. Chem.* **2016**, *55*, 1236-1244.
- (17) Becker, G.; Mundt, O.; Roessler, M.; Schneider, E., *Z. Anorg. Allg. Chem.* **1978**, *443*, 42-52.
- (18) Behrle, A. C.; Schmidt, J. A. R., *Organometallics* **2013**, *32*, 1141-1149.
- (19) Belli, R. G.; Burton, K. M. E.; Rufh, S. A.; McDonald, R.; Rosenberg, L., *Organometallics* **2015**, *34*, 5637-5646.
- (20) Berger, H. O.; Noeth, H., *J. Organomet. Chem.* **1983**, *250*, 33-48.
- (21) Boar, P.; Streithberger, M.; Lönnecke, P.; Hey-Hawkins, E., *Inorg. Chem.* **2017**, *56*, 7285-7291.
- (22) Bourumeau, K.; Gaumont, A.-C.; Denis, J.-M., *J. Organomet. Chem.* **1997**, *529*, 205-213.
- (23) Brooks, P.; Gallagher, M. J.; Sarroff, A., *Aust. J. Chem.* **1987**, *40*, 1341-1351.
- (24) Brown, A. C.; Carpino, L. A., *J. O. C.* **1985**, *50*, 1749-1750.

- (25) Brown, C. A.; Nile, T. A.; Mahon, M. F.; Webster, R. L., *Dalton Trans.* **2015**, 44, 12189-12195.
- (26) Brynda, M., *Coord. Chem. Rev.* **2005**, 249, 2013-2034.
- (27) Buhro, W. E.; Gladysz, J. A., *Inorg. Chem.* **1985**, 24, 3505-3507.
- (28) Buhro, W. E.; Zwick, B. D.; Georgiou, S.; Hutchinson, J. P.; Gladysz, J. A., *J. Am. Chem. Soc.* **1988**, 110, 2427-2439.
- (29) Bungabong, M. L.; Tan, K. W.; Li, Y.; Selvaratnam, S. V.; Dongol, K. G.; Leung, P.-H., *Inorg. Chem.* **2007**, 46, 4733-4736.
- (30) Burk, M. J., *Acc. Chem. Res.* **2000**, 33, 363-372.
- (31) Burk, M. J.; Gross, M. F.; Martinez, J. P., *J. Am. Chem. Soc.* **1995**, 117, 9375-9376.
- (32) Burk, M. J.; Harper, T. G. P.; Kalberg, C. S., *J. Am. Chem. Soc.* **1995**, 117, 4423-4424.
- (33) Burt, J.; Levason, W.; Reid, G., *Coord. Chem. Rev.* **2014**, 260, 65-115.
- (34) Busacca, C. A.; Farber, E.; De Young, J.; Campbell, S.; Gonnella, N. C.; Grinberg, N.; Haddad, N.; Lee, H.; Ma, S.; Reeves, D.; Shen, S.; Senanayake, C. H., *Org. Lett.* **2009**, 11, 5594-5597.
- (35) Butler, M. S.; Buss, A. D., *Biochem. Pharmacol.* **2006**, 71, 919-929.
- (36) Carpentier, J.-F.; Liu, B.; Sarazin, Y. In *Charge-neutral and cationic complexes of large alkaline earths for ring-opening polymerization and fine chemicals catalysis*, John Wiley & Sons, Inc.: 2014; pp 359-378, 351 plate.
- (37) Cernerud, M.; Adolfsson, H.; Moberg, C., *Tetrahedron: Asymmetry* **1997**, 8, 2655-2662.
- (38) Chen, G.-Q.; Kehr, G.; Daniliuc, C. G.; Wibbeling, B.; Erker, G., *Chem. Eur. J.* **2015**, 21, 12449-12455.
- (39) Chen, G.-Q.; Zhang, X.-N.; Wei, Y.; Tang, X.-Y.; Shi, M., *Angew. Chem. Int. Ed.* **2014**, 53, 8492-8497.
- (40) Cheow, Y. L.; Pullarkat, S. A.; Li, Y.; Leung, P.-H., *J. Organomet. Chem.* **2012**, 696, 4215-4220.
- (41) Chew, R. J.; Teo, K. Y.; Huang, Y.; Li, B.-B.; Li, Y.; Pullarkat, S. A.; Leung, P.-H., *Chem. Commun.* **2014**, 50, 8768-8770.
- (42) Ciganek, E., *Org. React. (Hoboken, NJ, U. S.)* **2008**, 72, 1-366.
- (43) Claridge, T. D. W., *High-Resolution NMR Techniques in Organic Chemistry*. Elsevier: 2009; Vol. 27.
- (44) Contrella, N. D.; Sampson, J. R.; Jordan, R. F., *Organometallics* **2014**, 33, 3546-3555.
- (45) Corbridge, D. E. C., *Phosphorus: Chemistry, Biochemistry, and Technology*. 6 ed.; CRC Press: Boca Raton, Florida, 2013; p 1473.
- (46) Cordell, D.; White, S., *Sustainability* **2011**, 3, 2027.
- (47) Costa, E.; Pringle, P. G.; Worboys, K., *Chem. Commun.* **1998**, 49-50.
- (48) Cox, P. A., *The Elements: Their Origin, Abundance, and Distribution*. Oxford University Press: Oxford 1989.
- (49) Crimmin, M. R.; Barrett, A. G. M.; Hill, M. S.; Hitchcock, P. B.; Procopiou, P. A., *Organometallics* **2007**, 26, 2953-2956.

- (50) Crimmin, M. R.; Barrett, A. G. M.; Hill, M. S.; Hitchcock, P. B.; Procopiou, P. A., *Organometallics* **2008**, 27, 497-499.
- (51) Crisp, G. T.; Salem, G.; Stephens, F. S.; Wild, S. B., *J. Chem. Soc., Chem. Commun.* **1987**, 600-602.
- (52) Crisp, G. T.; Salem, G.; Wild, S. B.; Stephens, F. S., *Organometallics* **1989**, 8, 2360-2367.
- (53) Davies, J. H.; Downer, J. D.; Kirby, P., *J. Chem. Soc. C* **1966**, 245-247.
- (54) Davies, L. H.; Harrington, R. W.; Clegg, W.; Higham, L. J., *Dalton Trans.* **2014**, 43, 13485-13499.
- (55) Davies, L. H.; Kasten, B. B.; Benny, P. D.; Arrowsmith, R. L.; Ge, H.; Pascu, S. I.; Botchway, S. W.; Clegg, W.; Harrington, R. W.; Higham, L. J., *Chem. Commun.* **2014**, 50, 15503-15505.
- (56) Davies, L. H.; Stewart, B.; Harrington, R. W.; Clegg, W.; Higham, L. J., *Angew. Chem. Int. Ed.* **2012**, 51, 4921-4924.
- (57) Davies, L. H.; Stewart, B.; Higham, L. J., *Organomet. Chem.* **2014**, 39, 51-71.
- (58) Davies, L. H.; Wallis, J. F.; Probert, M. R.; Higham, L. J., *Synthesis* **2014**, 46, 2622-2628.
- (59) Delacroix, O.; Gaumont, A. C., *Curr. Org. Chem.* **2005**, 9, 1851-1882.
- (60) Delavarenne, S. Y.; Viehe, H. G., *Chem. Ber.* **1970**, 103, 1198-1208.
- (61) Denmark, S. E.; Ober, M. H., *Adv. Synth. Catal.* **2004**, 346, 1703-1714.
- (62) Derrah, E. J.; Pantazis, D. A.; McDonald, R.; Rosenberg, L., *Angew. Chem. Int. Ed.* **2010**, 49, 3367-3370.
- (63) Deyris, P.-A.; Caneque, T.; Wang, Y.; Retailleau, P.; Bigi, F.; Maggi, R.; Maestri, G.; Malacria, M., *ChemCatChem* **2015**, 7, 3266-3269.
- (64) Di Giuseppe, A.; De Luca, R.; Castarlenas, R.; Perez-Torrente, J. J. J.; Crucianelli, M.; Oro, L. A., *Chem. Commun.* **2016**, 52, 5554-5557.
- (65) Douglass, M. R.; Marks, T. J., *J. Am. Chem. Soc.* **2000**, 122, 1824-1825.
- (66) Douglass, M. R.; Ogasawara, M.; Hong, S.; Metz, M. V.; Marks, T. J., *Organometallics* **2002**, 21, 283-292.
- (67) Douglass, M. R.; Stern, C. L.; Marks, T. J., *J. Am. Chem. Soc.* **2001**, 123, 10221-10238.
- (68) Drago, R. S., *Organometallics* **1995**, 14, 3408-3417.
- (69) Dubrovina, N. V.; Tararov, V. I.; Monsees, A.; Kadyrov, R.; Fischer, C.; Borner, A., *Tetrahedron: Asymmetry* **2003**, 14, 2739-2745.
- (70) Dupre, J.; Gaumont, A.-C.; Lakhdar, S., *Org. Lett.* **2017**, 19, 694-697.
- (71) Dutartre, M.; Bayardon, J.; Juge, S., *Chem. Soc. Rev.* **2016**, 45, 5771-5794.
- (72) Edwards, P. G.; Malik, K. M. A.; Ooi, L.-I.; Price, A. J., *Dalton Trans.* **2006**, 433-441.
- (73) Eric V. Anslyn, D. A. D., *Modern Physical Organic Chemistry*. University Science Books: 2006.
- (74) Erickson, K. A.; Dixon, L. S. H.; Wright, D. S.; Waterman, R., *Inorg. Chim. Acta* **2014**, 422, 141-145.
- (75) Erickson, K. A.; Stelmach, J. P. W.; Mucha, N. T.; Waterman, R., *Organometallics* **2015**, 34, 4693-4699.

- (76) Espinal-Viguri, M.; King, A. K.; Lowe, J. P.; Mahon, M. F.; Webster, R. L., *ACS Catal.* **2016**, *6*, 7892-7897.
- (77) Espinal-Viguri, M.; Mahon, M. F.; Tyler, S. N. G.; Webster, R. L., *Tetrahedron* **2017**, *73*, 64-69.
- (78) Falagas, M. E.; Kastoris, A. C.; Kapaskelis, A. M.; Karageorgopoulos, D. E., *Lancet Infect. Dis.* **2010**, *10*, 43-50.
- (79) Farras, J.; Ginesta, X.; Sutton, P. W.; Taltavull, J.; Egeler, F.; Romea, P.; Urpi, F.; Vilarrasa, J., *Tetrahedron* **2001**, *57*, 7665-7674.
- (80) Featherman, S. I.; Quin, L. D., *J. Am. Chem. Soc.* **1975**, *97*, 4349-4356.
- (81) Feng, J.-J.; Chen, X.-F.; Shi, M.; Duan, W.-L., *J. Am. Chem. Soc.* **2010**, *132*, 5562-5563.
- (82) Ficks, A.; Clegg, W.; Harrington, R. W.; Higham, L. J., *Organometallics* **2014**, *33*, 6319-6329.
- (83) Ficks, A.; Harrington, R. W.; Higham, L. J., *Dalton Trans.* **2013**, *42*, 6302-6305.
- (84) Ficks, A.; Hiney, R. M.; Harrington, R. W.; Gilheany, D. G.; Higham, L. J., *Dalton Trans.* **2012**, *41*, 3515-3522.
- (85) Ficks, A.; Martinez-Botella, I.; Stewart, B.; Harrington, R. W.; Clegg, W.; Higham, L. J., *Chem. Commun.* **2011**, *47*, 8274-8276.
- (86) Ficks, A.; Sibbald, C.; Ojo, S.; Harrington, R. W.; Clegg, W.; Higham, L. J., *Synthesis* **2013**, *45*, 265-271.
- (87) Field, L. D.; Thomas, I. P., *Inorg. Chem.* **1996**, *35*, 2546-2548.
- (88) Fleming, J. T.; Higham, L. J., *Coord. Chem. Rev.* **2015**, *297-298*, 127-145.
- (89) Fluck, E.; Issleib, K., *Chem. Ber.* **1965**, *98*, 2674-2680.
- (90) Fryzuk, M. D.; Bosnich, B., *J. Am. Chem. Soc.* **1978**, *100*, 5491-5494.
- (91) Gallagher, K. J.; Espinal-Viguri, M.; Mahon, M. F.; Webster, R. L., *Adv. Synth. Catal.* **2016**, *358*, 2460-2468.
- (92) Gallagher, K. J.; Webster, R. L., *Chem. Commun.* **2014**, *50*, 12109-12111.
- (93) Galloway, T.; Handy, R., *Ecotoxicology* **2003**, *12*, 345-363.
- (94) Gan, K.; Sadeer, A.; Xu, C.; Li, Y.; Pullarkat, S. A., *Organometallics* **2014**, *33*, 5074-5076.
- (95) Ganushevich, Y. S.; Miluykov, V. A.; Polyancev, F. M.; Latypov, S. K.; Lönnecke, P.; Hey-Hawkins, E.; Yakhvarov, D. G.; Sinyashin, O. G., *Organometallics* **2013**, *32*, 3914-3919.
- (96) Ganushevich, Y. S.; Miluykov, V. A.; Polyancev, F. M.; Latypov, S. K.; Lönnecke, P.; Hey-Hawkins, E.; Yakhvarov, D. G.; Sinyashin, O. G., *Organometallics* **2013**, *32*, 3914-3919.
- (97) Garner, M. E.; Parker, B. F.; Hohloch, S.; Bergman, R. G.; Arnold, J., *J. Am. Chem. Soc.* **2017**, *139*, 12935-12938.
- (98) Geer, A. M.; Serrano, A. L.; de Bruin, B.; Ciriano, M. A.; Tejel, C., *Angew. Chem. Int. Ed.* **2015**, *54*, 472-475.
- (99) Genet, C.; Canipa, S. J.; O'Brien, P.; Taylor, S., *J. Am. Chem. Soc.* **2006**, *128*, 9336-9337.
- (100) Ghebreab, M. B.; Bange, C. A.; Waterman, R., *J. Am. Chem. Soc.* **2014**, *136*, 9240-9243.

- (101) Ghebreab, M. B.; Shalumova, T.; Tanski, J. M.; Waterman, R., *Polyhedron* **2010**, 29, 42-45.
- (102) Glueck, D. S., *Chem. Eur. J.* **2008**, 14, 7108-7117.
- (103) Glueck, D. S., *Coord. Chem. Rev.* **2008**, 252, 2171-2179.
- (104) Glueck, D. S., *Dalton Trans.* **2008**, 5276-5286.
- (105) Glueck, D. S., *Top. Organomet. Chem.* **2010**, 31, 65-100.
- (106) Gobbini, M.; Armaroli, S.; Banfi, L.; Benicchio, A.; Carzana, G.; Fedrizzi, G.; Ferrari, P.; Giacalone, G.; Giubileo, M.; Marazzi, G.; Micheletti, R.; Moro, B.; Pozzi, M.; Scotti, P. E.; Torri, M.; Cerri, A., *J. Med. Chem.* **2008**, 51, 4601-4608.
- (107) Gregson, A. M.; Wales, S. M.; Bailey, S. J.; Keller, P. A., *J. Organomet. Chem.* **2015**, 785, 77-83.
- (108) Gu, X.; Zhang, L.; Zhu, X.; Wang, S.; Zhou, S.; Wei, Y.; Zhang, G.; Mu, X.; Huang, Z.; Hong, D.; Zhang, F., *Organometallics* **2015**, 34, 4553-4559.
- (109) Gusarova, N. K.; Chernysheva, N. A.; Klyba, L. V.; Shagun, V. A.; Yas'ko, S. V.; Smirnov, V. I.; Trofimov, B. A., *J. Organomet. Chem.* **2013**, 745-746, 126-132.
- (110) Gusarova, N. K.; Shaikhutdinova, S. I.; Kazantseva, T. I.; Malysheva, S. F.; Sukhov, B. G.; Belogorlova, N. A.; Dmitriev, V. I.; Trofimov, B. A., *Russ. J. Gen. Chem.* **2002**, 72, 371-375.
- (111) Gusarova, N. K.; Volkov, P. A.; Ivanova, N. I.; Khrapova, K. O.; Albanov, A. I.; Trofimov, B. A., *Russ. J. Gen. Chem.* **2016**, 86, 731-734.
- (112) Guterman, R.; Gillies, E. R.; Ragogna, P. J., *Dalton Trans.* **2015**, 44, 15664-15670.
- (113) Hajela, S. P.; Johnson, A. R.; Xu, J.; Sunderland, C. J.; Cohen, S. M.; Caulder, D. L.; Raymond, K. N., *Inorg. Chem.* **2001**, 40, 3208-3216.
- (114) Hao, X.-Q.; Huang, J.-J.; Wang, T.; Lv, J.; Gong, J.-F.; Song, M.-P., *J. Org. Chem.* **2014**, 79, 9512-9530.
- (115) Hao, X.-Q.; Zhao, Y.-W.; Yang, J.-J.; Niu, J.-L.; Gong, J.-F.; Song, M.-P., *Organometallics* **2014**, 33, 1801-1811.
- (116) Hayashi, T.; Niizuma, S.; Kamikawa, T.; Suzuki, N.; Uozumi, Y., *J. Am. Chem. Soc.* **1995**, 117, 9101-9102.
- (117) Henke, K. R.; Hutchison, A. In *Arsenic chemistry*, John Wiley & Sons Ltd.: 2009; pp 9-68.
- (118) Hiney, R. M.; Ficks, A.; Muller-Bunz, H.; Gilheany, D. G.; Higham, L. J., Air-stable chiral primary phosphines part (i) synthesis, stability and applications. In *Organometallic Chemistry: Volume 37*, The Royal Society of Chemistry: 2011; Vol. 37, pp 27-45.
- (119) Hiney, R. M.; Higham, L. J.; Mueller-Bunz, H.; Gilheany, D. G., *Angew. Chem. Int. Ed.* **2006**, 45, 7248-7251.
- (120) Holland, P. L.; Andersen, R. A.; Bergman, R. G., *Comments on Inorganic Chemistry* **1999**, 21, 115-129.
- (121) Hoye, P. A. T.; Pringle, P. G.; Smith, M. B.; Worboys, K., *J. Chem. Soc., Dalton Trans.* **1993**, 269-274.
- (122) Hu, H.; Cui, C., *Organometallics* **2012**, 31, 1208-1211.

- (123) Huang, J.-S.; Yu, G.-A.; Xie, J.; Wong, K.-M.; Zhu, N.; Che, C.-M., *Inorg. Chem.* **2008**, *47*, 9166-9181.
- (124) Huang, Y.; Chew, R. J.; Li, Y.; Pullarkat, S. A.; Leung, P.-H., *Org. Lett.* **2011**, *13*, 5862-5865.
- (125) Huang, Y.; Chew, R. J.; Pullarkat, S. A.; Li, Y.; Leung, P.-H., *J. Org. Chem.* **2012**, *77*, 6849-6854.
- (126) Huang, Y.; Pullarkat, S. A.; Li, Y.; Leung, P.-H., *Chem. Commun.* **2010**, *46*, 6950-6952.
- (127) Huang, Y.; Pullarkat, S. A.; Li, Y.; Leung, P.-H., *Inorg. Chem.* **2012**, *51*, 2533-2540.
- (128) Huang, Y.; Pullarkat, S. A.; Teong, S.; Chew, R. J.; Li, Y.; Leung, P.-H., *Organometallics* **2012**, *31*, 4871-4875.
- (129) Hutchins, R. O.; Hutchins, M. K., Magnesium–Methanol. In *Encyclopedia of Reagents for Organic Synthesis*, John Wiley & Sons, Ltd: 2001.
- (130) Imamoto, T.; Oshiki, T.; Onozawa, T.; Kusumoto, T.; Sato, K., *J. Am. Chem. Soc.* **1990**, *112*, 5244-5252.
- (131) Ingold, C. K.; Shaw, F. R., *J. Chem. Soc.* **1927**, 2918-2926.
- (132) Isley, N. A.; Linstadt, R. T. H.; Slack, E. D.; Lipshutz, B. H., *Dalton Trans.* **2014**, *43*, 13196-13200.
- (133) Itazaki, M.; Katsube, S.; Kamitani, M.; Nakazawa, H., *Chem. Commun.* **2016**, *52*, 3163-3166.
- (134) Ji, H.-m.; Wei, L.-q., *Wujing Houqin Xueyuan Xuebao, Yixueban* **2015**, *24*, 845-848.
- (135) Ji, P.; Sawano, T.; Lin, Z.; Urban, A.; Boures, D.; Lin, W., *J. Am. Chem. Soc.* **2016**, *138*, 14860-14863.
- (136) Jian, Z.; Kehr, G.; Daniliuc, C. G.; Wibbeling, B.; Erker, G., *Dalton Trans.* **2017**, *46*, 11715-11721.
- (137) Jimenez, M. V.; Perez-Torrente, J. J.; Bartolome, M. I.; Oro, L. A., *Synthesis* **2009**, 1916-1922.
- (138) Join, B.; Mimeau, D.; Delacroix, O.; Gaumont, A.-C., *Chem. Commun.* **2006**, 3249-3251.
- (139) Joseph, J.; RajanBabu, T. V.; Jemmis, E. D., *Organometallics* **2009**, *28*, 3552-3566.
- (140) Kagan, H. B.; Tahar, M.; Fiaud, J. C., *Tetrahedron Lett.* **1991**, *32*, 5959-5962.
- (141) Kamitani, M.; Itazaki, M.; Tamiya, C.; Nakazawa, H., *J. Am. Chem. Soc.* **2012**, *134*, 11932-11935.
- (142) Kawaoka, A. M.; Douglass, M. R.; Marks, T. J., *Organometallics* **2003**, *22*, 4630-4632.
- (143) Kawaoka, A. M.; Marks, T. J., *J. Am. Chem. Soc.* **2004**, *126*, 12764-12765.
- (144) Kazankova, M. A.; Efimova, I. V.; Kochetkov, A. N.; Afanas'ev, V. V.; Beletskaya, I. P.; Dixneuf, P. H., *Synlett* **2001**, 497-500.
- (145) Kazankova, M. A.; Shulyupin, M. O.; Borisenko, A. A.; Beletskaya, I. P., *Russ. J. Org. Chem.* **2002**, *38*, 1479-1484.

- (146) Kenaree, A. R.; Cuthbert, T. J.; Barbon, S. M.; Boyle, P. D.; Gillies, E. R.; Ragogna, P. J.; Gilroy, J. B., *Organometallics* **2015**, *34*, 4272-4280.
- (147) King, A. K.; Buchard, A.; Mahon, M. F.; Webster, R. L., *Chem. Eur. J.* **2015**, *21*, 15960-15963.
- (148) King, A. K.; Gallagher, K. J.; Mahon, M. F.; Webster, R. L., *Chem. Eur. J.* **2017**, *23*, 9039-9043.
- (149) Kissel, A. A.; Mahrova, T. V.; Lyubov, D. M.; Cherkasov, A. V.; Fukin, G. K.; Trifonov, A. A.; Del Rosal, I.; Maron, L., *Dalton Trans.* **2015**, *44*, 12137-12148.
- (150) Kojima, A.; Boden, C. D. J.; Shibasaki, M., *Tetrahedron Lett.* **1997**, *38*, 3459-3460.
- (151) Kojima, A.; Boden, C. D. J.; Shibasaki, M., *Tetrahedron Lett.* **1997**, *38*, 3459-3460.
- (152) Kojima, A.; Honzawa, S.; Boden, C. D. J.; Shibasaki, M., *Tetrahedron Lett.* **1997**, *38*, 3455-3458.
- (153) Komeyama, K.; Kawabata, T.; Takehira, K.; Takaki, K., *J. Org. Chem.* **2005**, *70*, 7260-7266.
- (154) Kondoh, A.; Yorimitsu, H.; Oshima, K., *J. Am. Chem. Soc.* **2007**, *129*, 4099-4104.
- (155) Koshti, V.; Gaikwad, S.; Chikkali, S. H., *Coord. Chem. Rev.* **2014**, *265*, 52-73.
- (156) Kovacik, I.; Wicht, D. K.; Grewal, N. S.; Glueck, D. S.; Incarvito, C. D.; Guzei, I. A.; Rheingold, A. L., *Organometallics* **2000**, *19*, 950-953.
- (157) Lapprand, A.; Dutartre, M.; Khiri, N.; Levert, E.; Fortin, D.; Rousselin, Y.; Soldera, A.; Juge, S.; Harvey, P. D., *Inorg. Chem.* **2013**, *52*, 7958-7967.
- (158) Lapshin, I. V.; Yurova, O. S.; Basalov, I. V.; Rad'kov, V. Y.; Musina, E. I.; Cherkasov, A. V.; Fukin, G. K.; Karasik, A. A.; Trifonov, A. A., *Inorg. Chem.* **2018**.
- (159) Lewis, F. D.; Zuo, X., *Spectrum (Bowling Green, OH, U. S.)* **2003**, *16*, 8-15.
- (160) Li, J.; Lamsfus, C. A.; Song, C.; Liu, J.; Fan, G.; Maron, L.; Cui, C., *ChemCatChem* **2017**, *9*, 1368-1372.
- (161) Liu, F.; Pullarkat, S. A.; Li, Y.; Chen, S.; Leung, P.-H., *Eur. J. Inorg. Chem.* **2009**, 4134-4140.
- (162) Liu, L.; Chan, C.; Zhu, J.; Cheng, C.-H.; Zhao, Y., *J. Org. Chem.* **2015**, *80*, 8790-8795.
- (163) Lorke, D. E.; Stegmeier-Petroianu, A.; Petroianu, G. A., *J. Appl. Toxicol.* **2017**, *37*, 13-22.
- (164) Lu, D.; Coote, M. L.; Ho, J.; Kilah, N. L.; Lin, C.-Y.; Salem, G.; Weir, M. L.; Willis, A. C.; Wild, S. B.; Dilda, P. J., *Organometallics* **2012**, *31*, 1808-1816.
- (165) Lu, D.; Salem, G., *Coord. Chem. Rev.* **2013**, *257*, 1026-1038.
- (166) Lu, J.; Ye, J.; Duan, W.-L., *Chem. Commun.* **2014**, *50*, 698-700.
- (167) Mairena, M. A.; Urbano, J.; Carbajo, J.; Maraver, J. J.; Alvarez, E.; Diaz-Requejo, M. M.; Perez, P. J., *Inorg. Chem.* **2007**, *46*, 7428-7435.
- (168) Maitra, K.; Catalano, V. J.; Clark, J., III; Nelson, J. H., *Inorg. Chem.* **1998**, *37*, 1105-1111.
- (169) Malisch, W.; Maisch, R.; Meyer, A.; Greissinger, D.; Gross, E.; Colquhoun, I. J.; McFarlane, W., *Phosphorus Sulfur* **1983**, *18*, 299-302.



- (170) Marquardt, C.; Balazs, G.; Baumann, J.; Virovets, A. V.; Scheer, M., *Chem. Eur. J.* **2017**, *23*, 11423-11429.
- (171) Masuda, J. D.; Jantunen, K. C.; Ozerov, O. V.; Noonan, K. J. T.; Gates, D. P.; Scott, B. L.; Kiplinger, J. L., *J. Am. Chem. Soc.* **2008**, *130*, 2408-2409.
- (172) Mimeau, D.; Gaumont, A.-C., *J. O. C.* **2003**, *68*, 7016-7022.
- (173) Mislow, K.; Baechler, R. D., *J. Am. Chem. Soc.* **1971**, *93*, 773-774.
- (174) Moglie, Y.; Gonzalez-Soria, M. J.; Martin-Garcia, I.; Radivoy, G.; Alonso, F., *Green Chem.* **2016**, *18*, 4896-4907.
- (175) Mohr, F.; Privér, S. H.; Bhargava, S. K.; Bennett, M. A., *Coord. Chem Rev.* **2006**, *250*, 1851-1888.
- (176) Monkowius, U. V.; Nogai, S. D.; Schmidbaur, H., *J. Am. Chem. Soc.* **2004**, *126*, 1632-1633.
- (177) Moquist, P.; Chen, G.-Q.; Mueck-Lichtenfeld, C.; Bussmann, K.; Daniliuc, C. G.; Kehr, G.; Erker, G., *Chem. Sci.* **2015**, *6*, 816-825.
- (178) Mori, T.; Inoue, Y., *Mol. Supramol. Photochem.* **2005**, *12*, 417-452.
- (179) Motta, A.; Fragala, I. L.; Marks, T. J., *Organometallics* **2005**, *24*, 4995-5003.
- (180) Mueller, G.; Brand, J., *Z. Anorg. Allg. Chem.* **2005**, *631*, 2820-2829.
- (181) Nakamura, E.; Sato, K., *Nat. Mater.* **2011**, *10*, 158-161.
- (182) Nigam, S.; Burke, B. P.; Davies, L. H.; Domarkas, J.; Wallis, J. F.; Waddell, P. G.; Waby, J. S.; Benoit, D. M.; Seymour, A.-M.; Cawthorne, C.; Higham, L. J.; Archibald, S. J., *Chem. Commun.* **2016**, *52*, 7114-7117.
- (183) Nigam, S.; Burke, B. P.; Davies, L. H.; Domarkas, J.; Wallis, J. F.; Waddell, P. G.; Waby, J. S.; Benoit, D. M.; Seymour, A.-M.; Cawthorne, C.; Higham, L. J.; Archibald, S. J., *Chem. Commun.* **2016**, *52*, 7114-7117.
- (184) Nyasse, B.; Grehn, L.; Ragnarsson, U., *Chem. Commun.* **1997**, 1017-1018.
- (185) Obata, T.; Kobayashi, E.; Aoshima, S.; Furukawa, J., *Polym J* **1993**, *25*, 1039-1048.
- (186) Ogura, T.; Yoshida, K.; Yanagisawa, A.; Imamoto, T., *Org. Lett.* **2009**, *11*, 2245-2248.
- (187) Ohmiya, H.; Yorimitsu, H.; Oshima, K., *Angew. Chem. Int. Ed.* **2005**, *44*, 2368-2370.
- (188) Otomura, N.; Okugawa, Y.; Hirano, K.; Miura, M., *Org. Lett.* **2017**, *19*, 4802-4805.
- (189) Otsuka, S.; Nakamura, A.; Kano, T.; Tani, K., *J. Amer. Chem. Soc.* **1971**, *93*, 4301-4303.
- (190) Pagano, J. K.; Bange, C. A.; Farmiloe, S. E.; Waterman, R., *Organometallics* **2017**, *36*, 3891-3895.
- (191) Pan, X.; Chen, X.; Li, T.; Li, Y.; Wang, X., *J. Am. Chem. Soc.* **2013**, *135*, 3414-3417.
- (192) Pei, Y.; Brade, K.; Brulé, E.; Hagberg, L.; Lake, F.; Moberg, C., *Eur. J. Org. Chem.* **2005**, *2005*, 2835-2840.
- (193) Perrier, A.; Comte, V.; Moise, C.; Le Gendre, P., *Chem. Eur. J.* **2010**, *16*, 64-67, S64/61-S64/69.

- (194) Preetz, A.; Baumann, W.; Fischer, C.; Drexler, H.-J.; Schmidt, T.; Thede, R.; Heller, D., *Organometallics* **2009**, *28*, 3673-3677.
- (195) Price, A. J.; Edwards, P. G., *Chem. Commun.* **2000**, 899-900.
- (196) Pringle, P. G.; Smith, M. B., *J. Chem. Soc., Chem. Commun.* **1990**, 1701-1702.
- (197) Pritzwald-Stegmann, J. R. F.; Loennecke, P.; Hey-Hawkins, E., *Dalton Trans.* **2016**, *45*, 2208-2217.
- (198) Pullarkat, S. A., *Synthesis* **2016**, *48*, 493-503.
- (199) Pullarkat, S. A.; Leung, P.-H., *Top. Organomet. Chem.* **2013**, *43*, 145-166.
- (200) Pullarkat, S. A.; Yi, D.; Li, Y.; Tan, G.-K.; Leung, P.-H., *Inorg. Chem.* **2006**, *45*, 7455-7463.
- (201) Quin, L. D., *A Guide to Organophosphorus Chemistry*. John Wiley & Sons: New York, 2000.
- (202) Ramón, D. J.; Yus, M., *European Journal of Organic Chemistry* **2000**, *2000*, 225-237.
- (203) Reuter, M.; Orthner, L. Trihydroxymethylphosphine. DE1035135, 1958.
- (204) Rigon, L.; Ranaivonjatovo, H.; Escudie, J., *Phosphorus, Sulfur Silicon Relat. Elem.* **1999**, *152*, 153-167.
- (205) Rodriguez, L. I.; Rossell, O.; Seco, M.; Muller, G., *J. Organomet. Chem.* **2009**, *694*, 1938-1942.
- (206) Rodriguez, L.-I.; Rossell, O.; Seco, M.; Grabulosa, A.; Muller, G.; Rocamora, M., *Organometallics* **2006**, *25*, 1368-1376.
- (207) Rodriguez, L.-I.; Rossell, O.; Seco, M.; Muller, G., *J. Organomet. Chem.* **2007**, *692*, 851-858.
- (208) Rodriguez, L.-I.; Rossell, O.; Seco, M.; Orejon, A.; Masdeu-Bulto, A. M., *J. Organomet. Chem.* **2008**, *693*, 1857-1860.
- (209) Rodriguez, L.-I.; Rossell, O.; Seco, M.; Orejon, A.; Masdeu-Bulto, A. M., *J. Supercrit. Fluids* **2011**, *55*, 1023-1026.
- (210) Rodriguez-Ruiz, V.; Carlino, R.; Bezzenine-Lafollee, S.; Gil, R.; Prim, D.; Schulz, E.; Hannedouche, J., *Dalton Trans.* **2015**, *44*, 12029-12059.
- (211) Roering, A. J.; Davidson, J. J.; MacMillan, S. N.; Tanski, J. M.; Waterman, R., *Dalton Trans.* **2008**, 4488-4498.
- (212) Roering, A. J.; Leshinski, S. E.; Chan, S. M.; Shalumova, T.; MacMillan, S. N.; Tanski, J. M.; Waterman, R., *Organometallics* **2010**, *29*, 2557-2565.
- (213) Roering, A. J.; Maddox, A. F.; Elrod, L. T.; Chan, S. M.; Ghebreab, M. B.; Donovan, K. L.; Davidson, J. J.; Hughes, R. P.; Shalumova, T.; MacMillan, S. N.; Tanski, J. M.; Waterman, R., *Organometallics* **2009**, *28*, 573-581.
- (214) Rogers, J. R.; Wagner, T. P. S.; Marynick, D. S., *Inorg. Chem.* **1994**, *33*, 3104-3110.
- (215) Rosca, S.-C.; Roisnel, T.; Dorcet, V.; Carpentier, J.-F.; Sarazin, Y., *Organometallics* **2014**, *33*, 5630-5642.
- (216) Rosenberg, L., *Coord. Chem. Rev.* **2012**, *256*, 606-626.
- (217) Rosenberg, L., *ACS Catal.* **2013**, *3*, 2845-2855.
- (218) Rossen, K.; Pye, P. J.; Maliakal, A.; Volante, R. P., *J. Org. Chem.* **1997**, *62*, 6462-6463.

- (219) Rotstein, B. H.; Yudin, A. K., *Synthesis* **2012**, *44*, 2851-2858.
- (220) Routaboul, L.; Toulgoat, F.; Gatignol, J.; Lohier, J.-F.; Norah, B.; Delacroix, O.; Alayrac, C.; Taillefer, M.; Gaumont, A.-C., *Chem. Eur. J.* **2013**, *19*, 8760-8764.
- (221) Sakae, R.; Yamamoto, Y.; Komeyama, K.; Takaki, K., *Chem. Lett.* **2010**, *39*, 276-277.
- (222) Sasaki, S.; Sutoh, K.; Shimizu, Y.; Kato, K.; Yoshifuji, M., *Tetrahedron Lett.* **2014**, *55*, 322-325.
- (223) Scriban, C.; Glueck, D. S., *J. Am. Chem. Soc.* **2006**, *128*, 2788-2789.
- (224) Scriban, C.; Glueck, D. S.; Zakharov, L. N.; Kassel, W. S.; DiPasquale, A. G.; Golen, J. A.; Rheingold, A. L., *Organometallics* **2006**, *25*, 5757-5767.
- (225) Serrano, A. L.; Casado, M. A.; Ciriano, M. A.; de Bruin, B.; Lopez, J. A.; Tejel, C., *Inorg. Chem.* **2016**, *55*, 828-839.
- (226) Sharpe, H. R.; Geer, A. M.; Lewis, W.; Blake, A. J.; Kays, D. L., *Angew. Chem. Int. Ed.* **2017**, *56*, 4845-4848.
- (227) Shendage, D. M.; Fröhlich, R.; Haufe, G., *Organic Lett.* **2004**, *6*, 3675-3678.
- (228) Shintani, R.; Ikehata, K.; Hayashi, T., *J. O. C.* **2011**, *76*, 4776-4780.
- (229) Shioji, K.; Ueno, Y.; Kurauchi, Y.; Okuma, K., *Tetrahedron Lett.* **2001**, *42*, 6569-6571.
- (230) Skinner, M. E. G.; Li, Y.; Mountford, P., *Inorg. Chem.* **2002**, *41*, 1110-1119.
- (231) Sowa, S.; Stankevic, M.; Szmigielska, A.; Maluszynska, H.; Koziol, A. E.; Pietrusiewicz, K. M., *J. O. C.* **2015**, *80*, 1672-1688.
- (232) Stelmach, J. P.; Bange, C. A.; Waterman, R., *Dalton Trans.* **2016**, *45*, 6204-6209.
- (233) Stewart, B.; Harriman, A.; Higham, L. J., *Organometallics* **2011**, *30*, 5338-5343.
- (234) Stewart, B.; Harriman, A.; Higham, L. J., Air-stable chiral primary phosphines part (ii) predicting the air-stability of phosphines. In *Organometallic Chemistry: Volume 38*, The Royal Society of Chemistry: 2012; Vol. 38, pp 36-47.
- (235) Stubenhofer, M.; Lassandro, G.; Balazs, G.; Timoshkin, A. Y.; Scheer, M., *Chem. Commun.* **2012**, *48*, 7262-7264.
- (236) Sugiura, J.; Kakizawa, T.; Hashimoto, H.; Tobita, H.; Ogino, H., *Organometallics* **2005**, *24*, 1099-1104.
- (237) Sylla-Iyarreta Veitia, M.; Brun, P. L.; Jorda, P.; Falguieres, A.; Ferroud, C., *Tetrahedron: Asymmetry* **2009**, *20*, 2077-2089.
- (238) Takaki, K.; Komeyama, K.; Kobayashi, D.; Kawabata, T.; Takehira, K., *J. Alloys Compd.* **2006**, *408-412*, 432-436.
- (239) Takaki, K.; Komeyama, K.; Takehira, K., *Tetrahedron* **2003**, *59*, 10381-10395.
- (240) Takaki, K.; Koshiji, G.; Komeyama, K.; Takeda, M.; Shishido, T.; Kitani, A.; Takehira, K., *J. O. C.* **2003**, *68*, 6554-6565.
- (241) Takaki, K.; Takeda, M.; Koshiji, G.; Shishido, T.; Takehira, K., *Tetrahedron Lett.* **2001**, *42*, 6357-6360.
- (242) Takeda, Y.; Nishida, T.; Minakata, S., *Chem. Eur. J.* **2014**, *20*, 10266-10270.
- (243) Tay, W. S.; Yang, X.-Y.; Li, Y.; Pullarkat, S. A.; Leung, P.-H., *Chem. Commun.* **2017**, *53*, 6307-6310.
- (244) Troev, K. D., *Reactivity of P-H Group of Phosphorus Based Compounds*. Academic Press: London, 2017.

- (245) Trost, B. M.; Bunt, R. C.; Lemoine, R. C.; Calkins, T. L., *J. Am. Chem. Soc.* **2000**, *122*, 5968-5976.
- (246) Turbervill, R. S. P.; Goicoechea, J. M., *Eur. J. Inorg. Chem.* **2014**, *2014*, 1660-1668.
- (247) Uberman, P. M.; Caira, M. R.; Martin, S. E., *Organometallics* **2013**, *32*, 3220-3226.
- (248) Uberman, P. M.; Lanteri, M. N.; Martín, S. E., *Organometallics* **2009**, *28*, 6927-6934.
- (249) Vedejs, E.; Lin, S., *J. O. C.* **1994**, *59*, 1602-1603.
- (250) Ward, B. J.; Hunt, P. A., *ACS Catal.* **2017**, *7*, 459-468.
- (251) Waterman, R., *Organometallics* **2007**, *26*, 2492-2494.
- (252) Waterman, R., *Curr. Org. Chem.* **2008**, *12*, 1322-1339.
- (253) Wauters, I.; Debrouwer, W.; Stevens, C. V., *Beilstein J Org Chem* **2014**, *10*, 1064-1096.
- (254) Werner, H., *Angew. Chem. Int. Ed.* **2004**, *43*, 938-954.
- (255) Wicht, D. K.; Kourkine, I. V.; Kovacik, I.; Glueck, D. S.; Concolino, T. E.; Yap, G. P. A.; Incarvito, C. D.; Rheingold, A. L., *Organometallics* **1999**, *18*, 5381-5394.
- (256) Wicht, D. K.; Kourkine, I. V.; Kovacik, I.; Glueck, D. S.; Concolino, T. E.; Yap, G. P. A.; Incarvito, C. D.; Rheingold, A. L., *Organometallics* **1999**, *18*, 5381-5394.
- (257) Wikteliuss, D.; Johansson, M. J.; Luthman, K.; Kann, N., *Org. Lett.* **2005**, *7*, 4991-4994.
- (258) Williams, J. O., *Angew. Chem. Int. Ed.* **1989**, *28*, 1110-1120.
- (259) Wu, Y.; Wu, F.; Zhu, D.; Luo, B.; Wang, H.; Hu, Y.; Wen, S.; Huang, P., *Org. Biomol. Chem.* **2015**, *13*, 10386-10391.
- (260) Wulfers, M. J.; Jentoft, F. C., *Journal of Catalysis* **2013**, *307*, 204-213.
- (261) Wuts, P. G. M.; Greene, T. W., Protection for the Amino Group. In *Greene's Protective Groups in Organic Synthesis*, John Wiley & Sons, Inc.: 2006; pp 696-926.
- (262) Yambushev, F. D.; Usmanov, Z. I.; Shagidullin, R. R.; Khalitov, F. G.; Galeev, A. M.; Tenisheva, N. K., *Zh. Obshch. Khim.* **1978**, *48*, 1766-1771.
- (263) Yang, M.-J.; Liu, Y.-J.; Gong, J.-F.; Song, M.-P., *Organometallics* **2011**, *30*, 3793-3803.
- (264) Yang, X.-Y.; Tay, W. S.; Li, Y.; Pullarkat, S. A.; Leung, P.-H., *Organometallics* **2015**, *34*, 5196-5201.
- (265) Yao, W.; Ma, M.; Zhang, N.; Li, Y.; Pullarkat, S. A.; Leung, P.-H., *J. Organomet. Chem.* **2016**, *801*, 1-5.
- (266) Yau, H. M.; Croft, A. K.; Harper, J. B., *Chem. Commun.* **2012**, *48*, 8937-8939.
- (267) Yoshifuji, M.; Shibayama, K.; Inamoto, N.; Matsushita, T.; Nishimoto, K., *J. Am. Chem. Soc.* **1983**, *105*, 2495-2497.
- (268) Younis, F. M.; Kriech, S.; Al-Shboul, T. M. A.; Goerls, H.; Westerhausen, M., *Inorg. Chem.* **2016**, *55*, 4676-4682.
- (269) Yuan, J.; Hu, H.; Cui, C., *Chem. Eur. J.* **2016**, *22*, 5778-5785.
- (270) Yuan, J.; Huang, Y.; Chi, J.; Yuan, F. antiviral agent for hepatitis C virus treatment. CN106674320A, 2017.

- (271) Zhang, W.; Zhang, X. In *Bisphosphacycles - from DuPhos and BPE to a diverse set of broadly applied ligands*, Wiley-VCH Verlag GmbH & Co. KGaA: 2011; pp 55-91.
- (272) Zhang, Y.; Qu, L.; Wang, Y.; Yuan, D.; Yao, Y.; Shen, Q., *Inorg. Chem.* **2018**, 57, 139-149.
- (273) Zhao, G.; Basuli, F.; Kilgore, U. J.; Fan, H.; Aneetha, H.; Huffman, J. C.; Wu, G.; Mindiola, D. J., *J. Am. Chem. Soc.* **2006**, 128, 13575-13585.
- (274) Zwick, B. D.; Dewey, M. A.; Knight, D. A.; Buhro, W. E.; Arif, A. M.; Gladysz, J. A., *Organometallics* **1992**, 11, 2673-2685.